Université de Montréal

Molecular and functional study of the mammalian double-stranded RNA-binding protein, Staufen

Par

Ming Luo

Département de Biochimie

Faculté de Médecine

Thèse présentée à la Faculté des Études Supérieures

en vue de l'obtention du grade de

Philosophiae Doctor (Ph.D.)

en Biochimie

Décembre 2000

Université de Montréal
Faculté des Etudes Supérieures

Cette thèse est intitulée:

Molecular and functional study of the mammalian double-stranded RNA-binding protein, Staufen

Présentée par:
Ming Luo

a été évaluée par un jury composé des personnes suivantes:

Léa Brakier-Gingras, Ph.D.,	Président du Jury
Luc DesGroseillers, Ph.D.,	Directeur de Recherche
Muriel Aubry, Ph.D.,	Membre du Jury
Sherif Abou Elela, Ph.D.,	Examinateur Externe
Patrick Hallenbeck, Ph.D.,	Le doyen ou son représentant

Thèse acceptée le: Février 2001

To my father, Guan-Zheng Luo
my mother, Ji-Nan Sun
my wife, Jing He
my son, Andy Luo

Résumé

La formation et le maintien de la polarité cellulaire nécessitent la distribution asymétrique de protéines dans la cellule. Il a récemment été démontré que le transport d'ARNm et leur traduction locale constituent une alternative efficace au ciblage des protéines, pour localiser différentes protéines à leur site fonctionnel. En dépit du nombre grandissant de systèmes dans lesquels la localisation d'ARNm fut observée, les mécanismes sous-jacents ne sont que pauvrement compris. Une des raisons qui expliquent cette lacune est le manque d'information concernant les protéines des complexes ribonucléoprotéiques responsables des étapes de transport et/ou de localisation de l'ARN. Chez la drosophile, la protéine Staufen (dStau) fut impliquée dans la localisation des transcrits *bicoid* et *oskar* aux pôles antérieurs et postérieurs de l'ovocyte en développement, respectivement. Dans les cellules somatiques, dStau est aussi nécessaire pour la localisation basale du transcrit *prospero* au cours de la division asymétrique de neuroblastes. Encore aujourd'hui, dStau est l'une des protéines les mieux caractérisées pour son rôle dans la localisation intracellulaire d'ARNm.

Afin de mieux comprendre les mécanismes moléculaires du transport de l'ARN chez les mammifères, mon projet de thèse avait pour but de caractériser les homologues humain (hStau) et murin (mStau) de Staufen tant au niveau moléculaire que cellulaire. Staufen lie l'ARN double brin via deux des quatre domaines consensus de liaison à l'ARN (dsRBD) et lie la tubuline par un domaine situé dans la région C-terminale de la protéine. Ceci suggère que hStau puisse lier certains ARN au cytosquelette et permettre leur déplacement dans la cellule. Des travaux antérieurs avaient montré que le gène *hStau* est présent dans le génome humain en une seule copie et est localisé dans la région

chromosomique 20q13.1. Nous avons examiné les sites d'initiation de la transcription des gènes humain et murin en utilisant différentes approches d'Amplification Rapide des Extrémités d'ADNc (RACE). Nous avons identifié le site d'initiation de la transcription et montré que ce site est conservé entre les espèces. Afin d'isoler la région du promoteur du gène *mStau*, une librairie génomique fut criblée en utilisant l'extrémité 5' de l'ADNc de mStau. Le séquençage des clones positifs a mis en évidence, en amont du site d'initiation, une région riche en G+C sans boîte TATA ou CATT canonique et présentant plusieurs sites possibles de liaison au facteur de transcription SP1, suggérant qu'un promoteur ubiquiste (housekeeping) soit à l'origine de l'expression très répandue de Staufen dans les cellules de mammifères.

Nous avons ensuite démontré que le gène *hStau* génère un minimum de quatre transcrits par épissage alternatif. L'expression transitoire des ADNc correspondant aux différents transcrits dans les cellules de mammifères a révélé que trois de ces transcrits codent une protéine de 55 kDa, alors que le quatrième transcrit code une protéine de 55 kDa. Les deux protéines ne diffèrent que par la séquence de leur extrémité N-terminale. Par microscopie à fluorescence, nous avons localisé hStau dans les structures cellulaires résistantes à une extraction au détergeant Triton X-100, démontrant que hStau n'est pas soluble dans la cellule mais bien associée à des structures et/ou organites sub-cellulaires. En microscopie confocale, hStau co-localise avec les marqueurs du réticulum endoplasmique rugueux (RER).

Nous avons confirmé par fractionnement cellulaire que Staufen est associée à des organites. De façon intéressante, nous avons montré que les isoformes endogènes de 55 et 63 kDa, Stau^{55} et Stau^{63}, sont associées aux ribosomes et au RER, respectivement. Ceci

démontre qu'elles sont incorporées dans différents complexes et suggère qu'elles jouent différents rôles dans la cellule.

Des études d'expression transitoires ont démontré que la protéine de 55 kDa issue de l'ADNc cloné a la même distribution sub-cellulaire que la protéine endogène. Elle peut donc être utilisée pour cartographier les déterminants moléculaires impliqués dans l'association de hStau^{55} avec les ribosomes. A cette fin, nous avons construit une série de mutants et analysé leur distribution sub-cellulaire par microscopie et fractionnement cellulaire. L'analyse de tous les mutants a révélé que le domaine 4 de liaison à l'ARN (dsRBD4) et le domaine liant la tubuline (TBD) forment le domaine minimal d'association aux ribosomes, chaque domaine ne pouvant pas lier les ribosomes séparément. Cette association est indépendante de la capacité de Staufen de lier l'ARN, démontrant que des interactions protéine-protéine sont produites. De façon intéressante, nous avons mis en évidence un domaine cryptique qui permet l'association de Staufen au RER. Le domaine dsRBD4 est suffisant pour promouvoir cette association, bien qu'une coopération moléculaire entre dsRBD4 et les domaines dsRBD2 et dsRBD3 favorise une association plus forte. Ce déterminant pourrait peut-être servir d'ancre pour l'isoforme de 63 kDa. Ces travaux suggèrent que l'association ribosomes/Stau^{55} réalisée par le déterminant dsRBD4/TBD puisse dépendre d'une association préliminaire ou simultanée avec le RER. hStau^{55} pourrait également constituer un pont entre le RER et les ribosomes.

Finalement, le rôle potentiel de Staufen dans le transport et la localisation de l'ARN fut étudié en collaboration avec deux laboratoires externes. D'abord, en collaboration avec Michael Kiebler, nous avons exprimé une protéine chimérique

hStau/GFP dans des neurones d'hippocampe de rats en culture. La protéine a été retrouvée dans le domaine somato-dendritique des cellules. La taille et la distribution des granules contenant hStau/GFP est similaire à celles observées par la protéine endogène. Ces granules co-localisent avec le marquage obtenu par le réactif SYTO14 (un réactif qui colore l'ARN), suggérant que les granules observés contiennent de l'ARN. Par vidéomicroscopie à saut temporel (time-lapse videomicroscopy), nous avons démontré que les granules contenant hStau/GFP se déplacent dans les dendrites à la vitesse moyenne de 6,4μm/min. Le déplacement est dépendent d'un réseau de microtubules intact. Ces résultats suggèrent fortement que hStau soit une composante d'un complexe impliqué dans une voie de transport de l'ARN dans les neurones. De même, en collaboration avec Andrew Mouland, nous avons montré que Staufen est impliquée dans la sélection de l'ARN génomique de rétrovirus, son transport intracellulaire et/ou son encapsidation dans les particules virales. Ces derniers résultats n'ont pas été inclus dans ma thèse.

En conclusion, les travaux présentés dans cette thèse supportent l'idée que Staufen soit conservée à travers l'évolution et qu'elle ait quatre propriétés biochimiques : la liaison à l'ARN double brin, la liaison aux microtubules, la capacité de s'associer au RER et la capacité de s'associer aux ribosomes. Ces propriétés biochimiques font de Staufen un excellent candidat pour un rôle dans le transport de l'ARN et/ou dans le contrôle de la traduction locale des transcrits associés. Enfin, en collaboration avec d'autres groupes, nous avons démontré que hStau, à l'image de la protéine chez la drosophile, est une composante importante d'une voie de transport intracellulaire de l'ARN.

Summary

The generation of a polarized cell requires asymmetric distribution of different proteins in the cell. Besides protein transport, accumulating examples have now demonstrated that mRNA localization constitutes an efficient way to localize numerous proteins to their subcellular functional sites. Although intracellular RNA localization has been well documented in many systems, the underlying mechanisms are not well understood. This is largely due to the lack of information on one of the principal constituents, the *trans*-acting factors in the ribonucleoprotein (RNP) complexes that mediate RNA transport and/or localization. The *Drosophila* double-stranded RNA (dsRNA)-binding protein, Staufen (dStau) has been demonstrated to be important for the proper localization of *bicoid* and *oskar* mRNAs to the anterior and posterior poles of the developing oocyte, respectively. In somatic cells, dStau is also required for basal localization of *prospero* mRNA in dividing neuroblasts. So far, it is one of the best-characterized *trans*-acting proteins involved in intracellular mRNA localization.

To understand the molecular mechanisms of RNA transport in mammals, my thesis project is focused on the molecular and cellular biology of the mammalian orthologue of dStau, including the human (hStau) and mouse (mStau) proteins. Previous studies have shown that the *hStau* is present as a single copy gene, is localized in the human chromosomal region 20q13.1, and is alternatively spliced producing multiple transcripts. For my thesis, we first examined the transcription initiation sites of human and mouse *stau* genes using different 5'RACE approaches and found that both genes share a conserved transcription initiation site at the same position. To further isolate the

possible promoter region of *mStau*, a mouse genomic library was screened using the 5' end of *mStau* cDNA and the genomic DNA fragment corresponding to the 5' upstream region of the cDNA was cloned and sequenced. A G+C-rich region that lacks the canonical TATA and CATT boxes and harbours multiple SP1-binding sites was found upstream of the most 5'RACE sequence, suggesting that a housekeeping-like promoter may drive the broad expression of Staufen in mammalian cells.

In humans, four alternatively spliced transcripts of hStau (termed T1 to T4 in Article 2) are produced in every tested tissue. By Western blotting, we found that hStau is expressed as two major protein isoforms of 63 ($hStau^{63}$) and 55 ($hStau^{55}$) kDa. When transiently expressed each of the four hStau transcripts in COS7 cells, we demonstrated that these transcripts code for two proteins with different N-terminal extremities, which co-migrate with the endogenous $hStau^{63}$ and $hStau^{55}$ respectively. From the deduced amino acid sequence, hStau contains 4 dsRNA-binding domains (dsRBDs) and a tubulin-binding domain (TBD). By immunofluorescent microscopy, we further demonstrated that hStau is associated with the detergent-insoluble fraction in the cell and colocalizes with markers of the rough endoplasmic reticulum (RER), implicating a role of this family of dsRNA-binding protein in the process of mRNA targeting to the site of translation.

To determine the molecular determinants involved in the subcellular localization of Stau and to explore the possible mechanisms of Stau-mediated RNA transport, a series of deletions and point mutations of hStau have been constructed. Using immunofluorescence microscopy and cell fractionation analysis, we first demonstrated that the endogenous $Stau^{55}$ and $Stau^{63}$, are differentially associate with ribosomes and the

RER respectively, suggesting that they may be incorporated in different complexes and play distinct roles in the cell.

We next mapped the determinants involved in hStau^{55} ribosome association. Two overlapping regions located in the N- and C-terminal ends (dsRBD2/3/4 and dsRBD4/TBD/5) of hStau^{55} were shown to promote RER and ribosome association, respectively. Fine mapping revealed that dsRBD4 is a RER binding domain and that it cooperates with dsRBD2 and dsRBD3 to promote full RER association. In contrast, the TBD alone is not sufficient to promote detectable ribosome binding. However, when fused with the RER-associated dsRBD4, TBD promotes basal ribosome association. Therefore, dsRBD4 and TBD together constitute a basal ribosome association domain. This ribosome association is independent of Staufen's RNA binding activity. Deletion of TBD from hStau^{55} shifted the distribution of the protein from the ribosomes to RER, further demonstrating that TBD is crucial for ribosome association. These results also revealed that hStau^{55} contains a cryptic determinant (dsRBD2/3/4) which has strong RER association capacity, thus hStau^{55} can associate not only with ribosomes but also with the RER. To further assess the role of dsRBD4 in ribosome association, we deleted this domain from hStau^{55}. Accordingly, this deletion modified hStau^{55} association with both ribosomes and the RER, demonstrating that dsRBD4 plays a pivotal role in the intracellular distribution of hStau^{55}. Taken together, these studies suggest that dsRBD4/TBD-mediated hStau^{55} ribosome association may depend on prior or simultaneous RER association and that hStau^{55} may be a bridging molecule between the RER and ribosomes through overlapping determinants.

The potential role of mammalian Staufen in RNA transport and localization in different systems has been explored by our collaboration with two other groups. In cultured living rat hippocampal neurons, transiently transfected hStau-green fluorescent protein (GFP) was found to be expressed in the somatodendritic domain, and to form fluorescent granules that were migrating into the distal dendrites in a microtubule-dependent way (see Article 4). These granules co-localize with RNA when labelled by SYTO14 (an RNA-staining dye), suggesting that hStau-GFP is a component of the ribonucleoprotein complex. In the mean time, the possible roles of hStau as a host cell RNA-binding protein in retroviral genomic RNA selection, intracellular transport and virion encapsidation have also been explored through collaboration with the group of Dr. Mouland (Mouland et al., 2000, not included in this thesis).

In summary, the studies presented in this thesis provide substantial evidence that mammalian Staufen belongs to an evolutionarily conserved protein with four distinct biochemical properties: dsRNA- and microtubule-binding, RER and ribosome association. These biochemical features have made Staufen a very good candidate for RNA transport and/or local translation. Finally, by collaboration with other groups we have demonstrated that human Staufen, similar to its *Drosophila* counterpart, may serve as an important component of the intracellular RNA transport pathway.

CONTENTS

List of Tables

I- Introduction

II- Article I

List of Figures

I- Introduction

II- Article 1

III- Article 2

IV- Article 3

V- Article 4

VI- Discussion

VII- Appendix

Abbreviations

bcd: *bicoid*

bp: base pair

BRE: Bruno response element

CaMKIIα: α-subunit of calcium/calmodulin-dependent protein kinase II

CEFs: chicken embryo fibroblasts

CNS: central nervous system

CPE: cytoplasmic polyadenylation element

CPEB: CPE-binding protein

CPSF: cleavage and polyadenylation specificity factor

dsRNA: double-stranded RNA

dsRBD: double-stranded RNA-binding protein

DRADA: double-stranded RNA adenosine deaminase

EF1α: elongation factor 1α

ELTP: expand long template PCR

FMRP: Fragile X mental retardation protein

GFP: green fluorescent protein

GMC: ganglion mother cell

grk: *gurken*

HA: hemagglutinin

hb: *hunchback*

HIV-1: human immunodeficiency virus type 1

hnRNP: heterogeneous nuclear ribonucleoprotein

Insc: Inscuteable

kDa: kilodalton

MAP1B: microtubule-associated protein 1B

MBP: myelin basic protein

METRO: messenger transport organizer

mGluRs: metabotropic glutamate receptors

mRNA: messenger RNA

mRNP: mRNA ribonucleoprotein complex

MTOC: microtubule organizing center

NLS: nuclear localization signal

NMR: nuclear magnetic resonance

nos: *nanos*

NRE: nanos response element

nt: nucleotides

osk: *oskar*

PCR: polymerase chain reaction

Pins: *Partner of Inscuteable*

PKA: protein kinase A

PKR: interferon-inducible dsRNA-dependent protein kinase

Pon: *Partner of Numb*

PNS: peripheral nervous system

Pros: Prospero

RACE: rapid amplification of cDNA ends

RBP: RNA binding protein

RER: rough endoplasmic reticulum

RGG: arginine/glycine-rich boxes

RLS: RNA localization signal

RNP: ribonucleoprotein

RRM: RNA recognition motif

RTS: RNA transport sequence

SOP: sensory organ precursor

Spnr: spermatid perinuclear RNA binding protein

SRE: Smaug response element

Stau: Staufen

TBD: tubulin-binding domain

TB-RBP: testis/brain RNA-binding protein

Tm: melting temperature

TRBP: TAR RNA binding protein

UTR: untranslated region

Vera: *Vg1* binding and ER associated protein

VgLE: *Vg1* localization element

Xlrbpa: *Xenopus* dsRNA-binding protein a

ACKNOWLEDGEMENTS

I wish to take this opportunity to express my sincere gratitude to my research director, Dr. Luc DesGroseillers, for accepting me to do my Ph.D. study in his laboratory, his guidance, encouragement, stimulating suggestions, and financial support throughout the course of the study.

I would like to thank Dr. Ivan R. Nabi for his help in performing immunofluorescence and confocal double-labelling microscopy, Drs. Guy Boileau and Philippe Crine for their valuable questions during the laboratory meetings, Drs. Michael Kiebler, Andrew Mouland, and Gopal Subramaniam, Mr. Thomas Duchaîne and Mr. George Elvira, for their critical reading of my paper manuscript.

I would also like to thank Ms. Louise Cournoyer for her excellent work to prepare cell culture and Ms. Annie Montmarquette for technical assistance, Mr. Pierre Methot for synthesizing oligonucleotides, Mrs. Manon Moreau and Mr. Gaston Lambert for photographic preparation.

I deeply appreciate my supervisor Dr. Luc DesGroseillers and Mr. Jean-Pierre Morello to critically read all the sections of this dissertation. I would also like to thank Mr. Thomas Duchaîne for his work to translate the summary of this thesis into French. I sincerely appreciate all the members of DesGroseillers lab, both present and past, for their friendship, encouragement, good sense of humor, technical assistance and helpful discussions throughout my study in University of Montreal.

I would also like to thank the members of my thesis jury for their time and work to evaluate this thesis.

Finally, I wish to express my sincere appreciation to my lovely wife, Jing He, and my family in China for their whole-hearted support, understanding and encouragement during the past five years. Without their support, I could not finish this thesis.

I- INTRODUCTION

I.1 Intracellular RNA localization

Biologists have long been fascinated by how cells target proteins to specific intracellular compartments and maintain their localized distributions. While a great deal of attention has been focused on the mechanisms by which proteins are sorted to the different compartments of the cell, particularly the membrane-bound organelles (Alberts et al., 1994a,b), relatively little is known about how proteins are targeted to different regions of the cytoplasm. During the last decade, an increasing number of examples indicate that a major mechanism by which this occurs is via the localization of messenger RNA (mRNA). Indeed, intracellular mRNA (even some structural RNAs) localization now appears to be an important and conserved mechanism to produce cellular asymmetries in a variety of organisms (see below).

I.1.1 The potential significance of intracellular RNA localization

From a biological standpoint, the intracellular localization of mRNAs is important for four major reasons. Firstly, mRNA localization can serve as an efficient way to target proteins to their corresponding functional sites in the cell. A single mRNA can be translated many times and give rise to many protein molecules, provided that it is associated with components of the translation machinery. Thus, the localization of mRNA instead of the protein itself has the potential of producing high local protein concentrations at a relatively low energy cost. Indeed, in many cases mRNAs are localized as ribonucleoprotein (RNP) complexes along with components of the translation machinery, ensuring that localized translation can occur efficiently.

A second reason why a specific mRNA might be localized is to ensure that the encoded protein is not expressed in the wrong region of the cell. For example, if the presence of one protein were sufficient to specify certain cell fates in oogenesis or embryogenesis, then exclusion of the protein from the remainder of the embryo would enable other developing fates to be adopted. Thus, mRNA localization and local translation might be required to ensure that a particular protein is not expressed throughout a developing embryo but only in a specific region where it is required. Later, I will discuss this scenario for several important cell fate determinants such as bicoid and nanos in *Drosophila* oogenesis and early embryogenesis. A similar scenario also occurs in somatic cells. For example, in oligodendrocytes, myelin basic protein (MBP) is an intracellular protein that interacts very strongly with membranes and causes them to compact. Unlike other components of myelin, which are exported to the myelinating cell processes by the secretory pathway, MBP is translated on free ribosomes from localized mRNA (Trapp et al., 1987). It would be very difficult to transport the MBP protein from the cell body to the sites of myelin formation, since the protein would stick to any membrane it came into contact with along the way. The localization of the mRNA avoids this problem and prevents the protein from compacting membranes in the main body of the cell (for review, see St Johnston 1995).

A third important reason comes from that localized translation opens up the possibility of local translational control. It is particularly attractive to speculate that the delivery of specific RNAs to dendrites would allow for localized translational regulation at the synapses. Transsynaptic activity such as synaptic stimulation could result in localization of certain RNAs to the activated postsynaptic sites and produce local

synthesis of specific proteins at the stimulated sites. Alternatively, transsynaptic activity may cause a translational switch, initiating translation of locally docked but translationally inactive mRNAs. The ability to induce the synthesis of selected proteins at the synapse would allow for long-lasting changes in structure and function of that synapse, thus modifying the synaptic plasticity (for review, see Tiedge et al., 1999).

A fourth reason why RNAs localize in the cell might be to subserve particular structural roles in a spatially restricted manner. It has been known that the localization of some non-protein-coding RNAs is important for the proper localization of certain mRNAs that code for important cell fate determinants and contributes to the establishment of polarized cell fates. For example, some structural RNAs such as *BC1* and *Xlsirts* have been found to localize in specific domains of mammalian neurons (Tiedge et al., 1991) and *Xenopus* oocytes (Kloc et al., 1993), respectively. *BC1* RNA is a component of ribonucleoprotein particles that are rapidly and selectively transported to dendrites (Muslimov et al., 1997) and is subject to activity-dependent regulation in hippocampal neurons (Muslimov et al., 1998). It has been suggested that *BC1* RNA plays an important role in the transport and/or translation of mRNA in dendrites, especially in the postsynaptic dendritic microdomains (Brosius and Tiedge, 1995). Accordingly, *Xlsirts* has been demonstrated to be important for the proper localization of *Vg1* mRNA, a *Xenopus* cell fate determinant, to the vegetal cortex of *Xenopus* oocytes (Kloc and Etkin, 1994), suggesting that it plays a structural role for the localization of other RNAs.

I.1.2 The list of intracellular localized RNAs

The first observation of localized RNA in a restricted region of the cell was made about 17 years ago, with the demonstration that actin mRNA is enriched in the myoplasm of ascidian eggs (Jeffery et al., 1983). Shortly thereafter, several maternal mRNAs that are asymmetrically localized during oogenesis were identified in *Xenopus* (Rebagliati et al, 1985) and *Drosophila* (Frigerio et al., 1986). The identification of the first localized *Drosophlia* maternal RNA *bicoid*, which plays a crucial role in specifying cell fates in the anterior half of the embryo, is a milestone in the demonstration that RNA localization *per se* is important for normal development (Frigerio et al., 1986, Berleth et al., 1988). More recently, localized mRNAs have been discovered in different types of somatic cells (for review, see St Johnston 1995, Bashirullah et al., 1998), and even in budding yeast (Long et al., 1997; Takizawa et al., 1997), making it clear that mRNA localization serves as a general mechanism for generating asymmetric distribution of proteins in the cytoplasm. To date, there are over 75 spatially restricted RNA transcripts identified in eggs, embryos, somatic cells, and single cell organisms (Bashirullah et al., 1998). Examples of intracellular RNA localization and their biological functions have been extensively reviewed recently (Bashirullah et al., 1998; Bassell and Singer, 1999; Carson et al., 1998; Kiebler and DesGroseillers, 2000; Mowry and Cote, 1999; Oleynikov et al., 1998; St Johnston, 1995). Here, I will first list the majority of these localized RNAs in different systems including eggs and early embryos of *Ascidians*, *Drosophila*, and *Xenopus* as well as in differentiated mammalian neurons (see Table 1). In the following sections, I will discuss some typical examples of localized RNAs in germline and somatic cells of different organisms, with an emphasis on the localization patterns, the possible localization mechanisms, and their biological significance and functions.

Table 1 Localized RNAs

Species	*Transcript name*	*Protein Product*	*Localization pattern*	*Cell*	*Reference*
Ascidians					
	Actin	Cytoskeletal component	Myoplasm and ectoplasm	Oocyte	105
	PCNA	Auxilary protein of DNA polymerase	Ectoplasm	Oocyte	291
	Ribosomal protein L5	Ribosomal component	Myoplasm	Oocyte	290
	YC RNA	Noncoding RNA	Myoplasm	Oocyte	289
Drosophila					
	Add-hts	Cytoskeletal component	Anterior	Oocyte and embryo	49,337
	Bicaudal-C	Signal transduction/ RNA-binding protein	Anterior	Oocyte	181
	Bicaudal-D	Cytoskeleton interacting protein (?)	Anterior	Oocyte	287
	bicoid	Transcription factor	Anterior	Oocyte and embryo	15, 281
	crumbs	Transmembrane protein	Apical	Cellular blastoderm	295
	Cyclin B	Cell cycle regulator	Posterior and perinuclear	Oocyte and embryo	233,329
	egalitarian	Novel	Anterior	Oocyte	180
	even-skipped	Transcription factor	Apical	Cellular blastoderm	173
	fushi tarazu	Transcription factor	Apical	Cellular blastoderm	58
	germ cell-less	Nuclear pore associated protein	Posterior	Oocyte and embryo	107,108
	gurken	Secreted growth factor	Anterior-dorsal	Oocyte	214
	hairy	Transcription factor	Apical	Cellular blastoderm	44
	Hsp83	Molecular chaperone	Posterior	Embryo	48
	inscuteable	Novel	Apical	Neuroblast	159
	K10	Novel	Anterior	Oocyte	37
	mtlrRNA	Noncoding RNA	Posterior	Oocyte and embryo	47,138

Table 1 *Continued*

Species	*Transcript name*	*Protein Product*	*Localization pattern*	*Cell*	*Reference*
	nanos	RNA binding protein	Posterior	Oocyte and embryo	73,315
	orb	RNA binding protein	Posterior	Oocyte and embryo	153
	oskar	Novel	Posterior	Oocyte and embryo	61,116
	Pgc	Noncoding RNA	Posterior	Oocyte and embryo	212
	prospero	Transcription factor	Apical/basal	Neuroblast	159
	pumilio	RNA binding protein	Posterior	Embryo	172
	runt	Transcription factor	Apical	Cellular blastoderm	77
	sevenless	Transmembrane receptor	Apical	Eye imaginal Epithelial cells	8
	tudor	Novel	Posterior	Oocyte	78
	wingless	Secreted ligand	Apical	Cellular blastoderm	7
	yemanuclein-α	Transcription factor	Anterior	Oocyte	4
Echinoderms					
	SpCOUP-TF	Hormone receptor	Lateral to animal-vegetal axis	Oocyte	313
Mammals					
	β-actin	Cytoskeletal component	Specialized periphery	Fibroblasts, myoblasts, and epithelial cells	36, 156 286
	Arc	Cytosketal component	Somatodendritic	Neurons	275
	BC-1	Noncoding RNA	Somatodentritic and axonal	Neurons	304,305
	BC-200	Noncoding RNA	Somatodendritic	Neurons	303
	CaMKIIα	Signalling component	Somatodendritic	Neurons	189
	F1/GAP43	PKC substrate	Somatodendritic	Neurons	275
	InsP3 receptor	Integral membrane receptor	Somatodendritic	Neurons	69

Table 1 *Continued*

Species	*Transcript name*	*Protein Product*	*Localization pattern*	*Cell*	*Reference*
	MAP2	Cytosketal component	Somatodendritic	Neurons	71
	MBP	Membrane protein	Myelinating membrane	Oligodendrocyte and Schwann cells	307
	Myosin heavy chain	Cytoskeletal component	Peripheral	Muscle	230
	OMP/odorant receptors	Integral membrane receptor	Axonal	Neurons	238,313
	Oxytocin	Neuropeptide	Axonal	Neurons	106
	Prodynorphin	Neuropeptide	Axonal	Neurons	199
	RC3	PKC substrate	Somatoden-dritic	Neurons	275
	tau	Cytoskeletal component	Axon hillock	Neurons	165
	Tropomyosin-5	Cytoskeletal component	Pre-axonal pole	Neurons	86
	V-ATPase subunits	Membrane protein	Specialized membrane	Osteoclasts	149
	Vassopressin	Neuropeptide	Axonal	Neurons	308
Xenopus					
	Actin	Cytoskeletal component	Periplasmic	Oocyte	226
	Anl (a and b)	Cyoplasmic protein (ubiquitin-like)	Animal	Oocyte	163,236
	An2	mt ATPase subunit	Animal	Oocyte	236,321
	An3	RNA binding protein	Animal	Oocyte	236
	An4 (a and b)	Novel	Animal	Oocyte	96
	βTrCP	Signaling molecule	Animal	Oocyte	96
	βTrCP-2	Signaling molecule	Vegetal	Oocyte	96
	βTrCP-3	Signaling molecule	Vegetal	Oocyte	96
	B6	NR[a]	Vegetal	Oocyte	119
	B7	NR	Vegetal	Oocyte	119
	B9	NR	Vegetal	Oocyte	119
	B12	NR	Vegetal	Oocyte	119
	C10	NR	Vegetal	Oocyte	119

Table 1 *Continued*

Species	*Transcript name*	*Protein Product*	*Localization pattern*	*Cell*	*Reference*
	G-proteins	Signaling molecule	Animal	Oocyte	221
	Oct60	Transcription factor	Animal	Oocyte	91
	PKCα	Signaling molecule	Animal	Oocyte	222
	α-tubulin	Cytoskeletal component	Periplasmic	Oocyte	226
	VegT (Antipodean)	Transcription factor	Vegetal	Oocyte	270,340
	Vgl	Signaling molecule	Vegetal	Oocyte	236
	Xcat-2	RNA-binding protein	Vegetal	Oocyte	200,341
	Xcat-3	RNA-binding protein	Vegetal	Oocyte	59
	Xcat-4	NR	Vegetal	Oocyte	119
	xl-21	Transcription factor (?)	Animal	Oocyte	133
	Xlan4	P-rich and PEST sequences	Animal	Oocyte	237
	Xlcaax-1	Membrane protein	Animal	Oocyte	132
	Xlsirt	Noncoding RNA	Vegetal	Oocyte	134
	Xwnt-11	Secreted ligand	Vegetal	Oocyte	142
Yeast					
	ASH1	Transcription factor	Budding site	Mother cell	166,293
Zebrafish					
	Vasa	RNA-binding protein	Cleavage plane	Early embryo	335

NR, not reported. Table adopted from Bashirullah et al., 1998.

I.2 RNA localization in embryonic development of *Drosophila*

The body patterns along the two major body axes (anterior-posterior and dorso-ventral) of *Drosophila melanogaster* are initiated by several maternal RNAs that are already localized in the newly formed unfertilized egg. These maternal mRNAs encode different positional information that specifies the development pattern of the early embryo. While the dorso-ventral (D-V) pattern arises from signaling between the oocyte and the overlying somatic follicle cells (for review, see van Eeden and St Johnston, 1999), the body pattern along the anterior-posterior (A-P) axis of the embryo is defined by two maternal mRNA determinants that are localized in the anterior and posterior poles of the egg, respectively. These two determinants, *bicoid* and *nanos*, generate two morphogenetic gradients emanating from each pole of the egg and direct the programming of the A-P body plan. In this section, I will mainly describe the following issues: 1) how RNA localization is related to the oocyte determination, 2) how the polarization of two axes are initiated, and 3) how the anterior and posterior determinants give rise to a series of localized mRNAs that specify cell fates along the anterior-posterior axis. To better understand these complex processes, I will first start with the morphological stages of *Drosophila* oogenesis and early embryogenesis.

I.2.1 Oogenesis and early embryogenesis

I.2.1.1 Oogenesis

In *Drosophila,* the eggs are formed within tubes called ovarioles, which are divided into chambers by transverse walls (see Fig. 1 for the depiction of oogenesis). The

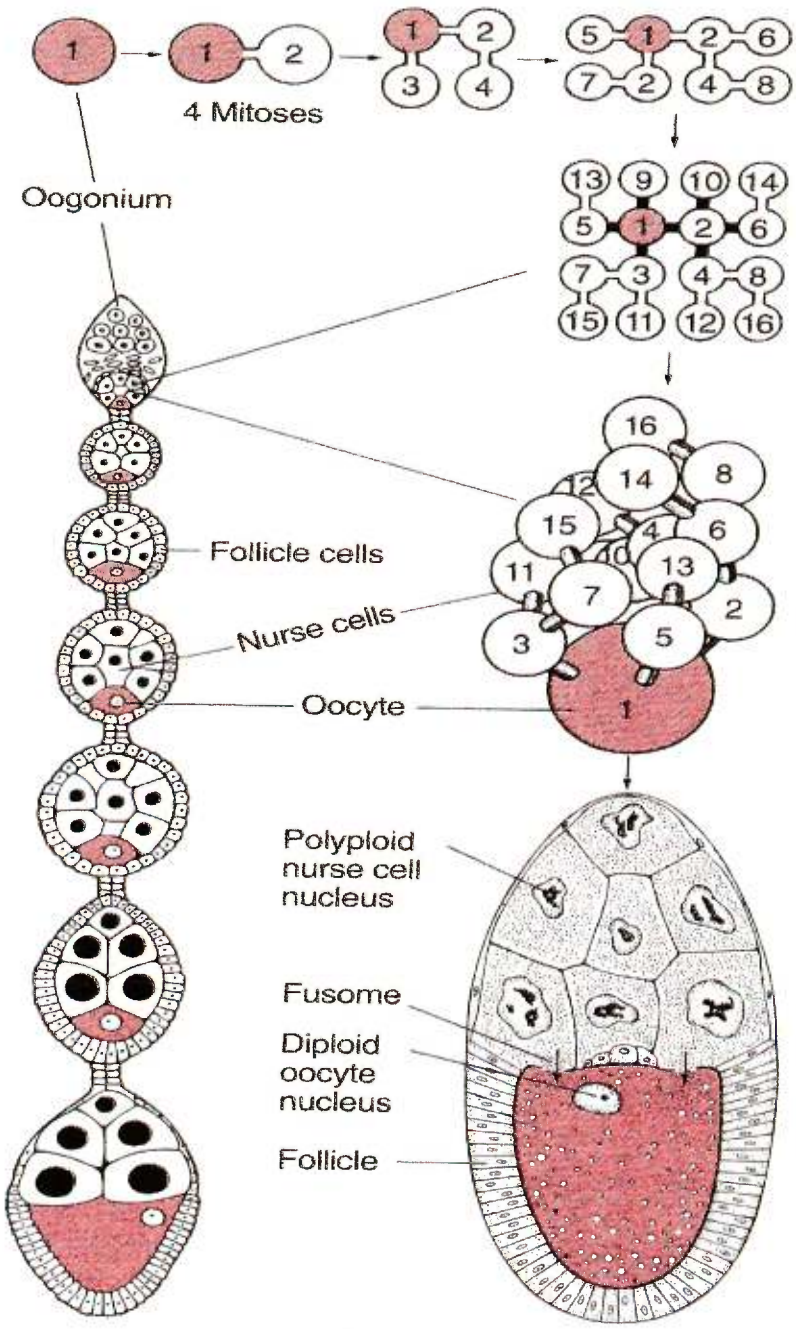

Fig. 1. *Drosophila* oogenesis. Schematic drawing of one tubular ovariole, containing oogonia close to its distal tip. Oocytes of progressive size and maturity are seen along the tube. The oocytes are accompanied by nurse cells and are surrounded by follicle cells. Enlarged details are shown outside the tube of the ovariole.

cells constituting the wall of an ovariole and surrounding the future egg are termed follicle cells by anology to the follicle cells in the ovary of vertebrates. In each chamber there is one female primordial germ cell, the oogonium. The oogonium undergoes four rounds of mitotic divisions, resulting in 16 cells. These remain interconnected by cytoplasmic bridges called ring canals or fusomes. In the center of the cluster, 2 of the 16 cells are connected with 4 sister cells; one of these 2 cells will become the oocyte, the future egg cell. The remaining 15 sister cells are fated to become nurse cells. While the oocyte remains diploid, and later will become haploid in the course of two meiotic divisions, the nurse cells become polyploid by replicating their DNA repeatedly; this amplification of the genome enables high transcriptional activity. The nurse cells will provide the oocyte with huge amounts of ribosomes and mRNAs that are enclosed in ribonucleoprotein particles (RNP). The nurse cell-oocyte complex is surrounded by somatic follicle cells which supply yolk and help to nourish the oocyte. By stage 10 of oogenesis, these follicle cells have migrated to cover the developing oocyte. As the oocyte matures, the nurse cells contract and dump their contents to the oocyte, while the follicle cells secrete the egg coverings. Both the nurse and follicle cells degenerate at the end of oogenesis. When the mature egg is laid, it is surrounded by the vitelline membrane and the chorion, and is filled with yolky cytoplasm (see Sprading 1993 for a full review of oogenesis).

I.2.1.2 Early embryogenesis

The embryonic development in *Drosophila* (Fig. 2) starts immediately following egg deposition. After fertilization, the zygotic nuclei go through a series of rapid cleavage

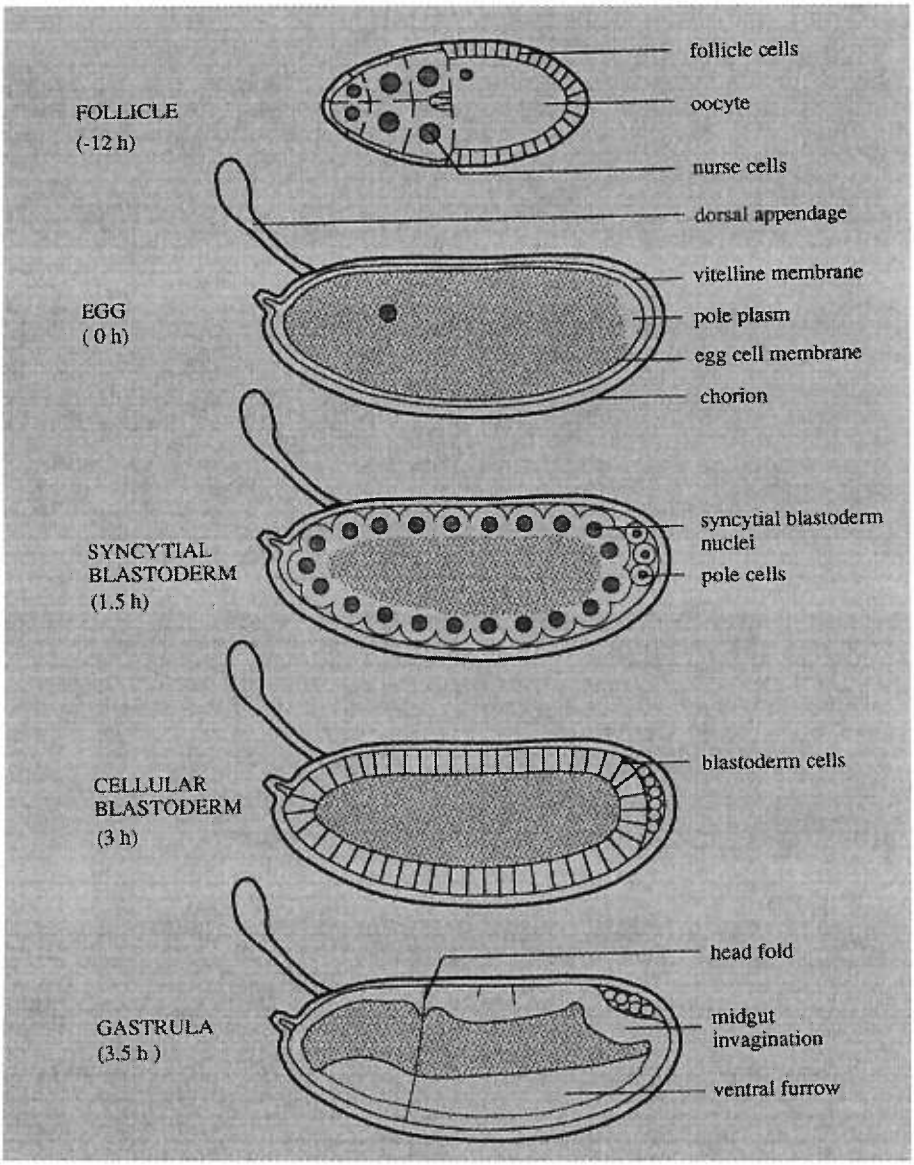

Fig. 2. Early embryogenesis in *Drosophila*. After fertilization, the zygotic nuclei go through a series of rapid cleavage divisions in the anterior of the egg. At the cleavage stage, nuclei are duplicated at a high frequency with intervals of only 9 minutes. After 13 rounds of replication about 6,000 nuclei are present. At this phase the egg represents a syncytium. During this stage, the 3-4 nuclei that have entered the pole plasm at the posterior pole form polar buds. Next cellularization is processed to create individual cells and to form cellular blastoderm. Later, gastrulation takes place with the invagination of the presumptive mesoderm through the ventral furrow and early organogenesis starts. Adapted from St Johnston and Nusslein-Volhard, 1992.

divisions in the interior of the egg. After nine divisions, the majority of the nuclei have migrated to the cortex to form the syncytial blastoderm. At this stage, the 3-4 nuclei that have entered the pole plasm at the posterior pole form polar buds, which will give rise to the pole cells, the precursors of the germline. The rest of nuclei divide four more times at the surface of the egg before being surrounded by cell membranes to give rise to nearly 6000 cells of the cellular blastoderm. Soon after cellularization is complete, gastrulation begins with the invagination of the presumptive mesoderm through the ventral furrow, the formation of the posterior midgut invagination that contains the pole cells, and appearance of the head fold (for review, see St Johnston and Nüsslein-Volhard, 1992).

I.2.2 Determination of the oocyte

Establishment of oocyte identity is a multistage process involving multiple factors and events. Localization of several mRNAs and proteins to a single cell within the 16-cell cyst first distinguishes the pro-oocyte from its neighbors. Two genes, *Bicaudal-D* (*Bic-D*) and *orb* play very important roles for the oocyte determination. *Bicaudal-D* encodes a protein that shares sequence similarity to myosin heavy chain tail domains (Suter et al., 1989). Null alleles of *Bic-D* abolish all signs of oocyte determination (Ran et al., 1994). In strong alleles of *orb*, a germ-line-specific RNA-binding protein, the 16-cell cyst formation is also disrupted (Lantz et al., 1992, 1994).

A key component implicated in oocyte determination is the microtubule cytoskeleton. Treating wild-type flies with microtubule-depolymerizing drugs such as colchicine causes a 16-nurse-cell phenotype. A microtubule-organizing-center (MTOC) is formed in the presumptive oocyte just after the formation of the 16-cell cluster. In *Bic-*

D mutants, this MOTC does not form (Theurkauf, 1993). The product of the *egalitarian* (*Egl*) gene has been shown to physically interact and colocalize with Bic-D in all stages of oogenesis (Mach and Lehmann, 1997). In *egalitarian* mutants, the microtubule network is not maintained (Theurkauf et al., 1993). In both *Bic-D* and *Egl mutants,* oocyte specific mRNAs fail to accumulate in a single cell and the cystocytes differentiate into 16 nurse cells with no oocyte (Theurkauf et al., 1993; Suter and Steward, 1991; Ran et al., 1994). These experiments have led to a model in which mRNAs are transported along the microtubule network into the single cell of the cyst that contains an MTOC, thereby determining this cell to become the oocyte.

I.2.3 Polarization of the A-P and D-V axes

Establishment of both anterior-posterior (A-P) and dorsal-ventral (D-V) axes involves multiple reciprocal communication events between the germline and the somatic follicle cells of the egg chamber. A common signal molecule, gurken (grk), plays a pivotal role in these events. *grk* mRNA is synthesized in the oocyte nucleus, encoding a TGF-α homolog, which acts as a ligand for the epidermal growth factor receptors (*torpedo/DER*) expressed in the somatic follicle cells (Neuman-Silberberg and Schupbach, 1993). The gurken-torpedo signalling pathway is essential for the polarization of both major body axes in *Drosophila* (Neuman-Silberberg and Schupbach, 1993, González-Reyes et al., 1995). *grk* RNA is first localized to the posterior pole of the oocyte at stage 7, then to both the anterior and posterior poles at stage 8, and finally to the anterodorsal corner from stage 8 through stage 10 (Neuman-Silberberg and Schupbach, 1993, 1994). Due to the posterior-localized *gurken* RNA, local production of the gurken

protein at the posterior end of the oocyte causes signalling to the posterior follicle cells. This signalling is essential for the establishment of the anterior-posterior oocyte axis and for the polarization of the oocyte microtubule-based cytoskeleton that plays a crucial role in RNA localization. Subsequently, anterodorsal localization of *grk* mRNA in the oocyte directs local grk protein synthesis, and generates a second oocyte-nurse cell signalling that establishes the dorso-ventral axis of the egg chamber.

I.2.4 bicoid RNA localization and anterior body patterning

Many RNAs that are later localized within the growing oocyte are first transcribed in the nurse cells but accumulate specifically in the pro-oocyte. All these RNAs are found at least transiently at the anterior margin of the oocyte before stage 7. For example, RNAs for *Bic-D, orb, oskar, K10, bicoid, gurken, hu-li tai shao (Adds-hts), Bic-C, tudor* and *cyclin-B* are all transiently localized at the anterior. This transient localization is consistent with their transport by the same microtubule-based mechanism that originally targeted them to the oocyte. Before stage 7, the microtubule-minus ends are located in the oocyte. After stage 7, the microtubule network is reorganized and the minus ends are present at the anterior cortex. Therefore, transport of these mRNAs by the minus-end directed motor would account for both pre- and post-stage 7 localization patterns. Late in oogenesis, all these transiently localized RNA transcripts undergo different localization pathways. Whereas most of these RNAs are uniformly distributed within the oocyte, some RNAs such as *bicoid* and *Add-hts* remain anteriorly localized until early cleavage embryogenesis, other RNAs such as *oskar, nanos* and *Pgc* retain posterior localization in

the early cleavage-stage embryos. Next, I will focus on one of the most studied anteriorly localized messenger RNA, *bicoid*.

I.2.4.1 Bicoid acts as an anterior morphogen

A. Bicoid is a transcrptional activator

Drosophila maternal effect gene, *bicoid* (*bcd*), encodes a protein that contains a homeodomain DNA recognition motif and a distinct transcriptional activation domain (Driever and Nusslein-Volhard, 1989a, 1989b, Struhl et al., 1989). *bcd* mRNA is first produced in the nurse cells and is transported to the oocyte and tightly localized to the anterior cortex during late oogenesis. After fertilization, this localized RNA is translated to Bicoid (Bcd) protein and gives rise to a steep concentration gradient emanating from the anterior to the posterior end of the early embryo (see Fig.3 for the schematic depiction of this process). This different concentration of Bicoid protein is then incorporated into the embryonic nuclei in the anterior region of the egg. The distinct concentration thresholds of bicoid protein along the A-P axis subsequently activate the transcription of a series of zygotic target genes including *hunchback*, a member of a class of genes called gap genes, in the anterior half of the embryo. Expression of these downstream zygotic genes finally direct the formation of the anterior head and thorax structures (Driever and Nusslein-Volhard, 1988, 1989a, 1989b; Struhl et al., 1989). Bicoid protein induces the anterior structures in a concentration-dependent manner since Bicoid mediates transcription activation by cooperative DNA binding of the homeodomain to different DNA targets. Therefore, the binding and activation of a former gene will help the activation of a downstream target gene with a decreased concentration (Burz et al., 1998; Ma et al., 1996).

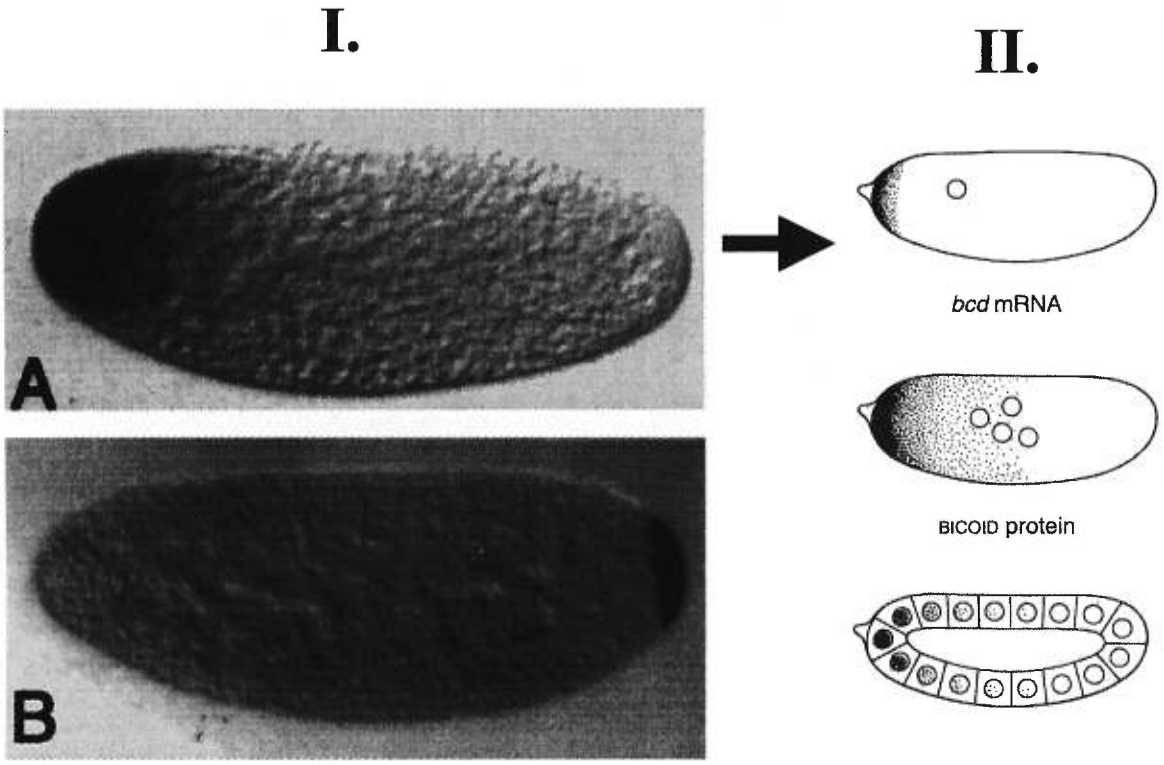

Fig. 3. Localized maternal mRNAs in early *Drosophila* embryos. I. *bicoid* (A) and *nanos* (B) mRNAs are localized in the anterior and posterior poles of stage 2 embryo, respectively. **II.** After fertilization, the anterior localized *bicoid* mRNAs are translated and give rise to a gradient of Bicoid protein in the nuclei of the blastoderm. The different concentrations of Bicoid protein subsequently activate a series of zygotic gap genes in the anterior part of the embryo and determine the head and thorax body pattern. Similarly, the posteriorly localized *nanos* mRNA generates an opposite protein gradient and determines the abdomen body pattern (not shown).

B *Bicoid is a translational repressor*

In addition to its role for transcriptional activation of a series of targeted zygotic genes, Bicoid protein determines the anterior cell fates partly by another function, translational repression of another maternal mRNA *caudal* (*cad*), in the anterior part of the embryo (Dubnau and Struhl, 1996; Rivera-Pomar et al., 1996). *cad* codes for another homeodomain protein which is involved in specifying the posterior pattern of the early embryo. Inappropriate expression of the *cad* gene in the anterior end of the embryo causes deletion of head and thoracic segmentation (Mlodzik et al., 1985; Macdonald and Struhl, 1986). Although *cad* mRNA is evenly distributed in the early cleavage-stage embryo, *cad* protein only forms a posterior-anterior concentration gradient before the initiation of zygotic gene expression. Bicoid binds to *cad* mRNA through the discrete target sequences within the 3'UTR of *cad* mRNA, and blocks the initiation of cad translation in the anterior part of the embryo.

I.2.4.2 Dynamics of bcd mRNA localization

bcd mRNA localization in *Drosophila* occurs through a complex process involving multiple successive steps which have different genetic requirements (St Johnston et al., 1989). Transcription of *bcd* mRNA begins in the nurse cells during stages 4 and 5 of oogenesis and the mRNA is immediately transported to the oocyte. As oogenesis proceeds, transport to the oocyte continues and *bcd* mRNA accumulates in a ring at the anterior margin of oocyte through stages 7-9. This localization is maintained in stages 9-10, and during this time, additional *bcd* mRNA is also seen in an apical region of the nurse cells. In *exuperantia* (*exu*) mutants, anterior concentration of *bicoid* RNA is

not maintained beyond stage 9 and the apical nurse cell localization is not observed (St Johnston et al., 1989). During stages 10-12, the nurse cells dump their cytoplasmic content to the oocyte, and the cytoplasmic streaming in the oocyte redistributes the *bcd* mRNA from across the entire anterior of the oocyte to a cap in the anterior cortex. Anterior localization persists into early embryogenesis, until the mRNA disappears shortly after formation of the cellular blastoderm (St Johnston et al., 1989). Mutation in s*wallow* (*swa*) affects *bcd* RNA localization in a late stage. In *swa* mutants, the distribution of *bcd* mRNA in nurse cells and the oocyte is normal through early stage 10. However, beginning in late stage 10, anterior concentration of *bcd* mRNA is not maintained and large quantities of *bcd* RNA that are transferred from the nurse cells at this time are distributed throughout the oocyte (Stephenson et al., 1988). Finally, *bcd* RNA is released from the anterior cortex at egg activation and is anchored in the anterior cytoplasm, and this anterior retention requires *staufen* (*stau*) activity. In eggs laid by *staufen* mutant female, *bcd* mRNA is not retained at the anterior pole and spreads posteriorly to form a shallow anterior-posterior gradient indicating that Stau is required to anchor *bcd* mRNA in the late stage of oogenesis.

I.2.4.3 The cis-acting elements

Recent work has been directed at understanding the molecular mechanisms underlying *bcd* RNA localization, focusing on the mapping of the relevant *cis*-acting signals and on the identification of the *bcd* RNA-binding proteins.

A A 625-base region in bcd 3'UTR acts as localization signal

Macdonald and Struhl (1988) demonstrated that the 5' untranslated region (5'UTR) and the entire bicoid coding sequence could be replaced without disrupting localization of the mRNA. In contrast, a 625-base region of the bicoid 3'UTR is necessary for correct localization and sufficient to direct the localization of the heterologous transcripts. This 625-nucleotide region is predicted to form a complex secondary structure including several long stem-loops (see Fig. 4). Similar stable secondary structures are also found in the *bcd* 3'UTRs of several other *Drosophila* species, which are able to direct the localization of their transcripts into the same pattern as the *bcd* 3'UTR of *D. melanoganster* (Macdonald, 1990; Seeger and Kaufman, 1990). Therefore, it is likely that the mechanism by which *bcd* mRNA localizes is by specifically recognizing the conserved secondary structure, rather than the primary sequence, of the 3'UTR.

B *Discrete and redundant localization elements*

Deletion analysis of the 3'UTR of *bcd* mRNA identified several discrete elements involved in specific steps of the localization pathway. Deletion of a 53-nucleotide region, denoted BLE1, which is located from nt 453-505 of the 817 nt *bcd* 3'UTR, prevents all stages of *bicoid* mRNA localization. In contrast, two copies of BLE1 are sufficient to direct the early steps of the localization process mediated by *bcd* 3'UTR, but are unable to maintain the anterior localization (Macdonald et al., 1993).

Further analysis of the *bcd* 3'UTR revealed two redundant RNA recognition events, designated as event A and event B, which serve to initiate largely overlapping programs of *bcd* mRNA localization (Macdonald and Kerr, 1997, 1998). Event A occurs

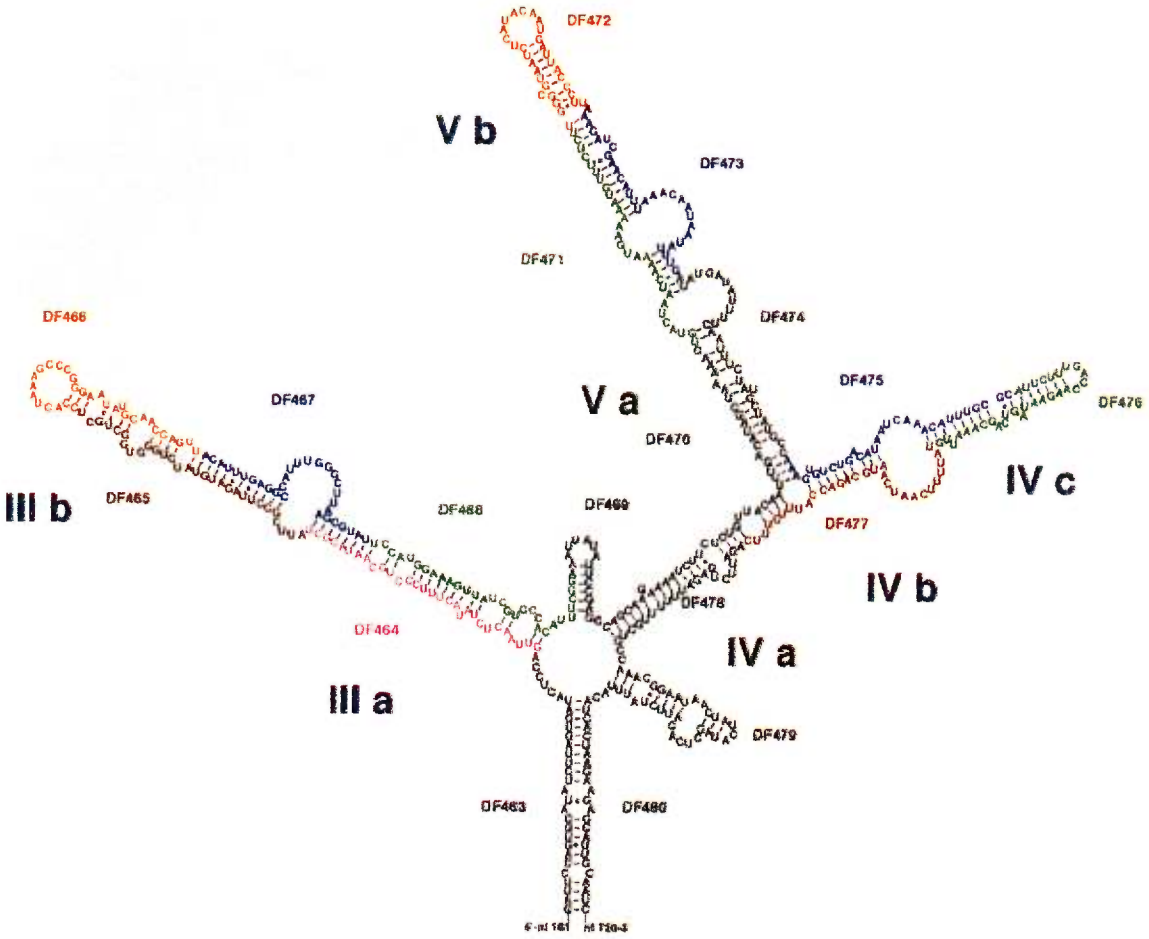

Fig. 4. A model for the secondary structure of the *bcd* 3'-UTR , showing the sequences required for the interaction with Staufen protein. The name of each stem-loop is indicated by Roman numerals. Stems IIIa, IIIb, Vb, IVc are predicted in most suboptimal foldings within 10% of the optimal folding energy. Each linker-scanning mutation that prevents the formation of Staufen-*bcd* 3`UTR complexes is shown in color. Three regions of the *bcd* 3'-UTR are important for Staufen-*bcd* interaction as demonstrated by linker-scanning mutations DF464-DF468, DF471-DF473 and DF475-DF477. The region drawn from *bcd* 3'-UTR starts exactly at the first nucleotide of DF463 (nucleotide 181) and ends at the last nucleotide of DF480 (nucleotide 720).

first and is solely responsible for the earliest transport of *bcd* to the oocyte during stages 4 to 6 of oogenesis. Subsequently, event B-dependent localization is initiated, and either RNA recognition event is sufficient for continued localization. Elimination of event A, by either a point mutation (G4496U) or a small deletion (nucleotides 4490-4507 in stem-loop V region), prevents early (stages 4-6) localization, but all later steps proceed normally. Elimination of event B is achieved through use of a subdomain of the localization signal consisting of stem-loops IV and V (IV-V) and has no detectable effect on localization during oogenesis, although a final step in embryogenesis is defective.

Transgenic approach in flies has been successful in identifying *cis*-acting elements involved in the RNA localization pathway. However, as mutations already disrupt the early steps in the localization pathway, transgenes are not suitable for the analysis of later events such as the interaction with Stau. To circumvent this problem, Ferrandon et al (1994) have developed an *in vivo* assay based on the injection of the *in vitro* synthesized transcripts into the embryo and showed that *bcd* 3'UTR is able to recruit endogenous Stau to form RNA-protein particles that are transported in a microtubule-dependent manner. Conjugation with linker-scanning mutational analyses, they mapped the sequences that specifically interact with Stau to three regions of the *bcd* 3'UTR (see Fig.4), namely nucleotides 211-360, nucleotides 42-510, and nucleotides 541-630. Each of these regions is predicted to form a long stem-loop structure (stem-loop III, V and IV, respectively). By introducing mutations into these interaction regions, the same group futher demonstrated that Stau binding to *bcd* 3'UTR requires the double-stranded conformation of the stems within the RNA localization signal (Ferrandon et al., 1997).

I.2.4.4 Trans-acting factors involved in bcd mRNA localization

As I mentioned earlier, the localization of *bcd* mRNA has so far been found to require three genes, *exuperantia* (*exu*), *swallow* (*swa*), and *staufen* (*stau*), each of which acts at a different point in the pathway. Proteins encoded by these three genes are good candidates for *trans*-acting factors involved in *bcd* mRNA localization. Although a direct interaction between Exu and *bcd* mRNA or Swa and *bcd* mRNA has not been reported yet, Staufen is the only demonstrated *trans*-acting RNA-binding protein involved in *bcd* mRNA localization. Later, I will discuss the nature of this protein and its roles in different RNA localization pathways in more details.

Macdonald et al (1995) have used 2 copies of BLE1 (2xBLE1) element (BLE1 is a short stretch of nucleotides in bicoid 3'-UTR which is important for bicoid mRNA localization) in an UV-crosslinking assay to search for directly interacting proteins. A single protein of 115 kDa called Exl was found to bind 2xBLE1 but not 1xBLE1, consistent with a role in localization. By further definition of the Exl-binding sites and mutations in BLE1, they demonstrated a correlation between *in vitro* Exl binding and one phase of *bcd* localization *in vivo* directed by BLE1. Furthermore, they found that the same phase of localization is disrupted in *exuperantia* mutants, suggestive of an interaction between the Exl and Exuperantia proteins.

Recently, Schnorrer et al (2000) demonstrated that the molecular motor dynein is involved in targeting Swallow and *bicoid* RNA to the anterior pole of *Drosophila* oocytes. In the latter section, I will discuss this in more detail. It now seems that Swallow protein functions as an adaptor, bridging bicoid mRNA to dynein, a molecular motor that would transport the complex to the anterior pole along microtubules.

I.2.5 RNA localization and posterior body patterning

Many RNAs are localized to the posterior pole of the developing oocyte during different stages of oogenesis. These RNAs include *oskar, nanos*, o*rb*, *Pgc*, *pumilio*, *tudor*, *gem cell-less*, and the noncoding mtlrRNA. Some maternal RNAs such as *Cyclin B* and *Hsp83* do not become posteriorly localized until later in oogenesis and early embryogenesis. Some RNAs such as *oskar, nanos* and *Pgc* retain posterior localization in early cleavage-stage embryos. Next, I will discuss two of the most studied posteriorly localized RNAs, *oskar* and *nanos*, which code for two important posterior morphological determinants.

I.2.5.1 nanos and oskar act as posterior and germ cell determinants

Normal abdominal segmentation is governed in part by successive actions of oskar (osk) and nanos (nos) proteins. While the major function of osk is nucleating the assembly of the posterior polar plasm (the precursor of germ cells)(Ephrussi et al., 1991; Ephrussi and Lehmann, 1991, 1992; Smith et al., 1992), posterior localization of *nos* mRNA requires prior posterior localization of the germ plasm components including the osk, vas and tud proteins (for review, see Lasko, 1999).

nanos acts as a key player in abdominal cell fate specification (Wang and Lehmann, 1991; Gavis and Lehmann. 1992). It possesses two zinc-finger DNA binding domains, binds to a uniformly distributed maternal mRNA *hunchback* (*hb*) through the NREs (Nanos response elements) located in *hb* 3'-UTR, and prevents its translation (Wharton and Struhl, 1991; Tautz, 1988; Irish et al., 1989, Struhl et al., 1992). Thus, the translation of the nos protein in the posterior half of the embryo blocks *hb* protein

synthesis in this region and leads to a *hb* protein concentration gradient complementary to that of nos. This prevents posterior cells from taking anterior identities in response to hunchback and enables 'default' abdominal fates to be adopted.

Oskar protein plays a key role in organizing the posterior pole cytoplasm which contains the determinants of the germ line and of the abdomen, thus osk acts indirectly as a posterior body patterning determinant (Ephrussi et al., 1991; Kim-Ha et al., 1991). Mislocalization of *oskar* RNA to the anterior pole by replacing the osk localization signal with that of *bicoid* leads to pole plasm assembly at the anterior pole (Ephrussi and Lehmann, 1992). At this ectopic site, germ cells form, nos RNAs become localized and translated, and a second abdomen develops in a mirror image to the posterior abdomen. Consequently, this ectopic expression is lethal.

I.2.5.2 Localization dynamics of oskar and nanos RNAs

Similar to *bicoid* mRNA in the anterior pole, the localization of *oskar* mRNA to the posterior of the oocyte also involves a number of intermediate steps with different genetic requirements. When the RNA is synthesized in the nurse cells, it is rapidly exported into the oocyte in a process that requires the activity of the *Bicaudal D* gene (Ephrussi et al., 1991; Kim-Ha et al., 1991; Ran et al., 1994). After stage 7, the RNA shows a transient accumulation at the anterior of the oocyte which is abolished in *cappuccino* and *spire* mutants. During stage 9, the RNA at the anterior margin of the oocyte is gradually transported to the posterior region to form a polar cap at stage 10; this process requires *staufen* and *mago nashi* activity (Newmark and Boswell, 1994). Once the RNA is localized to the posterior pole, on-site translation occurs and a posterior cap

of osk protein is formed. This translated protein in turn acts with other proteins such as Staufen to anchor *osk* mRNA at the posterior pole (Ephrussi et al., 1991; Kim-Ha et al., 1991, Markussen et al., 1995).

Like *osk*, *nos* RNA displays a progression of distribution patterns during oogenesis. It accumulates in the previtellogenic oocyte, although it is not present at detectable concentrations until stages 2-3 (Wang et al., 1994). During stages 7 and 8, it also transiently accumulates at the anterior pole of the oocyte. In contrast to *oskar*, *nanos* RNA appears uniformly within the oocyte by stage 10 while a high level of expression is detected in the nurse cells. This newly transcribed RNA is deposited to the oocyte with the contraction of the nurse cells following stage 10. Posteriorly localized *nos* RNA can be detected only at the very last stage of the oogenesis (Wang et al., 1994). At fertilization, much of the *nos* mRNA is distributed throughout the bulk cytoplasm of the egg and the remainder is localized at the posterior pole at somewhat higher concentrations. Posterior localization of *nos* is blocked by all mutations that abrogate *osk* mRNA localization and requires the osk, vas and tud proteins (Lasko, 1999).

I.2.5.3 The cis-acting localization elements

As with *bicoid*, the *cis*-acting signals responsible for localizing the posterior determinants map to the 3'-UTR of their respective RNA sequences.

A oskar 3'-UTR: dispersed and modular elements

For *oskar* RNA, different elements dispersed in the 3'-UTR are responsible for different stages of *oskar* RNA localization (Kim-Ha et al., 1993). Within 1043

nucleotides of the 3'-UTR, the region between nucleotides 532-791 is required for the accumulation of *oskar* RNA into the early oocyte. Two smaller regions, nucleotides 242-363 and 791-846, define *cis*-regulatory elements required for the release of *osk* RNA from the anterior pole. Finally, nucleotides 1-242 are essential for posterior localization of *osk* RNA. The presence of these distinct elements indicates that the *oskar* localization signal is also modular and that different 'modules' have distinct functions in the localization process (Lasko, 1999).

B *nanos 3'UTR: partially redundant and conserved elements*

The localization of *nanos* RNA is mediated by a localization elements composed of partially redundant localization sequences spread throughout a contiguous 547-nucleotide portion of the 3'-UTR (Gavis et al., 1996). Two overlapping subregions map within this larger region, each of which is capable of conferring localization, indicating partial functional redundancy. However, these subregions are 400 and 470 nt in length repectively, and can not be subdivided without disrupting localization. A deletion of nt 97-403 of the *nos* 3'UTR in a reporter gene construct abrogates early oocyte accumulation, but remains significant posterior localization ability, suggesting that localization of *nos* to the early oocyte is not necessary for eventual posterior accumulation (Gavis et al., 1996). Another deletion analysis suggests that full phenotypic rescue of the severe nos^{BN} mutant allele can be conferred by a nos transgene bearing only nt 1-184 of the 3-UTR (Dahanukar and Wharton, 1996). The *nos* 3'-UTRs from *D. melanogaster* and *D. Virilis* show extensive sequence conservation and are predicted to form similar stem-loop structures. Furthermore, the two 3'-UTRs can be replaced with

each other without changing their localization patterns, indicating an evolutionarily functional conservation (Gavis et al., 1996).

I.2.5.4 The trans-acting protein factors

Genetic analysis has identified many genes required for the localization of *oskar* and *nanos* RNA. These posterior group genes can be ordered in a pathway where the localization of one gene product is dependent on the correct localization of those genes above it in the hierarchy (see Fig. 5). Of the posterior group gene products, *oskar* is the first mRNA to be localized in the posterior pole and this localization constitutes a key step in the formation of the pole plasm (Micklem, 1995). The genes that affect *oskar* RNA localization also affect *nos* RNA localization.

So far, at least 10 genes are reported to affect *osk* RNA localization. These genes include *Bicaudal-D* (*BicD*), *cappuccino* (*capu*), *spire* (*spir*), *staufen* (*stau*), *mago nashi* (*mago*), *chickadee* (*chic*), *Tropomyosin-1* (*Tm1*), *orb*, *Notch* (*N*), *Delta* (*Dl*) and a maternal form of protein kinase A (*PKA*). The products of these genes can be considered as cofactors that contribute to *osk* mRNA localization.

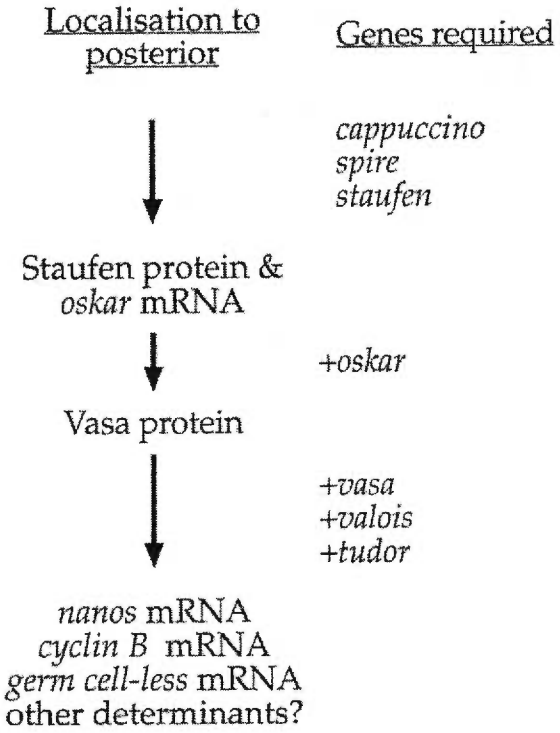

Fig. 5. Hierarchy of *Drosophila* posterior group genes. The posterior group genes can be ordered in a pathway where the localization of a gene product is dependent on the correct localization of those above it in the hierarchy. Adapted from Micklem, 1996.

I.3 RNA localization in oogenesis of *Xenopus laevis*

In addition to *Drosophila melanganster*, *Xenopus* oocytes offer another powerful model system to study the mRNA localization process. Numerous RNAs were found localized at either the animal or the vegetal hemisphere of the oocyte (see table 1 of the localized RNAs, for reviews, see Bashirullah et al., 1998; King et al., 1999; Mowry and Cote, 1999). The frog oocyte is a polarized cell approximately 100 times larger than a somatic cell. Its large size makes the events of RNA localization obvious and easy to detect compared with somatic cells. Most importantly, the significance of RNA localization can be addressed functionally by examining the consequences of mislocalization on development.

I.3.1 RNA targeting to the animal pole

The animal hemisphere (*An*) is the region in which the oocyte nucleus resides, the embryonic blastocoele forms and cells give rise to ectodermal, neural ectodermal, or mesodermal derivatives (King et al., 1999). The animal hemisphere enriched RNAs are grouped into three categories based on the proteins they encode. These contain nuclear proteins including transcription factors and nucleolar proteins such as An1, An3, Oct60, and xl-21, signal transduction components such as *PKC-α* and *G protein*, and others (see table 1). These RNAs are not tightly localized within the animal hemisphere but are at least four-fold enriched in this hemisphere relative to their vegetal concentrations. So far, little is known about the temporal regulation of RNA localization to the animal pole or other features of this pathway.

I.3.2 RNA targeting to the vegetal pole

In contrast to animal hemisphere RNAs, the vegetal localized RNAs exhibit highly restricted distribution patterns. These RNAs are highly concentrated (50-fold) within the cortical cytoskeleton of the vegetal pole. Analysis of vegetal localized RNAs shows that two distinct localization pathways operate to sort vegetal RNAs during oogenesis.

I.3.2.1 The early or microtubule-independent pathway

The early pathway involves RNA localization through a specialized region of the mitochondrial cloud called the messenger transport organizer (METRO), which was first described for the localization of *Xlsirt* RNA to the vegetal pole (Kloc et al., 1993). This specialized region, also known as the Balbiani body, is the site of mitochondrial proliferation and is also associated with the electron-dense RNA/protein granules of the germ plasm. So far, eight RNAs including *Xcat2, Xcat3* (*DEADSouth*), *Xdazl*, *Xlsirts*, *Xpat*, *Xwnt-11*, *C10* (*XFACS*), *B7* (*Fingers*) have been isolated that localize to the vegetal cortex via the METRO pathway. Most of them eventually segregate with germ plasm in the primordial germ cells (PGCs) and encode proteins required for germ cell specification or cell differentiation (Mosquera et al., 1993; King 1995; Houston et al., 1998; Hudson et al., 1998).

The early pathway occurs in three distinct steps (Kloc and Etkin, 1995): the movement of the transcripts from the germinal vesicles (GV) to the mitochondrial cloud, sorting of the individual transcripts within the cloud to their unique positions within the METRO, and their translocation and anchoring to the vegetal cortex (see Fig. 6 for the

description of the two pathways at different development stages, the early pathway is on the right). The association and movement of the RNAs with the METRO are neither microtubule- nor actin-dependent, but anchoring at the cortex is disrupted by the actin destabilizing drug cytochalasin B (Kloc and Etkin, 1995; Kloc et al., 1996).

I.3.2.2 The late or microtubule-dependent pathway

The second localization pathway begins at a later stage of oogenesis. Two RNAs, *Vg1* and *VegT*, have been characterized that use this late pathway. *Vg1* encodes a protein homologous to members of the TGF-β family and has been implicated in establishing the left-right asymmetry (Hyatt and Yost, 1998), dorsal mesoderm induction and endoderm specification (Joseph and Melton, 1998). Ectopic expression of processed Vg1 peptide leads to the induction of mesoderm in cells that normally would have become ectoderm (Thomsen and Melton, 1993). *VegT* encodes a novel T-box transcription factor involved in mesoderm patterning, and correct localization of *VegT* RNA is required for normal development as misexpressed VegT protein at the animal pole results in headless embryos (Zhang et al., 1996. 1998).

Unlike the METRO-associated RNAs that are translocated to the apex of the vegetal pole region during stages 1 and 2 of oogenesis, RNAs that are localized using the second pathway, such as Vg1 and vegT, are distributed evenly throughout the cytoplasm during stage 2 (see Fig.6 on the left for the late pathway). During stage 3, they appear to translocate through a region overlapping the positions of the early localized RNAs (Kloc and Etkin, 1995). During mid-oogenesis (stages III-IV), *Vg1* RNA is translocated to the vegetal hemisphere and cannot be detected in the animal hemisphere cytoplasm (Melton,

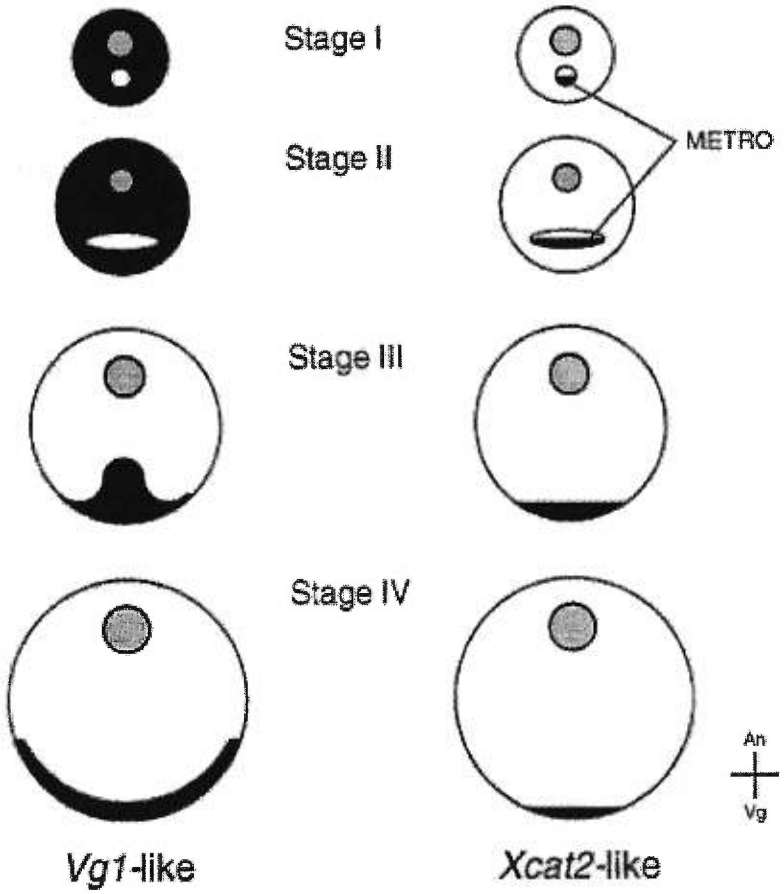

Fig. 6. Two RNA localization pathways during *Xenopus* oogenesis. RNA distribution patterns are shown in black. The *Vg1*-like pattern (the late pathway) is shown on the left and *Xcat-2*-like pattern (the early pathway) on the right. Oocytes from stages I-IV are schematized. An, animal pole; Vg, vegetal pole. The germinal vesicle (oocyte nucleus) is shown in grey and the METRO as a white circle (stage1) or ellipsoid (stage2). Adapted from Bashirullah, et al., 1988.

1987). By stages V-VI, *Vg1* mRNA occupies a tight cortical shell from the apex of the vegetal pole to the future marginal zone (Melton, 1987), where it will be anchored until maturation (Fig. 6, on the left). All steps of the RNA translocation process during the late pathway are dependent of the intact microtubule network, except the final anchoring step which requires actin filaments.

A *Vg1 localization elements*

The *cis*-acting RNA sequences required for localization have been identified within the 1300-nt 3'UTR by using *Vg1* deletion mutants injected into cultured oocytes. A 340-nt localization element (VgLE) was identified that is necessary and sufficient for vegetal localization of *Vg1* RNA (Mowry and Melton, 1992). Deletion analysis indicates that there is considerable redundancy within this region but that critical elements have been defined to lie at each end of this region (Gautreau et al., 1997). Two copies of a 85-nt subelement located at the 5'end, or one copy of it together with a 135-nt subelement located near the 3'end, are sufficient for localization (Gautreau et al., 1997).

B *Vg1 localization element-binding proteins*

In vitro and *in vivo* UV cross-linking and competition analysis experiments have revealed that a set of oocyte proteins bind in a sequence-specific manner to the *Vg1* localization element (Schwartz et al., 1992; Mowry, 1996; Deshler et al., 1997). Some or all of these proteins could play important roles as *Vg1* RNA localization was suggested to be mediated through formation of large RNP complex containing the *Vg1* localization elements and multiple proteins (Mowry, 1996). The different proteins within the RNP

complex may perform distinct roles in the localization process. Of these proteins, a 69 kDa *Vg1* RNA binding protein (Vg1RBP) that binds the Vg LE with high affinity *in vitro* has been reported to be a microtubule-associated protein and may mediate the binding of *Vg1* mRNA to microtubules (Elisha et al., 1995). Using UV cross-linking and competition experiments via the repeated elements found within the VgLE, Deshler et al (1997) have identified a single protein of 75 kDa called Vera that binds to *Vg1* and colocalizes with components of the endoplasmic reticulum (ER). Both Vera and Vg1-RBP have been directly correlated with *Vg1* mRNA localization.

I.4 RNA localization in nerve cells

In the mammalian central and peripheral nervous systems, neurons are highly polarized cells with long axons and complex dendritic trees. The dendrites of a neuron receive signals from other neurons through up to thousands of synapses, each of which may have its own unique molecular composition. This highly polarized nature of neuronal cells requires elaborate and accurate sorting mechanisms to establish and maintain their macromolecular components. There is now increasing evidence that an important aspect of gene expression in neurons involves the transport of certain mRNAs to particular subcellular domains such as axons and dendrites, or even more specialized regions such as subsynaptic locations. The differential transport and localization of mRNAs offer an opportunity for local synthesis of certain proteins in response to local signaling events.

The hypothesis that particular gene transcript is targeted to distinct subcellular domains in neurons was first suggested by the discovery that the protein synthesis machinery (e.g. polyribosomes and membranous cisterns) was selectively localized beneath postsynaptic sites on the dendrites of CNS neurons (Steward and Lewy 1982, Steward and Fass, 1983, Steward, 1983). Synapse-associated polyribosomes were found to be particularly prominent during the periods of synaptic growth, suggesting that dendritic RNA transport and local protein synthesis might play a role in synapse growth and plasticity. This hypothesis has been strengthened in recent years by the discovery of many types of mRNAs and nonmessenger RNAs in dendrites. Next, I will mainly describe the RNAs localized in the dendrites of nerve cells since a clear physiological relevance has been ascribed to this class of transcripts. Accordingly, another class of RNAs, often present in substantial amounts, is detected in axons of various nerve cell types. However, their physiological roles are less clear therefore, I will omit the discussion of these axonal RNAs.

I.4.1 RNAs targeting to the dendrites

The first identified mRNAs that were localized in mature dendrites are mRNAs encoding the high molecular weight microtubule-associated protein (MAP2) and the α-subunit of calcium/calmodulin-dependent protein kinase II (CaMKIIα) (Garner et al., 1988; Burgin et al., 1990). Later studies have revealed the presence of many other dendritic mRNAs (see Table 1). These mRNAs encode different proteins including, for example, the type 1 inositol 1,4,5-trisphosphate receptor ($InsP_3R1$; Furuichi et al., 1993), protein kinase C substrates such as F1/GAP43 and RC3 (Landry et al., 1994; Watson et al., 1992), a number of amino acid receptors such as glutamate and glycine receptors

(Miyashiro et al., 1994, Racca et al., 1997), the cytoskeleton-associated protein Arc (Link et al., 1995; Lyford et al., 1995), and growth factors and neurotransmitters such as BDNF (Dugich-Djordjevic et al., 1992), oxytocin and vasopressin (Mohr et al., 1995). Dendritic nonmessenger RNAs such as BC1 RNA (Tiedge et al., 1991), ribosomal RNAs (Kleiman et al., 1993, 1994), and tRNAs (Tiedge and Brosius, 1996) have also been reported.

I.4.1.1 Dendritic RNA targeting elements

Analogous to the elements required for subcellular RNA localization in other systems such as *Drosophila* and *Xenopus* oocytes, dendritic RNA transport is also mediated by *cis*-acting signals residing in the RNA itself and *trans*-acting proteins recognizing these cognate signals. In most cases examined, the structural elements that direct dendritic mRNA transport were also found in the 3'-untranslated region (3'-UTR). Mayford et al (1966) have demonstrated that the 3'-UTR of CaMKIIα mRNA can confer dendritic targeting to a transgenic bacterial β-galactosidase gene. Similarly, a chimeric mRNA containing the entire 3'-UTR of MAP2 (or a 640 nt region of the 3'-UTR) fused to a nondendritic reporter mRNA was detected in dendrites of hippocampal and sympathetic neurons (Blichenberg et al., 1999). Dendritic targeting signals of vasopressin (VP) mRNA are present as redundant elements since part of the coding sequence of VP mRNA and its 3'UTR are involved in its dendritic targeting. The full extent of dendritic targeting capacity to distal location was mapped to a fragment spanning nucleotide sequence from position 201 to 595 of the VP transcript which covers all the redundant elements, indicating a synergistic action of the various localizing elements (Prakash et al., 1997). However, for the nontranslated BC1 RNA, the *cis*-acting signal has been mapped

to the 5' region in no more than 62 nucleotides (Muslimov et al., 1997). Comparison of these different *cis*-acting elements did not reveal any apparent consensus sequences, suggesting that the targeting competence may be determined by secondary or higher-order structural motifs or by more than one motif in a modular fashion.

So far, little is known about the proteins involved in transport and anchoring of the mRNAs within dendrites. It is likely that RNA-binding proteins and motor proteins mediate the interactions between the 3'UTRs and the cytoskeleton, and mRNA ribonucleoprotein (mRNP) complexes may serve as the substrate for localization (for review, see Jansen 1999).

I.4.1.2 Mechanisms of dendritic RNA transport

Recent experimental approaches have tried to tackle the dynamics of the RNA transport to dendrites. Using the cell-permeable fluorescent dye SYTO 14, which preferentially interacts with RNA, Knowles et al. (1996, 1997) identified particles containing ribosomal RNA, mRNA and other protein components of the translation machinery which may potentially move along microtubules. The same granular appearance has been reported for several dendritic RNAs by high resolution *in situ* hybridization analysis (Racca et al., 1997; Wanner et al., 1997). The dendritic delivery rate was measured to be ~6μm/min (Knowles et al., 1996), which is within the range of fast transport. Similar transport rates have been reported for Arg3.1/Arc mRNA (Wallace et al., 1998) and BC1 (Muslimov et al., 1997) in neurons and are comparable to those measured for the directed translocation of myelin basic protein mRNA along microtubules in oligodendrite processes (Ainger et al., 1993). Taken together, these

studies support the hypothesis that dendritic RNAs may be delivered by active transport along the cytoskeleton in the form of ribonucleoprotein (RNP) particles.

I.4.1.3 Local translation of dendritic mRNAs

The presence of mRNAs and components of the translational machinery such as polyribosomes, tRNAs, and translation initiation factors in dendrites (Steward and Levy, 1982; Tiedge and Brosius, 1996) implies that proteins coded by these transcripts may be synthesized on-site. In addition, reticular structures that may function in glycoprotein and membrane protein synthesis were also found in dendrites (Racca et al., 1997; Martone et al., 1996; Torre and Steward 1996). However, direct evidence that specific mRNAs are translated within dendrites has not been reported. One study supporting the view of local translation in dendrites has been reported using transgenic mice technologies (Mayford et al., 1996). Transgene mice were generated bearing a reporter gene, the bacterial β-galactosidase gene, which was engineered to harbor an additional nuclear localization signal (NLS). Cell-specific expression was driven by the CaMKIIα gene promoter and the dendritic targeting of transgene mRNA was mediated by the CaMKIIα 3'-UTR. Histochemical β-galactosidase staining revealed, as expected, strong staining in the cell nuclei of the hippocampal formation. In addition, staining in the distal layer of the dendritic field was also found while proximal dendrites showed little staining. Obviously, the sorting machinery mediated by the NLS is capable to rapidly sequester protein synthesized in the cell somata and the proximal dendrites to the cell nucleus. The authors suggested that the β-galactosidase in the distal tips of dendrites may have arisen by local translation of the chimeric mRNA.

Recent work has established a direct link between local mRNA translation and synaptic plasticity, a process involving modification of the molecular composition and structure of individual or specific populations of synapses in order to adjust synaptic strength. Kang and Schuman (1966) have demonstrated that application of BDNF or neurotropin-3 (NT-3) to rat hippocampal brain slices enhanced synaptic transmission at the Schaffer collateral/CA1 pyramidal neuron synapse, which was significantly attenuated after preincubation with eukaryotic but not prokaryotic protein synthesis inhibitors. The requirement of immediate local *de novo* protein synthesis in the dendritic compartment rather than in the cell body layer is strongly suggested since the effect was still observed after microdissection of the pre- and/or postsynaptic cell bodies. Later work further established the importance of local mRNA translation versus synaptic plasticity. In an elegant set of experiments, Martin et al.(1997) have demonstrated that local application of serotonin (5-HT) to one synapse resulted in enhanced synaptic transmission only at that synapse. Protein synthesis inhibitors, when selectively applied to the synapse, block long-lasting, long-term facilitation (L-LTF) in cultured *Aplysia* neurons, indicating that local protein synthesis is important in eliciting a long-term facilitation and plays a role in memory storage. In vertebrates, high-frequency stimulation of hippocampal slices leads to an increase of CaMKIIα protein in dendrites, and this increase is blocked by translation inhibitors, indicating that local protein synthesis is induced by synaptic activation (Ouyang et al., 1997, 1999). In synaptodendritic preparations, the synthesis of a rat homolog of fragile X mental retardation protein (FMRP) is initiated within minutes by activation of the metabotropic glutamate receptors (mGluRs; Weiler et al., 1997; Comery et al., 1997). These observations support the

notion that transsynaptic activity could result in a translational switch and initiating translation of locally docked but translationally silent mRNAs, which further modifies the synaptic strength and plasticity.

I.4.1.4 Dendritic mRNA transport and synaptic plasticity

In another way, synaptic plasticity may be directly regulated by the local availability of certain mRNAs, through modulated transport or selective docking of the mRNAs to the dendritic target sites. Indeed, synaptic activity and/or application of neurotrophins or cAMP analogs have been shown to modulate the transport of different mRNAs or RNA-containing granules in dendrites. For example, dendritic delivery of BDNF and TRKB mRNAs is regulated, in an RNA synthesis-independent manner, by neuronal activity in hippocampal neurons (Tongiorgi et al., 1997). BC1 RNA, a noncoding pol III transcript, is found only in cultured hippocampal neurons that have made synaptic connections with other neurons, and its presence can be reversibly reduced by treatment with tetrodotoxin, which blocks the neuronal activity. Thus, the expression of BC1 RNA can be subjected to control through physiological activity in neurons (Muslimov et al., 1998). The dendritic localization of Arc mRNA is a direct function of synaptic input. In dentate granule cells, transsynaptic stimulation results in the selective localization of Arc mRNA only to the dendritic segments in which synapses were activated, and Arc protein was also found to be enriched in the same area. Moreover, the targeting of Arc mRNA was not disrupted by locally inhibiting protein synthesis, indicating the targeting signal resides in the mRNA itself (Steward et al., 1998). These data strongly suggest that local delivery and recruitment of RNA, rather than protein, is

responsible for long-lasting forms of activity-dependent synaptic modulation. Interestingly, the sorting of RNA granules to dendritic domains of living neurons has been shown to be stimulated by the neurotrophic factor NT-3, suggesting that neuronal plasticity may involve the redistribution of these RNA-granules in response to extracellular signals (Knowels and Kosik, 1997).

Taken together, specific mRNA transport to dendrites may facilitate localized translational regulation at the synapse and inducing the long-lasting changes in structure and function of that synapse. Therefore, it may represent an important aspect of synaptic plasticity and potentially be relevant to memory storage (for review, see Tiedge et al., 1999; Kiebler and DesGroseillers, 2000).

I.4.2 In neuroblasts of *Drosophila*

Besides many types of localized mRNAs observed in mammalian neurons, especially in the dendrites, asymmetric mRNA localization has recently been found in dividing neuroblasts of *Drosophila* and plays a role in *Drosophila* neurogenesis. The neural precursor cells in the *Drosophila* central nervous systems (CNS) are neuroblasts (NBs) that delaminate from the neuroectoderm. Each NB divides asymmetrically in a stem cell fashion to produce a large apical daughter cell that remains a NB and a smaller basal daughter cell called ganglion mother cell (GMC). While NBs undergo this type of asymmetric division repeatedly, GMCs divide only once to produce a pair of neurons. Thus, asymmetric cell division governs the generation of diverse cell types and directs the CNS development in *Drosophila* (for review, see Jan et al., 2000; Lu et al., 2000).

Recent studies have also revealed that *Prospero* mRNA localization play a role in asymmetric division of *Drosophila* neuroblasts.

I.4.2.1 Asymmetric partition of the cell fate determinants

One way to achieve asymmetric cell divisions is to segregate intrinsic cell fate determinants that are produced in the mother cell preferentially to one of the two daughter cells. In the *Drosophila* developing nervous system, Numb (Uemura et al., 1989; Rhyu et al., 1994) and Prospero (Pros; Hirata et al., 1995; Knoblich et al., 1995; Spana and Doe, 1995) proteins are candidates for such determinants.

Numb is a membrane-associated protein containing a protein-protein interaction domain known as phosphotyrosine binding (PTB) domain. It is localized asymmetrically in a crescent to one side of the sensory organ precursor cell (SOP) in the peripheral nervous system (PNS) and then segregated into one of two daughter cells to determine the different sibling cell fates (Rhyu et al., 1994). Similar role for Numb in cell fate decision of the MP2 neuroblast (a particular type of neuroblasts that divides only once) in CNS has also been demonstrated (Spana et al., 1995). Numb functions in these binary cell fate decisions in part by antagonizing Notch activity in the cells that inherit Numb (Frise et al., 1996; Guo et al., 1996). Although all NBs segregate Numb asymmetrically into their sibling GMC, its role in GMC is not clear.

Prospero is a homoeodomain-containing protein that is required for cell-fate specification in *Drosophila* CNS by functioning as transcriptional regulator (Vaessin et al., 1991; Doe et al., 1991). Similar to Numb, Pros protein segregates asymmetrically in dividing *Drosophila* neural precursor cells. In neuroblasts, the Pros protein can first be

detected shortly before mitosis, when it starts to accumulate at the apical side of the cell (Spana and Doe, 1995). During mitosis, Pros colocalizes with Numb into a crescent at the basal cell cortex, and, together with Numb, it segregates into the GMC. After mitosis, Pros translocates into the GMC nucleus to direct the specific GMC gene expression, whereas Numb is retained at the cell membrane (Knoblich et al., 1995; Spana and Doe, 1995; Hirata et al., 1995). Pros and Numb localization are independent each other, but their strikingly similar localization suggests that both proteins may be transported by a common localization machinery.

I.4.2.2 Localization machinery of the cell fate determinants

Asymmetric localization of the cell fate determinants is mediated by a complex process that has two prerequisites. First, it is necessary to establish a polarized cell and a means to direct the asymmetric localization of the determinants. Next, the plane of cell division must be oriented in a manner that is coordinated with the mechanisms for the localization of the determinants. Studies over the last few years have revealed that multiple proteins and RNAs involved in this process constitute a genetic pathway for the control of asymmetric division of *Drosophila* embryonic neuroblasts.

A Inscuteable is an essential organizing molecule

Inscuteable (Insc) is a cytoskeleton adapter protein that is localized in the apical cortex of dividing neuroblasts opposite to the basal Numb/Pros crescent (Kraut and Campos-ortega, 1996). Recent studies have shown that it plays multiple roles in directing asymmetric division of *Drosophila* NBs. Loss-of-function *Insc* mutants are defective in the formation and localization of the Numb/Pros crescent, indicating its function in

controlling Numb/Pros localization (Kraut et al., 1996). In addition to its role in protein localization, Insc is also required for coordinating the orientation of the mitotic spindle and the axis of protein localization (Kraut et al., 1996), and for the asymmetric localization of *pros* RNA (Li et al., 1997).

B *Pon, Miranda, and Stau act as adapter molecules of Insc*

Since the Insc crescent is localized to the opposite side of the Numb/Pros crescent and is delocalized before the completion of the cell cycle, it is unlikely that Insc directly localizes the cell fate determinants. Recent studies have revealed that Insc controls the localization of Numb, Pros and *pros* mRNA by indirectly controlling the asymmetric localization of three adapter proteins: Partner of Numb (Pon; Lu et al., 1998), Miranda (Mir; Shen et al., 1997; Ikeshima-Kataoka et al., 1997), and Staufen (Stau; Li et al., 1997; Broadus et al., 1998). Pon directly binds and colocalizes with Numb in dividing neural precursor cells and muscle precursor cells. In neuroblasts and SOP cells of Pon mutant embryos, the formation of Numb crescent is delayed although it is segregated normally by the end of mitosis. Numb localization is more severely affected in muscle precursor cells, which leads to abnormal muscle formation (Lu et al., 1988). Another adapter protein Miranda, identified by its interaction with the Pros asymmetric localization domain, is responsible for asymmetric Pros localization (Shen et al., 1997; Ikeshima-Kataoka et al., 1997). The Miranda protein itself is localized asymmetrically, along with the Pros protein, to the basal cell membrane during mitosis; a phenomenon that requires the Insc protein (Shen et al., 1997; Ikeshima-Kataoka et al., 1997). Stau protein has been demonstrated to be required for the localization of *bicoid* and *oskar* RNAs during *Drosophila* oogenesis. It is also expressed during *Drosophila* nervous system

development and colocalizes with the Pros protein and *pros* RNA in mitotic NBs (Li et al., 1997; Broadus et al., 1998; Shen et al., 1998). Biochemical studies have shown that Stau binds to the 3'-UTR of *pros* RNA and the carboxyl terminus of the Insc protein, therefore acting as a mediator in executing the RNA localization function of Insc (Li et al., 1997). Interestingly, the localization of Stau also requires Miranda, indicating that Miranda may play a more general role in asymmetric protein localization (Shen et al., 1998, Schuldt et al., 1998). All these adapter molecules function downstream of Insc to promote the asymmetric localization of Numb/Pros or *pros* mRNA.

C *Bazooka provides an apical cue for Insc localization*

Given that neuroblasts delaminate from the epithelial cell layer, a fascinating hypothesis has been proposed that the NBs may inherit the epithelial apical-basal polarity to establish their intracellular asymmetry. Recent studies of the gene *bazooka* have established the missing link between the NB polarity, manifested as the apical Insc crescent, and the apical-basal polarity of the epithelium.

The *Bazooka* gene is required for the polarity of the epithelial cells (Muller and wieschaus, 1996) where the Bazooka protein is localized in the apical cortex of these cells (Kuchinke et al., 1998). When NBs delaminate from epithelia, Bazooka is inherited and is colocalized with Insc at the apical cortex, suggesting that Bazooka links Insc with epithelial apical-basal polarity (Wodarz et al., 1999; Schober et al., 1999). Bazooka can bind directly to the Insc asymmetric localization domain in vitro and recruit the protein to the apical cortex of NBs after cotransfection (Schober et al., 1999). Removal of both maternal and zygotic bazooka activities results in a uniform distribution of the Insc protein in the NB cytoplasm and causes similar phenotypes both in the distribution of cell

fate determinants and in spindle orientation, as does the *loss of insc* mutation. These findings provide strong evidence that Bazooka serves as a component of the common molecular machinery to create polarity in both NBs and epithelial cells, and also acts as an apical cue for the localization of the Insc protein.

D *Pins is required for maintaining of the apical Insc complex*

Most recently, a new component called *partner of inscuteable (pins)*, which is required for asymmetric localization of Insc has been identified in a yeast two-hybrid screen using the central domain of Insc as bait (Yu et al., 2000). The same gene was identified independently by another group based on coimmunoprecipitation of its gene product and the Insc protein (Schaefer et al., 2000). In both maternal and zygotic *pins* mutant embryos, Insc is initially localized correctly to the apical stalk of a delaminating NB but becomes ubiquitously distributed in the NB after delamination, suggesting that pins is required not for the initiation but for the maintenance of Insc localization. Not surprisingly, *pins* mutants exhibit a phenotype similar to the *Insc* mutant phenotype, i.e., the spindle orientation becomes random, and Pon, Numb, Miranda, and Pros are all mislocalized. In *Insc* mutants, Pins becomes diffusely localized around the cortex of NBs. Thus, asymmetric localization of pins and Insc are mutually dependent.

Pins is predicted to encode a protein with 7 tetratricopeptide (TRP) repeats, a protein-protein interaction motif, and three GoLoco domains that are thought to bind and regulate Gα, the α subunit of heterotrimeric G-proteins. In vitro, Pins can bind inscuteable directly through its N-terminus, which contains the TPR repeats, and the inscuteable asymmetric localization domain. Therefore, Pins is a component of the multi-protein apical complex of the dividing NBs. Interestingly, Schaefer et al. (2000) found

that Gα may also be part of the apical complex, indicating that a heterotrimeric G protein signaling cascade may be involved in the control of asymmetric cell division.

I.4.2.3 Prospero mRNA localization in asymmetric cell division

In addition to directly segregating the proteins, the cell-fate determinants can be localized asymmetrically when the corresponding RNA transcripts are transported to one side of a cell where they are translated locally. For example, during *Drosophila* oogenesis, a complex RNA localization machinery is used to restrict *bicoid* and *nanos* RNA to the anterior and posterior poles of the oocyte, respectively. Recent experiments have revealed some intriguing parallels in RNA localization during *Drosophila* oogenesis and during asymmetric division in *Drosophila* NBs. As its encoded protein, the *pros* mRNA also shows a cell-cycle-specific asymmetric localization in NBs and is selectively partitioned to the daughter GMC (Li et al., 1997; Broadus et al., 1998). During interphase, most *pros* RNA is localized to the apical side of the NBs where it is found either in the cytoplasm or associated with the cortex. During mitosis, *pros* RNA is asymmetrically localized to the opposite side of the NB in a basal crescent. At cytokinesis, *pros* RNA is specifically segregated into the GMC.

The RNA-binding protein Stau has been demonstrated to be one of the major *trans*-acting proteins involved in RNA localization during *Drosophila* oogenesis and early embryogenesis. It is also detected in the embryonic CNS (St Johnston et al., 1991; Ferandon et al., 1994). In neuroblast cells, Stau colocalizes precisely with *pros* mRNA and Pros protein spatially and temporally, and is partitioned to the GMC along with *pros* mRNA and Pros protein. Homozygous *stau* mutant flies are defective in *pros* RNA

localization but not in Pros protein localization, indicating that Stau is required for the localization of *pros* RNA but not Pros protein (Li et al., 1997; Broadus et al., 1998). Stau protein localization is normal in *pros* null mutants and Pros protein localization is normal in *stau* null mutants. Thus, both Stau and Pros proteins are independently localized to the same region probably by binding to a common anchoring protein.

Loss of *pros* RNA localization, but not of Pros protein localization, in *stau* embryos does not alter GMC fate probably due to the redundant function of Pros protein localization. However, in hypomorphic (weakly active) alleles of *pros*, which have reduced Pros protein expression and generate an 'intermediate' GMC phenotype, loss of *pros* RNA localization due to *stau* mutation strongly enhances this phenotype. Therefore, *pros* RNA and Pros protein localization may act redundantly to specify GMC fate (Broadus et al., 1998). Since GMCs do not transcribe the *pros* gene (Broadus et al., 1998), inheritance of both *pros* mRNA and Pros protein from the neuroblast is essential for GMC specification.

I.4.2.4 A genetic pathway governing asymmetric neuroblast division

Studies over the last few years have revealed that a cascade of genes is involved in the control of asymmetric segregation of the cell-fate determinants to the GMCs and therefore governs the asymmetric division of *Drosophila* embryonic neuroblasts. This genetic pathway is still quite incomplete and is surely an oversimplification (for review, see Jan and Jan, 2000). Fig. 7 summarizes recent progress on the mechanisms of asymmetric cell division underlying the development of the *Drosophila* CNS.

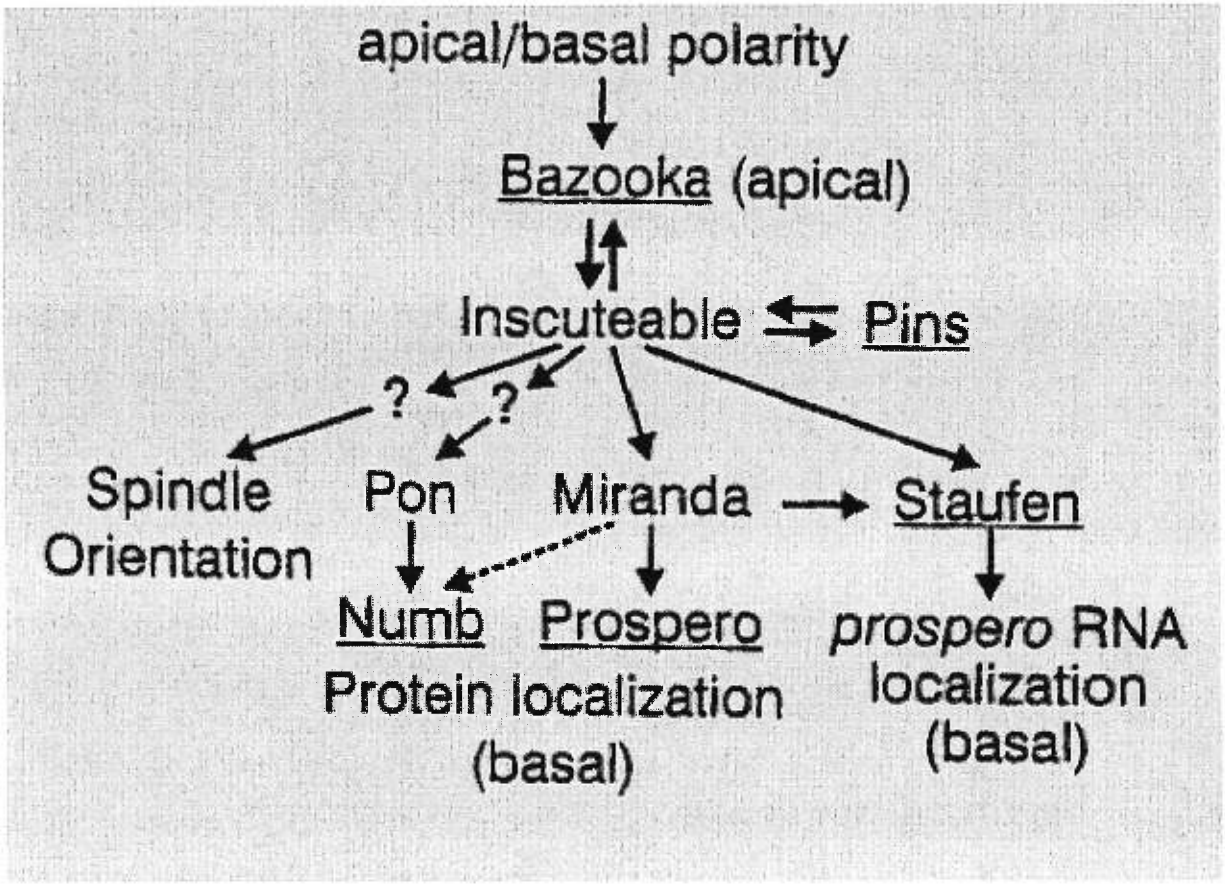

Fig. 7. A genetic pathway that controls the asymmetric cell division of the neuroblasts (NB) in *Drosophila.* Adapted from Jan et al, 2000.

I.5 RNA localization in budding yeast

Asymmetric cell division occurs not only in multicellular organisms to govern different cell fates but is also present in unicellular organisms such as prokaryotes and eukaryotic microbes. In the yeast *Saccharomyces cerevisiae,* recent studies of the mating-type switching have led to the discovery that asymmetric cell division can be achieved by the asymmetric distribution of intrinsic cell-fate determinants, a similar mechanism that was documented for the development of the *Drosophila* nervous system.

I.5.1 Mating-type switching and its determinant

The budding yeast *S.cerevisiae* is able to switch between two mating types, a and α. Among a pair of progeny cells only the older mother cell, which has previously divided, can switch mating types whereas the newly born daughter cell can not. This phenomenon ensures that the mother cell will not mate with its daughter. The different cell types a and α are determined by chromosomal changes at the mating-type locus *MAT*: *MATa* for a cells, and *MATα* for α cells. The yeast HO gene is responsible for mating-type switching due to its encoded endonuclease activity that initiates gene conversion at the *MAT* locus. Normally, *HO* gene activity is only expressed in the mother cells (for review, see Jacobs and Shapiro, 1998). Transcription of *HO* in mother cells is due to the unequal accumulation within the daughter cell nuclei of a HO transcription repressor called Ash1p. Ultimately, it is the differential localization of Ash1p that prevents mating-type switching in the daughter cell. Thus, Ash1p is the cell-fate determinant in budding yeast (Bobola et al., 1996; Sil and Herskowitz, 1996).

I.5.2 Ash1 RNA localization is required for mating-type switching

It has been demonstrated that asymmetric distribution of Ash1p in the nuclei of daughter cells requires asymmetric localization of its mRNA at the distal tip of the daughter cell during yeast division (Long et al., 1997, Takizawa et al., 1997). Three-dimensional imaging has also revealed that Ash1 mRNA is assembled into particles that associate with the daughter cell cortex (Takizawa et al., 1997). Under conditions in which Ash1 mRNA localization is disrupted, Ash1p accumulates asymmetrically in both mother and daughter nuclei therefore, localization of Ash1 mRNA creates an essential asymmetry in the distribution of Ash1p within mother and daughter cells of budding yeast and controls mating-type switching.

I.5.3 Mechanism of asymmetric Ash1 RNA localization

Similar to other localized RNA, asymmetric Ash1 RNA localization is probably mediated by *cis*-acting localization elements residing in the RNA sequence through interactions with putative *trans*-acting protein factors and the cytoskeletal elements.

I.5.3.1 The cis-acting Ash1 RNA localization elements

It was originally reported that the 3'-UTR of Ash1 mRNA is sufficient to localize a reporter RNA to the bud in the uninucleate small budded cells and to daughters in binucleate budded cells (Long et al., 1997, Takizawa et al., 1997). However, later studies have shown that its replacement has little or no effect on the localization of Ash1 mRNA and other sequence elements in the coding region are also involved in the asymmetric localization (Gonzalez et al., 1999; Chartrand et al., 1999). Three additional *cis*-acting elements have been found in the Ash1 coding region and each of them is sufficient to

direct the localization of a *LacZ* reporter mRNA to the bud (Chartrand et al., 1999). A fine-structure analysis of the 3'-UTR element has shown that its function in mRNA localization does not depend on a specific sequence but on the secondary or tertiary structure of a minimal 118-nt stem-loop. Similar structures also found in the localization elements of the coding region. Mutations in the stem-loop that affect the localization of the *LacZ* mRNA reporter also affected the formation of the localization particles in living cells. Therefore, the stem-loop structure in the localization elements is required for both localization and particle formation, suggesting that complex formation is part of the RNA localization mechanism (Chartrand et al., 1999).

I.5.3.2 The cytoskeletal elements and Ash1 RNA localization

Genetic studies have identified that five *SHE* genes (*SHE1* to *SHE5*) are important in the asymmetric expression of the HO endonuclease (*SHE*, symmetric HO expression) (Bobola et al., 1996). Mutations on these genes all have been found to affect Ash1 mRNA localization (Long et al., 1997; Takizawa et al., 1997; Bertrand et al., 1998). Three of these genes encode proteins that interact with or influence the actin cytoskeleton: *She1* is identical to a previously identified gene *MYO4*, which encodes an unconventional type V myosin and acts as an putative actin-based myosin motor (Jansen et al., 1996); *She5* encodes the Bni1 protein, which is involved in promoting actin-filament formation and polarization (Jansen et al., 1996); and *She4* encodes an uncharacterized protein also necessary for proper polarization of the actin cytoskeleton (Wendland et al., 1996). Analysis of these *She* mutants strongly suggests that the actin cytoskeleton plays an essential role in Ash1 RNA localization. Pharmacological studies

with the actin-depolymerizing agent (Takizawa et al., 1997) and mutations in tropomyosin, profilin, and actin itself (Long et al., 1997) have indeed revealed that Ash1 mRNA localization is dependent on an intact cytoskeletal network.

I.5.3.3 Dynamics of Ash1 RNA localization

Recent approaches to label mRNA with green fluorescent protein (GFP) have provided the first real-time images of RNA motility in living yeast and yielded new insights into the mechanism of mRNA transport (Bertrand et al., 1998; Beach et al., 1999). Bertrand et al. (1998) first developed a two-plasmid system in yeast. On one plasmid the GFP sequence was fused to the coding sequence of MS2 bacteriophage coat protein. On the second plasmid six MS2-binding sites were inserted between a reporter gene, *LacZ* and the Ash1 3'-UTR to make a reporter mRNA. A nuclear-localization signal was also engineered into the GFP-MS2 chimera so that it would be restricted to the nucleus if not complexed to RNA. Using these two sophisticated plasmids, Bertrand et al. first observed the formation of RNA particles induced by the *Ash1* 3'-UTR and followed the dynamics of mRNA movement and localization in budding yeast. They found that each *She* mutant reduced the proportion of cells containing *Ash1* particles. This effect is weakest for the *She5* mutant, but particles that do form often remain in the bud neck, suggesting movement was arrested en route. In the *She2* mutant strain, particle formation was almost completely abolished. In *She*3 mutant strain, the single and bright particle observed in wild type strains is found to be dispersed into many smaller particles, none of which localized. In *She4* mutant strain, fewer particles were seen and these were not localized about half the time, somewhat less than wild-type.

One of the most significant conclusions that Bertrand et al. have drawn is that the *She1/Myo4*gene, which encodes a putative Type V myosin motor, is required for particle movement and that She1p may serve as a motor to drive *Ash1* particle movement along actin microfilaments. This significant claim is based on a substantial body of evidence. First, the She1p and *Ash1* particles colocalize. Second, particle movement requires the *She1* gene. Third, *Ash1* mRNA particle movement occurs at velocities measured to be in the range of 200 to 400 nm/s. The rate of movement of actin bundles driven by purified chicken myosin V is 200-400 nm/s, implying that *Ash1* particle movement could be analogously driven by She1p.

A recent study using *in situ* colocalization and coprecipation of Myo4p and *Ash1* mRNA has demonstrated that a direct association between Myo4p and Ash1 mRNA is dependent on the She2 *and* She3 proteins, indicating a direct role for Myo4p myosin as a transporter of localized mRNAs (Münchow et al., 1999). This work also supports the concept of motor-driven RNA transport.

I.6 RNA localization in other somatic cells

In the previous sections, I have described the features of RNA transport and localization in the early embryonic development of *Drosophila* and *Xenopus*, and in polarized nerve cells and budding yeast. Asymmetric RNA localization occurs in many other types of polarized somatic cells. For example, the oligodendrocyte is one of the first systems in which subcellular RNA localization was described since mRNA coding

myelin basic protein (MBP) has been demonstrated to localize in the myelin compartment of the cell (for review, see Carson et al., 1998). By injecting fluorescently labeled MBP mRNA into living oligodendrocytes, Aniger and colleagues (1993) were the first to observe the formation of RNA granules and their subsequent transport to cellular processes. The same group also identified two elements within the 3'-UTR of MBP mRNA which are required for two distinct steps in its localization to the distal process of oligodendrocytes (Ainger et al., 1997). One element, termed RNA transport signal (RTS), is made of a 21-nucleotide sequence (GCCAAGGAGCCAGAGAGCAUG) and is required for the transport of MBP mRNA along the process. The second element, termed the RNA localization signals (RLS), contained within nucleotides 1130-1473 of the 3'-UTR of MBP mRNA, is required for localization of MBP mRNA to the myelin compartment. Computer analysis predicts that this region contains a stable secondary structure at a conserved position in rat, mouse, and human MBP mRNA. When RLS is deleted, the RNA forms granules that are transported along the process but fail to localize to the myelin compartment (Ainger et al., 1997). Interestingly, besides its function in transport, the RTS sequence has another role as a translational enhancer and confers translation enhancement to heterologous reporter RNAs (Kwon et al., 1999). This implies that translational regulation is an integral part of the RNA trafficking pathway and that the *cis*-acting signal for RNA trafficking may also act as the determinant for the regulation of translation.

Polarized somatic cells such as fibroblasts, myoblasts and epithelial cells represent another system in which intracellular mRNA localization has been documented. For example, in differentiating chicken myotubes, vimentin and desmin mRNAs are

highly localized to costameres and localized synthesis may be involved in the assembly of myofibrillar structures (Morris and Fulton, 1994). In chicken embryo fibroblasts (CEFs), β-actin mRNA is localized to the distal regions of the leading lamellae (Lawrence and Singer, 1986). Asymmetrically localized β-actin mRNA also exists in epithelia cells (Yeh and Svoboda, 1994) and early embryos (Bouget et al., 1996).

β-actin mRNA localization to the leading lamellae in the CEFs is independent of protein synthesis (Sundell and Singer 1990), and requires intact microfilaments (Sundell and Singer 1991). This asymmetric localization is mediated by conserved elements in the 3'UTR of β-actin mRNA (Kislauskis and Singer 1992; Kislauskis et al., 1993) including a 54-nt *cis*-acting signal termed "zipcode" (Kislauskis et al., 1994). The sorting of β-actin mRNA to the cell pheriphery is regulated by signal transduction mechanisms that influence the cytoskeletal organization of the leading edge (Hill et al., 1994; Latham et al., 1994). Treatment of CEFs with antisense oligonucleotides directed against the *cis*-acting zipcode led to delocalization of β-actin mRNA in the leading edge, and subsequent impairment of the cell polarity and motility in these delocalized cells. Thus, the asymmetric localization of β-actin mRNA to the leading edges of fibroblasts is important for the maintainance of cell polarity and motility (Kislauskis et al., 1997).

I.7 The RNA-binding proteins involved in RNA localization

Recently, progress has been made in identifying several families of *trans*-acting factors which are involved in the localization of mRNA in both germline and somatic cells of different organisms. Among the growing list of RNA-binding proteins, members of three different families have emerged: double-stranded RNA-binding protein (especially Staufen); zipcode binding proteins such as ZBP, Vera or Vg1RBP; and heterogeneous nuclear ribonucleoproteins (hnRNPs) (for review, see Kiebler and DesGroseillers, 2000). From the studies of these proteins, a particularly interesting theme has emerged is that the same RNA-binding protein may mediate the localization of different RNAs in distinct species via different pathways involving different cytoskeletal elements (Oleynikov and Singer, 1998; Micklem et al., 2000). This, combined with new evidence from the evolutionary conservation of some of these proteins, suggests a previously unanticipated uniformity in mRNA localization mechanisms. Next, I will mainly discuss three classes of *trans*-acting proteins, with an emphasis on Staufen which is so far the best-characterized protein family involved in RNA transport and localization.

I.7.1 The Staufen family

Staufen (Stau), a double-stranded RNA-binding protein, was first identified in *Drosophila melanoganster* in a genetic screen. The role of Staufen in the localization of several maternal mRNAs, which is essential for embryonic body programming during *Drosophila* oogenesis and early embryogenesis, has been well established. In somatic cells, Stau has also been shown to mediate RNA localization and play a role in asymmetric division during the development of the *Drosophila* central nervous system.

Recently, the cloning and characterization of the mammalian ortholog of Staufen has shown that Staufen is a conserved component of the RNA localization machinery.

I.7.1.1 Staufen is required for osk and bcd mRNA localization

Staufen plays an essential role in the localization of two maternal mRNAs that code for two important body pattern determinants during the early development of *Drosophila*. *Staufen* is one of the five genes required for the localization of *oskar* (*osk*) mRNA to the posterior pole of the oocyte where local synthesis of oskar protein directs the formation of abdomen and germline structures (Ephrussi et al., 1991; Kim-ha et al., 1991, 1995; St Johnston et al., 1991). In *stau* null mutants, *osk* mRNA persists in a ring at the anterior end of the oocyte and fails to move to the posterior pole. S*tau* is also one of the three genes required for the localization of *bcd* mRNA to the anterior pole. However, it functions at the final stage of *bcd* mRNA localization. After egg deposition Staufen is responsible for anchoring *bcd* mRNA at the anterior of the egg, where local synthesis of the bcd protein determines the head and thorax of the embryo (St Johnston et al., 1989). In *stau* null mutants, *bcd* mRNA shows a normal localization to the anterior end of the mutant oocytes, but has spread posteriorly to form a shallow gradient once the mutant egg has been laid.

I.7.1.2 Staufen is required for prospero mRNA localization

As I have discussed earlier, the function of the *stau gene* is not limited to oogenesis and early embryonic patterning in *Drosophila*. Zygotic Stau in *Drosophila* is expressed throughout the developing nervous system and participates in establishing

asymmetry by localizing *prospero* mRNA to the basal cortex of dividing neuroblast (Li et al., 1997; Broadus et al., 1998 Matsuzaki et al., 1998; Schuldt et al., 1998; Shen et al., 1998). This basal localization ensures the segregation of prospero mRNA only to the small GMC daughter cell after division. Since Prospero is a homeodomain containing transcription factor, asymmetric localization of its mRNA along with Prospero protein to the GMC will act redundantly to induce GMC-specific gene expression.

I.7.1.3 The nature of the Staufen-RNA ribonucleoprotein complex

Given that Staufen binds to any double-stranded RNA or RNA with internal double-stranded structures without sequence specificity, how could specific Staufen-RNA interactions be achieved *in vivo*? What are the other components of the specific Stau-RNA ribonucleoprotein complexes? And finally, how are the distinct Stau-RNA complexes transported and anchored to the different places? Although answers to these questions remain obscure, recent investigations are beginning to tackle these problems.

So far, the *cis*-acting sequences required for all steps of the *bcd* mRNA localization process have been mapped to a 625 nucleotide region of the 3'-UTR that is predicted to form a complex stem-loop secondary structure (see Fig. 4, Macdonald and Struhl, 1988; Ephrussi and Lehmann, 1992; Gavis and Lehmann, 1992; Macdonald et al., 1993). Using linker-scanning mutation analysis combined with microinjection, Ferrandon et al (1994) first mapped the sites essential for Stau recognition and Stau-RNA particles formation. These Stau binding sites coincide with the three predicted stem-loop structures of the 3'-UTR involving large double-stranded regions (stem-loop III, and the distal part of stem-loops IVc and Vb, see Fig. 4). To further test the relevance of the predicted

secondary structure for Stau binding, Ferrandon et al. (1997) designed sets of compensatory mutations on both strands of the putative helices and monitored Stau-particle formation after injection of the corresponding RNAs into the early embryo. They found that single mutation that disrupts each of the predicted stem structures prevented particle formation, while compensatory mutations that altered the primary sequences but not the helical structure restored the formation of Stau-containing granules. Thus, these results suggest that the double-stranded conformation of the *bcd* 3'-UTR plays a specific role in Stau-RNA interaction. dStau contains five dsRBD motifs and it has been recently shown that dsRBD1 and 4 bind dsRNA. However, their binding activity is weaker than that observed with dsRBD3 (Micklem et al., 2000). It is perceivable that specific interactions of Stau-*bcd* mRNA could be conferred by the correlation between the positions of the dsRBDs and the combined stem-loop structures of the 3'-UTR.

The nature of the specific Stau-*osk* mRNA interaction seems to be different from that of Stau-*bcd*. During oogenesis, Stau localizes exclusively with *osk* mRNA in the posterior region of the oocyte even though *bcd* mRNA is present at the anterior end (St. Johnston et al., 1991). In contrast, in the deposited egg and during early embryogenesis, Stau specifically binds *bcd* mRNA and does not bind injected *osk* mRNA (Ferrandon et al., 1994). Therefore, there is an apparent switch in specificity regarding Stau-RNA binding at the time between the end of oogenesis and the beginning of the egg deposition. The failure to form Stau-*osk* mRNA granules in the egg also suggests that other proteins not present in the egg cytoplasm are also required for the association of *osk* mRNA with Stau. Future work will need to elucidate the possible factors in the *Drosophila* oocyte which are involved in Stau-*osk* mRNA interaction.

Another significant point from the work of Ferrandon et al.(1997) comes from their claim that RNA-RNA interactions play a role in the formation of specific Stau-*bcd* mRNA ribonucleoprotein particles. This finding originated from an early observation that six conserved nucleotides in the distal loop of helix III are perfectly complementary to a side loop of the same helix (Macdonald, 1990) (see also Fig. 4). To test the possible interaction of these loops and their functional relevance in Stau binding, Ferrandon et al. introduced a set of compensatory mutations in each of the two loops. Interestingly, RNA containing the double compensatory mutations associates specifically with Stau in the embryo, whereas RNAs containing mutations on either single-stranded loop do not, suggesting that the two loops interact with each other through base-pairing. Further work confirmed that the base-pairing between the distal loops and side loop of Stem III is intermolecular and not intramolecular, indicating that dimers or multimers of the RNA localization signal associate with Stau. Thus, the formation of large ribonucleoprotein transport granules may be dependent on RNA-RNA interactions as well as RNA-protein interactions.

I.7.1.4 Staufen mediates RNA localization in both microtubule- and microfilament-dependent pathways

Staufen-mediated localization of *bicoid* and *oskar* mRNAs to the opposite poles of *Drosophila* oocytes is dependent on an intact microtubule network. Both RNAs are most likely transported in an active process involving microtubule-dependent motor proteins. However, recent studies on the localization of the prospero-Staufen complex have shown that it is microfilament-dependent since actin-destablizing, but not

microtubule-depolymerizing drugs, prevent prospero mRNA localization. Therefore, Staufen can mediate both microtubule- and actin-dependent mRNA localization.

A Staufen-mediated bcd mRNA localization is microtubule-dependent

Pokrywka and Stephenson have used microtubule-depolymerizing drugs to examine the late localization of *bcd* mRNA (Pokrywka and Stephenson, 1991, 1995). Treatment of stage 10 egg chambers in culture with nocodazole dislodges already localized *bcd* in the oocyte and nurse cells and prevents localization of newly synthesized *bcd* mRNA entering the oocyte. Interestingly, microtubule disruption by nocodazole is easily reversible after removing the drug. This relocalization of *bcd* mRNA suggests that the RNA is unlikely to be simply trapped at the anterior pole of the oocyte by a ubiquitous receptor as it enters the anterior oocyte from the nurse cells. In mutants where the oocyte develops as if it had two anterior ends, *bcd* mRNA localizes to the ectopic "anterior cortex" at the opposite end of the oocyte (Ruohola et al., 1991; Lane and Kalderon, 1994; Gonzalez-Reyes et al., 1995). This ectopic *bcd* mRNA cannot have been localized by being trapped as it entered the oocyte. Instead, *bcd* mRNA localization appears to occur via active transport towards the minus-ends of microtubules, since the sites of *bcd* mRNA localization coincide with the places where the minus ends of microtubules are thought to reside. Staufen is needed for the final stage of *bcd* mRNA localization in late oogenesis and early embryogenesis. When the 3'UTR of *bicoid* mRNA is injected into the early embryo, *bcd* mRNA recruits endogenous Stau to form Stau-containing ribonucleoprotein complexes which are localized in the vicinity of the astral microtubules of the mitotic spindles (Ferrandon et al., 1994). Since this localization

is disrupted by microtubule-depolymerizing drugs, and the time between mitoses is to short for any diffusion, it seems likely that the Stau-*bcd* mRNA complexes are actively transported along the microtubules, and possibly a microtubule-dependent motor protein is involved in this process. Most recently, the discovery that cytoplasmic dynein, a minus-end-directed microtubule motor protein, is involved in targeting Swallow and bicoid RNA to the anterior pole of *Drosophila* oocytes (Schnorrer et al., 2000) provides the missing link in *bicoid* mRNA localization. However, since Staufen is involved in *bcd* mRNA localization in a later phase than Swallow, it remains to determined if Staufen is recruited to the same complex containing Swallow and dynein.

B *Staufen-mediated osk mRNA localization is microtubule-dependent*

There is good evidence to suggest that the movement of Staufen-*oskar* mRNA from the anterior to the posterior pole of the oocyte is also due to active transport along microtubules. At stage 7, when *oskar* RNA begins to localize in the posterior of the oocyte, the nurse cell-oocyte microtubule array is reorganized to a clear anteroposterior polarity. The movement of Staufen protein and *oskar* mRNA to the posterior end correlates perfectly with the major reorganization of the oocyte cytoskeleton (Theurkauf et al., 1992).

Clark et al. (1994) demonstrated that the kinesin:β-gal fusion protein moves to the posterior region of the oocyte at the same stage as Staufen and *oskar* and that this movement is dependent on the activity of the kinesin motor domain. Treatment with the microtubule-depolymerizing drug colchicine prevents localization of Staufen, *oskar* mRNA, and the motor fusion. In *Notch*, *Delta*, and *gurken* mutants which result in

formation of a mirror-image microtubule skeleton, Staufen protein, *oskar* mRNA, and the kinesin:β-gal protein all mislocalize identically, to the center of the oocyte (Clark et al., 1994; Gonzalez-Reyes et al., 1995). In addition, movement of the reporter construct is disrupted by the same mutations (*cap, spire*) that affect Staufen and *oskar* mRNA localization but not by mutations in *staufen* and *oskar* themselves (Clark et al., 1994). These results indicate that the construct is not simply hitching a lift with Staufen or *oskar* mRNA but that it is sharing some aspects of the transport machinery which is disrupted in these mutants. In view of the fact that kinesin is well established as a microtubule-directed motor protein and colchicine treatment prevents the localization of the Staufen-oskar mRNA and the motor protein, it is very likely that this shared component of the transport machinery is the microtubules themselves. Further confirmation comes from an analysis of *cappuccino* and *spire* mutants (Theurkauf, 1994), which indicates that they result in the premature onset of cytoplasmic streaming immediately after loss of the posterior microtubule organizing center (MTOC). In these ovaries therefore, the anterior-posterior array of microtubules implicated in Staufen and *oskar* mRNA localization fails to form. This could account for the failure of Staufen and *oskar* to localize.

The apparently anterior nucleation of the anterior-posterior microtubule array (Theurkauf et al., 1993) and the fact that Staufen-*oskar* RNA always localizes to the same position as the kinesin:β-gal fusion protein (Clark et al., 1994) both support the notion that Staufen-*oskar* RNA is transported to the posterior pole along the microtubules by a plus end-directed motor. However, this simple model has been called into question by the discovery that the minus end-directed microtubule motor dynein also localizes to the posterior pole at the same time as *oskar* mRNA (Li et al., 1994). This raises the

possibility that at least some of the microtubules are oriented with their minus ends at the posterior and that *oskar* mRNA could therefore be localized by a minus-end directed motor such as dynein itself. Unlike the kinesin:β-gal fusion protein, which is thought to have an unregulated motor domain that moves along any microtubules it encounters, the activity of endogenous dynein is likely to be regulated. Thus, it is possible that dynein is merely being transported to the posterior end as another cargo for the motor that localizes the Staufen-*oskar* mRNA complex.

C *Staufen-mediated pros mRNA localization is microfilament-dependent*

Using *in vitro* culture of neuroblasts, Broadus and Doe (1997) investigated the role of the cytoskeleton in asymmetric localization of the Inscuteable, Prospero and Staufen proteins. They found that microtubule disruption has no effect on protein localization, but microfilament inhibitors result in delocalization of all three proteins. Inscuteable becomes uniform at the cortex, whereas Prospero and Staufen become cytoplasmic; inhibitor washout leads to recovery of the microfilaments and asymmetric localization of all three proteins. Staufen colocalizes with *Prospero* mRNA throughout the entire cell cycle. It is first concentrated on the apical side of the neuroblast at interphase, then forms a crescent on the basal side of the cell in prophase, where it remains through mitosis before partitioning to the GMC at cell division (Broadus et al., 1998; Schuldt et al., 1998). The dsRBD3 of Staufen can interact directly with the 3'-UTR of *Prospero* mRNA *in vitro* (Li et al., 1997) although the physiological relevance of this binding is hard to address since dsRBD3 of Staufen appears to bind any double-stranded RNA longer than 11 bp *in vitro*. Using an *in vivo* RNA injection assay, Schuldt et al.

(1998) demonstrated that Staufen specifically binds to the 3'-UTR of *prospero* mRNA to form ribonucleoprotein particles in *Drosophila* embryos, but not to the coding region of *prospero* mRNA. This behavior is similar to that of *bicoid* 3'-UTR in vivo. However, unlike the RNP particles formed between Staufen and the *bcd* 3'-UTR (Ferrandon et al., 1994), the Staufen/*Prospero* 3-UTR particles do not associate with astral microtubules, consistent with the obsevation that microtubles are not involved in Staufen-*Prospero* mRNA localization in the developing nervous system.

I.7.1.5 Structural features of Staufen

The only functional motif found in Staufen is the double-stranded RNA (dsRNA) binding domain (dsRBD), which consists of a 65 to 68 amino acid consensus sequence and binds to dsRNA or RNAs with extensive double-stranded structure (St Johnston et al., 1992). Staufen contains 5 copies of dsRBDs termed dsRBD1 to dsRBD5, the third dsRBD (dsRBD3) has been shown to strongly bind dsRNA *in vitro* (St Johnston et al., 1992). So far, the dsRBD has been found in a growing number of proteins from different organisms.

The structures of dsRBDs present in several proteins from different organisms have been determined by nuclear magnetic resonance (NMR) and X-ray crystallography, with highly consistent results. These proteins include *Escherichia coli* RNase III (Kharrat et al., 1995), *Drosophila melanogaster* Staufen (Bycroft et al., 1995), and human double-stranded RNA activated protein kinase PKR (Nanduri et al., 1998). Studies of these proteins have shown that the dsRBD folds into a compact α-β-β-β-α structure, and that the two α helices are packed along a face of a three-stranded anti-

parallel β sheet, with most of the potential RNA-binding residues exposed on one surface. The structure of the dsRBD3 from *Drosophila* Staufen is quite different from that of typical RNA binding domains such as RNP domain (β-α-β-β-α-β) and KH domain (β-α-α-β-β). However, it shares homology with the N-terminal domain of ribosomal protein S5 (Bycroft et al., 1995). Interestingly, the consensus derived from S5 protein family sequences shares several conserved residues with the dsRBD consensus sequence, indicating that the two domains share a common evolutionary origin (Bycroft et al., 1995). Two residues that are essential for dsRBD RNA binding, F32 and K50, are also conserved in the S5 protein family suggesting that the two domains interact with RNA in a similar way (Bycroft et al., 1995).

Recently, the 1.9 Å resolution crystal structure of dsRBD2 from the *Xenopus laevis* protein Xlrbpa complexed with dsRNA has been determined (Ryter et al., 1998). In this study, two dsRNAs, each 10bp long, are stacked end-wise to approximate a continuous helix. Three distinct regions of the protein interact with the RNA via direct or water-mediated interactions (see Fig. 8). Regions 1 and 2, which correspond to the N-terminal α helix (α1) and the loop between β1 and β2 respectively, interact with adjacent minor grooves. Region 3, which corresponds to the highly conserved residues at the beginning of the C-terminal helix (α2), spans the major groove formed by the two contiguous but distinct 10-mer fragments. The major groove seems to be wider than expected for continuous dsRNA, suggestive of partial unwinding of the A-form duplex. Consistent with this finding, the dsRBD can bind sequences containing mismatches and non-contiguous duplex regions (Bevilacqua et al., 1998; Tian et al., 2000), potentially allowing for a degree of specificity in dsRBD-RNA interactions. Most of these protein-

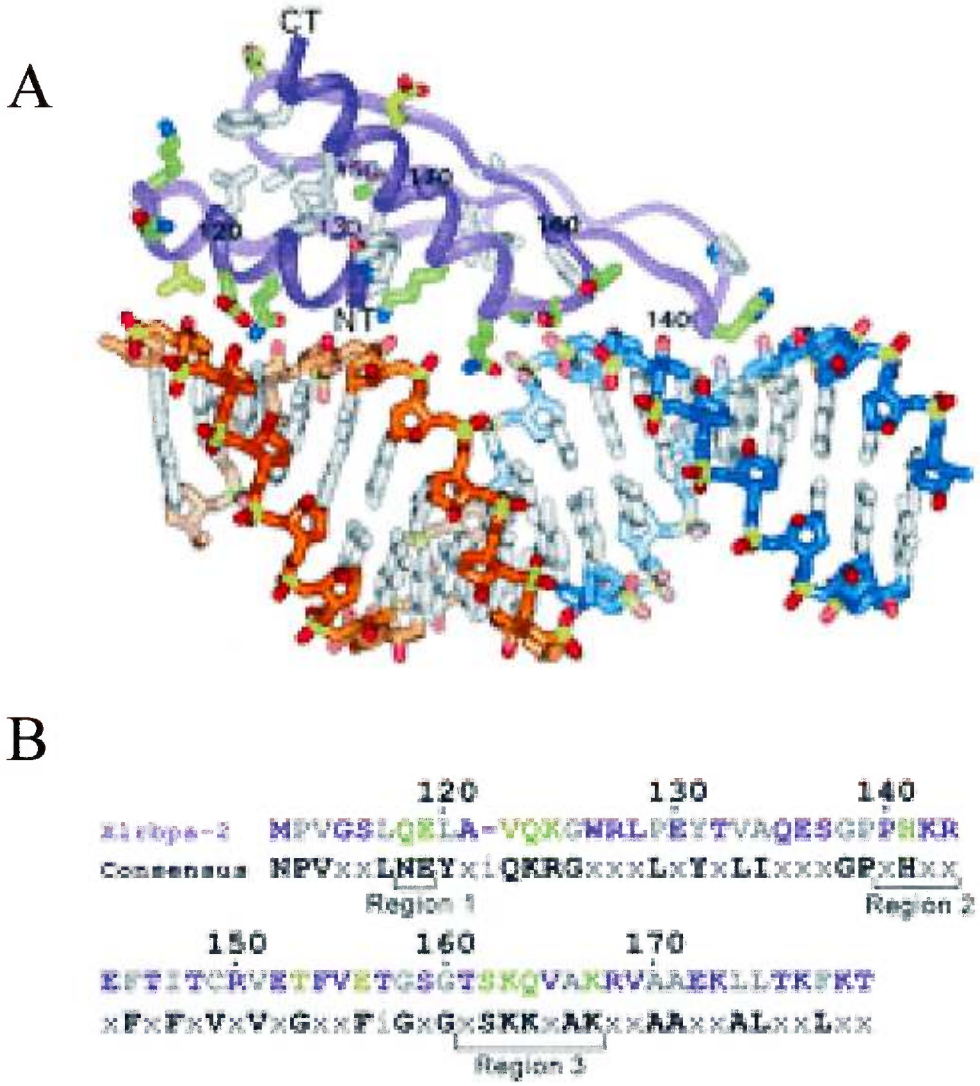

Fig. 8. Recognition of dsRNA by dsRBB2 of Xlrbpa. A. Structure of the complex between the Xlrbpa dsRBD2 (purple) and two pseudocontigious 10-nucleotide RNA duplexes (backbones shown in orange and blue). Protein segments interacting with the RNA are denoted by regions 1, 2 and 3 and critical sidechains are shown, as well as water molecues (blue spheres). CT, C-terminus; NT, N terminus. B. Sequence alignment of the Xlrbpa dsRBD2 with the dsRBD consensus sequence, indicating the regions involved in RNA interactions. Purple or X, nonconserved residues; green, hydrophilic residues matching the consensus sequence; grey, hydrophobic residues matching the consensus sequence; yellow, residues not matching the consensus sequence. Adapted from Ryter et al., 1998.

RNA interactions are with the phosphodiester backbone or ribose 2'-OH groups, which accounts for the discrimination against DNA. The limited number of base-specific interactions makes it likely that any specificity in RNA binding rests on sequence-specific structural features in the duplex. In keeping with this view, internal loops in dsRNA appear to play an important role in defining sites of cleavage by RNase III and of deamination by ADAR1 (Nicholson, 1996; Lehmann and Bass et al., 1999).

More recently, the RNA-protein interactions mediated by Staufen dsRBD3 and a 12 base-pair RNA stem-loop has also been demonstrated by NMR studies (Ramos et al., 2000). As the crystallographic structure of the complex between dsRBD2 of Xlrbpa and dsRNA, the same three regions (helix α1, loop 2 and loop 4) of Staufen dsRBD3 have been identified to interact with RNA (see Fig. 9). Mutations of amino acids in each of these regions abolish or reduce RNA-binding significantly whereas mutations in surface residues in other regions of the protein have no effect. While the loop between β-1 and β-2 (loop2) was shown to interact with the minor groove of RNA, loop 4 between the last β strand (β-3) and the second helix (α2) interacts with the phosphodiester backbone across the major groove. However, a very different description of the interaction between the N-terminal helix α1 and RNA was provided by the studies of the two RNA-protein complexes. In the crystal structure, helix α1 interacts with the minor groove of a second RNA duplex that abuts the first RNA molecule to form a pseudo-continuous double helix. As a consequence, the Xlrbpa dsRBD covers 16 bp across the junction between the two RNA molecules. In contrast, helix α1 of Staufen dsRBD3 interacts with a single-stranded tetraloop that caps a 12 bp stem of a perfect A-form RNA. Interactions between helix α1

I

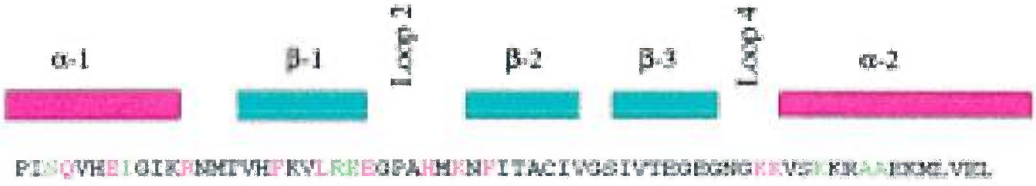

II

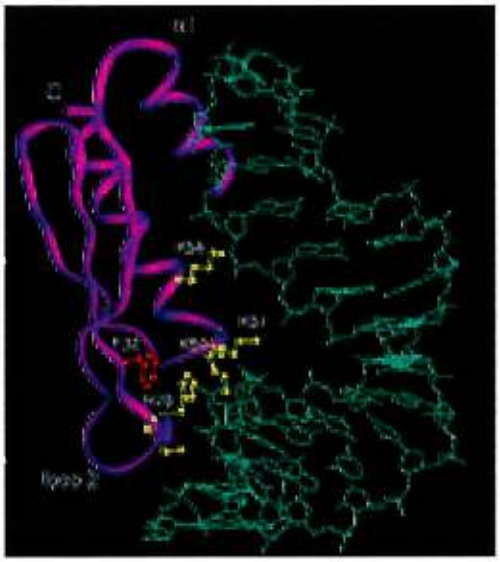

III

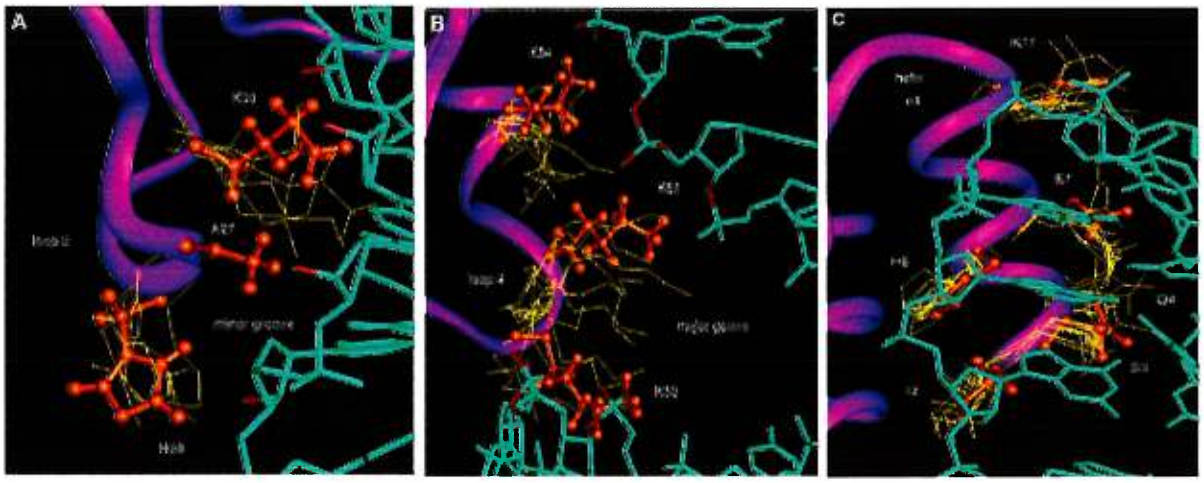

Fig. 9. The interactions of dsRBD3 of *Drosophila* Staufen and dsRNA. **I.** The schematic representation of the structure motifs of dsRBD3 (upper) and the amino acids that reduce(yellow) or abolish RNA binding. **II.** Stereo view of a low energy structure of the dsRBD3-RNA complex; Phe32 and five interfacial residues critical for Staufen function are shown explicitly. **III.** Intermolecular interactions between dsRBD3 and a RNA stem-loop in the superposition of 10 converged structures; one structure is represented in orange for clarity. (A) Interaction between loop 2 and the minor groove of the double-helical stem; Ala27 and His28 from the conserved GPAH sequence and the Lys30 side chain are shown explicitly; 2'-OH groups in close proximity to amino acids side chains are highlighted in red. (B) Interaction between loop 4 and the N-terminus of helix α2 and RNA phosphates (in red). (C) Interaction between helix α1 and the UUCG tetraloop. Adapted from Ramos et al., 2000.

of Staufen dsRBD3 and single-stranded RNA may provide important determinants of the specificity of dsRBD proteins *in vivo*.

I.7.2 The zipcode-binding proteins

A member of this class of RNA-binding proteins was first identified from an UV cross-linking and affinity purification approach to search for proteins that bind to the localization zipcode of β-actin mRNA in chicken fibroblasts (Ross et al., 1997). A 68-kDa protein termed ZBP-1 was found to specifically bind the zipcode and encode an RNA–binding protein containing a typical RNA recognition motif (RRM) and four KH (hnRNP K homology) domains. Similar approaches have also been used to identify *trans*-acting factors that bind to the *Vg1* localization element (VgLE), which functions in vegetal localization of *Vg1* RNA in *Xenopus* oocytes. A 75-kDa protein termed Vera was found to specifically bind to the VgLE and co-sediment with the endoplasmic reticulum (ER) (Deshler et al., 1997). Therefore, Vera may link Vg1 mRNA to the vegetal ER subcompartment while the ER is transported via microtubules to the vegetal pole. Previous experiments using UV-crosslinking of *Vg1* 3'-UTR and *Xenopus* oocyte extracts have also led to the identification of a 69-kDa protein called *Vg1* RNA-binding protein (Vg1RBP) (Schwartz et al., 1992). It was demonstrated that Vg1RBP is enriched in the microtubule fraction of oocytes and mediates the association of *Vg1* mRNA to microtubules *in vitro* (Elisha et al., 1995). Interestingly, sequence analyses have revealed that Vg1RBP or Vera is in fact the same protein and they are highly homologous to the microfilament-associatiated zipcode-binding protein (Havin et al., 1998). Thus, Vera/Vg1RBP and ZBP-1 are almost identical proteins operating on different cytoskeletal

elements in different cells of different species. The presence of the same RNA-binding protein mediating transport of different RNAs in different species suggests that ZBP represent a general and conserved factor in the RNA localization machinery.

In humans, a protein named KOC (KH-domain protein overexpressed in cancer cells) was found to be the homologue of ZBP-1 (Mueller-Pillasch et al., 1997). However, its function is unknown.

In developing neurons, β-actin mRNA is localized to granules that are sorted to dendritic and axonal growth cones (Bassell et al., 1998). In neuronal processes, these β-actin mRNA granules are closely associated with microtubules and delocalized after treatment with microtubule- but not microfilament-destabilizing drugs. This behavior is in contrast to β-actin mRNA localization in chicken fibroblasts. It is been proposed that the different features of β-actin mRNA localization in different cell types may be attributed to the presence of different *trans*-acting factors that have different cytoskeletal binding activities (Bassell and Singer, 1997). In agreement with this hypothesis, a second β-actin mRNA zipcode binding protein termed ZBP-2 has been found in neurons (preliminary results cited in Hazelrigg, 1998). Interestingly, ZBP-2 is also present in fibroblasts and is both nuclear and cytoplasmic. Therefore, different ZBP isoforms are expressed in the same cell but are likely to play distinct roles.

I.7.3 The heterogeneous nuclear ribonucleoproteins (hnRNPs)

hnRNPs are a large family of over 20 RNA-binding proteins, many of which are characterized by the presence of one or more RNA-binding domain motifs, and have been implicated in RNA transcription and pre-mRNA processing (for a review, see Dreyfuss et

al., 1993). These proteins may contain different RNA-binding motifs, e.g., RNA recognition motif (RRM), arginine/glycine-rich boxes (RGG), and KH (hnRNP K homology) domains that confer different RNA sequence binding preferences. Recent studies have revealed that several members of the hnRNP family are involved in RNA transport and localization.

The first member of hnRNP family that was found to be implicated in RNA transport is the 36-kDa hnRNP A2 which specifically binds to the 21-nt RNA transport signal (RTS) of MBP mRNA in mouse oligodendrocytes (Hoek et al., 1998). Western blotting indicates that hnRNP A2 is enriched in brain and testis, and immunostaining of oligodendrocytes indicates that the protein is found in both nucleus and cytoplasm where it appears in granules in the distal processes and myelin compartment, consistent with a role in RNA trafficking. Some hnRNPs including hnRNP A2 contain an unconventional nuclear localization signal called the M9 domain which binds to a nuclear import protein termed transportin, and shuttles between the nucleus and cytoplasm (Siomi and Dreyfuss, 1995; Pollard et al., 1996; Siomi et al., 1997). Thus, hnRNP A2 may function in nuclear export as well as in intracellular transport of RTS-containing RNA.

In *Xenopus oocytes*, localization of *Vg1* mRNA is directed by a 340 nt sequence (termed Vg1 localization element, VgLE) within the 5' half of its 3'-UTR (Mowry and Melton, 1992). VgLE contains a series of reiterated sequence motifs: E1 (UAUUUCUA, two copies), E2 (UUCAC, five copies), E3 (UGCACAGAG, two copies), E4 (CUGUUA, three copies) and VM1 (UUUCUA, three copies). The E2 element is reported to be the binding site for Vera (Deshler et al., 1998). The VM1 element have been shown to be required for the binding of VgRBP60, a protein previously identified as a VgLE-binding

protein (Mowry, 1996; Gautreau et al., 1997). Recently, the 60-kDa VgRBP has been cloned and found to be related to hnRNP I (Cote et al., 1999). Interestingly, when mutations were introduced into the VM1 elements, *Vg1* mRNAs was no longer localized and also failed to bind VgRBP60, implicating it in *Vg1* RNA localization (Cote et al., 1999).

In *Drosophila*, *Squid* (*Sqd*) encodes a hnRNP protein which is important for gurken (grk)-dependent dorsal-ventral (D-V) patterning during oogenesis (Kelley 1993). The *Sqd* gene is alternatively spliced to produce three protein isoforms: SqdA, SqdB, and SqdS. Interestingly, these isoforms display different subcellular distributions: both SqdB and SqdS are detected in germ-line cell nuclei, whereas SqdA is predominantly cytoplasmic. While the nuclear isoform (SqdS) is involved in the proper localization of *gurken* mRNA in the oocyte, the cytoplasmic isoform SqdA has no effect on *gurken* mRNA localization. Instead, it plays a role in preventing the translation of ventrally localized *grk* mRNA and causes the accumulation of gurken protein on the dorsal side of the egg chamber (Norvell et al., 1999). Therefore, distinct isoforms of Squid perform distinct roles in *gurken* mRNA localization and translation. The role of the hnRNP protein Squid in RNA localization has also been demonstrated using a mRNP microinjection assay. Lall et al (1999) have demonstrated that a synthetic, fluorescently tagged *fushi tarazu* (*ftz*) transcript, a *Drosophila* pair-rule gene product, is unable to localize after injection into blastoderm embryos but that preincubation with nuclear protein extracts leads to rapid and specific apical localization on an intact microtubule cytoskeleton. Further analysis shows that this activity can be attributed to the *Drosophila* Squid hnRNP protein, which selectively binds to the *ftz* 3-UTR. Moreover, related

human hnRNP proteins can substitute for Sqd activity, indicating that the localization-promoting activity of hnRNP proteins has been evolutionarily conserved. This represents the first direct demonstration that a specific protein accomplishes the localization of a transcript upon direct binding.

I.8 The cytoskeleton and cytoplasmic RNA localization

It is now believed that the cytoskeleton is widely used to transport or anchor mRNAs to their subcellular functional sites once they are synthesized in the nucleus. Studies in *Drosophila melanoganster* and *Xenopus laevis* oocytes, as well as in *Saccharomyces cerevisiae*, fibroblasts and neurons have implicated microtubules and microfilaments in localizing mRNAs and other determinants. It seems that microtubules are generally required for long-distance transport processes in large cells such as oocytes, neurons, or oligodendrocytes whereas microfilaments play a major role in smaller cell types such as fibroblasts and yeast. However, in certain cases both microtubules and microfilaments are required for RNA transport and subsequent protein synthesis (for a review, see Bassell and Singer 1997, Jansen 1999). It is possible that mRNA associates with various filament systems through a common mechanism and that these filaments, whether they be microtubules, actin or even intermediate filaments, could provide a solid surface for RNA-binding, preventing random movement of RNA within the cytoplasm and bringing it into contact with regulatory cofactors. Recent identification of a number

of RNA-binding proteins with cytoskeletal binding activity has proven to be essential mediators of the RNA-cytoskeleton association during RNA localization.

I.8.1 Microtubule-dependent RNA localization in *Drosophila* and *Xenopus* oocytes

In the previous section, I have described the importance of microtubules in the localization of *Drosophila* maternal mRNAs such as *bicoid and oskar*. Several lines of evidence suggest that microtubules play a more general role in *Drosophila* maternal mRNA localization. First, localization of the materal RNAs correlates with the rearrangement of the microtubule network. Over a dozen transcripts (e.g. *bicoid, nanos, orb, oskar, Bicaudal-C, Bicaudal-D, gurken, Pgc, K10, egalitarian*, and *tudor*) are synthesized in the nurse cells and specifically accumulate in the oocyte within early egg chambers. During these early stages, the microtubule nucleation site (the minus end) is located in the posterior end of the oocyte with microtubules oriented toward the nurse cells. Later in oocyte development, *bicoid*, *Bicaudal-D* and even some posteriorly localized RNAs such as *oskar* and *Pgc*, move from the posterior to the anterior end of the oocyte. During this time, the microtubule orientation undergoes a rearrangement with the nucleation site at the anterior end of the oocyte. In both cases, mRNAs move towards the minus end of the microtubules. Secondly, as mentioned in the last section, treating females with microtubule poisons such as colchicine leads to the redistribution of *bicoid* and *oskar* mRNA throughout the oocyte cytoplasm. Genetic mutations that alter microtubule organization in the oocyte also cause mislocalization of *bicoid* and *oskar* mRNAs. Thirdly, transport of mRNAs along microtubules indicates that microtubule-dependent motor proteins may be involved in this process. Indeed, several microtubule-

based motor proteins have been implicated in the localization of *Drosophila* maternal mRNAs. One such motor protein is cytoplasmic dynein which moves towards microtubule minus ends. It has been demonstrated that the light-chain subunit of cytoplasmic dynein (Dlc) specifically interacts with the coiled-coil domain of *Drosophila* Swallow (Schnorrer et al., 2000). *Swallow* is one of the genes required for anterior *bicoid* mRNA localization and encodes a protein with a coiled-coil domain as well as a domain with slight similarity to known RNA-binding motifs. Swallow transiently localizes to the anterior cortex in late-stage oocytes. This anterior localization depends on an intact microtubule network but not on Exuperantia activity or even the presence of *bicoid* mRNA (Schnorrer et al., 2000), indicating that the action of Swallow is upstream of *bicoid* mRNA localization. Thus, Swallow seems to have its own cellular address and may be used by *bicoid* mRNA to hitch a ride to the anterior cortex of the oocyte. Another candidate involving RNA localization during *Drosophila* oogenesis is kinesin, a microtubule-plus-end directed motor protein. A kinesin:β-galactosidase fusion protein has been shown to colocalize with oskar RNA when oskar RNA gradually moves away from the anterior and begins to accumulate at the posterior pole of the oocyte (Clark et al., 1994).

As discussed in the previous section, the dynamics of RNA localization to the vegetal pole of *Xenopus* oocytes can be generally classified into two different pathways exemplified by *Vg1* and *Xcat-2* RNAs. The *Vg1* pathway is microtubule-dependent and is abolished by treating oocytes with microtubule-depolymerizing drugs such as nocodazole or cochicine (Yisraeli et al., 1990). This microtubule-dependent transport process is possibly conserved between frogs and mammals as tau mRNA which is localized in the

axons of mammalian neurons, when injected into *Xenopus* oocytes, can take the same microtubule-dependent route to the vegetal cortex as does *Vg1* mRNA itself (Litman et al., 1996).

I.8.2 Microtubule-dependent RNA localization in somatic cells

Microtubules play an important role in RNA localization in some polarized somatic cells. In differentiated neurons, for example, tau mRNA is localized to the cell body and the proximal portion of the axons, and MAP2 mRNA is localized in the cell body and dendrites (Litman et al., 1994; Garner et al., 1988). Later studies have revealed that a number of other RNAs are also differentially localized to axonal or dendritic compartments (see previous section). In most cases, treatment with microtubule inhibitors can abolish the differential localization. The observations of localized RNAs in living cultured neurons have prompted investigators to suggest that they are present in particles composed of several RNAs and proteins, including some components of the translational machinery (Knowels et al., 1996). Moreover, these particles translocate inside the cell in a microtubule- but not microfilament-dependent manner (Knowels et al., 1996).

Studies with *MBP* mRNA injected into oligodendrocytes in culture also highlight the importance of microtubules in RNA transport. Injected MBP mRNA is rapidly assembled into RNA granules and moves from the cell body into the myelin processes (Ainger et al., 1993). Three-dimensional visualization indicates that MBP mRNA granules are often aligned in tracks along microtubules. These granules are not released by detergent extraction indicating that they are associated with the cytoskeletal network (Ainger et al., 1993). Recently, it has been directly demonstrated that the translocation of

MBP mRNA was inhibited by agents such as nocodazole and taxol which affect microtubules, but not by agents such as cytochalasin which affect microfilaments, indicating that MBP RNA transport requires intact microtubules but not microfilaments (Carson et al., 1997). Moreover, RNA translocation was inhibited when cells were treated with antisense oligonucleotides to suppress kinesin expression, indicating that kinesin may direct the microtubule-dependent MBP mRNA transport (Carson et al., 1997).

I.8.3 Microfilaments and RNA localization

Microfilaments have been found to be involved in asymmetric RNA localization solely in a few cases including the differential distribution of β-actin mRNA to the leading edges of chicken fibroblasts (Sundell and Singer, 1991) and Fucus embryos (Bouget et al., 1996). β-actin mRNA is also localized within neuronal processes and growth cones in a granular pattern however, its sorting in neurons is closely associated with microtubules (Bassell et al., 1998). It is possible that β-actin mRNA granules can interact with both microfilaments and microtubules and that the preferential usage of a particular filament system is characteristic of the specific cell type. This mechanism could involve *cis*-acting elements within the 3'-UTR of actin mRNA that interact with a set of cell type-specific RNA-binding proteins and/or motor proteins that promote preferential usage of one filament system over the other (Bassel and Singer, 1997). Indeed, a second zipcode-binding protein ZBP-2 has been identified in Singer's lab that binds to the 54-NT zipcode of β-actin and colocalizes with β-actin mRNA in neuronal processes (meeting report cited from Hazelrigg, 1998). Thus, in fibroblasts and neurons,

β-actin mRNA associates with different *trans*-acting proteins which in turn mediate its association with different cytoskeletal elements.

The actin-based microfilaments have also been found to be involved in the localization of several cell-fate determinants during asymmetric cell division. In *S. cerevisiae*, *Ash1* mRNA is localized to the budding tip of dividing yeast and then to the small daughter cell (Long et al., 1997; Takizawa et al., 1997). Mutations in proteins that are part of the microfilament network such as actin, myosin, profilin, and tropomyosin all affect *Ash1* mRNA localization. Furthermore, the unconventional myosin has been implicated as a motor protein for *Ash1* mRNA localization (Bertrand et al., 1998). In the developing nervous system of *Drosophila*, the *prospero* mRNA is also asymmetrically segregated into the daughter GMC cells in an actin filament-dependent fashion (Broadus and Doe, 1997, Broadus et al., 1998).

I.8.4 Ribonucleoprotein granules associated with the cytoskeleton

There is ample evidence that messenger RNAs can be found as integrated components of higher order structures throughout their lifetime. Such ribonucleoprotein (RNP) particles are one of the characteristics of RNA transport. *In situ* hybrization studies have revealed nonhomogenous granular patterns for a variety of localized mRNAs. These patterns include "punctuate actin mRNA in fibroblasts (Sundell and Singer, 1990), "island-like structures" of Xlsirt RNA in *Xenopus* (Kloc et al., 1993), "granules" of MBP mRNAs in oligodendrocytes (Ainger et al., 1993), formation of bicoid RNA "particles" in *Drosophila* (Ferrandon et al., 1994), and the motile RNA granules in living neurons (Knowles et al., 1996). Most recently, the movement of yeast

Ash1 RNA particles to the daughter cell was followed using two sophisticated reporter plasmids (Bertrand et al., 1998).

Analysis of mRNA-granules transport into neuronal processes using the RNA-labelling dye SYTO 14 indicates that mRNA forms granules that contain translational components and translocate along microtubules at a rate of 0.1 μm/second (Knowles et al., 1996). This rate is in agreement with the rate of the directed translocation of MBP mRNA along microtubules in oligodendrocyte processes (Ainger et al., 1993). Colocalization studies have shown that MBP mRNA granules contain arginyl-tRNA synthetase, EF1α, and ribosomes, suggesting the presence of a translational unit (Barbarese et al., 1995). Using dual-channel cross-correlation analysis of confocal images, MBP RNA granules were estimated to have a radius of between 0.6 and 0.8 μm, suggesting that RNA granules represent a supramolecular complex that could contain several hundred ribosomes (Barbarese et al., 1995).

I.8.5 RNA-binding proteins associated with the cytoskeleton

The identification of *trans*-acting proteins that bind to the *cis*-acting targeting sequences of localized RNAs has also shed light on mRNA-cytoskeletal association. Some of these RNA binding proteins also bind to cytoskeletal filaments which is consistent with the notion that RNA transport and localization is cytoskeleton dependent. Such proteins provide essential connections between RNAs and cytoskeleton during intracellular RNA transport and localization.

One of the best-characterized RNA-binding proteins that associates with the cytoskeleton and functions in mRNA localization is Staufen. Staufen is required for

oskar and *bicoid* mRNA localization to the opposite ends of *Drosophila* oocytes in a microtubule-dependent way (St Johnston, 1995). It also involves in the asymmetric segregation of *prospero* mRNA to the basal side of the dividing neuroblast and subsequently to the daughter GMC (Li et al., 1997; Broadus et al., 1998; Schuldt et al., 1998). In the latter case, its function relies on intact microfilaments but not microtubules (Broadus and Doe, 1997). Microinjection of the bicoid 3'-UTR into *Drosophila* embryos results in the formation of Staufen-RNA granules that associate with astral microtubules (Ferrandon et al., 1994). It has been proposed that the Staufen-*bicoid* RNA complex, but not Staufen itself, is recruited to microtubules because the *bicoid* mRNA might induce a conformational change in Staufen that is essential for its association with microtubules (Ferrandon et al., 1994). Whether the Staufen-*bicoid* RNA complex binds directly or indirectly to microtubules is unclear.

The 69 kDa Vg1RBP (*Vg1* RNA binding protein) binds to the essential targeting sequence of the 3'-UTR of *Vg1* mRNA and to microtubules (Elisha et al., 1995). Protein depletion experiments have demonstrated that *Vg1* mRNA attachment to microtubules is Vg1RBP dependent, implying that Vg1RBP is the link between cytoskeletal filaments and *Vg1* mRNA. Based on the fact that Vg1RBP is identical to Vera, a Vg1 binding and ER-associated protein (Havin et al., 1998), it has been suggested that Vg1RBP/Vera might attach Vg1 mRNA to a specific ER subcompartment of the oocyte, and that this ER subcompartment is subsequently transported along microtubules (Deshler et al., 1998).

Another protein termed TB-RBP (testis/ brain RNA binding protein) which was isolated first by binding to the 3'-UTR of protamine-1 mRNA has been shown to be a microtubule-associated protein (Han et al., 1995). TB-RBP is expressed ubiquitously

however the RNA binding activity is restricted to testis and brain. The protein recognizes conserved sequences called Y and H elements in a number of specific RNAs including the 3'-UTR of oligodendrocyte MBP mRNA, and mediates the attachment of mRNAs containing these sequences to microtubules (Han et al., 1995). In the mammalian testis, TB-RBP appears to have the dual functions of translational suppression of stored germ cell mRNAs (Kwon and Hecht, 1991,1993) and of mRNA transport through the intercellular bridges of male germ cells (Morales et al., 1998; Hecht 1998). In mouse brain, TB-RBP is involved in the formation of BC1 RNPs (Muramatsu et al., 1998). Recently, it was shown that TB-RBP associates with mRNPs in a sequence (Y element) dependent manner, and that blocking TB-RBP Y element binding site disrupts and mislocalizes α-CAMKII mRNA localization (Severt et al., 1999).

Spnr (spermatid perinuclear RNA binding protein) is another microtubule-associated RNA-binding protein that localizes to manchette, a microtubule-based structure, in differentiating spermatids (Schumacher et al., 1995). The RNA target of Spnr in vivo is unknown but has previously been suggested to be protamine 1 mRNA (Schumacher et al., 1995). Endogenous Spnr as well as recombinant versions can be precipitated along with murine testis microtubules even in the absence of any other microtubule-associated protein (Schumacher et al., 1998). These results suggest that Spnr, in addition to its function as an RNA-binding protein, might be a microtubule-associated protein.

I.9 Translational regulation during mRNA localization

RNA localization serves to restrict different protein activity to defined regions in the cytoplasm. To achieve this goal, mechanisms must exist to repress mRNAs that have not yet reached their proper destination in the cell. Conversely, once localized another mechanisms must exist to derepress the mRNAs and ensure efficient translation. Indeed, there is increasing evidence that RNA localization is often combined with local translation control (for review, see St Johnston 1995; Curtis et al., 1995; Macdonald and Smibert, 1996).

In recent years, studies in *Drosophila* body patterning have revealed that the mRNA localization and regulation of translation are of equal importance. So far, at least three different types of translational control have been found to act on the localized maternal RNAs, and substantial progress has been made in the identification and characterization of the *cis*-acting elements and *trans*-acting protein factors that mediate these different types of translational regulation. Most strikingly, several cascades of translation control events during oogenesis and embryogenesis have been found to direct the translation of several important body patterning determinants such as bicoid and caudal protein in the anterior, and oskar, nanos and hunchback in the posterior part of the oocyte. Fig.10 lists the cascades of translational control events that control the translation of these morphogenetic determinants. In the following text, I will discuss in more detail the translational regulation acting on the mRNAs encoding these determinants.

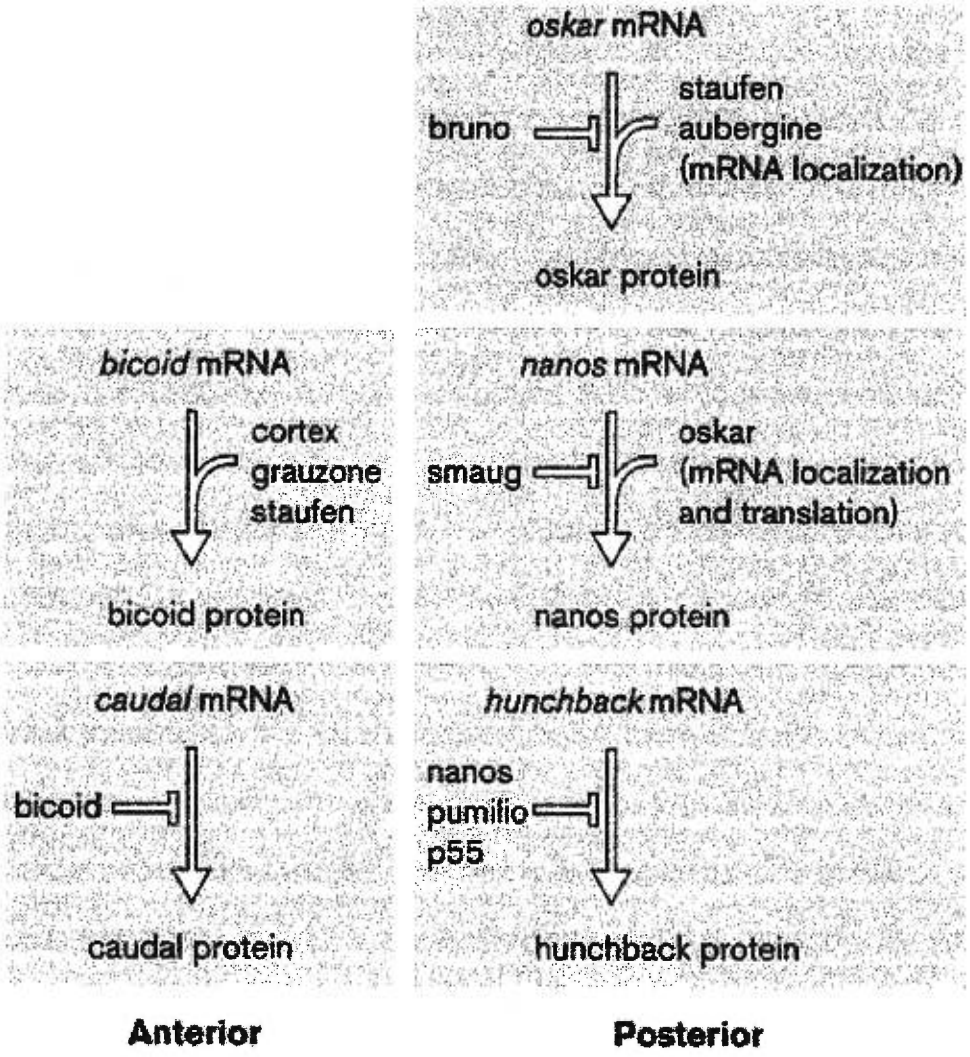

Fig. 10. Parallel cascades of translational control events in *Drosophila* body patterning. The first step in the posterior cascade (top right) occurs largely in the ovary, whereas all other stages are primarily embryonic. Each step in the cascades produces a protein product with a key role in the subsequent step..Multiple genes are required for each mRNA localization step are not indicated individually. Some of these genes may, as with Staufen, act in both mRNA localization and translation. Adapted from Macdonald and Smibert, 1996.

I.9.1 Translational activation by cytoplasmic polyadenylation

In oocytes, untranslated maternal mRNAs are stored in messenger ribonucleoprotein particles where they are bound to a set of proteins thought to "mask" the mRNA from the translational machinery (for review, see Wolffe and Meric, 1996). During meiotic maturation or after fertilization, translation of many of the maternal mRNAs is activated. Early observations in clam oocytes have shown that this activation process is often accompanied by extending of the poly (A) tail (Rosenthal et al., 1983). Elongation of poly(A) tails now appears to be a common mechanism by which maternal mRNAs are unmasked in different systems including mouse, *Xenopus* and *Drosophila* (reviewed by Jackson, 1993; Seydoux et al., 1996). In *Drosophila*, the poly(A) tail of the *bicoid* mRNA is extended after fertilization and bicoid protein is translated at this time (Salles et al., 1994). Full-length *bicoid* mRNA injected into embryos lacking bicoid activity is polyadenylated and can rescue the *bicoid* mutant phenotype. In contrast, *bicoid* mRNA deleted for a portion of its 3'-UTR does not undergo cytoplasmic polyadenylation and does not have rescuing activity. Addition of a synthetic 175-residue poly(A) tail partially restores rescuing activity to the truncated *bicoid* mRNA (Salles et al., 1994). Thus, a long poly(A) tail is required, and appears sufficient, for translation of bicoid protein.

So far, regulated cytoplasmic polyadenylation has been characterized primarily in *Xenopus*. Sequences that mediate this process reside in the 3'-UTR and include the canonical AAUAAA motif required for nuclear polyadenylation and a nearby U-rich sequence (e.g. UUUUAU) called the cytoplasmic polyadenylation element (CPE) (Fox et al, 1989, McGrew et al., 1989, for review, see Richter 1996). CPEs are required for

cytoplasmic polyadenylation but their activity is context-dependent and can be modulated by other sequences present in the 3'-UTR (Stebbins-Boaz and Richter, 1994). Besides *cis*-acting RNA signals, at least three *trans*-acting proteins play a role in the control of cytoplasmic polyadenylation and/or translation. One such protein in *Xenopus* is CPEB (for CPE-binding protein) (Hake and Richter, 1994), which contains two RNA recognition motifs and shares sequence similarity with Orb, an RNA binding protein from *Drosophila* (Lantz et al., 1992, 1994). Immunodepletion of CPEB inhibits the polyadenylation of seven CPE-containing mRNAs in *Xenopus* egg extracts (Stebbins-Boaz et al., 1996), suggesting that this protein may be required generally for cytoplasmic polyadenylation during oocyte maturation. A second factor identified biochemically is the cleavage and polyadenylation specificity factor (CPSF), a multi-subunit factor that binds preferentially to RNAs containing the CPE and AAUAAA sequences. This factor is required for nuclear polyadenylation but is probably also critical in cytoplasmic polyadenylation (Bilger et al., 1994). Finally, poly(A) polymerases have been detected immunologically in the cytoplasm of Xenopus oocytes and are likely related to their counterparts in nuclei (Ostareck-Lederer et al., 1994). Recently, two loci in *Drosophila*, *cortex* and *grauzone*, have been shown to be required for the cytoplasmic polyadenylation and translation of *bicoid* and other maternal mRNAs (Lieberfarb et al., 1996). Mutations in the genes *cortex* and *grauzone* disrupt cytoplasmic polyadenylation in both the ovary and the embryo, leading to both abbreviated and hyperextended poly(A) tails. These opposite effects suggest that both genes may be involved in the regulation of cytoplasmic polyadenylation (Lieberfarb et al., 1996). It will be interesting to determine whether proteins encoded by these loci correspond to some of the biochemically defined

components identified in other systems. The effects of polyadenylation on *bicoid* mRNA translation comprise part of a cascade of translational regulation, acting in anterior body patterning.

I.9.2 Translational activation by localization

Oskar and *nanos mRNAs* are required for formation of the posterior region of *Drosophila*, and both mRNAs are localized to the posterior pole of the oocyte and early embryo (reviewed by St Johnston, 1995). To reach that destination, the mRNAs must move across the oocyte after they enter the anterior end of the oocyte from nurse cells. Translational repression of *oskar* mRNA during this transit is mediated by the 68 kDa protein Bruno, which binds to Bruno responsive elements (BRE) in the *oskar* 3'-UTR and colocalizes with oskar mRNA to the posterior pole (Kim-Ha et al., 1995, Webster et al., 1997). Three BREs are present in the *oskar* 3'-UTR that share a 7- to 9-nt motif; mutations in these elements abolish Bruno binding *in vitro* (Kim-Ha et al., 1995). In oocytes produced by females with a transgene lacking BREs (*oskar*-BRE$^-$), *oskar* is prematurely translated during stages 7 and 8 producing gain-of-function phenotypes with double-posterior regions in progeny embryos (Kim-Ha et al., 1995). Repression by Bruno may involve deadenylation, as a rapid deadenylation signal in Eg2 mRNA of Xenopus contains consensus BRE sequence that may interact with a Xenopus homologue of Bruno Etr (Bouvet et al., 1994; Webster et al., 1997). However, regulation of *oskar* mRNA does not appear to be accompanied by changes in its poly(A) length (Webster et al., 1997). Activation of *oskar* mRNA translation, or relief from bruno repression, accompanies the posterior localization of *oskar* mRNA. Mutants that prevent *oskar* mRNA localization

lack oskar activity (Markussen et al., 1995; Rongo et al., 1995). However, when the Bruno-mediated repression is eliminated, most of these mutants regain oskar activity proving that localization does indeed activate translation.

Stau, a gene that is required for *oskar* mRNA localization, is also needed for the accumulation of oskar protein even when Bruno-mediated repression is eliminated (Kim-Ha et al., 1995). Thus, Staufen acts in at least two process: the localization and translation of *oskar* mRNA. Staufen contains 5 dsRBDs (dsRBD1, 3, and 4 can bind dsRNA whereas dsRBD2 and dsRBD5 only contain half-consensus dsRNA-binding domains and therefore can not bind dsRNA *in vitro*, Micklem et al., 2000). When a transgene bearing a dsRBD5 deletion ($Stau^{\Delta dsRBD5}$) is introduced into flies lacking wild type Stau, $Stau^{\Delta dsRBD5}$ completely rescues the posterior localization of *oskar* mRNA. However, the localized RNA can not produce Oskar protein suggesting that domain 5 is required to activate the translation of oskar mRNA at the posterior pole (Micklem et al., 2000). Interestingly, when the $Stau^{\Delta dsRBD5}$ transgene is crossed into the Stau null and osk BRE^{-} background, $Stau^{\Delta dsRBD5}$ activates the translation of derepressed *oskar* mRNA. This experiment further suggests that dsRBD5 is specifically required for the activation of translation once the mRNA has been localized. The significance of this linkage is still unknown. Besides Staufen, another translational activator of *oskar* mRNA is encoded by *aubergine* (Wilson et al., 1996). The role of this gene seems to act during the later stages of oogenesis and not to override bruno-mediated repression.

Recently, a discrete element situated at the 5'-UTR of *oskar* mRNA has been demonstrated to specifically activate the translation of the RNA (Gunkel et al., 1998). This element is only active at the posterior pole and is only required when the transcript

is repressed through the BRE, suggesting that it functions as a derepressor of BRE-mediated repression rather than as a simple enhancer of translation. Interstingly, two proteins of 50-(p50) and 68-kDa (p68) selectively bind to the derepressor element, and this binding is related to the translational derepression (Gunkel et al., 1998).

As with *oskar* mRNA, the *Drosophila* posterior determinant *nanos* mRNA is localized at the posterior pole of the oocyte although at a much later stage of oogenesis. Similarly to *oskar* mRNA, translation of *nanos* mRNA depends on this posterior localization as delocalized transcripts are translationally repressed (Gavis and Lehmann, 1994). Much of the recent work in this area focuses on how nonlocalized *nanos* mRNA is translationally repressed. Repression of mislocalized nanos RNA requires stem-loop structures in its 3'-UTR that most likely interact with the embryonic protein Smaug (Gavis et al., 1996; Smibert et al., 1996; Dahanukar and Wharton, 1996). Smaug binds specifically to two sites called Smaug reponse elements (SRE) in the *nanos* mRNA 3'-UTR (Smibert et al., 1996). When these sites are mutated, a fraction of nanos mRNA that fails to be localized under normal conditions is now translated. Consequently, body patterning is perturbed with lethal consequences therefore, regulation of nanos translation is essential. Activation of *nanos* mRNA translation in the posterior requires Oskar (Gavis and Lehmann, 1994) and the Vasa protein (Gavis et al., 1996), a posteriorly localized RNA helicase (Liang et al., 1994). Thus, Vasa protein might remove a uniformly distributed repression by destabilizing an RNA secondary structure to which the repressor binds.

I.9.3 Spatial or temporal regulation of translational repression

The end result of translational activation through mRNA localization is to generate a localized source of protein. Another way to achieve this goal is to locally inhibit a uniformly distributed mRNA. In recent years, several examples of locally repressed mRNAs have been described in *Drosophila* oogenesis and early embryogenesis.

The first example comes from *caudal* mRNA. The *caudal* mRNA codes another homeodomain transcription factor and is uniformly distributed in the oocyte (Mlodzik et al., 1985). Remarkably, the homeodomain transcription factor Bicoid binds to the Bicoid response element in the 3'-UTR of *caudal* mRNA and is required for translational repression of this RNA (Dubnau and Struhl, 1996; Rivera-Pomar et al., 1996). Thus, once *bicoid* mRNA is activated, the anterior-posterior gradient of Bicoid protein will silence the uniformly distributed *caudal* mRNA at the anterior region, resulting in the creation of an opposite Caudal protein gradient in the posterior which promotes the development of posterior structures in the *Drosophila* embryo.

At the posterior end of the oocyte, a superficially analogous cascade of translational regulation occurs. *hunchback* mRNA, which is spread throughout the embryo and encodes a transcriptional regulator of the anterior gap genes, must be repressed in the presumptive posterior (Tautz, 1988). This repression is mediated by nanos response elements (NREs) in the 3'-UTR of the *hunchback* mRNA and is dependent on nanos protein (Wharton and Struhl, 1991). Recent analyses have revealed that nanos does not interact detectably with the NRE. In contrast, a protein called Pumilio and another unidentified 55-kDa protein (p55) directly bind to this sequence. Binding of

pumilio to maternal *hunchback* mRNA is required for posterior patterning of *Drosophila* embryos (Murata et al., 1995). The interaction of pumilio-*hunchback* mRNA is functionally significant, as the repression of *hunchback* mRNA translation is defective in *pumilio* mutant embryos. The role of the 55 kDa factor however, is less clear. The finding that pumilio binding is important for *hunchback* repression suggested a model in which pumilio first binds the NRE of *hunchback* mRNA to form a core complex and subsequently recruits Nanos protein to form a translational-repression competent complex (Murata et al., 1995).

I.10 Summary: A model for cytoplasmic RNA localization

Intracellular RNA localization is used by many polarized cells as a means of generating regional distribution of proteins at distinct functional microdomains. Whereas the types of localized transcripts vary, mRNA localization in all systems shares several common features (Wilhelm and Vale, 1993; St Johnston, 1995; Bassell and Singer, 1997; Carson et al., 1998, Kiebler and DesGroseillers, 2000). First, most of the localized RNAs contain *cis*-acting localization signals that generally reside in the 3'-UTR of the transcripts. Second, the transport of localized RNAs from the nucleus to their final destinations depends on either microtubules or microfilaments as tracks. Third, RNA transcripts are anchored at their sites of localization through attachment to cytosketal elements and then activated for local translation. Fourth, most of the localized RNAs

have been observed as granules or particles that is closely associated with the cytoskeleton. In some cases the components of the translational machinery are colocalized with the granules. Moreover, several studies report microtubule- or microfilament-dependent movements of these RNA granules in living cells at rates consistent with the caculated velocities of certain microtubule- or microfilament-directed motor proteins. These lines of evidence point out a model of active RNA transport along the cytoskeleton at distinct steps or events (see Fig. 11). These events involve: 1) the recognition of the RNA *cis*-acting signals, mostly localized in the 3'UTR of the transcripts, by specific trans-acting factors and the assembly of the initial RNP particle, 2) the formation of transport-competent large RNA-protein complexes, 3) the migration of these complexes to their final destination via elements of the cytoskeleton, and 4) the anchoring of the localized RNA to the cytoskeletal component to allow local translation of the transcripts.

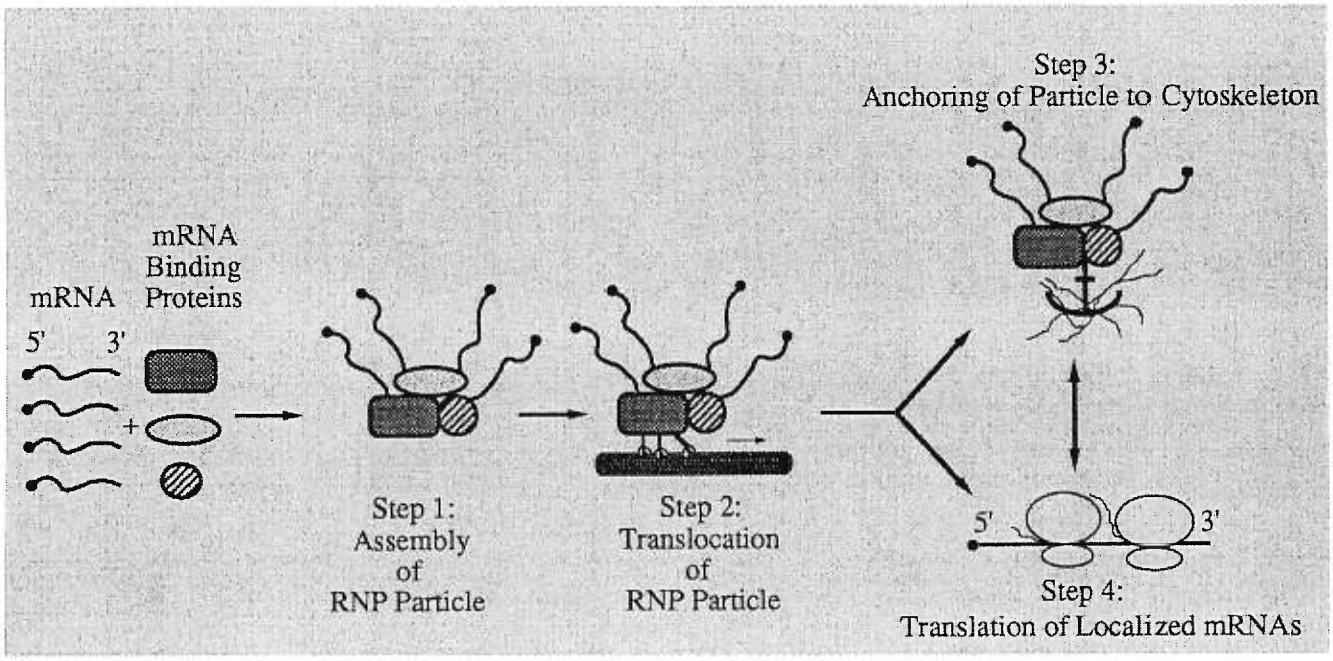

Fig. 11. A model of mRNA transport pathway. See text for details, adapted from Wilhelm and Vale, 1993.

I.11 Objectives and strategies of research

As I have described in the previous sections, asymmetric mRNA localization has emerged as a powerful means of intracellular protein targeting in all polarized cell types. Based on investigations of a large number of localized RNAs in different organisms, an ordered pathway for mRNA localization has been proposed including several successive steps (see Fig. 11). In this pathway, the formation of a multi-component ribonucleoprotein (RNP) complex is the key step for RNA localization. To date, extensive studies have been done to map the *cis*-acting elements required for RNA localization and in most cases, these signals reside in the 3'UTR of the localized RNAs. However, the *trans*-acting proteins in the RNP complex that are involved in RNA transport, anchoring and translation regulation are poorly understood. Staufen, a double-stranded RNA-binding protein (dsRBP), is so far the best-demonstrated *trans*-acting protein required for RNA transport and translation regulation during *Drosophila* early embryonic development. This dsRBP interacts specifically through one or more dsRBDs with the 3'UTRs of *bicoid* and *oskar* mRNAs at the anterior pole of the embryo and the posterior pole of the oocyte, respectively. In *Drosophila* neuroblasts, it also serves to localize *prospero* mRNA properly. To understand the mechanisms of mRNA transport in mammals and determine the nature of the RNA-binding protein involved in this process, the research projects outlined in this thesis are aimed at studying the mammalian homologue of the *Drosophila staufen* gene and to characterize its encoded protein from several different approaches.

❖ **Characterization of the transcription initiation sites of the human and mouse *stau* genes and isolation of the putative promoter region of mouse *stau***

From previous work of our laboratory, the human and mouse *staufen* cDNAs were partially cloned from a human central nervous system and a mouse embryo cDNA library, respectively. In order to get information on the transcription initiation site of the human or mouse *staufen* gene, two experimental approaches have been used. The first approach is to clone and sequence the most 5' end of human and mouse *stau* transcripts by 5' RACE and cDNA library screening. A second approach is to screen a mouse genomic library to clone the 5' flanking region of mouse *stau* gene and to isolate the possible promoter region. The positive genomic DNA clones were subcloned and sequenced. The results are presented in Article 1 in the following chapter.

❖ **Molecular characterization of human Staufen proteins and their subcellular localization in mammalian cells**

As a first step in characterizing the encoded protein of the *staufen* gene, I first used a Western blotting assay to investigate the expression of endogenous Staufen protein in different human cell lines. Two mammalian *Staufen* isoforms were observed in this experiment. Subsequently, I have transiently transfected different clones of human staufen cDNAs into mammalian cells and confirmed that these cloned cDNAs can produce different proteins that co-migrate with the two endogenous isoforms. Using double labelling immunofluorescence microscopy, we

further studied the localization of each cloned human Staufen isoform. The experimental results are presented in Article 2.

❖ **Determination of the molecular determinants involved in hStau ribosome- and RER-association**

By confocal microscopy, we (Article 2, Wickham et al., 1999) and others (Marion et al., 1999) have determined that hStau is localized to the rough endoplasmic reticulum. Using sucrose gradient sedimentation analysis, the latter group further demonstrated that hStau is also associated with polysomes (Marion et al., 1999). To get more insight into the subcellular localization of different hStau isoforms, I have used a discontinuous sucrose gradient sedimentation assay to examine the association of hStau with the RER or ribosomes in the same sucrose gradient. Together with immunofluorescence microscopy, I have examined the localization of endogeneous Stau isoforms and a series of hStau mutants expressed in *trans*. These experiments have allowed us to determine the difference in localization of two endogenous Stau isoforms and to map the molecular determinants involved in hStau RER and ribosome association. The results of these studies are presented in Article 3.

❖ **Study of the potential function of hStau involved in RNA transport**

The overall organization of human and mouse proteins and their corresponding dsRBDs are quite similar to that of *Drosophila* Staufen protein (Article 2). Thus, the mammalian protein most probably has conserved functions with its *Drosophila* counterpart. Biochemical studies have revealed that mammalian Staufen has the capacity of binding RNAs and microtubules (Article 2), and is associated with the

RER and ribosomes *in vivo* (Article 3). Since microtubules and the RER have been demonstrated to be involved in intracellular RNA localization and ribosomes serve as the machinery for protein translation, the distinct properties of mammalian Staufen have made it a good candidate for mRNA transport, localization and local translation regulation. To gain direct clues in the function of mammalian Staufen in RNA transport and localization, I have taken part in the study of hStau in neurons and in HIV-1 infected mammalian cells. The work in these studies was a collaboration with two different groups.

In cultured rat hippocampal neurons, we transiently transfected a hStau-GFP fusion protein and followed its expression in living neurons in real time by time lapse-videomicroscopy. This experiment has allowed us to study hStau-involved granule formation and its movement in distal dendrites and to characterize a novel microtubule-dependent transport pathway involving RNA-containing granules with Staufen as a core component (see Article 4). Finally, in human immunodeficiency virus type 1 (HIV-1) infected cells, the role of hStau in HIV-1 genomic RNA selection, intracellular transport and virion encapsidation has been explored (Mouland et al., 2000, not included in this thesis).

II- Article 1

Genomic Organization of the Human and Mouse *stau* Genes

Frédéric Brizard, Ming Luo, and Luc DesGroseillers

DNA and Cell Biology, 2000 19(6):331-339

My contribution:

In this paper, I isolated three *stau* genomic DNA clones that may contain the putative promoter region from a mouse genomic library. Positive clones were subcloned and the DNA sequence upstream of the 5' untranslated region of mouse *stau* (*mstau*) cDNA was sequenced (see Fig. 3). In order to determine *mstau* gene transcription initiation site, different 5'RACE approaches have been applied. A single transcription start site was observed in *mstau* gene. Similar 5'RACE approaches were applied to *hstau*, and both genes have conserved transcription initiation sites at the same position (see Fig. 3). Analysis of genomic sequence has revealed that an extremely G+C-rich region is present upstream of the transcription initiation site. This region lacks the canonical TATA and CAAT boxes but harbours multiple SP-1 binding consensus sequences, suggesting that a housekeeping-like promoter drives the broad expression of Staufen in mammalian cells. F. Brizard did the full mapping of human and mouse *stau* intron/exon junction sites.

DNA AND CELL BIOLOGY
Volume 19, Number 6, 2000
Mary Ann Liebert, Inc.
Pp. 331–339

Genomic Organization of the Human and Mouse *stau* Genes

FRÉDÉRIC BRIZARD, MING LUO, and LUC DESGROSEILLERS

ABSTRACT

Mammalian Staufen is a double-stranded RNA-binding protein potentially involved in mRNA transport and localization. Recently, we reported that the human gene is located on chromosome 20, region q13.1. We now report the genomic organization of both the human and mouse *stau* genes. Amplification of genomic DNA and sequencing of the resulting PCR products indicated that the human and mouse genes are fragmented into 15 and 12 exons, distributed over at least 65 and 17 kb of genomic DNA, respectively. The three additional exons found in the human gene are subjected to differential splicing, generating four different transcripts. Corresponding exons have not been found in mouse transcripts. Apart from those three exons, the overall organization of the *stau* gene is similar in the two species, and the positions of the exon–intron junctions are perfectly conserved. Even an alternative choice between two splicing acceptor sites, which causes an insertion of 18 nucleotides in exon 5, is conserved in both humans and mice. An extremely G+C-rich region lacking canonical TATA and CAAT boxes was found upstream of the most 5′ RACE sequence, suggesting that a housekeeping-like promoter drives the broad expression of Staufen in mammalian cells. This work represents the first step toward production of knockout mice and the elucidation of putative Staufen-linked hereditary diseases in humans.

INTRODUCTION

In eukaryotes, RNA-binding proteins play critical roles in diverse biologic functions such as pre-mRNA processing, translational regulation, and the establishment of cell polarity. Characterization of these proteins has led to the identification of several RNA-binding motifs (Burd and Dreyfuss, 1994). One of these specifically binds double-stranded RNAs (dsRNAs), RNA with extensive secondary structure, or both. The double-stranded RNA-binding domain (dsRBD) consists of a 65- to 68-amino acid consensus sequence that is required for binding (St. Johnston *et al.*, 1992). Short domains, which retain the last 21 amino acids at the C-terminal end of the complete motif, are usually present in RNA-binding proteins, along with the complete domain. These short domains do not bind dsRNA. Proteins bearing these motifs are involved in diverse cellular functions such as protection against viral pathogens (Feng *et al.*, 1992; Burd and Dreyfuss, 1994), upregulation of some HIV-1 genes (Gatognol *et al.*, 1991), adenosine deamination (Wang *et al.*, 1995), and mRNA transport (reviewed in Kiebler and DesGroseillers, 2000).

In our laboratory, we have cloned human and mouse cDNAs coding for the mammalian Staufen homolog (Wickham *et al.*, 1999). In *Drosophila*, Staufen (Stau) is a dsRNA-binding protein involved in the asymmetric localization of specific mRNAs that are required for oocyte polarization (St. Johnston, 1995). Genetic and molecular studies have shown that Staufen is required to properly target *oskar* and *bicoid* maternal mRNAs, an activity that is essential for anterior–posterior axis formation in a developing *Drosophila* oocyte (reviewed in St. Johnston, 1995). Later, during larval development, Staufen is expressed in neurons, where it is part of a process leading to the asymmetric division of mitotic neurons and hence is involved in cell fate decisions (Li *et al.*, 1997; Broadus *et al.*, 1998). Mammalian Staufen is a member of the double-stranded RNA-binding family and has four dsRBDs, which correspond to domains 2 to 5 of *Drosophila* Staufen (see Fig. 3B). In mammals, Staufen is expressed in most, if not all, tested tissues (Marión *et al.*, 1999; Wickham *et al.*, 1999). *In vitro*, Staufen binds dsRNAs, although with no apparent sequence specificity, and tubulin (Marión *et al.*, 1999; Wickham *et al.*, 1999). Accordingly, in neurons, Staufen is found in close proximity to microtubules, and its presence in dendrites is dependent on an intact microtubule network (Kiebler *et al.*, 1999; Köhrmann *et al.*, 1999).

University of Montreal, Department of Biochemistry, Montreal, Canada.

TABLE 1. OVERLAPPING PCR PRODUCTS AMPLIFIED FROM MOUSE *stau* GENE

PCR number[a]	Primer sequence 5' → 3'[b]	PCR method[c]	PCR annealing T (°C)	Expected size (kbp)	PCR product size (kbp)
PCR 2	TAATGCTGCTGAGAACATGCTGG TGCCCTGGTGAAATCTTTGGTG	Taq	55	0.301	1.5
PCR 55	CCATCCATCCAGACAGAAACCAGCCCCAAC GCACTAGGAGCCACAATGCTCTTCCCC	ELTP	63	0.784	0.7
PCR 62	CATGGTATCGGCAAGGATGTGGAGTC GTCCGTTTCCTGTTCTTGGCATCTCTG	ELTP	63	0.115	0.5
PCR 67	CAGTTGGGGAATTTGTAGGGGAAGGAGAAGGG GCGACGTGGAAGACCTCGTTCTG	Taq	61	0.281	1.8
PCR 68	GGATGAATCCTATTAGTAGACTTGCAC TCTCTTCTGATTTGAGTGCTGGCTTGGCAGGC	Taq	61	0.261	0.9
PCR 84	GACCCTTACTCTCGGATGCAGTCCACC GGGCATCGTGTTTCACGGGTGGTCTCATC	ELTP	63	0.178	1.1
PCR 85	GACCACCCGTGAAACACGATGCCCC CAAAATTCACAGGCAAATTCCGCTTC	ELTP	57	0.174	3.4
PCR 86	GGAAGAGAAGCAGAGGAAGAAAACC GCCTCCTAAGCTGCTCCAGAACAGCC	ELTP	57	0.256	5.6
PCR 92	TAATGCTGCTGAGAACATGCTGG TAGTCCCATTTTCATCCCCA	Taq	58	0.164	1.3
PCR 93	GTCGGGGTTAGTCAAGGACACCACACCAAAG CTCCACATCCTTGCCGATGCC	Taq	58	0.336	0.8
PCR 94	CTGCACTGAACATTTTAAAGCTGCTGTC CAGCACAACCAGGGCTACCAC	Taq	55	0.267	0.5

[a]Only PCR fragments representing the last step of intron characterization are shown.
[b]The first and second primers represent forward and reverse oligonucleotides, respectively.
[c]PCRs were performed as described in Materials and Methods.

Significant colocalization of Staufen with an endoplasmic reticulum marker was also observed. Both endogenous Staufen and transiently expressed Staufen–green fluorescent protein (GFP) are found in ribonucleoprotein particles, as visualized by the RNA-specific dye SYTO14 (Kiebler *et al.*, 1999; Köhrmann *et al.*, 1999). When transfected into neurons, Staufen-GFP forms granules that move in a saltatory fashion from the cell body into dendrites and vice versa (Köhrmann *et al.*, 1999). In fibroblasts, confocal microscopy showed that both the endogenous and the overexpressed Staufen colocalize with markers of the rough endoplasmic reticulum but not with other intracellular or organellar markers (Marión *et al.*, 1999; Wickham *et al.*, 1999). From all these studies, it is now apparent that Staufen is involved in mRNA transport and localization in mammals.

We previously reported that the human *stau* gene maps to chromosome 20q13.1 (DesGroseillers and Lemieux, 1996). In this paper, we report the exon–intron organization of the human and mouse *stau* genes and show that their genomic organization is conserved, demonstrating that the two genes are derived from a common ancestor. This study should facilitate the eventual production of knockout mice in order to find the role of mammalian Staufen *in vivo*.

MATERIALS AND METHODS

Isolation of genomic DNA

Genomic DNA was extracted and purified from the kidneys of BALB/c mice using the DNA purification kit (Boehringer Mannheim, Laval, Québec, Canada) according to the manufacturer's instructions. Human genomic DNA isolated from whole blood also was purchased from Boehringer Mannheim.

PCR-based methods for genomic mapping

The PCR amplifications of the murine and human *stau* genes were carried out using the primers described in Tables 1 and 2. Primers were designed and melting temperatures (T_m) were calculated with the OSP program (Hillier and Green, 1991). Amplifications were done in a programmable thermocycler (Perkin Elmer, Palo Alto, CA, USA) according to the PCR protocols described below.

Standard amplifications (Taq DNA polymerase)

Amplifications (<2.5 kb) were carried out in a total volume of 50 μl in the presence of 0.2 mM each dNTP (Boehringer

TABLE 2. OVERLAPPING PCR PRODUCTS AMPLIFIED FROM HUMAN *stau* GENE

PCR number[a]	Primer sequence 5' → 3'	PCR Method	PCR annealing T (°C)	Expected size (kbp)	PCR product size (kbp)
PCR 15	GTGGGTAAAGGATGTGGGCAGCAGCAG CGCAGGGCTACCAGGTTTTCCATACGG	ELTP	65	1.137	1.1
PCR 48	CCATCTGCTGCTCTCTCAGGGAGCC CCTCGGGGGATAAGCACCTCCTCTC	Other	63	0.315	~ 15
PCR 61	CATGGTATCGGCAAGGATGTGGAGTC GTCCGTTTCCTGTTCTTGGCATCTCTG	ELTP	63	0.115	1.2
PCR 63	GGTTGGGGAGTTTGTGGGGGAAGGTG CTGTGAGGAGCGTGTACTCTGG	Taq	61	0.266	1.3
PCR 64	GGGGATCAATCCGATTAGCCGAC CTGACTTGAGTGCGGGTTTGGTGGGC	ELTP	57	0.257	3.2
PCR 71	TAATGCTGCTGAGAACATGCTGG TAGTCCCATTTTCATCCCCA	Taq	55	0.164	1.6
PCR 72	ACACCCATAAAGAAACCAGG TGCCCTGGTGAAATCTTTGGTG	Taq	55	0.213	0.4
PCR 75	CCACTTAACCTCTCAGAACTGAAC TGGCTCCCTGAGAGAGCAGCAGATGGGTTC	Other	63	0.205	7.4
PCR 87	GACCCTTACTCTCGGATGCAGTCCACC CGCTTTGGCAGCAGCATCGTGTTTCGC	ELTP	63	0.189	2.3
PCR 88	GCGAAACACGATGCTGCTGCCAAAGCG CTCGAAATTCACAGGCAAGTTCCGTTTAAGTGC	ELTP	60	0.168	~ 15
PCR 89	GCACTTAAACGGAACTTGCCTGTGAATTTCGAG CTGTGAGGAGCGTGTACTCTGG	ELTP	60	0.352	~ 15
PCR 95	GGTCGCCCAGGCTGTAGGAGTTAG GATCAGAGGTGGCTGAGAGGAG	Taq	58	0.322	0.9
PCR 96	CGCTGAACATCTTAAAGTTGCTGTCTG CTGCTGCTGCCCACATCCTTTACCCAC	Taq	58	0.234	1.3

[a]See footnotes to Table 1.

Mannheim), 0.5 μM each primer, 100 ng of genomic DNA, and 1.5 U of *Taq* DNA polymerase (Pharmacia, Baie d'Urfé, Québec) in 1.5 mM $MgCl_2$, 50 mM KCl, 10 mM Tris HCl, pH 8.3, 0.001% gelatin. Amplification conditions were 35 cycles at 94°C for 45 sec, at the annealing temperature (as specified in Tables 1 and 2) for 45 sec and at 72°C for 2 min with a 5-sec extension time per cycle.

Long-range PCR amplifications

Genomic DNA (100 ng) was incubated with 0.5 μM each primer, 0.35 mM each dNTP, and 2.6 U of Expand™ Long Template PCR (ELTP) polymerase (Boehringer Mannheim) in 1× Buffer 1 (Boehringer Mannheim) in a total volume of 50 μL. The PCR samples 48 and 75 were prepared with 0.50 mM each dNTP and 1× Buffer 2. Perfect match solution (Stratagene, La Jolla, CA) was added to PCR 15. Amplification conditions were an initial denaturation step at 94°C for 2 min, followed by 30 cycles at 94°C for 45 sec, at the annealing temperature (as specified in Tables 1 and 2) for 90 sec and at 68°C for either 2 min (PCRs 15, 61, 62, 87), 5 min (PCRs 64, 86), 8 min (PCRs 55, 84, 85), or 10 min (PCRs 88, 89). The elongation step at 68°C was extended 20 sec per cycle for the last 20 cycles. All programs ended with a final extension step at 68°C for 7 min.

DNA sequencing

The amplified DNA fragments were separated on 1%–4% agarose gels and visualized by ethidium bromide staining. When necessary, isolated fragments were cloned in pCR2.1 (Invitrogen, Carlsbad, CA) for sequencing. Exon–intron boundaries of cloned fragments were identified by nucleotide sequencing according to the Sanger dideoxynucleotide chain termination method with T7 DNA polymerase (Pharmacia). The exon–intron boundaries of many PCR fragments were directly

TABLE 3. EXON–INTRON BOUNDARIES IN MURINE *stau* GENE

Exon number[a]	INTRON 3'-acceptor site	EXON 5'-end	Size (kbp)	3'-end	INTRON 5'-donor site	Intron size (kbp)
1		GGCGGGC	(>0.265)	CAGCCAG	gtaagg....	?[b]
2	...	AAAGTAT	(0.139)	CCCCCAG	gtatgtg...	0.9
3	...accettgtgtttgtag	ATACTTT	(0.166)	GTTGGAG	gtaaggt...	3.2
4	...attactcttctgtcag	GTAAATG	(0.099)	TTTTGAG	gtaagcc...	5.3
5a	...tcacgctttcactcag	TCTTTCCT	(0.231)			
or						
5b	...agtctttccttctgacacag	GTGGCCC	(0.213)	CTGCAAG	gtagagc...	1.5
6	...tgtctttcagctacag	ACAGCCC	(0.138)	GATGCAG	gtgagtt...	0.6
7	...ttggtgttttacacag	GTAAAGG	(0.147)	AGAGAAG	gtgactg...	1.1
8	...atttttctttcttaag	ACTCCAG	(0.076)	GGAACTA	gtaaggt...	0.2
9	...ctgtgtcccctgcgag	GTAACAA	(0.320)	ATTCCAG	gtaaccg...	0.5
10	...tgctgtttttccttag	GTTGAAT	(0.123)	TGATATG	gtatgtg...	0.4
11	...tcattcaccttttctag	GCTGCAC	(0.086)	TTTCAGC	gtgagtgc...	0.3
12	...ttcttcttcctaaag	GTGCGGG	(>0.991)	CTAGTGC		
Consensus	$(y)_{12}$ n c a g (65 100 100)	N		AG (64 73)	g t a a g t (100 100 62 68 84 62)	

[a]Exon 1 is defined according to the 5′ end of the cDNA.
[b]The size of this intron appeared to exceed the potential of the Expand™ Long Template PCR.

sequenced using the Thermo Sequenase™ cycle sequencing kit (Amersham Life Science, Oakville, Ontario, Canada) or the SequiTherm EXCEL™ DNA Sequencing kit (Epicentre Technologies, Markham, Ontario).

Isolation of genomic clones

Mouse and human genomic DNA libraries were screened with the 5′-most *Eco*RI-*Sac*I fragment of the cDNA (nt 1–225). The probe was labeled with [α-^{32}P]-dCTP using an Oligolabelling kit (Pharmacia). Phage DNA was isolated and purified, and restriction fragments were subcloned in pBluescript SK$^+$ (Stratagene) for sequencing.

RESULTS

Genomic organization

In order to identify exon–intron junctions, we PCR-amplified genomic DNA using oligonucleotide primers that generated overlapping fragments covering the whole nucleotide sequence of the human and mouse cDNAs (Tables 1 and 2). Because PCR fragments could be of any size, we elaborated several PCR conditions. The resulting fragments were either cloned and then sequenced or directly sequenced by PCR to confirm the presence of introns and precisely map their position in the genomic DNA fragments. In both mouse and human, only the primer pairs covering the 3′-untranslated region (3′-UTR) amplified a fragment whose size was identical to that of the corresponding region in the cDNA, demonstrating that the 3′-UTR is not fragmented. In contrast, all other fragments were larger than the corresponding region in the cDNA, suggesting that multiple introns are spread throughout both genes. When necessary, pairs of nested oligonucleotide primers were used until each intron had been identified. This allowed us to define the position of the introns, the sequence of the exon–intron junctions, and the size of each intron in both humans and mice (Tables 3 and 4). A schematic representation of the genomic organization of the human and mouse *stau* genes is presented in Figure 1.

The human and mouse genes spanned at least 65 and 17 kb of genomic DNA and consisted of 15 and 12 exons, respectively. The three additional exons found at the 5′ end of the human gene were not found in mice and have been labeled E1a, E1b, and E1c, for consistency with the mouse gene. These exons were identified from alternatively spliced transcripts (Fig. 2A) (Wickham *et al.*, 1999). The size of the exons ranged from 75 bp (E1b) to >1270 bp (E12) in humans and from 76 bp (E8) to >991 bp (E12) in mice. The introns ranged in size from 0.2 kb (E8–E9) to about 15 kb (E1c–E2 and E3–E4) in humans and from 0.2 kb (E8–E9) to about 5.3 kb (E4–E5) in mice. All splice sites re-

TABLE 4. EXON–INTRON BOUNDARIES IN HUMAN *stau* GENE

Exon number[a]	INTRON 3'-acceptor site	EXON 5'-end	EXON Size (kbp)	EXON 3'-end	INTRON 5'-donor site	Intron size (kbp)
1				...CAGCCAG	...	?[b]
1a	...	CAGCAGC	(0.132)	TTACAGG	...	?[b]
1b	...	AGTTTAT	(0.075)	AAAAAAG	gtacat...	7.2
1c	...cctttacaacttttag	GTAGAAC	(0.289)	GCTGCAG	gtaagca....	~15
2	...ttctttttctttgcag	AAAGCAT	(0.139)	CCCCGAG	gtatgtg...	2.1
3	...ctcctttttatttctag	GTACTTT	?	...	...	~15
4	...	...	?	TTTCGAG	...	~14
5a	...gctttcactcag	TCTTTCC	(0.231)			1.0
or 5b	...agtctttcccctctgaaacag	GTGGCCC	(0.213)	AGTCAAG	gtgagaa...	
6	...cttgtttgttcctcag	CCACAGA	(0.144)	GATGCAG	gtgggtc...	3.0
7	...tgacttctttgtgcag	GTGAAGG	(0.147)	GGAGAAG	gtgagtg...	1.4
8	...ttcttctttttttaag	ACACCCA	(0.076)	GGGACTA	gtaagtg...	0.2
9	...tgtatgtcccctcccag	GTAATAA	(0.320)	ATTCCAG	gtaactg...	0.6
10	...ctctttttcccccttag	GTTGAAT	(0.123)	TGATATG	gtacgtc...	1.1
11	...ttccattccccactag	GCTGCGC	(0.086)	TGTCTGT	gtgagtg...	1.1
12	...tttttcttccttaaag	GTGTGGG	(>1.270)	CCCTGCG		
Consensus	$(y)_{12}$ n c a g (65 100 100)	N		AG (64 73)	G t a a g t (100 100 62 68 84 63)	

[a]Exon 1 is defined according to the 5′ end of the cDNA.
[b]The size of these introns appeared to exceed the potential of the ELTP.

spected the GT (5′-end) and AG (3′-end) consensus rule. Interestingly, very large introns were concentrated at the 5′ end of the gene, while smaller ones were found downstream. The ATG initiation start site generating the 55-kD protein (Wickham *et al.*, 1999) was found in E2. An additional ATG, found exclusively in the human genome, was located in the differentially spliced E1c and generated the 63-kD protein (Fig. 1). In both humans and mice, another differential splicing event generates two transcripts, which differ by an insertion of 18 nt in the coding region (Duchaîne and DesGroseillers, unpublished work). Our data now show that this phenomenon is attributable to an alternative choice of splicing acceptor sites at the 5′ end of E5 (Tables 3 and 4); (Fig. 2B). Altogether, our results demonstrate that the overall organization of the *stau* gene is similar in the two species and that the position of the exon–intron junctions is perfectly conserved.

With both human and mouse genomic DNAs, we have not been able to PCR amplify the most-5′ intron of the genes, even if we amplified the corresponding cDNA sequences using the same conditions and primers (data not shown). It is likely that the size of these introns exceeded the capacity of ELTP. To overcome this problem, we screened human and mouse genomic libraries with the 5′-most cDNA fragment as a probe. Although no clone was retrieved from the human library, many overlapping clones were isolated and purified from the mouse library. Restriction mapping and DNA sequencing (Fig. 3) allowed us to map the position of the first intron in mice. A splicing consensus sequence is found where the cDNA and genomic sequences diverged (Table 3). Exon E2 was not found in these clones, confirming the large size of this intron.

Characterization of the 5′ flanking sequence

To characterize the 5′ flanking sequence of the mouse *stau* gene, we sequenced the genomic DNA clone in the region that corresponds to the 5′ end of the cDNA (Fig. 3). In parallel, we used the 5′ RACE approach to determine the transcription initiation site(s). Purified mRNA was reversed transcribed with Staufen-specific primers, and the resulting fragments were elongated at their 3′ ends with terminal transferase, PCR amplified, cloned, and sequenced. This technique was repeated

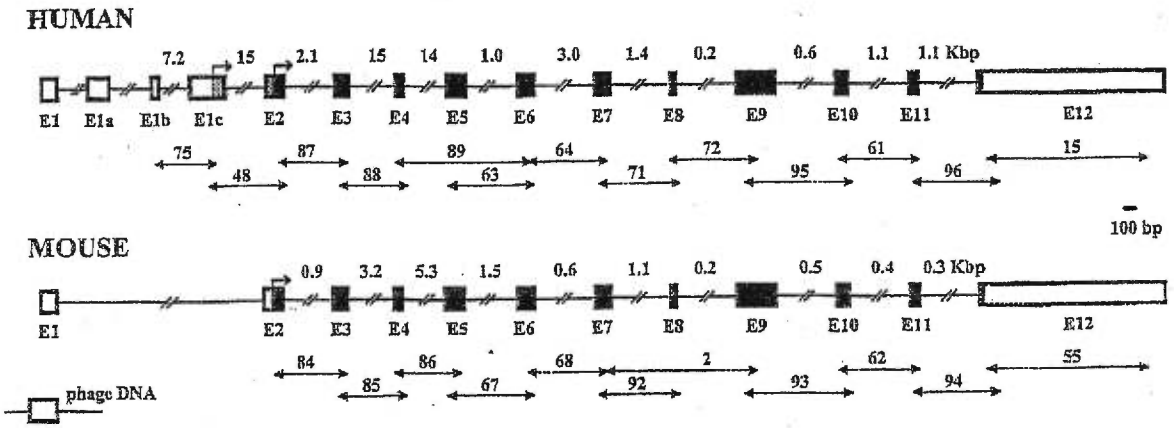

FIG. 1. Schematic representation of the human and mouse *stau* genes. Boxes and lines represent exon and intron sequences, respectively. Open and black boxes are untranslated and coding regions, respectively. The gray boxes represent additional coding sequences found in the 63-kD isoform. Translation initiation sites are shown by arrows above E1c and E2. The size of each intron is written above the lines. The number and position of each PCR-amplified fragment are given below the maps. Only PCR fragments representing the last step of intron characterization are shown. The position of the murine phage DNA is indicated below the maps. Exons are labeled E1 to E12.

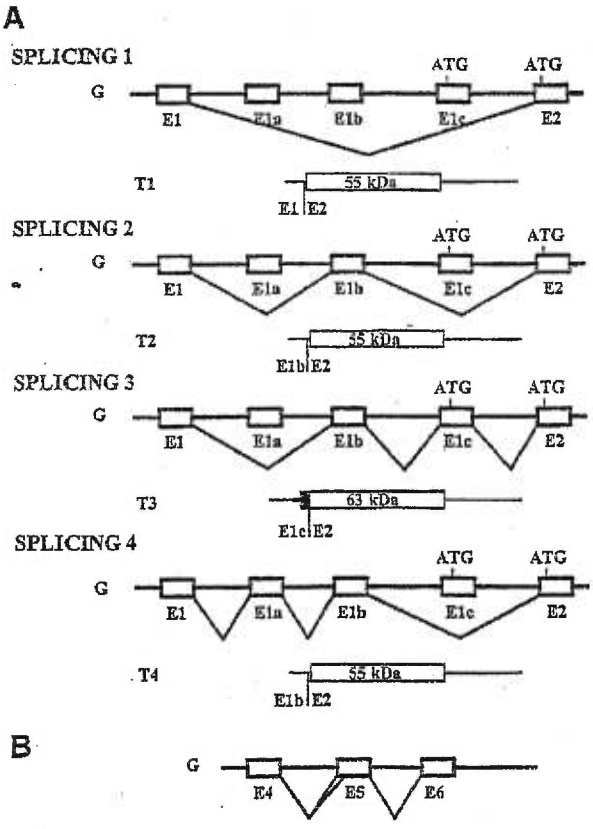

FIG. 2. Alternative splicing events of the *stau* genes. (**A**) Schematic representation of the differential splicing events at the 5′ end of the human transcripts, as deduced from this study and from those of differentially spliced transcripts (Wickham *et al.*, 1999). (**B**) Alternative choice between two splicing acceptor sites found at the 5′ end of E5 of the human and mouse genes. Boxes and lines represent exon and intron sequences, respectively. The size of the proteins generated from each resulting transcript is written in the boxes. G, genomic DNA; T, transcript. Not drawn to scale.

three times with different mRNA preparations and Staufen primers. A single transcription start site was observed in the mouse *stau* gene (Fig. 3). The transcription initiation site of the human gene was found at the same position (not shown). Because the putative site of transcription initiation is downstream of a G+C-rich region, we also performed a 5′ RACE assay at high temperature using the *Tth*I thermoresistant reverse transcriptase. The same results were obtained using this enzyme. We then hybridized poly(A)$^+$ mRNA with a probe derived from the 5′-end flanking region. No signal was detected (not shown), demonstrating that this sequence represents either the promoter region or an additional intron.

Upstream from the region corresponding to the most-5′ end of the cDNA, no canonical TATA or CAAT boxes were found. However, a very rich G+C region, as well as multiple SP1 and other consensus sequences for binding putative *trans*-acting transcription factors, were observed, typical of many housekeeping gene promoters.

DISCUSSION

In this paper, we report the molecular characterization of the human and mouse *stau* genes. Using PCR amplification of genomic DNA, we show that the organization of the mouse gene is similar to that of the human gene, with perfect conservation of the position of all exon–intron junctions. However, the human *stau* gene is about four times the size of its mouse homolog because of its larger introns. In addition, it contains three exons that are not present in the mouse gene (Wickham *et al.*, 1999).

The PCR amplification of genomic DNA, analysis of differentially spliced transcripts, and screening of genomic libraries allowed us to map most introns of the human and murine *stau* genes. The only uncharacterized intron lies between exons 3 and 4 of the human *stau* gene. We nevertheless established the presence of an intron in this region, as we amplified a fragment of about 15 kb that hybridized with a nested cDNA fragment. We were unable to clone or sequence the fragment, and

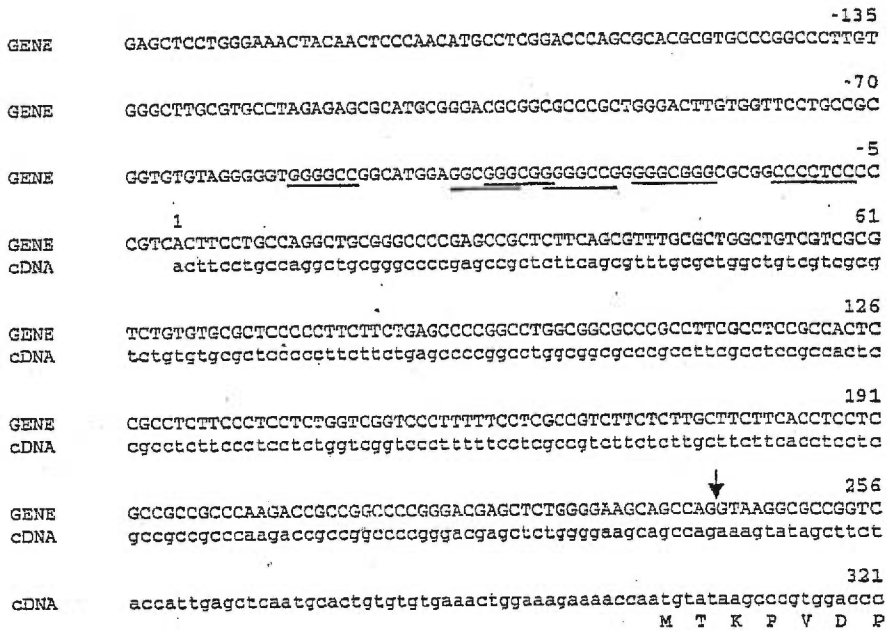

FIG. 3. Sequence of the 5′ flanking region. Mouse genomic (uppercase letters) and cDNA (lowercase letters) sequences are aligned. The position of the translation start site is indicated by the protein sequence below the sequence, and the position of the exon–intron junction is indicated by an arrow. The SP1 transcription binding sites in the promoter are underlined.

therefore, the sequence and position of the exon–intron junction is still unknown. However, considering the perfect conservation in the human and mouse *stau* genes, it is almost certain that the exon–intron junction will be identical to the corresponding junction in the mouse genome. The position of the first four introns at the 5′ end of the human gene was first localized by comparison of alternatively spliced transcripts (Wickham *et al.*, 1999). The position of three of these introns was then validated by PCR amplification of genomic DNA and sequencing or by comparison with the mouse genomic organization. Only the position of the second intron (E1a–E1b) has not been confirmed experimentally. It is probable that the distance between E1 and E1b is too large for PCR amplification, and the fact that E1a is an Alu sequence in reverse orientation precludes the use of additional primers within this exon to shorten the amplified fragment.

One of the four differentially spliced transcripts allows the synthesis of an additional human Staufen isoform (Wickham *et al.*, 1999). Its role is still unknown. The fact that this isoform is not found in mice suggests that it may be either redundant or necessary only for some specialized functions. In contrast, the splicing of exon E5 at two different acceptor sites is conserved in the two species and may represent a mechanism to regulate human Staufen function in mammalian cells. The resulting transcripts, which either contain or do not contain an 18-nb insertion, are expressed at about the same level in every cell. Interestingly, this insertion generates a protein with impaired RNA-binding capacity (Duchaîne and DesGroseillers, unpublished data).

The 5′ flanking region has many features characteristic of promoters of housekeeping genes. The absence of a TATA box and the presence of a G+C rich region (74%), high frequency of potential methylation sites (CpG pairs), and multiple SP1-binding sites are observed in the *stau* gene promoter. The presence of such a promoter in the mouse *stau* gene would be consistent with the broad expression of *stau* mRNA in both species (Wickham *et al.*, 1999; Duchaîne and DesGroseillers, unpublished data). Nevertheless, we do not exclude the possibility that the G+C-rich region impeded the processing of the reverse transcriptase or of the PCR polymerase, even at high temperature, precluding isolation of full-length cDNA. If not the promoter, the 5′ flanking region is likely to be an intron, as a probe derived from this region did not hybridize with mRNA. Putative splicing consensus sequences are present in this region.

The position of exon–intron junctions has also been determined for other members of the dsRNA-binding protein family. The genomic organization of the human adenosine deaminase (DRADA) and of the human interferon-inducible dsRNA-dependent protein kinase (PKR) has been published (Wang *et al.*, 1995; Kuhen *et al.*, 1996). As observed for the human and mouse *stau* genes, *PKR* (about 50 kb; 17 exons) (Kuhen *et al.*, 1996) and *DRADA* (30 kb; 15 exons) (Wang *et al.*, 1995) are relatively long genes that consist of several exons. Interestingly, these maps also allowed us to compare the splicing junctions in the regions of the dsRBDs as an indication of their evolutionary relations. Whereas *DRADA* and *PKR* share splicing junctions within each of the dsRBDs, the positions of the introns are different for the *stau* gene, even between copies of Staufen's dsRBDs (Fig. 4A). In the former cases, introns divide dsRBDs into identical-size NH_2 and COOH regions. This is interesting considering the fact that full-size and short dsRBDs mostly differ in their NH_2 half, whereas the

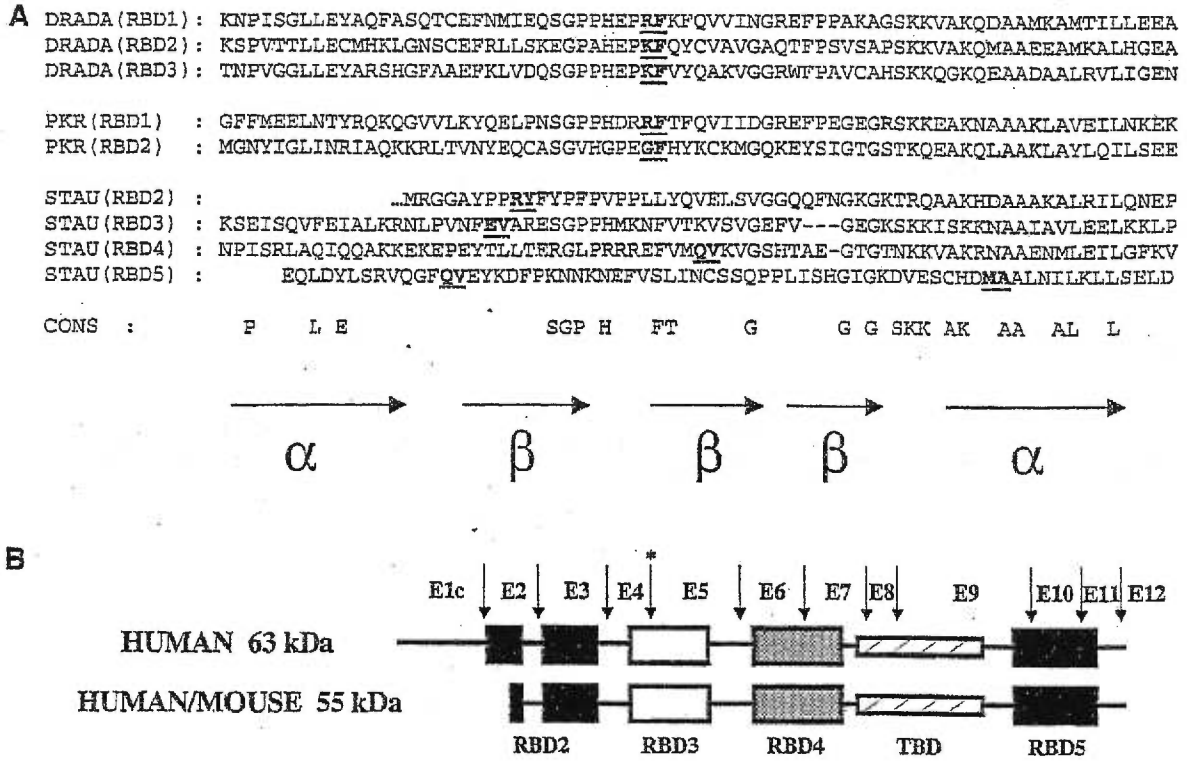

FIG. 4. Comparison of the exon–intron junctions in the dsRBDs. (A) Amino acid sequences of the 3, 2, and 4 dsRBDs of human adenosine deaminase (DRADA), human interferon-inducible dsRNA-dependent protein kinase (PKR), and mammalian Staufen (STAU), respectively. The positions of exon–intron junctions are bold and underlined. A consensus sequence (CONS) of all the dsRBDs is given below (Wang *et al.*, 1995). The proposed position of α-helixes and β-sheets (Bycroft *et al.*, 1995; Nanduri *et al.*, 1998) is aligned below the sequences. (B) Intron localization in comparison with Staufen proteins. Black, gray, and open boxes represent dsRBDs with no, weak, and significant RNA-binding capacity, respectively. The hatched box represents the tubulin-binding domain. The positions of introns are indicated by vertical arrows. Asterisk indicates the position of the alternative choice of splicing acceptor sites in E5. The dsRBDs are labeled RBD2 to RBD5 (RBD1 being absent in mammals) for consistency with Staufen in *Drosophila*. TBD, tubulin-binding domain. Exons are labeled E1c to E12.

COOH half is more conserved (St. Johnston *et al.*, 1992). It was suggested that dsRBDs may be made from different combinations of the NH_2 and COOH half units by exon shuffling or alternative splicing (Wang *et al.*, 1995). This finding also suggests that duplication of a single ancestor domain containing an intron may have led to the repetition of this domain in DRADA and PKR. These exons may be specific for proteins whose enzymatic activity depends on RNA binding. However, because the *stau* gene shows a different pattern (Fig. 4A), the dsRBDs may have originated from a different ancestor gene or evolved independently. In humans and mice, dsRBD3 and dsRBD4 correspond to full-size domains and are able to bind dsRNAs (Wickham *et al.*, 1999). Interestingly, as observed in DRADA and PKR, the domains are also divided into NH_2 and COOH units by an intron, although the sites of splicing are different. In contrast, dsRBD2 and dsRBD5 do not bind dsRNAs *in vitro* (Wickham *et al.*, 1999). From sequence comparisons, it was suggested that dsRBD2 is a split domain, in which the N- and C-terminal halves are separated by inserts of different sizes (Micklem, 1998). Interestingly, we show that each conserved region of the split domain is flanked by introns (Fig. 4B). For its part, dsRBD5 is divided into three units, the well-conserved C-terminal consensus sequence being spliced.

This study constitutes the first step in establishing a link between Staufen and genetic diseases. Indeed, genetic diseases such as Fanconi anemia (Steinlein *et al.*, 1992), maturity onset diabetes of the young type 1 (Rothschild *et al.*, 1993), epilepsy/benign familial neonatal convulsions type 1 (Beck *et al.*, 1994; Malafosse *et al.*, 1992), electroencephalographic variant 1 convulsions (Steinlein *et al.*, 1992), nocturnal frontal lobe epilepsy (Phillips *et al.*, 1995), and some myeloproliferative disorders or myelodysplastic syndromes (Asimakopoulos *et al.*, 1994; Smith *et al.*, 1994) map to the region in which *stau* has been located.

ACKNOWLEDGMENTS

We thank Jean-Pierre Morello for critical reading of manuscript. We also thank Louise Wickham for her technical assistance and Wagner Yotov and André Royal for the generous gifts of the human and mouse genomic library, respectively.

This work was supported by a Natural Sciences and Engineering Research Council of Canada (NSERC) grant to LDG.

REFERENCES

ASIMAKOPOULOS, F.A., WHITE, N.J., NACHEVA, E., and GREEN, A.R. (1994). Molecular analysis of chromosome 20q deletions associated with myeloproliferative disorders and myelodysplastic syndromes. Blood **84,** 3086–3094.

BECK, C., MOULARD, B., STEINLEIN, O., GUIPPONI, M., VALLEE, L., MONTPIED, P., BALDY-MOULINIER, M., and MALAFOSSE, A. (1994). A nonsense mutation in the alphâ-4 subunit of the nicotinic acetylcholine receptor (CHRNA4) cosegregates with 20q-linked benign neonatal familial convulsions (EBN1). Neurobiol. Dis. **1,** 95–99.

BROADUS, J., FUERSTENBERG, S., and DOE, C.Q. (1998). Staufen-dependent localization of prospero mRNA contributes to neuroblast daughter-cell fate. Nature **391,** 792–795.

BURD, C.G., and DREYFUSS, G. (1994). Conserved structures and diversity of functions of RNA-binding proteins. Science **265,** 615–621.

BYCROFT, M., GRÜNERT, S., MURZIN, A.G., PROCTOR, N., and ST. JOHNSTON, D. (1995). NMR solution structure of a dsRNA binding domain from Drosophila Staufen protein reveals homology to the N-terminal domain of ribosomal protein S5. EMBO J. **14,** 3563–3571.

DESGROSEILLERS, L., and LEMIEUX, N. (1996). Localization of a human double-stranded RNA-binding protein gene to band 20q13.1 by fluorescence *in situ* hybridization. Genomics **36,** 527–529.

FENG, G.S., CHONG, K.L., KUMARA, A., and WILLIAMS, B.R.G. (1992). Identification of double-stranded RNA-binding domains in the interferon-induced double-stranded RNA-activated p68 kinase. Proc. Natl. Acad. Sci. USA **89,** 5447–5451.

GATIGNOL, A., BUCKLER-WHITE, A., BERKHOUT, B., and JEANG, K.-T. (1991). Characterization of a human TAR RNA-binding protein that activates the HIV-1 LTR. Science **251,** 1597–1600.

HILLIER, L., and GREEN, P. (1991). OSP: A computer program for choosing PCR and DNA sequencing primers. Genome Res. **1,** 124–128.

KIEBLER, M.A., HEMRAJ, I., VERKADE, P., KÖHRMANN, M., FORTES, P., MARIÓN, R.M., ORTIN, J., and DOTTI, C.G. (1999). The mammalian Staufen protein localizes to the somatodendritic domain of cultured hippocampal neurons: Implications for its involvement in mRNA transport. J. Neurosci. **19,** 288–297.

KIEBLER, M.A., and DESGROSEILLERS, L. (2000). Molecular insights into mRNA transport and local translation in the mammalian nervous system. Neuron **25,** 1–10.

KÖHRMANN, M., LUO, M., KAETHER, K., DESGROSEILLERS, L., DOTTI, C.G., and KIEBLER, M.A. (1999). Microtubule-dependent recruitment of Staufen-GFP into large RNA-containing granules and subsequent dendritic transport in living hippocampal neurons. Mol. Biol. Cell. **10,** 2945–2953.

KUHEN, K.L., SHEN, X., CARLISLE, E.R., RICHARDSON, A.L., WEIER, H.-U.G., TANAKA, H., and SAMUEL, C.E. (1996). Structural organization of the human gene (PKR) encoding an interferon-inducible RNA-dependent protein kinase (PKR) and differences from its mouse homolog. Genomics **36,** 197–201.

LI, P., YANG, X., WASSER, M., CAI, Y., and CHIA, W. (1997). Inscuteable and Staufen mediate asymmetric localization and segregation of prospero RNA during *Drosophila* neuroblast cell divisions. Cell **90,** 437–447.

MALAFOSSE, A., LEBOYER, M., DULAC, O., NAVELET, Y., PLOUIN, P., BECK, C., LAKLOU, H., MOUCHINO, G., GRANDSCENE, P., VALLEE, L., GUILLOUD-BATAILLE, M., SAMOLYK, D., BALDY-MOULINIER, M., FEINGOLD, J., and MALLET, J. (1992). Confirmation of linkage of benign familial neonatal convulsions of D20S19 and D20S20. Hum. Genet. **89,** 54–58.

MARIÓN, R.M., FORTES, P., BELOSO, A., DOTTI, C., and ORTIN, J. (1999). A human sequence homologue of Staufen is an RNA-binding protein that is associated with polysomes and localizes to the rough ER. Mol. Cell. Biol. **19,** 2212–2219.

MICKLEM, D.R. (1998). *Trans*-acting factors required for the posterior localization of *oskar* mRNA. Ph.D. Thesis (Cambridge University, Cambridge, UK).

NANDURI, S., CARPICK, B.W., YANG, Y., WILLIAMS, B.R.G., and QIN, J. (1998). Structure of the double-stranded RNA-binding domain of the protein kinase PKR reveals the molecular basis of its dsRNA-mediated activation. EMBO J. **17,** 5458–5465.

PHILLIPS, H.A., SCHEFFER, I.E., BERKOVIC, S.F., HOLLWAY, G.E., SUTHERLAND, G.R., and MULLEY, J.C. (1995). Localization of a gene for autosomal dominant nocturnal frontal lobe epilepsy to chromosome 20q13.2. Nature Genet. **10,** 117–118.

ROTHSCHILD, C.B., AKOTS, G., HAYWORTH, R., PETTENATI, M.J., RAO, P.N., WOOD, P., STOLZ, F.M., HANSMANN, I., SERINO, K., KEITH, T.P., FAJANS, S.S., and BOWDEN, D.W. (1993). A genetic map of chromosome 20q12-q13.1: Multiple highly polymorphic microsatellite and RFLP markers linked the maturity-onset diabetes of the young (MODY) locus. Am. J. Hum. Genet. **52,** 110–123.

SMITH, C.L., KEITH, T., HANSMANN, I., WEISSENBACH, J., ASIMAKOPOULOS, F.A., BOWDEN, D.W., DELEUZE, J.F., DUTTON, E.R., FASMAN, K.H., GREEN, T., HADCHOUEL, M., HAZEN, J., HILGARTNER, S., STEINLEIN, D.K., WHITE, N., and WILLIAMSON, C.M. (1994). Report of the First International Workshop on Human Chromosome 20 Mapping, 1993. Cytogenet. Cell Genet. **66,** 78–82.

STEINLEIN, O., FISCHER, C., KEIL, R., SMIGRODZKI, R., and VOGEL, F. (1992). D20S19, linked to low voltage EEG, benign neonatal convulsions, and Fanconi anaemia, maps to a region of enhanced recombination and is localized between CpG islands. Hum. Mol. Genet. **1,** 325–329.

ST. JOHNSTON, D., BROWN, N.H., GALL, J.G., and JANTSCH, M. (1992). A conserved double-stranded RNA-binding domain. Proc. Natl. Acad. Sci. USA **89,** 10979–10983.

ST. JOHNSTON, D. (1995). The intracellular localization of messenger RNAs. Cell **81,** 161–170.

WANG, Y., ZENG, Y., MURRAY, J.M., and NISHIKURA, K. (1995). Genomic organization and chromosomal location of the human dsRNA adenosine deaminase gene: The enzyme for glutamate-activated ion channel RNA editing. J. Mol. Biol. **254,** 184–195.

WICKHAM, L., DUCHAÎNE, T., LUO, M., NABI, I.R., and DESGROSEILLERS, L. (1999). Mammalian Staufen is a double-stranded RNA- and tubulin-binding protein which localizes to the rough endoplasmic reticulum. Mol. Cell. Biol. **19,** 2220–2230.

Address reprint requests to:
Dr. Luc DesGroseillers
Department of Biochemistry
University of Montreal
P.O. Box 6128, Station Centre Ville
Montreal, Québec, Canada H3C 3J7

E-mail: desgros@bcm.umontreal.ca

Received for publication January 20, 2000; received in revised form and accepted March 13, 2000.

III- Article 2

Mammalian Staufen Is a Double-Stranded-RNA- and Tubulin-Binding protein which localizes to the Rough Endoplasmic Reticulum

Louise Wickham, Thomas Duchaîne, Ming Luo, Ivan R. Nabi, AND **Luc DesGroseillers**

Molecular and Cellular Biology, Mar. 1999, 19(3):2220-2230

My contribution:

This is the first paper that describes the molecular cloning and characterization the human(hStau) and mouse(mStau) homologues of *Drosophila* Staufen, which is so far the best-studied double-stranded RNA (dsRNA) binding protein involved in RNA transport and localization. My contribution in this paper is: 1). Determination of the 5' transcription start site of hstau by 5'RACE (Fig. 1). 2) Characterization of two hStau cDNAs and proteins in vitro (Fig. 2, B and C). 3) Study of the cell biology of hStau (Fig.7 and Fig. 8).

Fig. 1 showed the cDNA and amino acid sequences of 4 different hStau transcripts produced by alternative splicing. Using 5'-RACE (rapid amplification of 5'-cDNA ends), I completed the cDNA sequence in the 5'-untranslated regions (5'-UTR).

Fig. 2B showed the presence of two endogenous hStau protein isoforms by Western Blotting. To determine whether the two protein bands observed in the Western blot come from the translation of our cloned cDNAs, I subcloned two full-length cDNAs (T2 and T3, see Fig. 1) in a mammalian expression vector and transiently expressed them in mammalian cells. Each cDNA gives rise to a single overexpressed protein which perfectly comigrates with one of the endogenous proteins (Fig. 2C).

Next, I determined the subcellular distribution and cytoskeletal association of Stau in vivo: 1) Using GFP-tagged fusion protein, I showed that Stau is present in the cytoplasm and associated with the detergent-insoluble fraction in vivo (Fig. 7).

2) Using confocal immunofluorescence of two different ER markers and HA-tagged Stau, I demonstrated that Stau localizes to the rough endoplasmic reticulum, implicating its role in the transport of RNAs to the site of translation (Fig. 8). 3) Using confocal microscopy, I also determined that the two cloned hStau proteins colocalize when coexpressed in mammalian cells (picture not shown in paper). These studies constitute a substantial part of the paper.

MOLECULAR AND CELLULAR BIOLOGY, Mar. 1999, p. 2220–2230 Vol. 19, No. 3
0270-7306/99/$04.00+0

Mammalian Staufen Is a Double-Stranded-RNA- and Tubulin-Binding Protein Which Localizes to the Rough Endoplasmic Reticulum

LOUISE WICKHAM,[1] THOMAS DUCHAÎNE,[1] MING LUO,[1] IVAN R. NABI,[2] AND LUC DESGROSEILLERS[1]*

Departments of Biochemistry[1] and Pathology and Cell Biology,[2] University of Montreal, Montreal, Quebec, Canada H3C 3J7

Received 9 September 1998/Returned for modification 23 October 1998/Accepted 17 November 1998

Staufen (Stau) is a double-stranded RNA (dsRNA)-binding protein involved in mRNA transport and localization in *Drosophila*. To understand the molecular mechanisms of mRNA transport in mammals, we cloned human (*hStau*) and mouse (*mStau*) *staufen* cDNAs. In humans, four transcripts arise by differential splicing of the *Stau* gene and code for two proteins with different N-terminal extremities. In vitro, hStau and mStau bind dsRNA via each of two full-length dsRNA-binding domains and tubulin via a region similar to the microtubule-binding domain of MAP-1B, suggesting that Stau cross-links cytoskeletal and RNA components. Immunofluorescent double labeling of transfected mammalian cells revealed that Stau is localized to the rough endoplasmic reticulum (RER), implicating this RNA-binding protein in mRNA targeting to the RER, perhaps via a multistep process involving microtubules. These results are the first demonstration of the association of an RNA-binding protein in addition to ribosomal proteins, with the RER, implicating this class of proteins in the transport of RNA to its site of translation.

It is now believed that the cytoskeleton is widely used to transport mRNAs between their transcription and processing sites in the nucleus and their translation and degradation sites in the cytoplasm (3, 42, 44). One consequence of the interaction between mRNAs and the cytoskeleton is to promote differential localization and/or transport of mRNAs in subcellular compartments. Indeed, examples of mRNA targeting have been observed in both germinal and somatic cells throughout the animal kingdom (51, 55, 63). The universal use of this mechanism is also apparent when we consider the nature of the proteins which are coded by the transported mRNAs; asymmetric localization involving mRNAs coding for cytosolic, secreted, membrane-associated, or cytoskeletal proteins have all been reported. Localization of mRNAs in the cytoplasm is now considered an essential step in the regulation of gene expression and an efficient way to unevenly distribute proteins in polarized cells. In general, it is believed that mRNA localization is used to determine and/or regulate local sites of translation (46, 51, 55). Indeed, ribosomes and many translational cofactors were found in association with the cytoskeletal elements, preventing both mRNAs and translation factors from being diluted by the cellular fluid (44). Transport and local translation of specific mRNAs have been shown to play an important role in processes such as learning and memory (38), synaptic transmission (9, 22, 26, 51, 61), axis formation during development (reviewed in reference 55), cell motility (30), and asymmetric cell division (7, 36, 37, 56).

The mechanisms underlying mRNA localization are not yet fully understood, mainly because of the lack of information on the principal constituents of the ribonucleoprotein (RNP) complexes involved in this process. Nevertheless, it is known to involve both *cis*-acting signals in mRNA and *trans*-acting RNA-binding proteins which bind to this signal (55). The signals that allow mRNAs to be recognized as targets for transport and then to be localized have been mapped within their 3′ untranslated regions (UTRs) (55, 63). In contrast, the nature of the RNA-binding proteins is still obscure. Recently, a 68-kDa protein which binds the β-*actin* mRNA zipcode localization domain was isolated and its transcript was cloned from chicken cDNA libraries (47). This protein, which binds to microfilaments, contains RNA-binding domains (RBDs) which share strong sequence similarities with the RNP and KH motifs. In addition, 69- and 78 kDa proteins in *Xenopus laevis* oocyte extracts have been shown to bind to the localization signal of *Vg1* mRNA (12, 50). While the 69-kDa protein was shown to bind microtubules (15), the 78-kDa Vera protein colocalized with a subdomain of the smooth endoplasmic reticulum (SER) (12). Surprisingly, molecular cloning of the two proteins revealed that they are identical and are similar to the chicken zipcode-binding protein (13, 23).

Genetic and molecular studies have shown that the activity of the *staufen* gene product in *Drosophila* is necessary for the proper localization of *bicoid* and *oskar* mRNAs to the anterior and posterior cytoplasm of oocytes, respectively, and of *prospero* mRNA in neuroblasts (7, 16, 28, 36, 52, 53). Staufen (Stau), a member of the double-stranded RNA (dsRNA)-binding protein family, contains (i) three copies of a domain consisting of a 65- to 68-amino-acid consensus sequence which is required to bind RNAs having double-stranded secondary structures and (ii) two copies of a short domain which retains the last 21 amino acids at the C-terminal end of the complete motif (53, 54). In vitro, it has been demonstrated that Stau binds directly to *bicoid* and *prospero* mRNAs (36, 54). However, since Stau seems to bind to any dsRNA in vitro, it is not clear whether it binds directly to these RNAs in vivo or needs cellular cofactors which make up part of a larger RNP complex to localize each mRNA. Many experiments have demonstrated that the localization of *oskar*, *prospero*, and *bicoid* mRNAs

* Corresponding author mailing address: Department of Biochemistry, University of Montreal, P.O. Box 6128, Station Centre Ville, Montreal, Quebec, Canada H3C 3J7. Phone: (514) 343-5802. Fax: (514) 343-2210. E-mail: desgros@bcm.umontreal.ca.

occurs through a multistep mechanism of active transport that is dependent on elements of the cytoskeleton (7, 17, 45, 55, 58).

To understand the mechanisms of mRNA transport in mammals and determine the nature of both the RNAs and proteins in the RNA-protein complexes, we began the cloning of the human and mouse *staufen* (*hStau* and *mStau*) cDNAs and the characterization of their encoded proteins. Recently, we showed by both Southern blot analysis of human DNA and fluorescent in situ hybridization on human chromosomes in metaphase that the human gene is present as a single copy in the human genome and is localized in the middle of the long arm of chromosome 20 (11). We now report the sequence of the hStau and mStau and show that the transcript is found in all tested tissues. We further demonstrate that Stau binds both dsRNA and tubulin in vitro via specific binding domains. Stau is also shown to be present in the cytoplasm in association with the rough endoplasmic reticulum (RER), implicating this protein in the targeting of RNA to its site of translation.

MATERIALS AND METHODS

Molecular cloning and sequencing of the cDNAs. To clone an *hStau* homologue, we searched the GenBank database with *Drosophila* dsRBD sequences to find consensus sequences and eventually design degenerate oligonucleotide primers for reverse transcription (RT)-PCR. However, searching in the expressed sequence tag database identified a partial sequence, clone HFBDQ83 (GenBank accession no. T06248), with high homology to the *Drosophila* sequence. This clone was purchased from the American Type Culture Collection and used as a probe to screen both human brain (Clontech) and fetal total mouse (a generous gift from A. Royal) cDNA libraries as described previously (62). DNA from the isolated λgt10 clones was subcloned into a pBluescript vector (Stratagene). Double-stranded DNA (dsDNA) was sequenced by the dideoxynucleotide method according to Sequenase protocols (United States Biochemical Corp.).

Construction of fusion proteins. The 1.2-kbp *Bam*HI fragment of the human HFBDQ83 cDNA was subcloned in frame in either pQE32 (Qiagen) or pMAL-c (New England Biolabs), thus generating the protein fused to a hexahistidine tag or to the maltose-binding protein (MBP), respectively. The protein was expressed in bacteria by induction with isopropyl-β-D-thiogalactopyranoside (IPTG) as recommended by the manufacturer.

Full-length and internal fragments of the mStau protein were PCR amplified and cloned into pMal-c to produce MBP fusion proteins. For the expression of the internal domains, which do not contain an endogenous stop codon, the PCR fragments were cloned in a modified pMal-c vector (pMal-stop) in which stop codons were introduced at the *Hin*dIII site, by the ligation of the annealed complementary oligonucleotides 5′-AGCTTAATTAGCTGAC-3′ and 5′-AGC TGTCAGCTAATTA-3′. The MBP-mStau fusion protein, containing the full-length mStau sequence, was generated by PCR amplification with Vent DNA polymerase (New England BioLabs), using the primer pair 5′-CCTGGATCCG AAAGTATAGCTTCTACCATTG-3′ plus 5′-TACATAAGCTTCTAGATGG CCAGAAAAGGTTCAGCA-3′. The resulting 1,562-bp fragment was digested with *Hin*dIII and *Bam*HI and ligated in the pMal-c vector. The C-terminal fragment (mStau-C) was amplified with the primer pair 5′-GGATGAATCCTA TTAGTAGACTTGCAC-3′ plus 5′-TACATAAGCTTCTAGATGGCCAGAA AAGGTTCAGCA-3′, digested with *Hin*dIII, and cloned in the *Eag*I* and *Hin*dIII sites of pMal-c. *Eag*I* was created by filling in the cohesive ends of *Eag*I-digested pMal-c vector, using the Klenow fragment of DNA polymerase I. This fusion vector was then digested with *Sac*I and *Eco*RI, and the resulting fragment was subcloned in the pMal-stop vector to generate the mStau-RBD3 construct. The mStau-tubulin-binding domain (TBD) construct was prepared by PCR using the primer pair 5′-GCTCTAGATTCAAAGTTCCCCAGGCGCA G-3′ plus 5′-TTAAGCTTCTCAGAGGGTCTAGTGCGAG-3′; the product was digested with *Xba*I and *Hin*dIII and cloned in the pMal-stop vector. mStau-RBD2 and mStau-RBD1 were constructed by first amplifying a fragment using the primer pair 5′-CAATGTATAAGCCCGTGGACCC-3′ and 5′-AAAAAGC TTGTGCAAGTCTACTAATAGGATTCATCC-3′. The resulting product was digested with *Hin*dIII and cloned in the *Eag*I* and *Hin*dIII sites of the pMal-stop vector. This vector was then used to purify the 398-bp *Pst*I and *Hin*dIII fragment, which was subcloned in the pMAL-stop vector to generate the mStau-RBD2 construct. In the same way, the mStau-RBD1 vector was obtained by digestion with *Sma*I and *Stu*I, followed by recircularization of the digestion product using T4 DNA ligase. The mStau-RBD4 was PCR amplified by using the primer pair 5′-ATAGCCCGAGAGTTGTTG-3′ plus 5′-TACATAAGCTTCTAGATGGC CAGAAAAGGTTCAGCA-3′. The resulting fragment was digested with *Hin*dIII and ligated in the pMal-stop vector at the *Stu*I and *Hin*dIII sites. All MBP-Stau fusion plasmids were transformed in BL-21 *Escherichia coli*. The fusion proteins were obtained after induction with 1 mM IPTG for 2 to 3 h. Cells were lysed in sodium dodecyl sulfate-polyacrylamide gel electrophoresis (SDS-PAGE) loading buffer for immediate use, or frozen at −80°C for storage.

Antibody production and Western blotting. For the production of antibodies, a large amount of the His-hStau fusion protein was purified on Ni-nitrilotriacetic acid (NTA) resin (Qiagen) as recommended by the manufacturer and injected into rabbits as done previously (2). For Western blotting, cells were lysed in 1% *n*-octylglucoside–1 mM phenylmethylsulfonyl sulfoxide–aprotinin (1 μg/ml)–pepstatin A (1 μg/ml) in phosphate-buffered saline (PBS). Protein extracts were quantified by the Bradford method (Bio-Rad), and similar amounts of proteins were separated on SDS–10% polyacrylamide gels and transferred onto nitrocellulose membranes. Membranes were blocked for 30 min in TBS (Tris-buffered saline; 10 mM Tris [pH 8.0], 150 mM NaCl)–5% dry milk and incubated with primary antibodies in TBS–0.05% Tween for 1 h at room temperature. Detection was accomplished by incubating the blots with peroxidase-conjugated anti-rabbit immunoglobulin G (IgG) antibodies (Dimension Labs) followed by Supersignal Substrate (Pierce) as recommended by the manufacturer.

RNA-binding assay. Bacterial extracts from IPTG-induced cultures were separated on SDS–10% polyacrylamide gels and the proteins were transferred onto nitrocellulose membranes. Membranes were incubated in the presence of ^{32}P-labeled RNA probes in 50 mM NaCl–10 mM $MgCl_2$–10 mM HEPES (pH 8.0)–0.1 mM EDTA–1 mM dithiothreitol–0.25% milk for 2 h at room temperature, washed in the same buffer for 30 min, and exposed for autoradiography. For competition assays, a 100- to 1,000-fold excess of cold homopolymers (Pharmacia) was added to the hybridization mixture along with the labeled probe. The 3′ UTR of *bicoid* cDNA (positions 4016 to 4972), which was PCR amplified from *Drosophila* genomic DNA and subcloned in the pBluescript vector, was transcribed by using T7 RNA polymerase in the presence of [α-^{32}P]CTP. Synthetic RNAs (Pharmacia) were labeled with T4 polynucleotide kinase in the presence of [γ-^{32}P]ATP. The specific activities of the *bicoid* and synthetic RNA probes were 1.4×10^6 and 0.5×10^6 cpm/μg, respectively.

For RNA-binding assay in solution, dilutions of the purified human His-Stau fusion protein were incubated with in vitro-labeled *bicoid* RNA (3′ UTR), poly(rI)-poly(rC), poly(rI), or poly(rC) (20,000 cpm; specific activity, 10^6 cpm/μg) in 10 mM $MgCl_2$–50 mM NaCl–0.1 mM EDTA–1 mM dithiothreitol–10 mM HEPES (pH 8.0) for 30 min at room temperature. The RNA-protein complexes were then filtered through a nitrocellulose membrane (0.45-μm pore size), washed, and counted. Analyses were done with the Graph Pad PRISM (version 2.01) software.

Tubulin-binding assay. Bacterial extracts from IPTG-induced cultures were separated on SDS–10% polyacrylamide gels, and the MBP-tagged proteins were transferred onto nitrocellulose membranes. Membranes were incubated in TBS–1% Tween 20 for 45 min prior to an overnight overlay with tubulin (7 μg/ml; Sigma) in TBS–0.2% Tween 20. Blots were washed several times in TBS–0.2% Tween 20 and then incubated with a mixture of mouse monoclonal anti-α- and anti-β-tubulin antibodies (ICN). Bound antibodies were detected with secondary peroxidase-conjugated anti-mouse IgG antibodies (Dimension Labs) and Supersignal substrate (Pierce) as stated previously. Separate assays were performed with actin and antiactin antibodies (both from Sigma).

Immunofluorescence. HStau-hemagglutinin (HA) and hStau-green fluorescent protein (GFP) were constructed by PCR amplification of the full-length cDNA, using the primer pair 5′-TACATGTCGACTTCCTGCCA/GGGCTGC GGG-3′ plus 5′-TACAATCTAGATTATCAGCGGCCGCACCTCCCACACA CAGACAT-3′. The 3′ primer was synthesized with a *Not*I site just upstream from the stop codon allowing ligation of a *Not*I cassette containing either three copies of the HA tag or the GFP sequence. The resulting fragment was cloned in pBluescript following digestion with *Sal*I and *Xba*I. The *Kpn*I/*Xba*I fragment was then subcloned in the pCDNA3/RSV vector (25), and a *Not*I cassette was introduced at the *Not*I site. For the TBD-GFP fusion protein, the TBD was PCR amplified with oligonucleotides on each side of this region (5′-TACATAAGCT TAAGCCACCATGGTCAAAGTTCCCCAGGCGC-3′ and 5′-TACAATCTA GAGCGGCCGCGCTCAGAGGGTCTAGTGCGAG-3′). The sense primer contained an ATG initiation codon and the Kozak consensus sequence upstream from the TBD sequence. The antisense primer contained a *Not*1 site just upstream from a stop codon. The resulting fragment was digested with *Hin*dIII and *Xba*I and cloned into the pCDNA3/RSV vector. The GFP *Not*I cassette was then introduced at the *Not*I site.

Mammalian cells were transiently transfected with the cDNAs by the calcium phosphate precipitation technique, fixed in 4% paraformaldehyde in PBS for 25 min at room temperature, and permeabilized with 0.3% Triton X-100 in PBS containing 0.1% bovine serum albumin (BSA). The cells were then blocked with 1% BSA in PBS–0.3% Triton X-100 and incubated with mouse anti-HA, rabbit anticalreticulin, or rabbit anticalnexin antibodies for 1 h at room temperature, as indicated. Cells were washed in permeabilization buffer and incubated with fluorescein-conjugated or Texas red-conjugated species-specific secondary antibodies (Jackson Immunoresearch Laboratories, West Grove, Pa.) in blocking buffer for 1 h. GFP and GFP fusion proteins were detected by autofluorescence. Mounting was done in ImmunoFluor mounting medium (ICN). For the analysis of cytoskeleton-associated proteins, transfected cells were first extracted in 0.3% Triton X-100–130 mM HEPES (pH 6.8)–10 mM EGTA–20 mM $MgSO_4$ for 5 min at 4°C as previously described (10). They were then fixed in 4% paraformaldehyde in PBS and processed for immunofluorescence as described above.

FIG. 1. Amino acid sequences of the *hSau* cDNAs. Shown is alignment of the cDNAs and PCR fragments with the translation of the putative protein sequences. Numbers refer to the sequence of the short cDNA. Positions of the four consensus dsRBDs (RBD1 to RBD4) and of the TBD are indicated between brackets above the sequence.

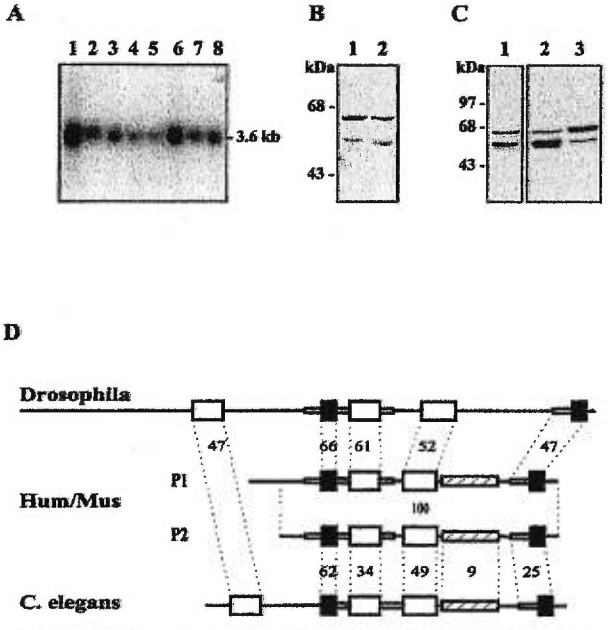

FIG. 2. Characterization of the *hStau* mRNA and proteins. (A) Northern blot analysis of *hStau* expression in human tissues. A human multiple-tissue Northern blot (Clontech) was hybridized with the 1.2-kbp *Bam*HI fragment of *hStau* cDNA. Lane 1, brain; lane 2, pancreas; lane 3, heart; lane 4, skeletal muscles; lane 5, liver; lane 6, placenta; lane 7, lung; lane 8, kidney. (B) Western blot experiment with anti-hStau antibodies. Lane 1, HeLa cell extracts; lane 2, HEK 293 cell extracts. (C) HEK 293 cells were transfected with cDNAs coding for either the short (lane 2) or the long (lane 3) hStau isoform, lysed, and analyzed by Western blotting using the anti-hStau antibodies. Mock-transfected cells are shown in lane 1. (D) Schematic representation of the *Drosophila* (accession no. M69111), human and mouse (Hum/Mus), and *C. elegans* (accession no. U67949) Stau proteins. The human protein P1 has an insertion of 81 amino acids at its N-terminal extremity compared to protein P2. Large open and black boxes represent the full-length and short dsRBDs, respectively. Small boxes and lines are regions of high and low sequence similarity, respectively. The hatched boxes indicate the position of the region which is similar to the MAP1B microtubule-binding domain. The percentage of identity between the domains of the human and invertebrate proteins is indicated.

Cells were visualized by immunofluorescence, using the 63× planApochromat objective of a Zeiss Axioskop fluorescence microscope.

Confocal microscopy was performed with the 60× Nikon Plan Apochromat objective of a dual-channel Bio-Rad 600 laser scanning confocal microscope equipped with a krypton-argon laser and the corresponding dichroid reflectors to distinguish fluorescein and Texas red labeling. No overlap was observed between the fluorescein and Texas red channels. Confocal images were printed with a Polaroid TX1500 video printer.

Nucleotide sequence GenBank accession numbers. The human and mouse sequences were deposited in the GenBank database under accession no. AF061938, AF061939, AF061940, and AF061941 (human) and AF061942 (mouse).

RESULTS

Molecular cloning of mammalian *staufen* cDNAs. To understand the mechanism of mRNA transport in mammalian cells, we cloned the human and mouse *staufen* homologues. Thirteen overlapping human cDNAs, ranging in size between 0.8 and 2.5 kb, were isolated from a human central nervous system cDNA library, using the expressed sequence tag HFBDQ83 cDNA as a probe (Fig. 1). Purified human HeLa cell poly(A)$^+$ RNAs were also reverse transcribed and PCR amplified, using different 5′ RACE (rapid amplification of 5′ cDNA ends) protocols, allowing us to clone the 5′ end of the transcript. Two different cDNAs of 3,217 and 3,506 nucleotides were identified from overlapping clones (see below). One of the human cDNAs was then used to screen a fetal total mouse cDNA library under low-stringency conditions, which led to the isolation of a full-length cDNA (*mStau*). The human and mouse proteins are 90% identical (98% similarity).

Hybridization of a human multiple-tissue Northern blot with a human cDNA reveals that *hStau* mRNA is found in every tested tissue (Fig. 2A), unlike the *Drosophila staufen* gene, which is exclusively expressed in oocytes and in the central nervous system at the larval stage (53). The size of the cDNAs is close to that of the transcripts, which migrate on a Northern blot as an unresolved large band of around 3.6 kb.

A differential splicing event generates two *hStau* proteins. Characterization of the human cDNAs revealed the presence of two types of transcripts which differ only by an insertion of 289 bp at position 324 (T2 and T3 in Fig. 1). To confirm this result and determine the relative expression of the two classes of transcripts, we used RT-PCR to amplify the region of the transcript which overlaps the site of insertion. Unexpectedly, four different fragments were amplified. Cloning and sequencing of the fragments revealed that two correspond to the cDNA sequences (Fig. 1). Compared to the smallest cloned cDNA sequence (T2), a third fragment (T4) has an insertion of 132 bp at position 249, which corresponds to an *Alu* Sq sequence in an inverted orientation, while the other one (T1) has a deletion of 75 bp between positions 249 and 324. Within a single tissue, the four bands are not expressed at the same level, T2 being the most abundant. However, from one tissue to the other, the relative ratios of the four bands are roughly the same (not shown).

Translation of the cDNAs suggests that three of the four transcripts (T1, T2, and T4) may give rise to a protein of 55 kDa. Interestingly, the DNA insertion in transcript T3 introduces an ATG initiation codon upstream from the first one found in the other transcripts (Fig. 1). This finding suggests that a second putative protein of 63 kDa, exhibiting an 81-amino-acid extension at its N-terminal extremity compared to the other protein, may be translated. Using anti-hStau antibodies in Western blot experiments, we observed two protein bands of around 63 and 55 kDa in human cell extracts (Fig. 2B). To determine whether our cDNAs could account for the presence of the two proteins, we subcloned the T2 and T3 transcripts in an expression vector and expressed them in mammalian cells. As seen in Fig. 2C, each cDNA gives rise to a single overexpressed protein which perfectly comigrates with one of the endogenous proteins. Altogether, these results demonstrate that the *hstaufen* gene produces four different transcripts and that the transcripts code for two highly homologous proteins which differ in their N-terminal extremities.

Comparison of the mammalian and *Drosophila* Stau proteins. The amino acid sequences of the mammalian proteins are similar to that of the *Drosophila* Stau protein and of the product of an uncharacterized open reading frame on the X chromosome of *Caenorhabditis elegans* (Fig. 2D). The overall structures and relative positions of the full-length and short RBDs are well conserved, and high sequence identity is found between corresponding dsRBDs. This is highly significant since an alignment of the domains found in the members of the dsRNA-binding protein family shows an average of only 29% amino acid identity to one another (54). In addition, domains 1 and 4 in the human sequence, which are short domains compared to the consensus, are nevertheless highly similar to the corresponding fly sequences, even in the region that extends far beyond the N-terminal side of the consensus sequence, suggesting that they must play an essential role in Stau function.

Mammalian Stau does not contain the first dsRBD or the

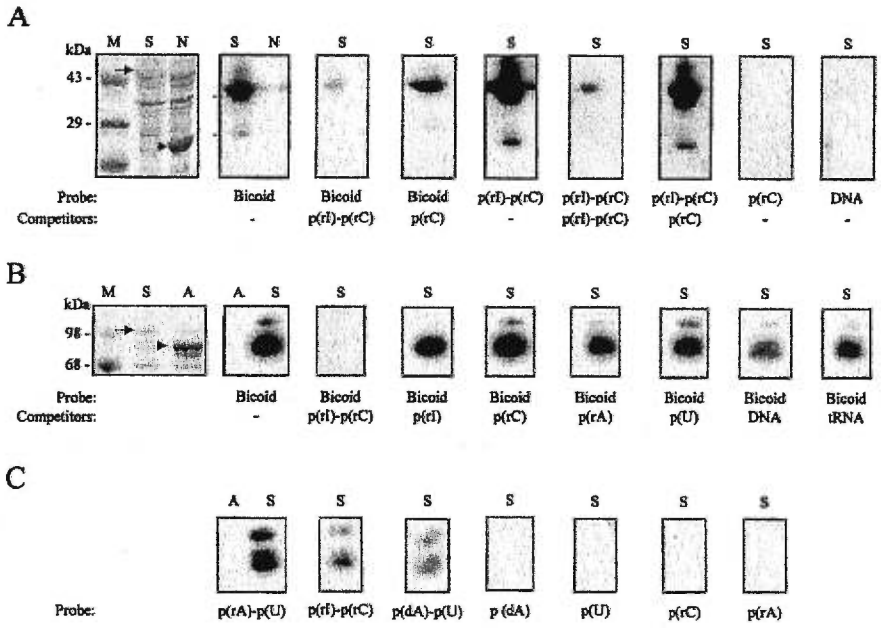

FIG. 3. RNA-binding assay. Bacterially expressed His-hStau (A, lanes S) and His-neutral endopeptidase (A, lane N) fusion proteins or bacterially expressed MBP-mStau (B and C, lanes S) or MBP-aminopeptidase (B and C, lanes A) fusion proteins were electrophoresed on a polyacrylamide gel, transferred to nitrocellulose, and incubated with ^{32}P-labeled nucleic acids, in the presence or absence of cold competitors, as indicated below each gel. After extensive washing, binding was detected by autoradiography. A representative Coomassie blue staining of the blots is shown on the left (A and B). Arrows, positions of overexpressed Stau; arrowheads, positions of overexpressed control proteins. Lanes M, molecular weight markers.

long N-terminal sequence of the *Drosophila* protein which was shown to bind to oskar protein (5). In addition, a putative TBD located between the third and fourth dsRBDs of mammalian Stau is not found in the *Drosophila* protein, at least at the amino acid level. This region contains a stretch of 91 amino acids which show 25% amino acid identity (66% similarity) to a microtubule-binding domain of microtubule-associated protein 1B (MAP1B) (65). It is meaningful that the sequence similarity covers the full microtubule-binding domain of MAP1B and that it is restricted to this domain. Putative nuclear localization signals are also present.

***hStau* and *mStau* bind dsRNAs.** As seen in Fig. 2D, mammalian Stau proteins contain multiple dsRBDs. To determine whether Stau binds RNAs, we used two bacterially expressed fusion proteins, His-hStau and MBP-mStau, in an RNA-binding assay. The fusion proteins were probed with in vitro-labeled *bicoid* mRNA, which is known to adopt an extensive secondary structure and to strongly bind to *Drosophila* Stau protein, both in vivo and in vitro (18, 54). Both fusion proteins strongly bind this RNA. The binding is competed by a 100-fold excess of cold poly(rI)-poly(rC) but not by a 1,000-fold excess of poly(rI), poly(rC), poly(rA), or poly(U) or by tRNA or dsDNA (Fig. 3A and B), suggesting that mammalian Stau recognizes double-stranded structures in the RNA rather than a sequence-specific region. Both fusion proteins also directly bind labeled dsRNAs and RNA-DNA hybrids but not single-stranded RNA or DNA homopolymers (Fig. 3A and C). As controls, bacterial extracts containing overexpressed His-neutral endopeptidase or MBP-aminopeptidase fusion proteins were also included on each blot; they did not bind any of these nucleic acids. We also tested other in vitro-labeled RNAs such as those coding for tubulin, neuropeptides from *Aplysia*, and nuclear RNP B. All of these RNAs bind to Stau in vitro, as reported previously for other members of the dsRNA-binding protein family. This finding demonstrates that both hStau and mStau, regardless of the protein to which they are fused, are able to bind dsRNAs. However, there is no sequence specificity, as reported for other members of the dsRNA-binding protein family (21, 54, 55).

Filter binding assays, using Ni-NTA-purified His-hStau (inset), were used to determine the binding affinity of Stau (Fig. 4). High-affinity binding, with a K_d of about 10^{-9} M, was observed when the 3′ UTR of *bicoid* or double-stranded RNA was used as a probe (Fig. 4A). The resulting sigmoidal curves suggest that Stau cooperatively binds dsRNAs. In contrast, only low-affinity binding was observed with single-stranded RNAs, confirming that Stau specifically binds dsRNAs (Fig. 4B).

hStau and mStau bind tubulin in vitro. As described above, Stau contains a region which is similar to the microtubule-binding domain of MAP1B. To determine whether mammalian Stau can bind tubulin, bacterially expressed MBP-Stau fusion proteins were used in a tubulin-binding assay. As shown in Fig. 5, hStau binds tubulin in vitro. As a control, the bacterially expressed MBP-aminopeptidase fusion protein was also included on the blot; it did not show any tubulin-binding capability. Under the same conditions, hStau cannot bind actin (Fig. 5), which suggests that the binding of tubulin to Stau is specific. The same results were obtained with the MBP-mStau fusion protein (Fig. 6B, lane 1). Binding to mRNAs and microtubules are two of the characteristics expected of localizing proteins, making hStau and mStau very good candidates for mRNA transport and localization in mammals.

Molecular mapping of the RBD and TBD. To determine which Stau domain(s) is involved in RNA and/or tubulin binding, the MBP-mStau fusion protein was used to construct a series of deletion mutants (Fig. 6). The production and relative abundance of each fusion protein was first verified by Western blotting (not shown). Using the RNA-binding assay, we dem-

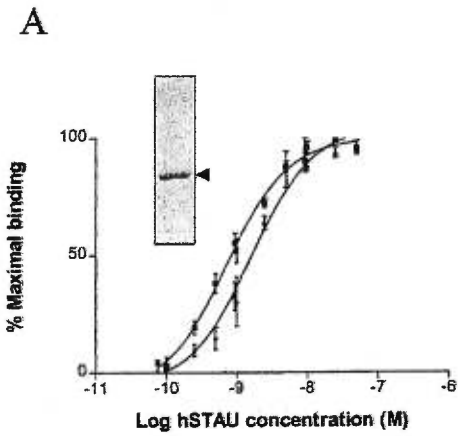

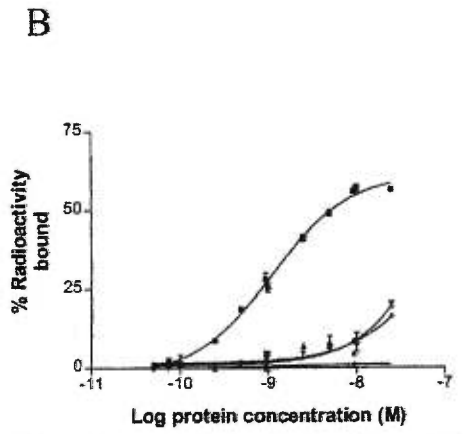

FIG. 4. RNA-binding assay in solution. Dilutions of the purified His-hStau fusion protein were incubated with fixed amounts of labeled RNAs, and the RNA-protein complexes were filtered through nitrocellulose membranes. (A) RNA-binding affinity to dsRNAs. Triangles, 3' UTR of *bicoid* RNA; squares, poly(rI)-poly(rC). The results are presented as a percentage of maximal retained probe and are the averages of three independent experiments done in duplicate. Inset, Coomassie blue staining of Ni-NTA-purified His/hStau after separation by SDS-PAGE. (B) RNA-binding affinity to RNAs. Squares, poly(rI)-poly(rC); triangles, poly(rI); inverted triangles, poly(rC); diamonds, BSA with poly(rI)-poly(rC), used as a control. The results are presented as a percentage of bound radioactivity and represent a single experiment done in duplicate. The same results were obtained in two other independent experiments.

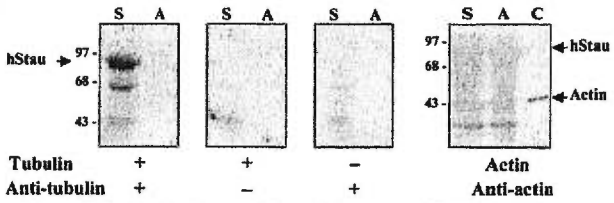

FIG. 5. Tubulin-binding assay. Bacterially expressed MBP-hStau (lanes S) or MBP-aminopeptidase (lanes A) fusion proteins were electrophoresed on SDS-polyacrylamide gels, transferred to nitrocellulose, and incubated with tubulin or actin. After extensive washing, tubulin and actin were detected with monoclonal antitubulin and antiactin antibodies, respectively. As controls, the same experiments were performed in the absence of either tubulin or antitubulin antibodies. Purified actin was also loaded on the gel as a control (lane C). Sizes are indicated in kilodaltons.

onstrated that both of the full-size dsRBDs (dsRBD2 and dsRBD3) are independently sufficient to bind bicoid RNA (Fig. 6A). In contrast, the two short domains (dsRBD1 and dsRBD4) were unable to bind dsRNA in this assay. We also demonstrated that the C-terminal half of mStau is able to bind tubulin (Fig. 6B, lane 4). More specifically, the region which is similar to the MAP1B microtubule-binding domain is sufficient to bind tubulin (Fig. 6B, lane 6). These experiments confirm that the regions that we identified by sequence comparison as putative dsRBDs and TBDs are biochemically functional.

Stau is associated with the detergent-insoluble fraction in vivo. We next addressed the cellular distribution and cytoskeletal association of the two hStau proteins in vivo. To do so, we fused GFP or an HA tag to the 63- and 55-kDa hStau isoforms, respectively. Using confocal microscopy, we first showed that the two fusion proteins colocalize when coexpressed in mammalian cells (not shown). Then, we showed that they are nonhomogeneously distributed throughout the cytoplasm and label numerous vesicular and tubular structures which concentrate in the perinuclear region (Fig. 7A). Minimal staining was found in the nucleus. When the cells were treated with Triton X-100 prior to fixing, allowing soluble proteins to be separated from the cytoskeleton and cytoskeleton-associated proteins (44), the tubulovesicular labeling was still present, demonstrating that hStau is associated with the detergent-insoluble material in vivo (Fig. 7B). Labeled structures were also present in cell processes, suggesting that Stau may target mRNAs to peripheral ER elements. The same results were obtained following expression of the GFP-mStau protein (not shown). The association between hStau and the cytoskeletal-associated material was confirmed by in vitro cell fractionation in the presence of Triton X-100. In this assay, hStau partitioned mainly in the cytoskeleton-associated fractions, although a significant fraction was found in a soluble form, as judged by Western blotting (not shown).

To determine whether the tubulin-binding domain identified in vitro is truly involved in this function in vivo, we transfected mammalian cells with a cDNA coding for a fusion protein in which the minimal TBD was fused to GFP. In contrast to the full-length protein, the TBD-GFP fusion protein is randomly distributed in the cytoplasmic and nuclear domains of the cells (Fig. 7C), as is the GFP protein used as a control (Fig. 7D). This staining was completely extracted by the Triton X-100 treatment (not shown), suggesting that the minimal TBD found in vitro is not sufficient to render the protein insoluble and form a stable association with the microtubule network and/or the cytoskeleton-associated material.

Stau localizes to the RER in vivo. Interestingly, the pattern of localization of Stau resembles that of the ER. To test a putative localization of Stau to the ER, we transfected mammalian cells with a cDNA coding for a fusion protein in which a HA tag was introduced at the C-terminal end of the short hStau protein. We then double labeled transfected cells with anti-HA, to recognize hStau, and with anticalreticulin or anticalnexin, two markers of the ER. Using a confocal microscope, we showed that hStau completely colocalizes with anticalreticulin, although HA-staining appears to be absent in some parts of the ER, in particular around the nucleus (Fig. 8A to C). To confirm these results, we examined the colocalization of Stau and calnexin, a specific marker for the RER (24) (Fig. 8D to F). The patterns of staining obtained with anti-hStau and anticalnexin were identical, demonstrating that hStau colocalizes exclusively with the RER.

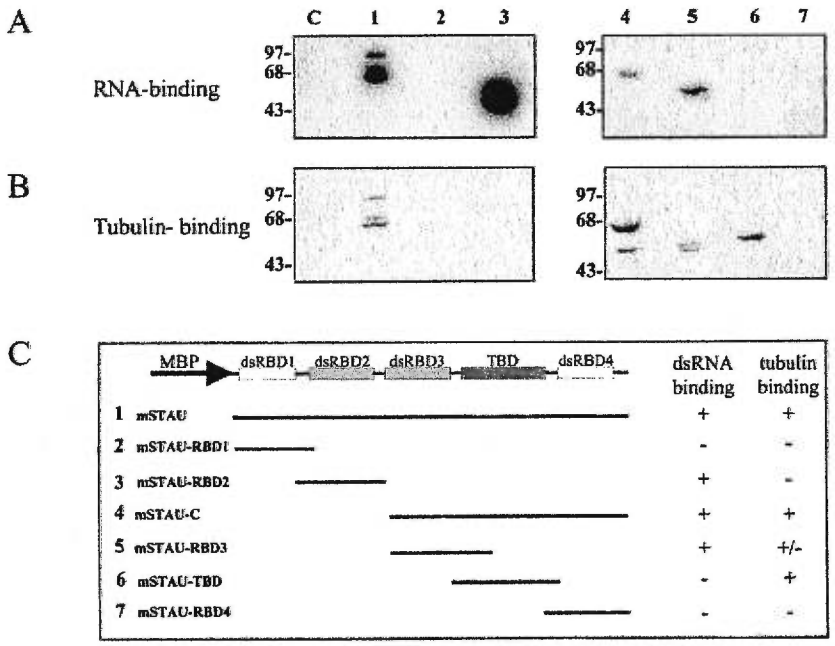

FIG. 6. Molecular mapping of the dsRBD and TBD. Bacterially expressed MBP-mStau (lanes 1), MBP-mStau deletion mutants (lanes 2 to 7), or MBP-aminopeptidase (lanes C) fusion proteins were electrophoresed on a polyacrylamide gel, transferred to nitrocellulose, incubated with either ^{32}P-labeled 3′-UTR *bicoid* RNA (A) or tubulin and antitubulin antibodies (B), and revealed as described above. (C) Schematic representation of the mutant proteins. Their RNA- and tubulin-binding responses are indicated.

DISCUSSION

The transport and localization of specific mRNAs have important functions in cell physiology. For example, mRNA targeting plays a key role in the formation of cytoskeletal filaments and in the establishment of morphogenetic gradients (55). However, the nature of the RNP complexes as well as the mechanisms involved in these processes are still largely uncharacterized. In this paper, we describe a novel RNA-binding protein which localizes to the RER in mammalian cells. Although its precise role is still unclear, its biochemical and molecular properties strongly suggest that it is involved in mRNA transport and/or localization. Consistent with such a role, we recently demonstrated that hStau is involved in human immunodeficiency virus type 1 genomic RNA encapsidation (41). Mammalian Stau was also found in the dendrites of rat hippocampal neurons in culture, but not in the axons, and colocalizes with RNPs known to contain mRNA, ribosomes, and translation factors, suggesting a role for Stau in the polarized transport and localization of mRNAs in mammalian neurons (27).

A differential splicing event generates four *hStau* transcripts. The significance of the four different classes of transcripts is unknown. They arise by differential splicing since each of the inserts that appears in the 5′ end of the cDNAs is flanked by large introns containing typical consensus splicing sequences (6). They are observed in all the tissues tested by RT-PCR, suggesting that they are not cloning artifacts. The multiplicity of the transcripts and the short size of the alternatively spliced exons may explain the fact that a single but diffuse band is visible on the Northern blot, despite the presence of four transcripts. This alternative splicing, which changes the 5′ UTR of the transcripts, could represent a mechanism by which translation is regulated, although the presence of similar relative levels of the four transcripts in each tissue argues against this possibility. Alternatively, these different classes of transcripts may result from aberrant or incomplete splicing events. In fact, an unusually large number of cDNA clones containing intron sequences were isolated, and this may indicate that the splicing of the premature transcripts is a slow process. The presence of an *Alu* sequence in the 5′ UTR may arise by the activation of a resident intronic *Alu* element as an exon, as reported previously (35). Many examples of recruitment, via splicing or intron sliding, of a segment of a resident *Alu* element into an mRNA have been reported. It is thought that the presence of a polypyrimidine tract which is the complement of the A-rich tail of the element when inserted in the reverse orientation contributes to the creation of the splicing acceptor site. A point mutation, downstream from this site, may generate the splicing donor site, as reported previously. The presence of an old *Alu* subfamily sequence and of only the right subunit segment of the *Alu* element is consistent with this interpretation.

Structure and function of Stau. We observed that mammalian Stau, like all members of the dsRNA-binding protein family (55), can bind any dsRNA or RNAs forming double-stranded structures in vitro, regardless of its primary sequence, as well as RNA-DNA hybrids. The latter adopt a conformation that is more closely related to that of dsRNA than dsDNA, which probably explains why they can bind to Stau. The fact that the full-length Stau protein, as observed with single dsRBD, binds to any dsRNA in vitro suggests that the correspondence between the position of the dsRBDs, and the arrangement of double-stranded stems in the folded RNAs may not be sufficient for specificity; posttranslational modifications and/or essential cofactors capable of forming complex RNP structures along with mRNA molecules could be necessary to discriminate between different RNA secondary structures. Packaging of mRNAs into RNP complexes (1, 18, 20, 32), the

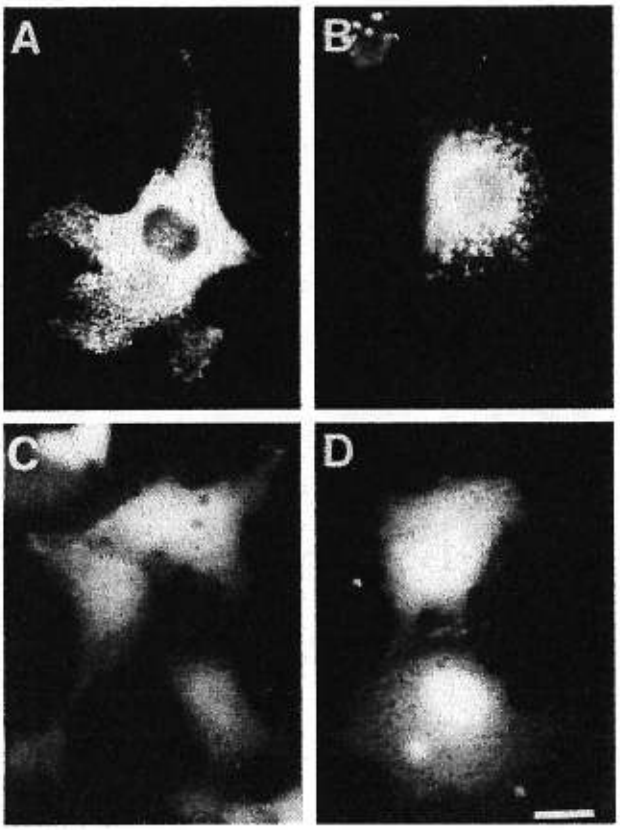

FIG. 7. Subcellular localization of the hStau-GFP fusion proteins. COS7 cells were transfected with cDNAs coding for either the hStau-GFP (A and B) or TBD-GFP (C) fusion protein, or GFP alone (D). Untreated (A, C, and D) or Triton X-100-treated (B) cells were fixed and visualized by autofluorescence. Bar = 20 μm.

intermolecular dimerization of the localization signal of *bicoid* mRNA (19), and the involvement of untranslatable hnRNAs in mRNA transport (31, 59, 60) are consistent with this interpretation. Until now, specific mRNA-Stau interactions were shown in vivo only after injection of different RNAs into *Drosophila* embryos, but the mechanisms underlying the specificity are not known (18). Since specific RNA binding cannot be obtained in vitro, it precludes the use of classic techniques to isolate and identify relevant RNAs which would bind staufen in vivo. Cross-linking of mRNA to Stau in vivo and isolation of the resulting complexes will be necessary to identify the nature of bound RNAs.

Regardless of their limitations, the in vitro assays did allow us to map the molecular determinants which are necessary and sufficient to bind RNAs. The presence of two functional domains in the mammalian Stau contrasts with what has been reported for other members of the dsRNA-binding protein family, which contain multiple full-length dsRBDs but only one that is biochemically functional (21, 34, 39, 48). Interestingly, full-length dsRBDs incapable to bind dsRNA by themselves can do so when joined to another inactive full-length domain, suggesting that multiple domains present in a given protein exhibit cooperative binding effect (34, 48). Whether the two mStau dsRBDs exhibit similar or different affinities is not yet clear.

We mapped the TBD to a region which is similar to a microtubule-binding domain of MAP1B. Although this region can efficiently bind tubulin in vitro, it is not sufficient to bring a TBD-GFP fusion protein to the microtubule network. Binding of Stau to microtubules in vivo may involve more than one molecular determinant or the proper localization and folding of the TBD in the full-length protein. Indeed, in our in vitro assay, the fusion protein which contains the C-terminal region in addition to the TBD binds tubulin more efficiently than does the TBD alone, suggesting that this region may be necessary for binding to microtubules in vivo. Interestingly, the corresponding region of the *Drosophila* Stau protein was shown to bind inscuteable (36), a protein with ankyrin domains which is believed to associate with the cytoskeleton (33), suggesting that corresponding regions of the mammalian and *Drosophila* proteins may have functional similarities.

Alternatively, binding may be weak and/or transitory in vivo, for example during the early steps of mRNA recruitment, during mRNA transport, and/or at mitosis, as found in *Drosophila* (18, 45, 55). These steps may be difficult to observe by immunofluorescence in some cell lines (18) and/or be masked by the anchoring of the protein to the RER. A similar conclusion was reached when binding of MAP1B to the microtubule network was studied (65), suggesting that weak binding to the cytoskeleton may be a characteristic of proteins containing this type of TBD. These steps may nevertheless be necessary to allow the efficient and flexible transport of RNA along the cytoskeleton. Interestingly, the immunoelectron microscopic observation of dendrites of hippocampal neurons in culture showed the presence of abundant gold particles close to microtubules, strongly arguing in favor of a Stau-microtubule association in these cells (27). In *Drosophila*, there is no evidence that Stau directly binds to the microtubule network, although Stau-dependent mRNA transport was shown to rely on this structure (45, 55).

Our studies demonstrate that Stau is anchored to the RER and that the putative TBD is not involved in this function. Indeed, preliminary results suggest that the binding of Stau to the RER is carried out by one of the RBDs (40). Similar domains in other members of the dsRNA-binding proteins were previously shown to be involved in protein dimerization and/or in protein-protein interactions (4, 8). This finding also suggests that different Stau molecular determinants are necessary for binding to tubulin and anchoring to the RER. This is consistent with previous findings demonstrating that in *Xenopus* and *Drosophila*, mRNA localization was likely to occur via successive steps involving different elements of the cytoskeleton and overlapping molecular determinants (55).

Localization of Stau to the RER. When expressed in mammalian cells, Stau isoforms show a tubulovesicular pattern of localization which is found more abundantly in the perinuclear region. Besides ribosomal proteins, Stau is the first RNA-binding protein shown to be associated with the RER in mammals. No signal peptide or putative hydrophobic transmembrane domains are present in either the long or short Stau proteins, indicating that they are cytosolic proteins and not residents of the RER and that their association to the RER is likely to reflect their mRNA transport function. Two recent papers also suggest that mRNA transport may be linked to the ER or ER-like structures. In *Xenopus* oocytes, Vera, a *Vg1* mRNA-binding protein, was shown to cosediment with TRAPα, a protein associated with the protein translocation machinery of the ER. However, in contrast to Stau, Vera-*Vg1* complexes were found associated only with a small subdomain of the ER, which was of the smooth variety (12). Similarly, in *Drosophila*, at least some steps in mRNA transport in nurse cells and oocytes seem to occur within ER-like cisternae (64).

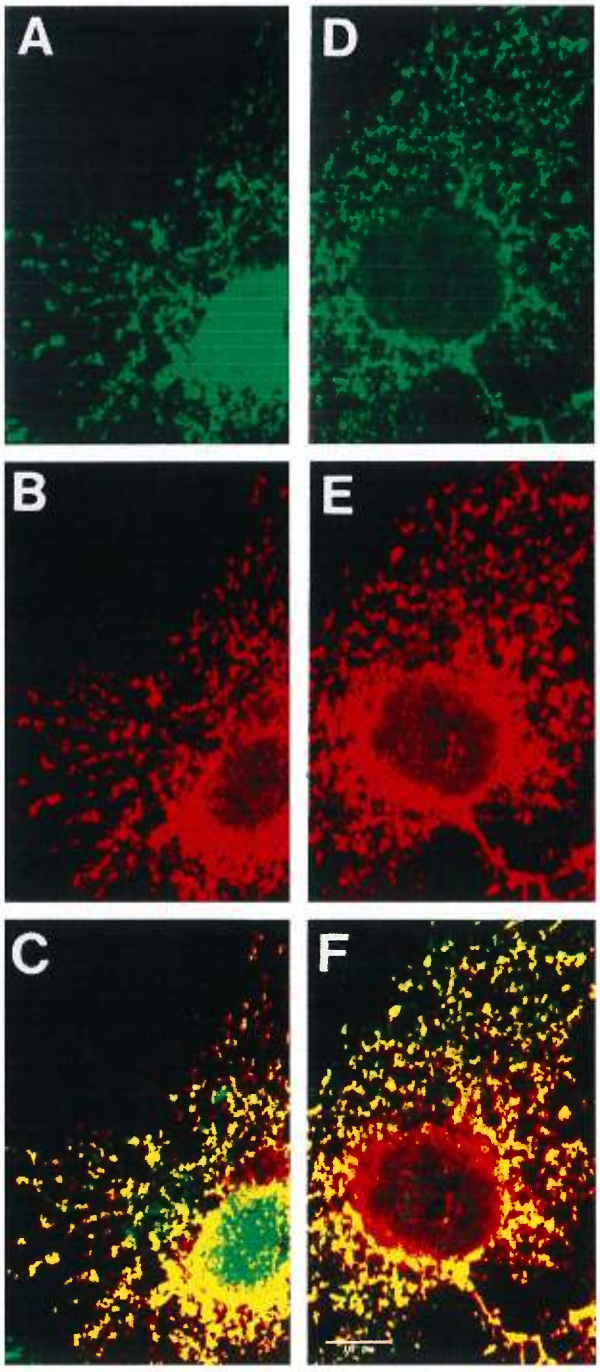

FIG. 8. Colocalization of hStau with markers of the RER by confocal microscopy. A cDNA coding for an hStau-HA fusion protein was transfected into COS7 cells. Triton X-100-treated cells were fixed and double labeled with anti-HA (B) and anticalreticulin (A) or with anti-HA (E) and anticalnexin (D). Anti-HA was detected with Texas red-coupled anti-mouse IgG antibodies, using the Texas Red channel; anticalreticulin and anticalnexin were detected with fluorescein-conjugated anti-rabbit IgG antibodies, using the fluorescein channel. Panels C and F are superpositions of panels A plus B and D plus E, respectively. No overlap was observed between the fluorescein and Texas red channels. Bar = 10 μm.

As observed for the *Vg1* mRNA-SER interaction in *Xenopus*, this structure seems to exclude most ribosomes, suggesting that translation is not the major function of these associations.

hStau and mStau represent new members of a large family of proteins involved in the transport and/or localization of mRNAs to different subcellular compartments and/or organelles. Stau, the TAR RNA-binding protein and *X. laevis* homologue Xlrbpa, and Spnr were shown to colocalize with the RER (this paper), with ribosomes and hnRNPs (14), and with the microtubular array of spermatids (49), respectively. Our results strongly suggest that Stau-mRNA RNP complexes are transported along the microtubule network and then anchored to the RER. It is well known that the ER is associated with the microtubule cytoskeleton (57). Therefore, a transient interaction between microtubules and Stau may facilitate the localization of Stau and the targeting of mRNA to the RER. One of the roles of Stau might be to transport and localize specific mRNAs to the RER, such as those coding for secreted or membrane proteins which have to be translocated to the RER. This would bring them in proximity to the signal recognition particles and RER, thus facilitating translation and translocation. The presence of Stau in cell processes, in association with ER structures, may represent a first clue to understanding the role of many mRNAs which were found to be localized in neuronal processes (51). Stau may facilitate the transport of mRNAs to cell processes to ensure efficient local translation and translocation. In addition, the presence of multiple Stau-like proteins in mammals creates the possibility that different members of the family can target subclasses of mRNAs to different subdomains of the ER. This phenomenon has been described before and is thought to be the first step in the differential targeting of proteins in polarized cells (43).

We do not exclude the possibility that Stau plays additional roles in mammals; Stau may first be linked to the RER for storage, and then a subset of molecules may be recruited by specific mRNAs and/or cofactors to form RNP complexes that will be transported along microtubules toward their final destination. The presence of large amounts of Stau in the perinuclear region, which could be awaiting the nucleocytoplasmic transport of mRNAs, is consistent with this possibility. The presence of a putative nuclear localization signal even suggests that Stau transits through the nucleus before being localized in the cytoplasm and plays a role in mRNA or rRNA export. Alternatively, Stau may play key roles in the translational regulation of localized mRNAs, as is the case for *Drosophila* Stau, which is essential for the translation of *oskar* mRNA, once it is localized at the posterior pole (29). Indeed, since polysomes and ER-bound ribosomes are not extracted by Triton X-100, it is possible that Stau is associated with the RER via ribosomes and/or mRNAs. Characterization of mRNAs and putative cofactors which bind to staufen will be necessary to understand the process.

In vertebrates, the mechanisms which underly the transport of mRNAs have not yet been deciphered. Characterization of the RNAs and proteins involved in transport and localization is particularly important since understanding the mechanisms responsible for the transport of mRNAs is fundamental for learning more on the development of polarity in cells, both during mammalian development and in somatic cells, at a time where RNA-based gene therapy is being considered as a possible approach to cure different disorders.

ACKNOWLEDGMENTS

We thank Luis Rokeach (Department of Biochemistry, University of Montreal) for the anticalreticulin antibodies, John Bergeron (McGill University) for the anticalnexin antibodies, and André Royal (Depart-

ment of Pathology and Cell Biology) for the mouse cDNA library. We thank Luis Rokeach and Lea Brakier-Gingras for comments and discussion and Michael Kiebler for sharing unpublished information.

The first two authors contributed equally to this work.

This work was supported by a Natural Sciences and Engineering Research Council of Canada grant to L.D., a National Health Research Development Program grant to L.D., and a Medical Research Council of Canada grant to I.R.N.

REFERENCES

1. **Ainger, K., D. Avossa, F. Morgan, S. J. Hill, C. Barry, E. Barbarese, and J. H. Carson.** 1993. Transport and localization of exogenous myelin basic protein mRNA microinjected into oligodendrocytes. J. Cell Biol. **123**:431–441.
2. **Aloyz, R. S., and L. DesGroseillers.** 1995. Processing of the L5-67 precursor peptide and characterization of LUQIN in the central nervous system of Aplysia californica. Peptides **16**:331–338.
3. **Bassell, G., and R. H. Singer.** 1997. mRNA and cytoskeletal filaments. Curr. Opin. Cell Biol. **9**:109–115.
4. **Benkirane, M., C. Neuveut, R. F. Chun, S. M. Smith, C. E. Samuel, A. Gatignol, and K.-T. Jeang.** 1997. Oncogenic potential of TAR RNA binding protein TRBP and its regulatory interaction with RNA-dependent protein kinase PKR. EMBO J. **16**:611–624.
5. **Breitwieser, W., F.-H. Markussen, H. Horstmann, and A. Ephrussi.** 1996. Oskar protein interaction with Vasa represents an essential step in polar granule assembly. Genes Dev. **10**:2179–2188.
6. **Brizard, F., and L. DesGroseillers.** Submitted for publication.
7. **Broadus, J., S. Fuerstenberg, and C. Q. Doe.** 1998. Staufen-dependent localization of prospero mRNA contributes to neuroblast daughter-cell fate. Nature **391**:792–795.
8. **Cosentino, G. P., S. Venkatesan, F. C. Serluca, S. Green, M. B. Mathews, and N. Sonenberg.** 1995. Double-stranded-RNA-dependent protein kinase and TAR RNA-binding protein from homo- and heterodimers in vivo. Proc. Natl. Acad. Sci. USA **92**:9445–9449.
9. **Crino, P. B., and J. Eberwine.** 1996. Molecular characterization of the dendritic growth cone: regulated mRNA transport and local protein synthesis. Neuron **17**:1173–1187.
10. **Davis, L., G. A. Banker, and O. Steward.** 1987. Selective dendritic transport of RNA in hippocampal neurons in culture. Nature **330**:477–479.
11. **DesGroseillers, L., and N. Lemieux.** 1996. Localization of a human double-stranded RNA-binding protein gene (*STAU*) to band 20q13.1 by fluorescence in situ hybridization. Genomics **36**:527–529.
12. **Deshler, J. O., M. I. Highett, and B. J. Schnapp.** 1997. Localization of Xenopus Vg1 mRNA by Vera protein and the endoplasmic reticulum. Science **276**:1128–1131.
13. **Deshler, J. O., M. I. Highett, T. Abramson, and B. J. Schnapp.** 1998. A highly conserved RNA-binding protein for cytoplasmic localization in vertebrates. Curr. Biol. **8**:489–496.
14. **Eckmann, C. R., and M. F. Jantsch.** 1997. Xlrbpa, a double-stranded RNA-binding protein associated with ribosomes and heterogeneous nuclear RNPs. J. Cell Biol. **138**:239–253.
15. **Elisha, Z., L. Havin, I. Ringel, and J. K. Yisraeli.** 1995. Vg1 RNA binding protein mediates the association of Vg1 RNA with microtubules in Xenopus oocytes. EMBO J. **14**:5109–5114.
16. **Ephrussi, A., L. K. Dickinson, and R. Lehmann.** 1991. Oskar organizes the germ plasm and directs localization of the posterior determinant nanos. Cell **66**:37–50.
17. **Erdelyi, M., A. M. Michon, A. Guichet, J. B. Glotzer, and A. Ephrussi.** 1995. Requirement for Drosophila cytoplasmic tropomyosin in oskar mRNA localization. Nature **377**:524–527.
18. **Ferrandon, D., L. Elphick, C. Nüsslein-Volhard, and D. St Johnston.** 1994. Staufen protein associates with the 3′UTR of bicoid mRNA to form particles that move in a microtubule-dependent manner. Cell **79**:1221–1232.
19. **Ferrandon, D., I. Koch, E. Westhof, and C. Nüsslein-Volhard.** 1997. RNA-RNA interaction is required for the formation of specific *bicoid* mRNA 3′UTR-staufen ribonucleoprotein particles. EMBO J. **16**:1751–1758.
20. **Forristall, C., M. Pondel, and M. L. King.** 1995. Patterns of localization and cytoskeletal association of two vegetally localized RNAs, Vg1 and Xcat-2. Development **121**:201–208.
21. **Gatignol, A., C. Buckler, and K.-T. Jeang.** 1993. Relatedness of an RNA-binding motif in human immunodeficiency virus type 1 TAR RNA-binding protein TRBP to human P1/dsI kinase and *Drosophila* Staufen. Mol. Cell. Biol. **13**:2193–2202.
22. **Gazzaley, A. H., D. L. Benson, G. W. Huntley, and J. H. Morrison.** 1997. Differential subcellular regulation of NMDAR1 protein and mRNA in dendrites of dendate gyrus granule cells after perforant path transection. J. Neurosci. **17**:2006–2017.
23. **Havin, L., A. Git, Z. Elisha, F. Obeerman, K. Yaniv, S. P. Schwartz, N. Standart, and J. K. Yisraeli.** 1998. RNA-binding protein conserved in both microtubule- and microfilament-based RNA localization. Genes Dev. **12**: 1593–1598.
24. **Hochstenback, F., V. David, S. Watkins, and M. B. Brenner.** 1992. Endoplasmic reticulum resident protein of 90 kilodaltons associates with the T- and B-cell antigen receptors and major histocompatibility complex antigens during assembly. Proc. Natl. Acad. Sci. USA **89**:4734–4738.
25. **Jockers, R., A. Da Silva, A. D. Strosberg, M. Bouvier, and S. Marullo.** 1996. New molecular and structural determinants involved in β2-adrenergic receptor desensitization and sequestration. J. Biol. Chem. **271**:9355–9362.
26. **Kang, H., and E. M. Schuman.** 1996. A requirement for local protein synthesis in neurotrophin-induced hippocampal synaptic plasticity. Science **273**: 1402–1406.
27. **Kiebler, M.** Personal communication.
28. **Kim-Ha, J., J. L. Smith, and P. M. Macdonald.** 1991. Oskar mRNA is localized to the posterior pole of the Drosophila oocyte. Cell **66**:23–35.
29. **Kim-Ha, J., K. Kerr, and P. M. Macdonald.** 1995. Translational regulation of oskar mRNA by Bruno, an ovarian RNA-binding protein, is essential. Cell **81**:403–412.
30. **Kislauskis, E. H., X. Zhu, and R. H. Singer.** 1997. β-Actin messenger RNA localization and protein synthesis augment cell motility. J. Cell Biol. **136**: 1263–1270.
31. **Kloc, M., and L. D. Etkin.** 1994. Delocalization of Vg1 mRNA from the vegetal cortex in Xenopus oocytes after destruction of Xlsirt RNA. Science **265**:1101–1103.
32. **Knowles, R. B., J. H. Sabry, M. E. Martone, T. J. Deerinck, M. H. Ellisman, G. J. Bassell, and K. S. Kosik.** 1996. Translocation of RNA granules in living neurons. J. Neurosci. **16**:7812–7820.
33. **Kraut, R., and J. A. Campos-Ortega.** 1996. Inscuteable, a neural precursor gene of Drosophila encodes a candidate for a cytoskeletal adaptor protein. Dev. Biol. **174**:66–81.
34. **Krovat, B. C., and M. F. Jantsch.** 1996. Comparative mutational analysis of the double-stranded RNA binding domains of Xenopus laevis RNA-binding protein. A. J. Biol. Chem. **271**:28112–28119.
35. **Labuda, D., E. Zietkiewicz, and G. A. Mitchell.** 1995. Alu elements as a source of genomic variation: deleterious effects and evolutionary novelties, p. 1–24. *In* R. J. Maraia (ed.), The impact of short interspersed elements (SINEs) on the host genome. R. G. Landes Company, Austin, Tex.
36. **Li, P., X. Yang, M. Wasser, Y. Cai, and W. Chia.** 1997. Inscuteable and staufen mediate asymmetric localization and segregation of prospero RNA during Drosophila neuroblast cell divisions. Cell **90**:437–447.
37. **Long, R. M., R. H. Singer, X. Meng, I. Gonzalez, K. Nasmyth, and R.-P. Jansen.** 1997. Mating type switching in yeast controlled by asymmetric localization of ASH1 mRNA. Science **177**:383–387.
38. **Martin, K. C., A. Casadio, H. Zhu, E. Yaping, J. C. Rose, M. Chen, C. H. Bailey, and E. R. Kandel.** 1997. Synapse-specific, long-term facilitation of Aplysia sensory to motor synapses: a function for local protein synthesis in memory storage. Cell **91**:927–938.
39. **McCormack, S. J., L. G. Ortega, J. P. Doohan, and C. E. Samuel.** 1994. Mechanism of interferon action: motif 1 of the interferon-induced, RNA-dependent protein kinase (PKR) is sufficient to mediate RNA-binding activity. Virology **198**:92–99.
40. **Ming, L., and L. DesGroseillers.** Unpublished data.
41. **Mouland, A. J., J. Mercier, L. Wickham, L. DesGroseillers, and E. A. Cohen.** Submitted for publication.
42. **Nakielny, S., U. Fischer, W. M. Michael, and G. Dreyfuss.** 1997. RNA transport. Annu. Rev. Neurosci. **20**:269–301.
43. **Okita, T. W., X. Li, and M. W. Roberts.** 1994. Targeting of mRNAs to domains of the endoplasmic reticulum. Trends Biochem. Sci. **4**:91–96.
44. **Pachter, J. S.** 1992. Association of mRNA with the cytoskeletal framework: its role in the regulation of gene expression. Crit. Rev. Eukaryotic Gene Expr. **2**:1–18.
45. **Pokrywka, N. J., and E. C. Stephenson.** 1995. Microtubules are a general component of mRNA localization systems in Drosophila oocytes. Dev. Biol. **167**:363–370.
46. **Rings, E.H.H.M., H. A. Büller, A. M. Neele, and J. Dekker.** 1994. Protein sorting versus messenger RNA sorting? Eur. J. Cell Biol. **63**:161–171.
47. **Ross, A. F., Y. Oleynikov, E. H. Kislauskis, K. L. Taneja, and R. H. Singer.** 1997. Characterization of a β-actin mRNA zipcode-binding protein. Mol. Cell. Biol. **17**:2158–2165.
48. **Schmedt, C., S. R. Green, L. Manche, D. R. Taylor, Y. Ma, and M. B. Mathews.** 1995. Functional characterization of the RNA-binding domain and motif of the double-stranded RNA-dependent protein kinase DAI (PKR). J. Mol. Biol. **249**:29–44.
49. **Schumacher, J. M., K. Lee, S. Edelhoff, and R. E. Braun.** 1995. Spnr, a murine RNA-binding protein that is localized to cytoplasmic microtubules. J. Cell Biol. **129**:1023–1032.
50. **Schwartz, S. P., L. Aisenthal, Z. Elisha, F. Oberman, and J. K. Yisraeli.** 1992. A 69-kDa RNA-binding protein from Xenopus oocytes recognizes a common motif in two vegetally localized maternal mRNAs. Proc. Natl. Acad. Sci. USA **89**:11895–11899.
51. **Steward, O.** 1997. mRNA localization in neurons: a multipurpose mechanism? Neuron **18**:9–12.
52. **St. Johnston, D., W. Driever, T. Berleth, S. Richstein, and C. Nüsslein-Volhard.** 1989. Multiple steps in the localization of bicoid RNA to the

anterior pole of the Drosophila oocyte. Dev. Suppl. **107**:13–19.
53. **St Johnston, D., D. Beuchle, and C. Nüsslein-Volhard.** 1991. Staufen, a gene required to localize maternal RNAs in the Drosophila egg. Cell **66**:51–63.
54. **St Johnston, D., N. H. Brown, J. G. Gall, and M. Jantsch.** 1992. A conserved double-stranded RNA-binding domain. Proc. Natl. Acad. Sci. USA **89**:10979–10983.
55. **St Johnston, D.** 1995. The intracellular localization of messenger RNAs. Cell **81**:161–170.
56. **Takizawa, P. A., A. Sil, J. R. Swedlow, I. Herskowitz, and R. D. Vale.** 1997. Actin-dependent localization of an RNA encoding a cell-fate determinant in yeast. Nature **389**:90–93.
57. **Terasaki, M., L. B. Chen, and K. Fujiwara.** 1986. Microtubules and the endoplasmic reticulum are highly interdependent structures. J. Cell Biol. **103**:1557–1568.
58. **Tetzlaff, M. T., H. Jäckle, and M. J. Pankratz.** 1996. Lack of Drosophila cytoskeletal tropomyosin affects head morphogenesis and the accumulation of oskar mRNA required for germ cell formation. EMBO J. **15**:1247–1254.
59. **Tiedge, H., R. T. Fremeau, Jr., P. H. Weinstock, O. Arancio, and J. Brosius.** 1991. Dendritic localization of neural BC1 RNA. Proc. Natl. Acad. Sci. USA **88**:2093–2097.
60. **Tiedge, H., A. Zhou, N. A. Thorn, and J. Brosius.** 1993. Transport of BC1 RNA in hypothalamo-neurohypophyseal axons. J. Neurosci. **13**:4214–4219.
61. **Tongiorgi, E., M. Righi, and A. Cattaneo.** 1997. Activity-dependent dendritic targeting of BDNF and TrkB mRNAs in hippocampal neurons. J. Neurosci. **17**:9492–9505.
62. **Wickham, L., and L. DesGroseillers.** 1991. A bradykinin-like neuropeptide precursor gene is expressed in neuron L5 of Aplysia californica. DNA Cell Biol. **10**:249–258.
63. **Wilhelm, J. E., and R. D. Vale.** 1993. RNA on the move: the mRNA localization pathway. J. Cell Biol. **123**:269–274.
64. **Wilsch-Bräuninger, M., H. Schwarz, and C. Nüsslein-Volhard.** 1997. A sponge-like structure involved in the association and transport of maternal products during Drosophila oogenesis. J. Cell Biol. **139**:817–829.
65. **Zauner, W., J. Kratz, J. Staunton, P. Feick, and G. Wiche.** 1992. Identification of two distinct microtubule binding domains on recombinant rat MAP1B. Eur. J. Cell Biol. **57**:66–74.

IV- Article 3

Multiple determinants in human RNA-binding protein Staufen are involved in ribosome and rough endoplasmic reticulum association

Ming Luo and Luc DesGroseillers

Journal of Biological Chemistry, submitted.

Multiple determinants in human RNA-binding protein Staufen are involved in ribosome and rough endoplasmic reticulum association

Ming Luo and Luc DesGroseillers*

Department of Biochemistry, University of Montreal, Montreal, Canada, H3C 3J7

* To whom correspondence should be addressed:

Dr Luc DesGroseillers

Department of Biochemistry

University of Montreal

P.O. Box 6128, Station Centre Ville

Montreal, (Que), Canada

H3C 3J7

Running title: Mapping of hStau functional domains

Keywords: RNA-binding protein/ mRNA localization/ mRNA transport/ cytoskeleton/ RNA-binding activity/ribosomes

SUMMARY

The human double-stranded (ds) RNA-binding protein Staufen (hStau) is believed to mediate intracellular RNA transport. In this paper, we show by immunofluorescence microscopy and cell fractionation that endogenous Stau^{55} and Stau^{63} isoforms differentially cofractionate with ribosomes and the rough endoplasmic reticulum (RER), respectively, suggesting that they are incorporated into different complexes and are likely to play different roles. Analysis of hStau^{55} mutants indicated that the dsRNA-binding domain 4 (dsRBD4) and the tubulin-binding domain (TBD) together constitute the basal ribosome association domain. This association is independent of Staufen's RNA-binding activity. Deletion of TBD from hStau^{55} shifts the distribution of the protein from ribosomes to the RER, demonstrating that TBD is crucial for ribosome association and that hStau^{55} carries a cryptic determinant (dsRBD2/3/4) that allows its full association with the RER. Therefore, hStau^{55} can associate not only with ribosomes but also with the RER. Accordingly, deletion of dsRBD4 from hStau^{55} modified hStau^{55} association with both ribosomes and the RER, demonstrating that dsRBD4 has a pivotal role in Staufen distribution. Together with the fact that dsRBD4 alone cofractionates with the RER marker, these results suggest that dsRBD4/TBD-mediated ribosome association is dependent on RER association, show that hStau^{55} may be a bridging molecule between the RER and ribosomes through overlapping determinants and that hStau^{55} is likely to play some role in translation.

INTRODUCTION

Mammalian Staufen is an RNA-binding protein which recognizes and binds dsRNAs and RNAs with extensive secondary structures[1;2]. Molecular dissection of the protein *in vitro* revealed that Stau contains two functional dsRNA-binding domains (dsRBD3 and dsRBD4), the major one corresponding to dsRBD3 of *Drosophila* Staufen (dStau)[2]. Mammalian Staufen was also shown *in vitro* to bind tubulin via a region similar to the microtubule-binding domain of MAP-1B[2]. Electron microscopy and pharmacological studies in rat hippocampal neurons were consistent with the possibility that Stau associates with microtubules, although direct interaction *in vivo* has not been documented[3;4]. In both neurons and fibroblasts, Staufen mainly colocalizes with markers of the RER[1-3]. Cell fractionation and sedimentation analyses further indicated that Stau cofractionates with ribosomes and polysomes[1]. Association with polysomes was confirmed by the change in Staufen sedimentation properties following polysomes dissociation by puromycin or EDTA treatment[1]. hStau is a functional component of RNA-containing granules that migrate in dendrites of hippocampal neurons[4] and is encapsidated along with HIV-1 RNA into virus particles[5], strongly suggesting that hStau might be involved in mRNA transport.

Staufen isoforms with apparent molecular masses of 55 ($Stau^{55}$) and 63/65 ($Stau^{63}$) kDa have been observed by Western blotting in human, mouse and rat and cDNAs coding for $Stau^{55}$ have been isolated in these species[1-3;6]. So far, cDNA coding for the 63/65 kDa isoform has not been isolated in any species. We previously reported in human cells a differentially spliced transcript that codes for a protein of 63 kDa which comigrates with the 63 kDa protein observed on Western blots[2], suggesting that the cloned 63 kDa isoform and the common 63 kDa protein are the same protein. However, this is clearly not the case since their subcellular distribution is different (Luo and DesGroseillers, unpublished) and since similar differentially spliced

transcripts have not been found in mouse and rat[6;7], demonstrating that the cloned transcript is specifically expressed in humans.

To understand further the role of Staufen in mammals, we studied the subcellular distribution of the endogenous isoforms as well as a series of hStau[55] mutants expressed in *trans*. These experiments revealed the presence of two different Staufen-containing particles suggesting that Staufen isoforms play different roles in mammals. In addition, we identified two major domains involved in hStau[55] subcellular distribution *in vivo*. Each of them requires multiple contributions for full activity and determines the binding of the protein to different intracellular targets.

EXPERIMENTAL PROCEDURES

Cell culture and microscopy

Mammalian cells grown in Dulbecco's Modified Essential Medium (DMEM) supplemented with 10% fetal bovine serum and penicillin/streptomycin were transiently transfected with cDNAs using the calcium/phosphate precipitation technique. Cells were fixed less than 16 h post-transfection to prevent overexpression of the proteins, and stained with antibodies as previously described[2]. The green fluorescence protein (GFP) and GFP-fusion proteins were detected by autofluorescence. For the analysis of cytoskeleton-associated proteins, transfected cells were first extracted in 0.3% Triton X-100 prior to fixation. Cells were visualized by immunofluorescence (IF) using the 63X Plan-Apochromat objective of a Zeiss Axioskop fluorescence microscope.

Construction and molecular cloning of the fusion proteins

All the mutants were constructed by PCR amplification of the cDNAs coding for hStau[55], using the Vent DNA polymerase (New England Biolabs, Berverly, MA). The resulting fragments were digested with appropriate restriction enzymes and cloned in pCDNA3/RSV[8]. When necessary, a hemagglutinin (HA_3) tag or GFP was added to the C-terminal of the mutants as described previously[2]. To construct RBD2/3/4 we used the sense primer P1 (5'-AATTGGTACCTGCACTGTGCGTGAAACTTGGA-3', underlined: *Kpn*I restriction site) in pairs with the antisense primer P2 (5'-ATATTCTAGATTAGCGGCCGCTCTCCTCTGACTTGAGTGC-3', underlined: *Xba*I and *Not*I restriction sites). RBD4, RBD4/TBD/5 and RBD4/TBD were constructed with the sense primers P3 (5'-ATATAAGCTTAAGCCACCATGGTCAAGCCACAGACAAGC-3', underlined : *Hind*III

restriction site and Kozak's consensus sequence) and antisense primers P2, P4 (5' TACAATCTAGATTATCAGCGGCCGCACCTCCCACACACAGACAT-3') and P5 (5' TACAATCTAGATTAGCGGCCGCGCTCAGAGGGTCTAGTGCGAG-3'), respectively. TBD/5 was amplified with the sense primer P6 (5' TACATAAGCTTAAGCCACCATGGTCAAAGTCCCGCAGCGGC-3') and the antisense primer P4. To construct hStau^{55}ΔTBD, the sense primer 5' ATGATAGCCCGAGAGTTGTTGTATGGG 3' was paired to the antisense primer 5' GACTTTGAAACCAAGGATCTCCAGCAT 3'. The PCR reaction was treated with *Dpn*I (Roche Molecular Biochemicals), T4 PNK Kinase (Pharmacia) and self-ligated. To construct hStau^{55}Δ4, the sense primer 5' ACCAAACCCGCACTCAAGTCAGAGGAG 3' and antisense primer 5' TGGGCTTGTCTGTGGCTTGACTATGGG 3' were used and the resulting PCR fragment was self-ligated. Finally, to construct hStau^{55}Δ5, the sense primer 5'-AATTGGTACCTGCACTGTGCATGAAACTTGGA-3' (underlined: *Kpn*I restriction site) and antisense primer 5'-TATATCTAGATTAGCGGCCGCACAACTCTCGGGCTATCATGGC-3' were used.

All the fusion and mutated proteins were first expressed in COS7 cells and analyzed by SDS-PAGE to test their level of expression and stability (Fig. 1). Accordingly, we decided to fix or harvest the cells 16 h post-transfection to prevent overexpression of the proteins in subsequent studies. The half-life of wild-type and of several mutants has been reported elsewhere[5].

Site-directed mutagenesis

Phenylalanine residues at position 135 and 238 in dsRBD3 and dsRBD4, respectively, were mutated into alanine using two sense primers carrying mutations, P7 (5'-

TTTTCCCGGGAGAGTGGCCCACCCCACATGAAGAACGCTGTGACCAAG-3', underlined: endogenous *Sma*I restriction site, italic: mutated nucleotides), and P8 (5'-TTTTAGGCCTCCCGCGCCGCAGGGAGGCTGTGATGCAG-3', (underlined: endogenous *Stu*I restriction site, italic: mutated nucleotides) and the antisense primer P9 (5'-CTACAGCCTGGGCGACCTCGG-3'), located downstream from the endogenous *Eco*RI restriction site. The resulting fragments were digested with *SmaI/Eco*RI and *StuI/Eco*RI, respectively, substituted for the corresponding wild type fragment in hStau^{55} cDNA, and sequenced. All fusion proteins and mutants were expressed in COS7 cells and analyzed by SDS-PAGE showing comparable expression levels and stabilities, as described above (Fig. 1).

Protein purification, Western blotting and RNA-binding assay

To determine the RNA-binding capacity of hStau^{55}/3* and hStau^{55}/3*/4*, we substituted the HA_3 tag by a His_6 tag at the C-terminal end of the mutants using the annealed oligonucleotides 5'-GGCCACCATCACCATCACCATTA-3' and 5'-GGCCTAATGGTGATGGTGATGGT-3'. After transfection into HEK293 cells, cells were harvested and lysed. hStau^{55}-his_6 fusion proteins were isolated on Ni-NTA columns as described before[2]. Expression of the mutants was determined by Western blotting. Their RNA-binding capacity was determined by Northwestern blotting as described before[2].

Cell fractionation on sucrose gradient

Cell fractionation was done by sedimentation through sucrose gradients (Antebi and Fink, 1992). COS7 cells were rinsed with cold PBS (pH 7.5) and harvested. Approximately 4 x 10^7 cells were resuspended in 3 ml of lysis buffer (10 mM Hepes, pH 7.5, 12.5% sucrose, 1 mM EDTA, 1 mM PMSF, 1 μg/ml pepstatin, 1 μg/ml aprotinin) and subjected to at least 10 strokes in

a Dounce homogenizer. Two centrifugations at 700 x *g* and 1000 x *g* were performed and the resulting supernatant was layered onto a step gradient of 9 fractions of 22 to 60% (w/v) sucrose in 10 mM HEPES, pH 7.5, 1 mM $MgCl_2$. The gradients were centrifuged at 37,000 rpm (SW40 rotor, Beckman Instruments) for 2.5 h at 4°C. Fifteen fractions (0.77 ml) were taken sequentially from the top of the tube and aliquots of each fraction were analyzed by SDS-PAGE. Proteins were transferred to nitrocellulose and probed with either anti-HA (generous gift from Dr M. Bouvier, Université de Montréal, Montréal, Canada), anti-hStau[2], anti-calnexin (Stressgene, BC, Canada) or anti-ribosomal L7a (generous gift from Dr A. Ziemiecki, University of Berne, Switzerland). Quantification of the protein amounts that cofractionate with ribosomes, the RER or soluble proteins was done with a HP ScanJet (6100C) using the NIH Image processing and analysis program.

RESULTS

Two Staufen isoforms are differentially associated with ribosomes and the RER

It was previously shown that hStau is mainly localized to the RER[1;2]. Cell fractionation further revealed that it is associated with polysomes in mammalian cells[1]. To gain more insight into the distribution of Staufen, we determined the sedimentation profile of endogenous Staufen in a sucrose gradient that allowed the migration of ribosomes and RER microsomes to different fractions. Each fraction of the gradient was tested by Western blotting with anti-hStau, anti-calnexin, anti-L7a and anti-αtubulin antibodies to detect respectively Staufen, RER, ribosomes and soluble proteins. Interestingly, $Stau^{63}$ and $Stau^{55}$ presented different sedimentation profiles: while $Stau^{63}$ cofractionated with the RER marker, $Stau^{55}$ was predominantly found in ribosome-containing fractions like L7a (Fig. 2A). These results indicate that Stau isoforms can be associated with at least two distinct subcellular compartments or organelles.

We then determined by sucrose density gradient sedimentation whether transiently transfected $hStau^{55}$-HA_3 has the same subcellular distribution as the endogenous protein. Transfected cells were harvested about 16 h post-transfection to prevent overexpression of the protein. The exogenous proteins are then expressed at a lower level than endogenous isoforms (Fig. 1). As shown in Figure 2B, the cloned $hStau^{55}$-HA_3 cofractionated with the ribosomes, as observed above for endogenous $hStau^{55}$. These results indicated that transiently expressed $hStau^{55}$-HA_3 has the same subcellular distribution as the endogenous protein and that it can be used to identify the molecular determinant(s) involved in $Stau^{55}$ ribosome association.

N- and C-terminal determinants cofractionate with the RER and ribosomes, respectively

To identify the molecular determinants involved in ribosome association, we first expressed a series of hStau[55] mutants (Fig. 3) in COS7 cells and determined their subcellular localization by immunofluorescence microscopy and velocity sedimentation. The N-terminal mutant (RBD2/3/4-HA_3) localized to tubulovesicular structures that resemble RER (Fig. 4C) and colocalized with calnexin, a marker of the RER, as revealed by confocal microscopy (not shown). The localization was not altered by Triton X-100 treatment (Fig. 4D), which removes soluble proteins and retains cytoskeleton-associated proteins. This behavior was similar to that of the wild-type protein (Fig. 4 A,B)[2], demonstrating that this region contains a strong determinant for localization and suggesting that the C-terminal region may be dispensable. Accordingly, the C-terminal mutant (RBD4/TBD/5-HA_3) showed a diffuse cellular staining in both the cytoplasm and nucleus (Fig. 4E). However, once soluble proteins were removed by Triton X-100 treatment, a tubulovesicular Triton-resistant staining was visible (Fig. 4F), suggesting that a second independent determinant can promote hStau[55] localization.

When analyzed by sucrose gradient sedimentation, RBD2/3/4-HA_3 cofractionated with the RER marker, in a pattern similar to that of hStau[63] (Fig. 5A). Quantification indicates that the amount of RBD2/3/4-HA_3 is proportional to that of calnexin all across the gradient, suggesting that RBD2/3/4-HA_3 is exclusively associated with the RER. In contrast, RBD4/TBD/5-HA_3 fractionation pattern was similar to that of the full-length 55 kDa protein (Fig. 5B), although, consistent with the immunofluorescence observation, about 35% of the protein was found with the soluble proteins. Altogether, these results demonstrate that two independent determinants are present along the protein subdomains, each of them recognizing a different subcellular structure/organelle; that hStau[55]/ribosome association depends on determinants located in

dsRBD4, TBD or dsRBD5; and that RBD2/3/4 has full binding capacity and must be present to increase and stabilize the C-terminal-dependent hStau^{55}/ribosome association. However, in the context of hStau^{55}, the C-terminal determinant is dominant over the N-terminal determinant for proper targeting of the protein to its subcellular localization.

RBD4/TBD is essential and sufficient for ribosome association

We then mapped the minimal domain in the C-terminal region that is required for hStau^{55}/ribosome association observed after Triton treatment. Deletion of dsRBD5 from the C-terminal mutant (RBD4/TBD-HA$_3$) had no effect on the subcellular distribution of the protein, demonstrating that this domain is not involved in ribosome association (Fig. 6A,C). Accordingly, in the sedimentation assay RBD4/TBD-HA$_3$ showed a profile similar to RBD4/TBD/5-HA$_3$ (Fig. 7A). In contrast, TBD-GFP[2] and TBD/RBD5-HA$_3$ were completely extracted by Triton treatment (Fig. 6 B,D) and in the sedimentation assay TBD/RBD5-HA$_3$ was mostly found with the soluble proteins (Fig. 7B). RBD4 alone (RBD4-HA$_3$) did not cofractionate with ribosomes (Fig. 7C). Altogether, these results demonstrate that both dsRBD4 and TBD are necessary for the localization of the C-terminal mutant to ribosomes and constitute the basal ribosome association domain.

TBD is critical for ribosome association

Although TBD alone cannot promote the association of a heterologous fusion protein with Triton resistant organelles[2], comparison of the subcellular distribution of RBD2/3/4-HA$_3$ (Fig. 5A) and RBD4/TBD-HA$_3$ (Fig. 7A) suggests that TBD is critical for *in vivo* ribosome association. To prove this point, we either fused TBD to the RER-associated RBD2/3/4-HA$_3$ mutant or deleted TBD from the ribosome associated full-length protein and determined the

subcellular distribution of the resulting proteins by velocity sedimentation. Adding TBD to RBD2/3/4-HA_3 (hStau^{55}Δ5-HA_3) shifted the distribution of the protein from the RER (Fig. 5A) to ribosomes (Fig. 8A). Deletion of TBD from the full-length protein (hStau^{55}ΔTBD-HA_3) had the reverse effect and relocalized the protein to the RER (Fig. 8B). This result demonstrates that TBD is critical for hStau-ribosome association.

dsRBD4 independently associates with the RER and plays a dual role in RER and ribosome association

When analyzed on sucrose gradient, more than 50% of RBD4-HA_3 cofractionated with the RER (Fig. 7C), demonstrating that this domain is an independent determinant for RER association. In contrast, RBD2-HA_3 and RBD3-HA_3 were found with soluble proteins at the top of the gradients (not shown). These results demonstrate that, in the absence of TBD, dsRBD4 is sufficient for RER association. However, in the presence of TBD, dsRBD4 becomes an essential cofactor for ribosome association, suggesting that RER association through dsRBD4 is important for ribosome association and that dsRBD4 allows a transition between the RER and ribosome association.

To understand further the role of the RER-associated dsRBD4 on hStau^{55}/ribosome association, we deleted dsRBD4 from hStau^{55} and analyzed the localization of the resulting protein by sucrose gradient. Despite the fact that dsRBD4 is essential for basal association with ribosomes, its deletion from hStau^{55} (hStau^{55}Δ4-HA_3) seemed to have no effect on the strong ribosome association of the protein (Fig. 8C). However, when deletion of dsRBD4 was paired to a point mutation in dsRBD3 that abolished Staufen RNA-binding activity (Fig. 9B), hStau^{55}/3*/Δ4-HA_3 showed random cytoplasmic/nuclear distribution (not shown) and

cofractionated with soluble proteins (Fig. 8D). Therefore, hStau^{55}Δ4-HA$_3$ associates with ribosomes via an RNA-binding dependent molecular mechanism in contrast to hStau^{55}-HA$_3$ and RBD4/TBD/5-HA$_3$ whose association is independent of RNA-binding activity (see below, Fig. 10B). These results both demonstrate that dsRBD4 plays a significant role in hStau^{55} association with ribosomes and emphasize its critical role for RER association.

dsRNA-binding activity plays indirect role in ribosome association

Since hStau^{55} contains functional RNA-binding domains (dsRBD3 and dsRBD4), we asked whether RNA-binding activity is involved in hStau^{55} distribution in mammals. One possibility is that binding dsRNA induces a structural shift in Staufen that changes its affinity for subcellular targets. To address this point, we introduced point mutation in dsRBD3 alone (F135A) or in both dsRBD3 (F135A) and dsRBD4 (F238A), to generate hStau^{55}/3*-his$_6$ and hStau^{55}/3*/4*-his$_6$. We first tested whether the point mutations introduced in the dsRBDs abolished the dsRNA-binding capacity of the protein. Both hStau-his$_6$, hStau^{55}/3*-his$_6$ and hStau^{55}/3*/4*-his$_6$ were overexpressed in mammalian cells and purified on Ni-NTA columns. Levels of expression were determined by Western blotting (Fig. 9A) and RNA-binding activity by Northwestern assay (Fig. 9B). This experiment showed that the mutations are sufficient to abolish the dsRNA-binding capacity of the mutants and that dsRBD3 is critical for this activity.

In transiently transfected COS7 cells, both hStau^{55}/3*-HA$_3$ (not shown) and hStau^{55}/3*/4*-HA$_3$ (Fig. 9A) proteins cofractionated with the ribosome marker, as did hStau^{55}-HA$_3$. However, the amounts of protein associated with the soluble proteins increased. When analyzed by IF, the proteins were randomly distributed, but significant amounts were retained in tubulovesicular structures after Triton treatment (not shown). Mutation in dsRBD4 alone

(hStau^{55}/4*-HA$_3$) has no effect on hStau^{55} distribution (not shown). These results indicated that dsRBD3 RNA-binding activity plays additional roles in the subcellular localization of hStau^{55}, especially on the strength of hStau^{55}/organelle association. However, it did not change the RER-ribosome distribution of the protein. Interestingly, overexpression of hStau^{55}/3*-HA$_3$ or hStau^{55}/3*/4*-HA$_3$ induces the formation of large Staufen-containing granules around the nucleus. As determined by confocal microscopy, these granules colocalize with calnexin (not shown, see Fig. 3 in the Appendix), suggesting that RNA-binding activity may play a more important role in transporting Staufen-containing particles and/or RER vesicles than in targeting the complexes to subcellular organelles.

We also tested whether RNA-binding activity is important in the context of the minimal domains involved in ribosome association. F238A point mutation was introduced in the C-terminal mutants to generate RBD4*/TBD/5-HA$_3$. Both IF analyses in the presence or absence of Triton X-100 (not shown) and cell fractionation (Fig. 10B) indicate that mutation that abolished the RNA-binding activity of dsRBD4 had no effect on RBD4*/TBD/5-HA$_3$ distribution as compared to that of RBD4/TBD/5-HA$_3$ (Fig. 5B). This indicated that basal ribosome binding is completely independent of RNA binding activity.

DISCUSSION

From its predicted protein sequence, mammalian Stau is expected to be a modular protein. Recently we demonstrated that three regions are functional for binding dsRNA (dsRBD3 and dsRBD4) or tubulin (TBD) *in vitro*[2]. In this paper, we tested hStau^{55} domains for their ability to localize the protein to subcellular organelles/structures *in vivo*. We demonstrate that Stau^{55} and Stau^{63} isoforms differentially co-fractionate with ribosomes and the RER and that they are likely to play different roles in RNA localization or processing. Basal Stau^{55} association with the ribosomes relies on both dsRBD4 and TBD but dsRBD2 and dsRBD3 play additional roles for full association. Although hStau^{55} isoform is mainly associated with ribosomes, it has the potential to be associated with the RER through a cryptic molecular determinant overlapping dsRBD2, dsRBD3 and dsRBD4. hStau^{55} RNA-binding activity stabilizes Staufen association with the ribosome and may be important for putative RER-mediated mRNA transport.

Multiple domains are involved in hStau^{55} subcellular distribution

Our results demonstrate that multiple domains are required for hStau^{55} stable association with ribosomes. Among them, dsRBD4 and TBD are the most important ones. Indeed, RBD4/TBD is sufficient and necessary for ribosome association. Interestingly, deletion of TBD shifts the distribution of the protein from ribosomes to the RER whereas deletion of dsRBD4 modifies both ribosome and RER associations. These results can be explained either by a single determinant that overlaps the two regions, or by two determinants playing complementary roles. In the former case, an additional subdomain in dsRBD4 must be present to allow its association with the RER. In the latter case, TBD is crucial for ribosome association but its function is

dependent of RER association through dsRBD4. In both cases, dsRBD4 is a central determinant involved in both the RER and ribosome association. Basal hStau^{55}/ribosome association through RBD4/TBD is independent of RNA-binding activity, suggesting that protein/protein interactions occur. Therefore, the molecular mechanism is likely to differ from that involving other members of the dsRNA-binding proteins family: association of the double-stranded dependent protein kinase (PKR) with ribosomes requires the presence of functional RBDs, although an additional independent ribosome-association site was mapped outside of the RBDs[9;10].

Interestingly, deletion of TBD reveals a cryptic determinant involved in RER association. This determinant works independently of ribosome association. dsRBD4 which associates with the RER is the major determinant. The addition of dsRBD2 and dsRBD3 strengthens Staufen dsRBD4/RER association. Indeed, the fusion of the three domains reconstitutes the full binding activity of the protein. These domains may induce an RNA-dependent conformational change in dsRBD4 or contribute to create a ribonucleoprotein complex that is recognized by other RNA-binding proteins, cofactors and/or receptors, facilitating hStau association with the RER. dsRBD4 seems to contribute very little to the RNA-binding activity of the full-length protein. Therefore, it is likely to bind components of the RER through protein/protein interactions. Protein-protein interactions mediated by dsRBDs have been reported for *Drosophila* Staufen and other members of the dsRNA-binding protein family[11-14].

The complex process of RER association requires the cooperation of multiple determinants consisting of dsRBD2, dsRBD3 and dsRBD4. It is likely that the RER-associated Stau^{63} protein uses the same N-terminal determinants (RBD2/3/4) to promote its association with the RER. So far we have no evidence for expression of transcripts coding for a Staufen isoform with a modified or truncated C-terminus which would delete TBD (Duchaîne and DesGroseillers, unpublished). Therefore, in the context of Stau^{63}, TBD function must be modulated somehow to

prevent its association with ribosomes. The additional amino acid sequence found in Stau[63] compared to Stau[55] or specific cofactors may play this role. The cloning of its cDNA will allow us to test our hypothesis.

RNA-binding activity mediated by dsRBD3 seems to further strengthen Staufen association with subcellular organelles. Mutations that abolish RNA-binding activity release significant amounts of bound proteins but do not relocalize the protein to novel subcellular targets. However, the role of RNA-binding activity in Staufen association with subcellular structures will be markedly underestimated if transfected mutants form dimers with the endogenous Staufen already associated with ribosomes. dsRBD4/TBD would then specify dimer formation rather than ribosome association. Formation of dimers between endogenous Staufen isoforms has been proposed before[15].

Staufen as a molecular bridge between the RER, ribosomes and cytoskeleton

Our results are consistent with the possibility that hStau[55] association with ribosomes requires prior or simultaneous association with the RER and that hStau[55] represents a bridging molecule between ribosomes and the RER. The presence of dsRBD4, a functional RER-binding domain as a cofactor for ribosome association, supports this hypothesis. In addition, RBD4/TBD-mediated ribosome association is strengthened by the addition of the full N-terminal RER-binding domain and is weakened by mutation that destroyed the RNA-binding activity, as observed for RER association (Luo and DesGroseillers, unpublished). Interestingly, overexpression of hStau[55] increases the percentage of protein associated with RER fractions (see Fig. 2B). This would be expected if a putative RER to ribosome transition step is saturable. Therefore, ribosome association seems to be dependent on RER association. dsRBD4 which is

involved in both RER and ribosome association may be the molecular switch for the ribosome/RER transition.

TBD was also shown to bind tubulin *in vitro*[2]. In COS7 cells, we have no evidence for hStau/microtubule colocalization, but the size of the cell may not allow one to observe the transport of a small population of Staufen-containing particles. In contrast, Stau distribution[3] and movement within dendrites of neurons in culture[4] are sensitive to drugs that disrupt microtubules. Altogether, these results suggest that hStau also bridges the RER and the microtubules, at least in some cell compartments. A dynamic translocation of hStau-containing complexes between ribosomes, RER and microtubules may be important for hStau function(s) in mammals.

Putative role of Stau^{55} isoform in vivo

Our results are consistent with the possibility that each Staufen isoform plays a different role in mammals. It was previously suggested that Staufen is involved in mRNA transport in neurons[4]. This view was based on the fact that Staufen-GFP labeled granules move from the cell body into dendrites in a microtubule-dependent manner. This paper now suggests that Stau^{55} plays additional role in the cell. It is likely that Stau^{55} is rather involved in a ribosome-related function. The fact that Stau^{55} association with ribosomes is independent of its dsRNA-binding activity suggests that it may directly modulate ribosomal proteins, ribosome-associated proteins or translation factors and eliminates the possibility that Stau^{55} indirectly associates with ribosomes via translation of Stau^{55}-bound RNAs. This is consistent with previous studies that showed that Staufen still cofractionated with ribosomal subunits after treatment of the polysomes with EDTA[1]. Therefore, Stau^{55} may directly modulate ribosome functions and be involved for example in translation regulation. Genetic studies involving *oskar* mRNA and Staufen in *Drosophila*[16] are consistent with this possibility. It will be interesting to determine whether Stau^{55}

is involved in the derepression of mRNA translation as does its *Drosophila* homologue[17] or whether it plays other role(s). In the former hypothesis, dsRBD5 might functionally cooperate with the identified ribosome association domain (TBD) to regulate translation since *Drosophila* dsRBD5 was shown to be involved in the derepression of *oskar* mRNA translation once localized[17]. We nevertheless do not exclude the possibility that, though Stau[55] perfectly co-fractionates with ribosomes, it is associated not with ribosomes but with a ribonucleoprotein complex of the same density. Identification of endogenous RNAs and proteins that are bound to Stau[55] will be very important to further characterize the role(s) of this Staufen isoform in the cell.

ACKNOWLEDGMENTS

We thank A. Montmarquette for technical assistance; Drs. A. Mouland, R. Subramanian and M. A. Kiebler for critical reading of the manuscript; Judith Kashul for editing the manuscript; Dr Michel Bouvier (Département de Biochimie, University of Montreal) for the anti-HA antibodies and Dr A. Ziemiecki (University of Berne, Switzerland) for the anti-ribosomal L7a antibodies; and L. Cournoyer for help with tissue culture. This work was supported by a grant from the Natural Sciences and Engineering Research Council of Canada (NSERC) to LDG.

FIGURE LEGENDS

Figure 1. Western blot analyses of transiently expressed Staufen mutants. COS7 cells were transfected with cDNAs coding for hStau^{55}-HA$_3$ or mutants. Sixteen (lanes 3 to 10) or 48 (lane 2) hours post-transfection cells were lysed and the proteins analyzed by SDS-PAGE. Staufen mutants were detected with anti-Staufen **(A)** to compare their level of expression to that of the endogenous Stau^{63} (black arrow) and Stau^{55} (arrow head) isoforms, or anti-HA **(B)** antibodies. Lane 1, mock-transfected cells. Lanes 2 and 3, hStau^{55}-HA$_3$. Lane 4, hStau^{55}/3*/4*-HA$_3$. Lane 5, hStau^{55}/Δ4-HA$_3$. Lane 6, hStau^{55}/ΔTBD-HA$_3$. Lane 7, hStau^{55}/Δ5-HA$_3$. Lane 8, RBD2/3/4-HA$_3$. Lane 9, RBD4/TBD/5-HA$_3$. Lane 10, RBD4/TBD-HA$_3$. Asterisk indicates the position of a non-specific band.

Figure 2. Differential association of Staufen isoforms with the RER and ribosomes. (A) Untransfected COS7 cells were homogenized and fractionated on sucrose gradient. Each fraction was collected and the proteins separated by SDS-PAGE. Staufen, RER, ribosomes and soluble proteins were detected as indicated with anti-Staufen, anti-calnexin, anti-L7a and anti-αtubulin antibodies, respectively. Molecular mass (kDa) of the proteins is indicated on the right. The fast migrating proteins of about 53 kDa are generated from Stau^{55} by differential translation initiation at different ATGs (Luo and DesGroseillers, unpublished). **R**: ribosome. **RER**: rough endoplasmic reticulum. **(B)** COS7 cells were transfected with cDNAs coding for hStau^{55}-HA$_3$, lysed 16 h post-transfection and analyzed as described in (A), except that fusion proteins were detected with the anti-HA antibody. L7a is also detected in RER fractions on overexposed blots. Schematic representation of transfected protein is shown below the gel. White and dotted boxes represent the major and minor RNA-binding domains, respectively, while black boxes represent regions

with RNA-binding consensus sequence but lacking RNA-binding activity *in vitro*. The hatched box indicates the position of the region similar to the MAP1B microtubule-binding domain.

Figure 3. Schematic representation of hStau mutants. Left side: schematic representation of Staufen mutants. The color code is the same as in the legend of Figure 2. A: mutations F135A or F238A. Right side: summary of results obtained by IF and cell fractionation (gradients). IF: +, full association with subcellular organelles/structures in the absence or presence of Triton X-100; -, random cytosolic/nuclear distribution before Triton treatment and complete protein removal after Triton treatment; +/-, random cytosolic/nuclear distribution before Triton treatment but significant association with subcellular organelles/structures after Triton treatment. Gradients: **RER**, cofractionation of Staufen with the RER; **R**, cofractionation of Staufen with ribosomes; -, cofractionation of Staufen with soluble proteins.

Figure 4. Subcellular localization of hStau^{55}-HA$_3$, RBD2/3/4-HA$_3$ and RBD4/TBD/5-HA$_3$ fusion proteins. COS7 cells were transfected with cDNAs coding for either hStau^{55}-HA$_3$ **(A,B)**, RBD2/3/4-HA$_3$ **(C,D)** or RBD4/TBD/5-HA$_3$ **(E,F)** fusion proteins. Untreated **(A,C,E)** or Triton X-100 treated **(B,D,F)** cells were fixed and visualized by fluorescence using anti-HA antibodies. Scale bar = 20 μm.

Figure 5. RBD2/3/4-HA$_3$ and RBD4/TBD/5-HA$_3$ cofractionate with the RER and ribosomes, respectively. COS7 cells were transfected with cDNAs coding for either RBD2/3/4-HA$_3$ **(A)** or RBD4/TBD/5-HA$_3$ **(B)** and fractionated on sucrose gradient. Each fraction was collected and the proteins separated by SDS-PAGE and analyzed as described in Figure 2.

Figure 6. Subcellular localization of C-terminal mutants. COS7 cells were transfected with cDNAs coding for either RBD4/TBD-HA_3 **(A,C)** or TBD/RBD5-HA_3 **(B,D)** fusion proteins. Untreated **(A,B)** or Triton X-100 treated **(C,D)** cells were fixed and visualized by fluorescence with the anti-HA antibodies. Scale bar = 20 μm.

Figure 7. Fine mapping of the determinant involved in ribosome association. COS7 cells were transfected with cDNAs coding for either RBD4/TBD-HA_3 **(A)**, TBD/RBD5-HA_3 **(B)** or RBD4-HA_3 **(C)** and fractionated on sucrose gradient. Each fraction was collected and the proteins separated by SDS-PAGE and analyzed as described in Figure 2.

Figure 8. Critical role of TBD in ribosome association. COS7 cells were transfected with cDNAs coding for either hStau^{55}Δ5-HA_3 **(A)**, hStau^{55}ΔTBD-HA_3 **(B)**, hStau^{55}Δ4-HA_3 **(C)** or hStau^{55}/3*/Δ4-HA_3 **(D)** and fractionated on sucrose gradient. Each fraction was collected and the proteins separated by SDS-PAGE and analyzed as described in Figure 2.

Figure 9. Point mutations in dsRBDs abolish hStau^{55} RNA-binding activity. cDNAs coding for either hStau^{55}-his_6, hStau^{55}/3*-his_6 or hStau^{55}/3*/4*-his_6 were transfected in HEK293 cells and the his-tagged proteins were purified on Ni-NTA columns. **A)** Western blot experiment with anti-hStau antibodies. **B)** RNA-binding assay. The fusion proteins were electrophoresed on a 10% polyacrylamide gel, transferred to nitrocellulose, and incubated with ^{32}P-labeled bicoid 3'UTR RNA as described previously[2]. After extensive washing, RNA binding was detected by autoradiography.

Figure 10. RNA-binding activity plays additional role in Staufen distribution. COS7 were transfected with hStau^{55}/3*/4*-HA$_3$ **(A)** or RBD4*/TBD/5-HA$_3$ **(B)** and fractionated on sucrose gradient. Each fraction was collected and the proteins separated by SDS-PAGE and analyzed as described in Figure 2.

REFERENCE LIST

1. Marión, R. M., Fortes, P., Beloso, A., Dotti, C., and Ortin, J. (1999) *Mol.Cell Biol.* **19,** 2212-2219

2. Wickham, L., Duchaîne, T., Luo, M., Nabi, I. R., and DesGroseillers, L. (1999) *Mol.Cell Biol.* **19,** 2220-2230

3. Kiebler, M. A., Hemraj, I. A., Verkade, P., Köhrmann, M., Fortes, P., Marión, R. M., Ortín, J., and Dotti, C. G. (1999) *J.Neurosci.* **19,** 288-297

4. Köhrmann, M., Luo, M., Kaether, C., DesGroseillers, L., Dotti, C. G., and Kiebler, M. A. (1999) *Mol.Biol.Cell* **10,** 2945-2953

5. Mouland, A. J., Mercier, J., Luo, M., Bernier, L., DesGroseillers, L., and Cohen, E. A. (2000) *J.Virol.* **74,** 5441-5451

6. Monshausen, M., Putz, U., Rehbein, M., Schweizer, M., DesGroseillers, L., Kuhl, D., Richter, D., Kindler, S. (2001) *J. Neurochem.* **76,** 155-165

7. Brizard, F., Luo, M., and DesGroseillers, L. (2000) *DNA Cell Biol.* **19,** 331-339

8. Jockers, R., Da Silva, A., Strosberg, A. D., Bouvier, M., and Marullo, S. (1996) *J.Biol.Chem.* **271,** 9355-9362

9. Zhu, S., Romano, P. R., and Wek, R. C. (1997) *J.Biol.Chem.* **272,** 14434-14441

10. Wu, S., Kumar, K. U., and Kaufman, R. J. (1998) *Biochemistry* **37,** 13816-13826

11. Cosentino, G. P., Venkatesan, S., Serluca, F. C., Green, S. R., Mathews, M. B., and Sonenberg, N. (1995) *Proc.Natl.Acad.Sci.USA* **92,** 9445-9449

12. Schmedt, C., Green, S. R., Manche, L., Taylor, D. R., Ma, Y., and Mathews, M. B. (1995) *J.Mol.Biol.* **249,** 29-44

13. Li, P., Yang, X., Wasser, M., Cai, Y., and Chia, W. (1997) *Cell* **90,** 437-447

14. Schuldt, A. J., Adams, J. H. J., Davidson, C. M., Micklem, D. R., Haseloff, J., St Johnston, D., and Brand, A. H. (1998) *Genes Dev.* **12,** 1847-1857

15. Duchaîne, T., Wang, H. J., Luo, M., Steinberg, S. V., Nabi, I. R., and DesGroseillers, L. (2000) *Mol.Cell Biol.* **20,** 5592-5601

16. Kim-Ha, J., Kerr, K., and Macdonald, P. M. (1995) *Cell* **81,** 403-412

17. Micklem, D. R., Adams, J., Grunert, S., and St Johnston, D. (2000) *EMBO J.* **19,** 1366-1377

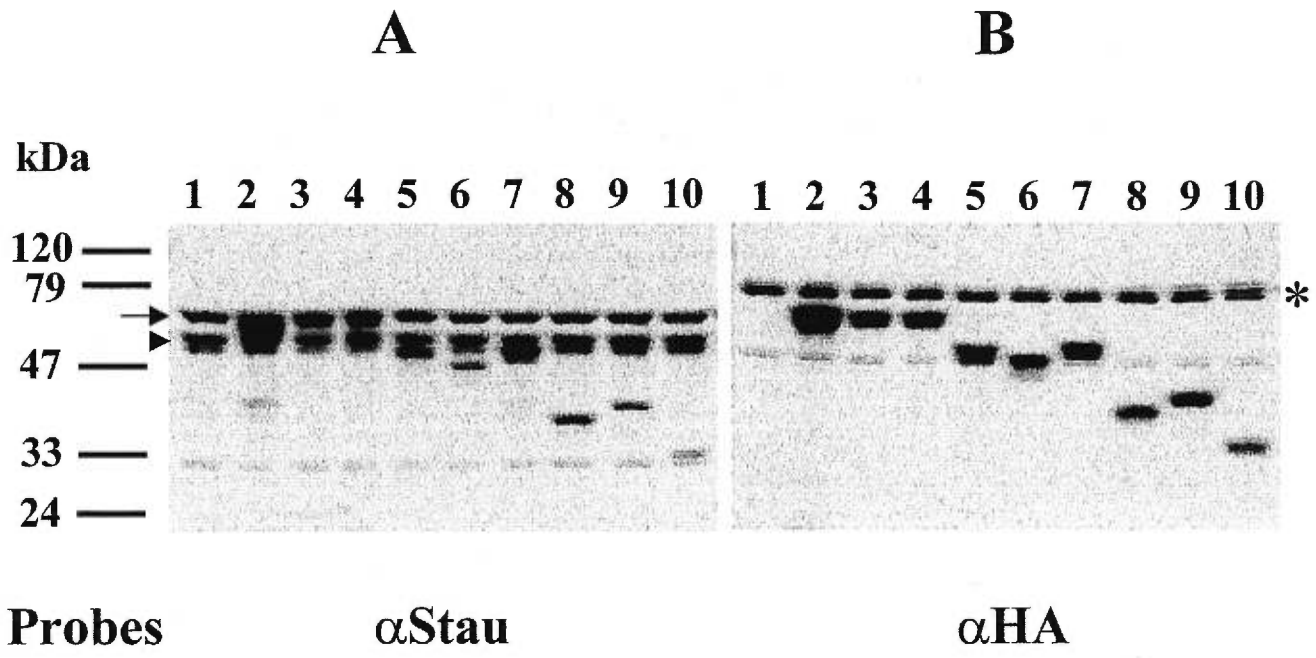
A
B
kDa
1 2 3 4 5 6 7 8 9 10
1 2 3 4 5 6 7 8 9 10
120
79
47
33
24
*
Probes
αStau
αHA

Fig. 1

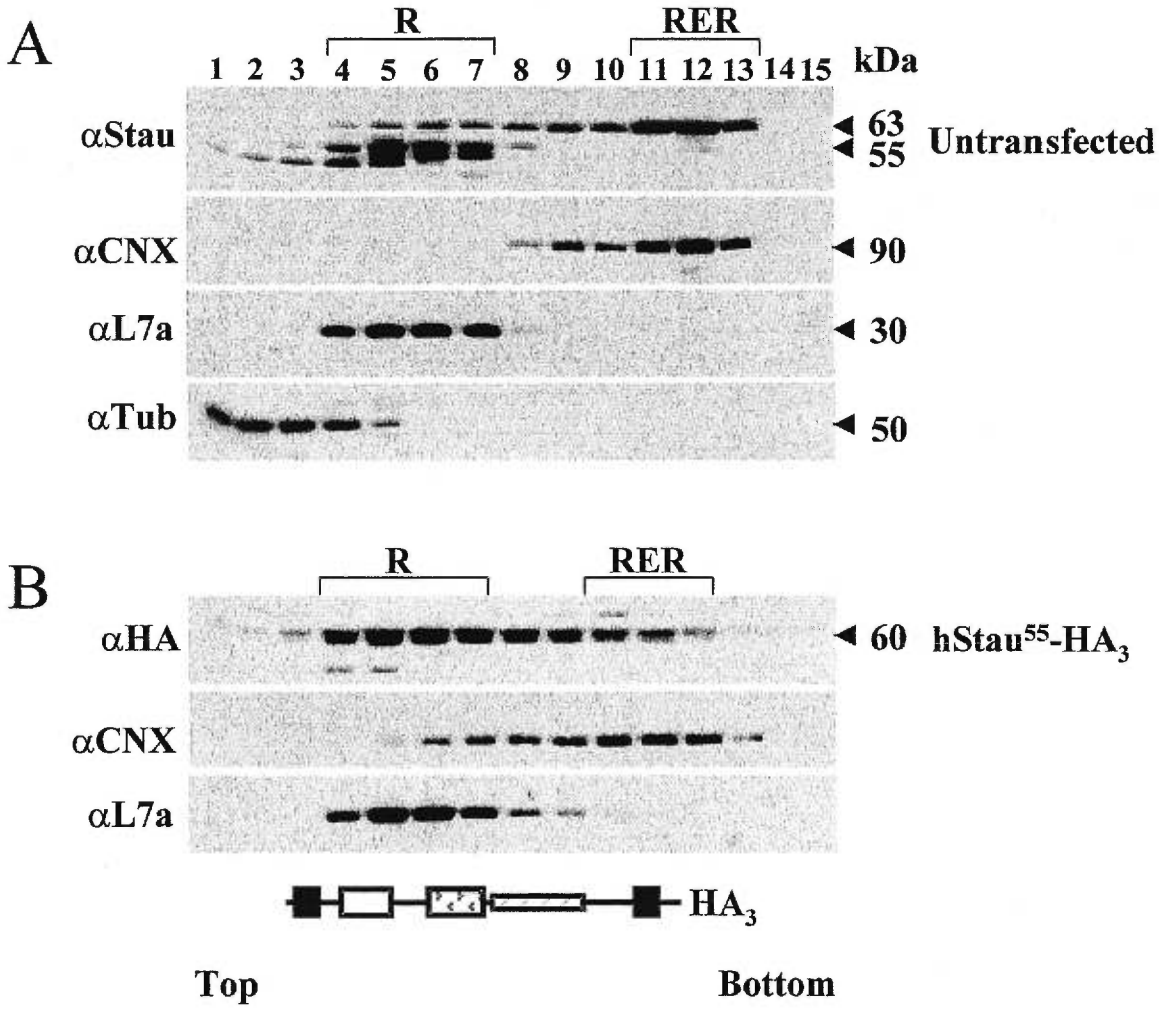
A
R
RER
1 2 3 4 5 6 7 8 9 10 11 12 13 14 15
kDa
αStau
63
55
Untransfected
αCNX
90
αL7a
30
αTub
50
B
R
RER
αHA
60
hStau55-HA3
αCNX
αL7a
HA3
Top
Bottom

Fig. 2

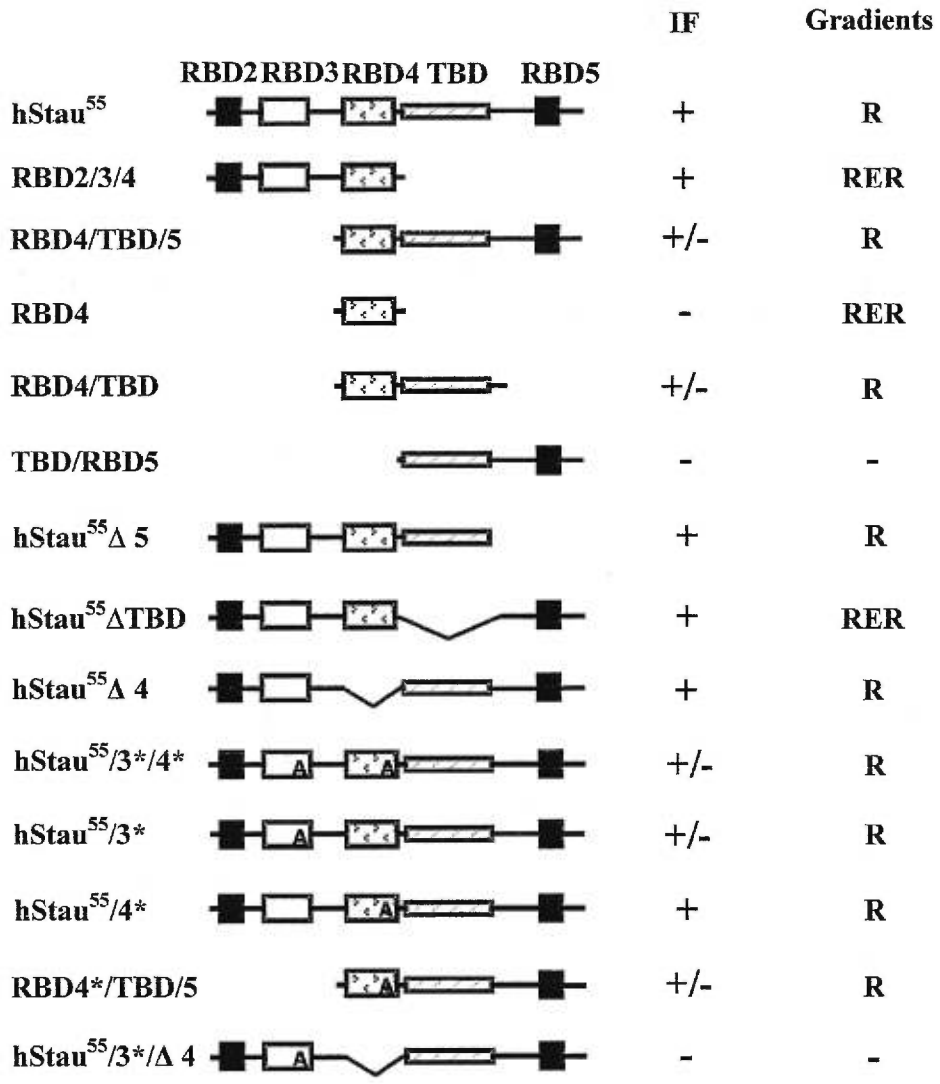
IF
Gradients
RBD2 RBD3 RBD4 TBD RBD5
hStau55
+
R
RBD2/3/4
+
RER
RBD4/TBD/5
+/-
R
RBD4
-
RER
RBD4/TBD
+/-
R
TBD/RBD5
-
-
hStau55Δ 5
+
R
hStau55ΔTBD
+
RER
hStau55Δ 4
+
R
hStau55/3*/4*
+/-
R
hStau55/3*
+/-
R
hStau55/4*
+
R
RBD4*/TBD/5
+/-
R
hStau55/3*/Δ 4
-
-

Fig. 3

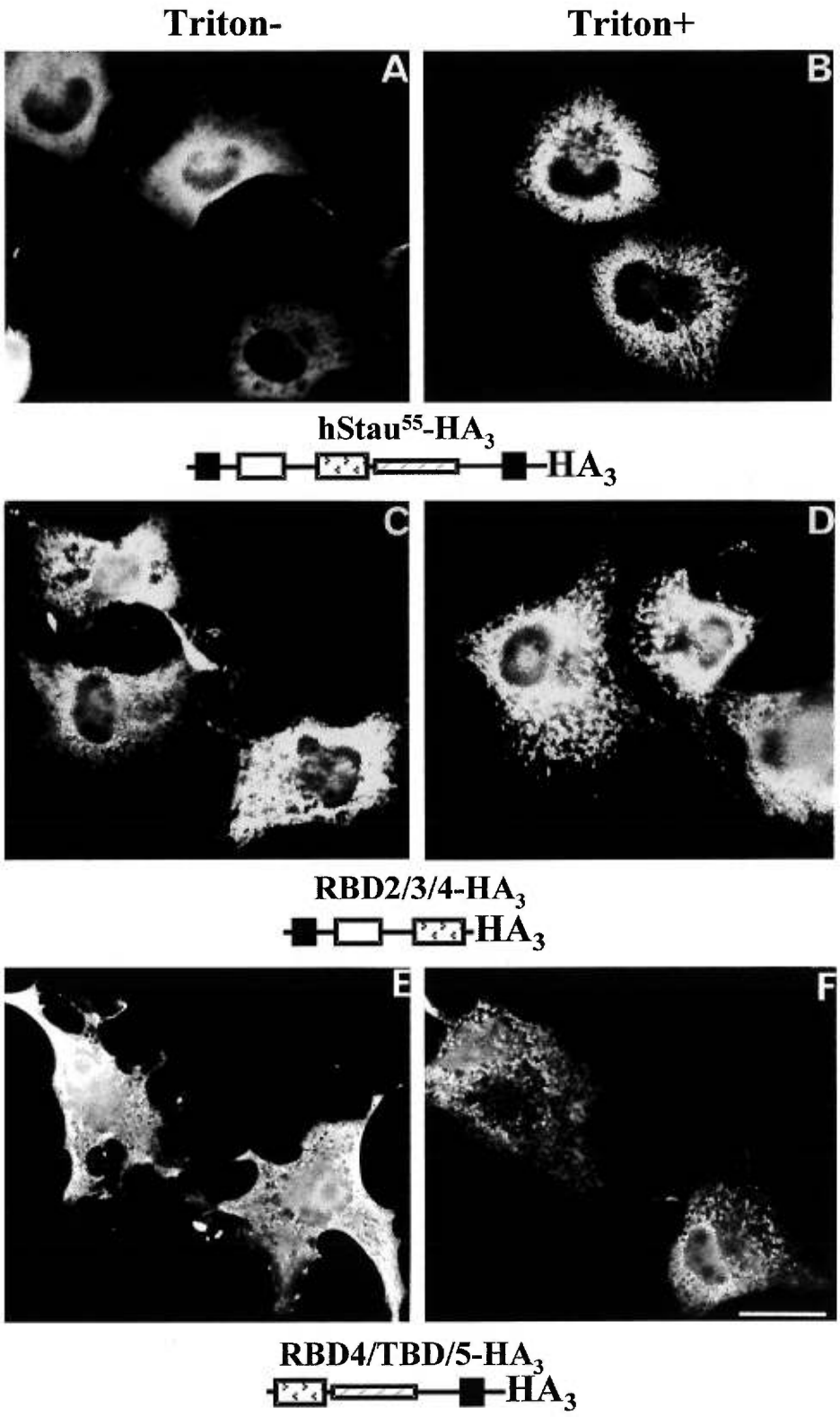
Triton-
Triton+
A
B
hStau55-HA3
HA3
C
D
RBD2/3/4-HA3
HA3
E
F
RBD4/TBD/5-HA3
HA3

Fig. 4

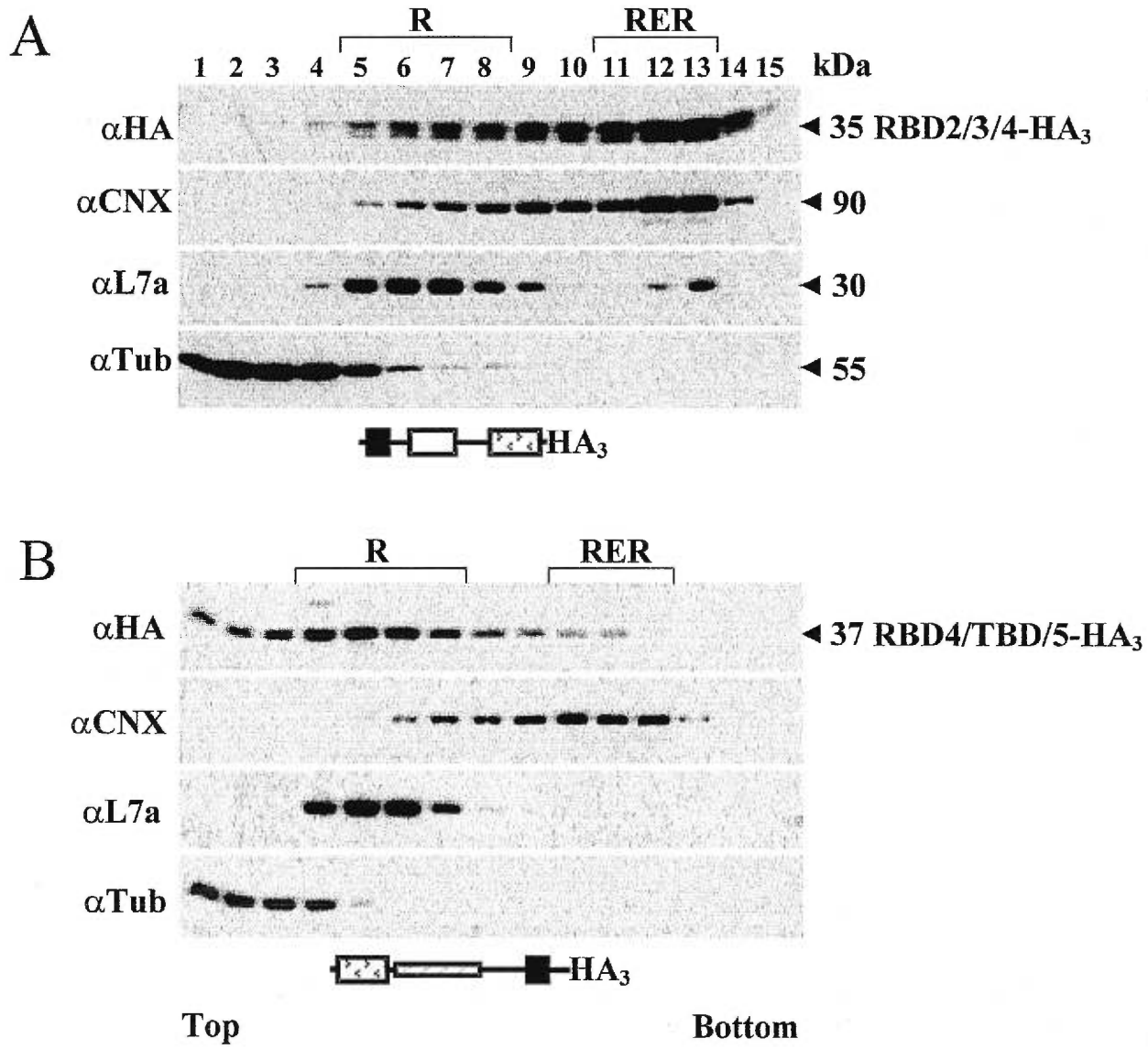
A
R
RER
1 2 3 4 5 6 7 8 9 10 11 12 13 14 15 kDa
αHA
αCNX
αL7a
αTub
35 RBD2/3/4-HA3
90
30
55
HA3
B
R
RER
αHA
αCNX
αL7a
αTub
37 RBD4/TBD/5-HA3
HA3
Top
Bottom

Fig. 5

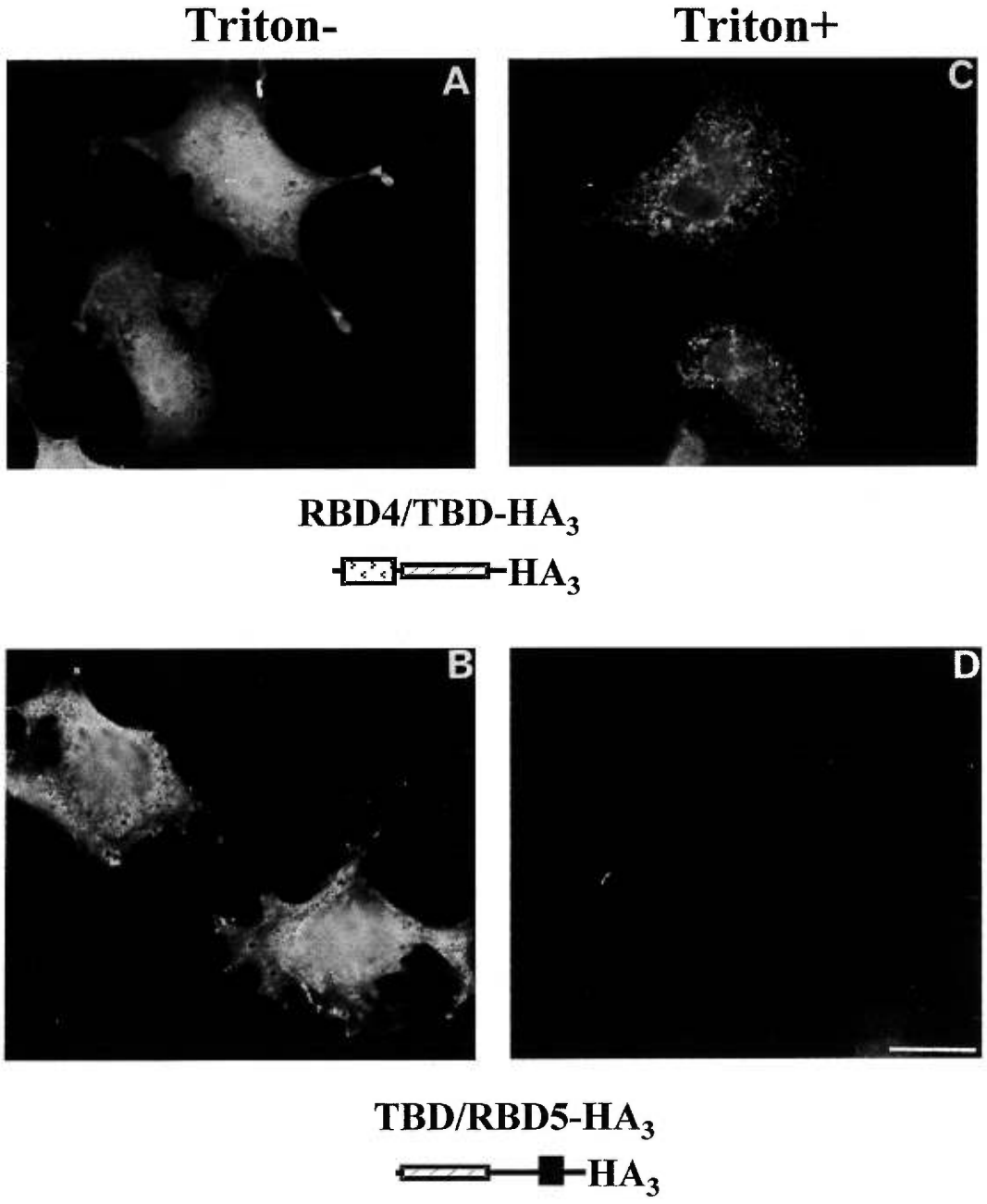

Fig. 6

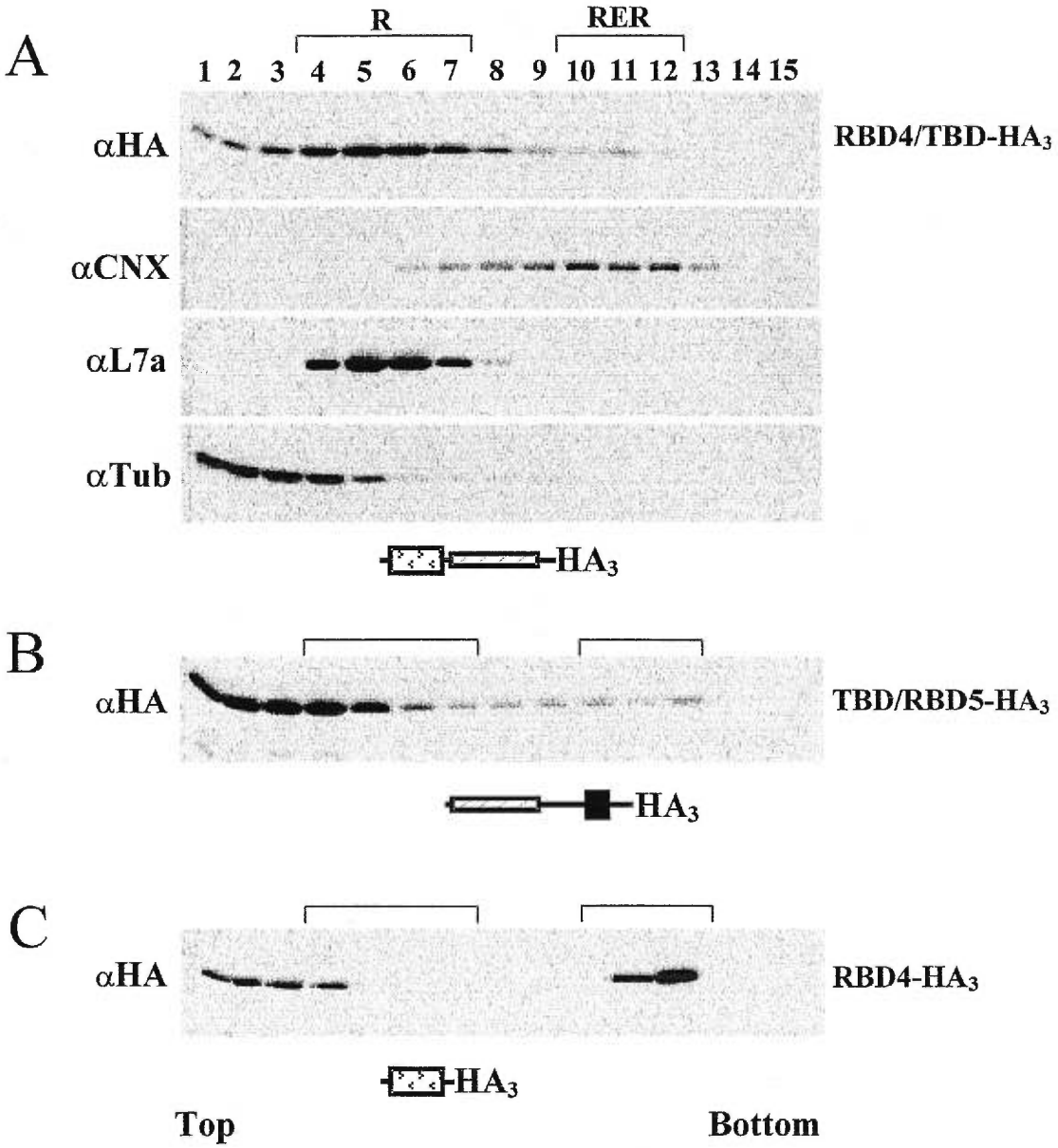
A
R
RER
1 2 3 4 5 6 7 8 9 10 11 12 13 14 15
αHA
RBD4/TBD-HA3
αCNX
αL7a
αTub
HA3
B
αHA
TBD/RBD5-HA3
HA3
C
αHA
RBD4-HA3
HA3
Top
Bottom

Fig. 7

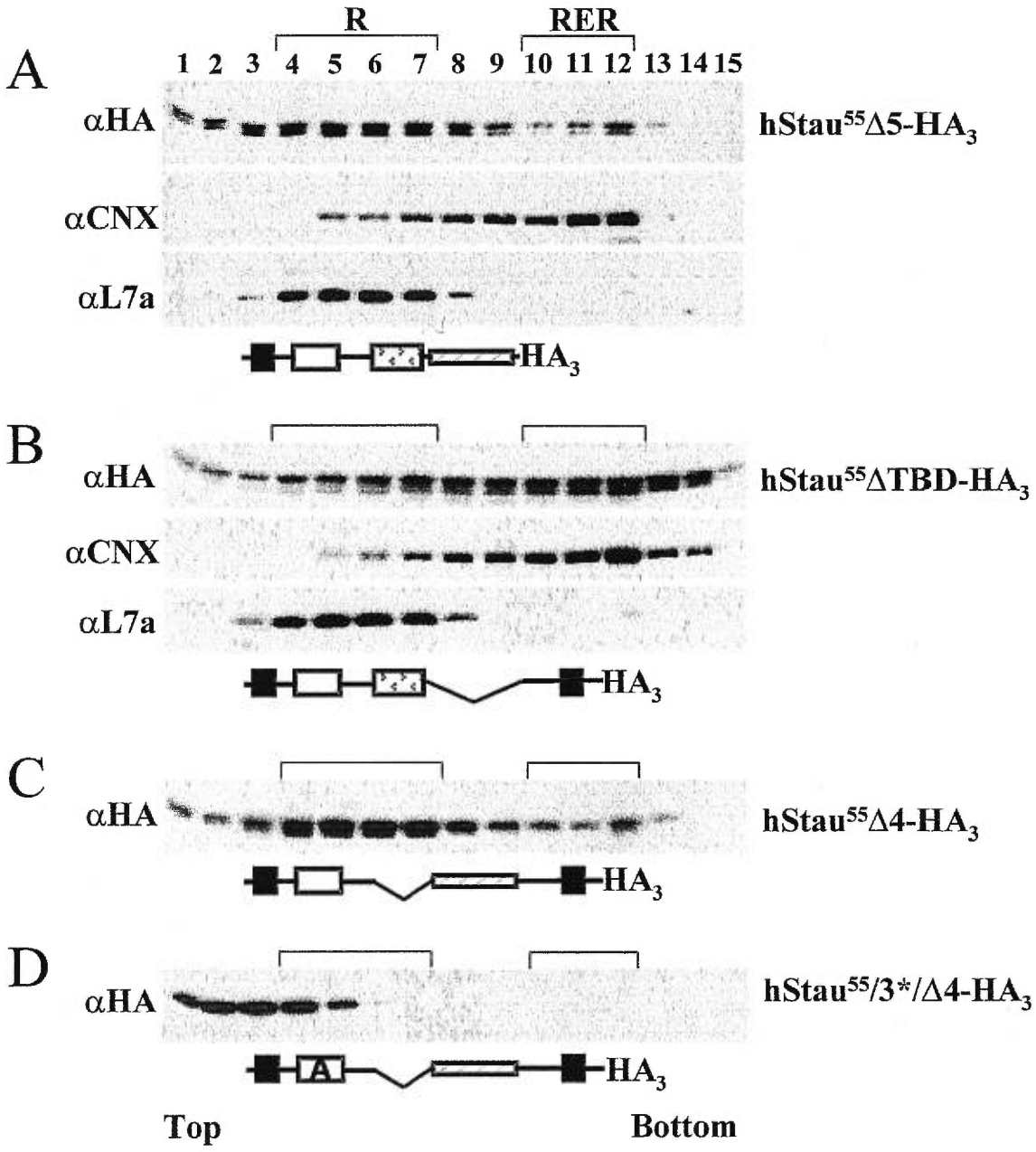
R
RER
1 2 3 4 5 6 7 8 9 10 11 12 13 14 15
A
αHA
αCNX
αL7a
hStau55Δ5-HA3
HA3
B
αHA
αCNX
αL7a
hStau55ΔTBD-HA3
HA3
C
αHA
hStau55Δ4-HA3
HA3
D
αHA
hStau55/3*/Δ4-HA3
A
HA3
Top
Bottom

Fig. 7

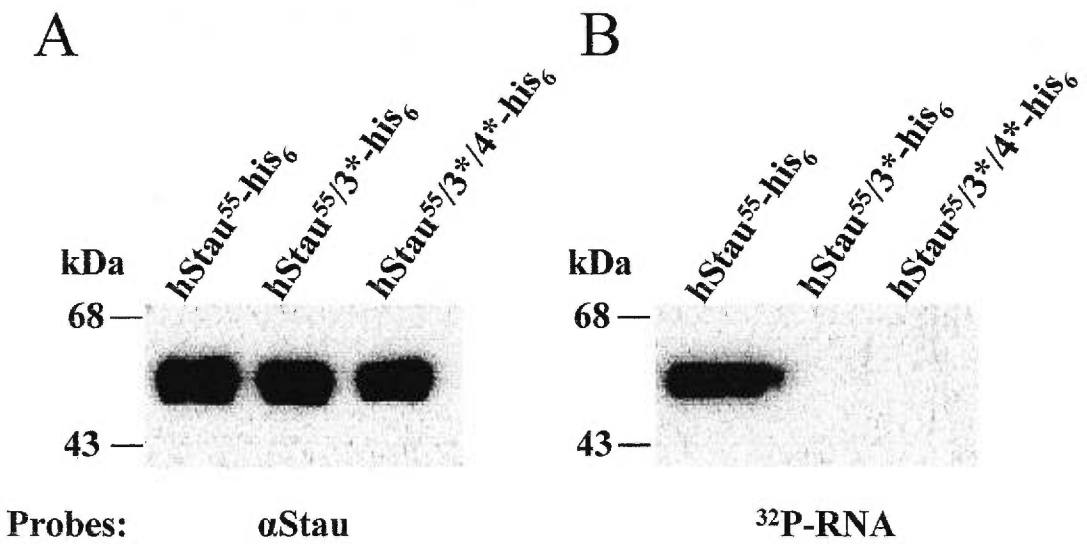
A
B
hStau55-his6
hStau55/3*-his6
hStau55/3*/4*-his6
kDa
68
43
Probes:
αStau
32P-RNA

Fig. 9

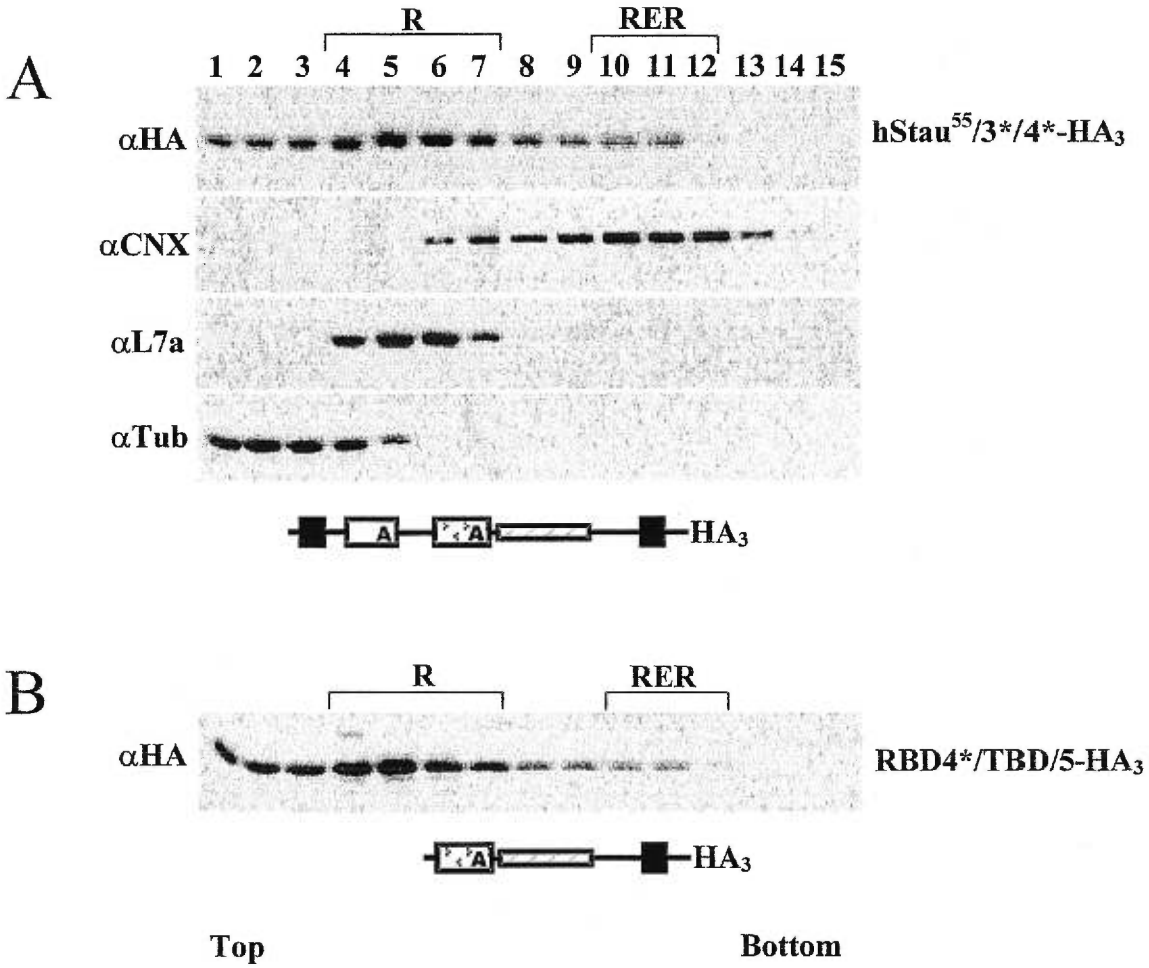
A
R
RER
1 2 3 4 5 6 7 8 9 10 11 12 13 14 15
αHA
αCNX
αL7a
αTub
hStau55/3*/4*-HA3
A
A
HA3
B
R
RER
αHA
RBD4*/TBD/5-HA3
A
HA3
Top
Bottom

Fig. 10

V- Article 4

Microtubule-dependent Recruitment of Staufen-Green Fluorescent Protein into Large RNA-Containing Granules and Subsequent Dendritic Transport in Living Hippocampal Neurons

Martin Köhrmann, Ming Luo, Christoph Kaether, Luc DesGroseillers, Carlos G Dotti, and Michael A. Kiebler

Molecular Biology of the Cell, September 1999, 10:2945-2953

My contribution:

This paper studied the movement of a human Stau-GFP fusion protein in living hippocampal neurons. hStau-GFP granules colocalize with RNA and are shown to move from the cell body into the dendrites in a bidirectional and microtubule-dependent manner. In this paper, I constructed the 63 kDa hStau-GFP fusion protein and confirmed that it was well expressed in mammalian cells with a predictable molecular weight about 90 kDa in Western blotting assay. This construct was subsequently transferred to Dr, Kiebler's lab for further study in living hippocampal neurons.

Molecular Biology of the Cell
Vol. 10, September 2945–2953, 1999

Microtubule-dependent Recruitment of Staufen-Green Fluorescent Protein into Large RNA-containing Granules and Subsequent Dendritic Transport in Living Hippocampal Neurons[V]

Martin Köhrmann,*† Ming Luo,‡ Christoph Kaether,* Luc DesGroseillers,‡ Carlos G. Dotti,* and Michael A. Kiebler*†§

*European Molecular Biology Laboratory, Cell Biology Programme, 69117 Heidelberg, Germany; †Max-Planck-Institute for Developmental Biology, Department of Physical Biology, 72076 Tübingen, Germany; and ‡Department of Biochemistry, University of Montreal, Montreal, Quebec, Canada, H3C 3J7

Submitted February 12, 1999; Accepted July 2, 1999
Monitoring Editor: Jennifer Lippincott-Schwartz

Dendritic mRNA transport and local translation at individual potentiated synapses may represent an elegant way to form synaptic memory. Recently, we characterized Staufen, a double-stranded RNA-binding protein, in rat hippocampal neurons and showed its presence in large RNA-containing granules, which colocalize with microtubules in dendrites. In this paper, we transiently transfect hippocampal neurons with human Staufen-green fluorescent protein (GFP) and find fluorescent granules in the somatodendritic domain of these cells. Human Stau-GFP granules show the same cellular distribution and size and also contain RNA, as already shown for the endogenous Stau particles. In time-lapse videomicroscopy, we show the bidirectional movement of these Staufen-GFP–labeled granules from the cell body into dendrites and vice versa. The average speed of these particles was 6.4 μm/min with a maximum velocity of 24.3 μm/min. Moreover, we demonstrate that the observed assembly into granules and their subsequent dendritic movement is microtubule dependent. Taken together, we have characterized a novel, nonvesicular, microtubule-dependent transport pathway involving RNA-containing granules with Staufen as a core component. This is the first demonstration in living neurons of movement of an essential protein constituent of the mRNA transport machinery.

INTRODUCTION

The concept of localized mRNAs within a mammalian cell to achieve a spatially restricted answer to a local stimulus has attracted significant attention lately (for review, see St. Johnston, 1995; Carson *et al.*, 1998; Kuhl and Skehel, 1998; Tiedge *et al.*, 1999). Prominent examples of asymmetrically distributed mRNAs range from the budding yeast (ASH1 mRNA; Bertrand *et al.*, 1998), *Drosophila* (bicoid and oskar; Driever *et al.*, 1988; Ephrussi *et al.*, 1991), *Xenopus* (Vg1; Deshler *et al.*, 1997), fibroblasts (β-actin mRNA; Bassell *et al.*, 1998) to mammalian oligodendrocytes (myelin-basic protein mRNA; Holmes *et al.*, 1988) and neurons (many mRNAs; for review, see Kuhl and Skehel, 1998). The asymmetric localization of mRNAs to the somatodendritic domain has been observed together with the translational machinery in the nervous system. However, the mechanism of mRNA delivery and functional significance has not been analyzed in molecular detail.

In the past year, the first molecular components of the mRNA trafficking pathway have been identified (for review, see Hazelrigg, 1998). Among these were several potential mRNA-binding proteins, which recognize *cis*-acting sequences in the 3′-untranslated region (UTR) of localized mRNAs (e.g., Mayford *et al.*, 1996). These proteins include hnRNP A2 in oligodendrocytes (Hoek *et al.*, 1998), actin zipcode-binding protein in fibroblasts and *Xenopus* (Ross *et al.*, 1997; Deshler *et al.*, 1998), and Staufen in *Drosophila* (St. Johnston *et al.*, 1991). Upon binding to their cognate mRNAs, these mRNA-binding proteins were then recruited to particles as shown in the *Drosophila* embryo in oligodendrocytes and neurons (Ainger *et al.*, 1993; Ferrandon *et al.*, 1994; Wang and Hazelrigg, 1994; Knowles *et al.*, 1996). These granules may therefore represent the active transport unit to deliver mRNAs to their final destination

§ Corresponding author. E-mail address: Michael.Kiebler@Tuebingen.mpg.de.

[V] Online version of this article contains video material for Figure 4. Online version available at www.molbiolcell.org.

within the cell (Wilhelm and Vale, 1993). Finally, data have accumulated suggesting this transport requires intact microtubules (Knowles *et al.*, 1996; Carson *et al.*, 1997) or actin in the case of ASH1 mRNA (Bertrand *et al.*, 1998). Besides mRNA and their cognate RNA-binding protein(s), the described granules may also contain microtubule-associated proteins, potentially a kinesin-like or dynein-like molecular motor protein (or an unconvential myosin V motor in the case of ASH1 mRNA), aminoacyl-tRNA-synthetases, elongation factors, components of the translational machinery, and even subunits of ribosomes (for review, see Carson *et al.*, 1998).

Recently, in vivo labeling using the green fluorescent protein (GFP) has been successfully applied to study mRNA transport in *Drosophila* and yeast. In *Drosophila*, the movement of the RNA-binding protein exuperantia was visualized (Wang and Hazelrigg, 1994), whereas in yeast, the fate of the mRNA itself could be indirectly followed using two sophisticated reporter plasmids (Bertrand *et al.*, 1998). In neurons, however, these granules have only recently been visualized using the RNA-specific, fluorescent dye SYTO14 (Knowles *et al.*, 1996). Because SYTO14 labels all RNA, including mitochondrial RNA, the characterization and transport of these granules in living neurons have been problematic. Therefore, labeling of a known protein constitutent would be a more specific approach to visualize these RNA-containing granules. We took advantage of the first known protein component of these granules, the RNA-binding protein Staufen (St. Johnston *et al.*, 1991). Human Staufen binds microtubules and colocalizes with polysomes in HeLa cells (Marión *et al.*, 1999; Wickham *et al.*, 1999). In fixed neurons, rat Staufen localized to the somatodendritic domain of hippocampal neurons in large RNA-containing granules (Kiebler *et al.*, 1999) that colocalize with microtubules. To determine whether Staufen-containing granules move in vivo, we transiently transfected hippocampal neurons with human Stau-GFP (hStau-GFP) and studied the formation of fluorescent granules and their transport along distal dendrites by time lapse video microscopy.

MATERIALS AND METHODS

Materials and Reagents

The following antibodies were used in the indicated dilutions: polyclonal antibody against human Staufen (Kiebler *et al.*, 1999) at 1:300; polyclonal anti-GFP antibody (antiserum D2) (Wacker *et al.*, 1997) at 1:300; and monoclonal anti-tubulin antibody (Amersham, Arlington Heights, IL; N356, 1:10,000). Phalloidin (phalloidin-rhodamine; Molecular Probes, Eugene, OR; R-415, 1:500) staining was performed as described (Bradke and Dotti, 1999). As secondary antibodies, an FITC-conjugated donkey anti-rabbit immunoglobulin (Ig) (Amersham; N1034, 1:100), a rhodamine-conjugated goat anti-rabbit IgG (Cappel, West Chester, PA; 55674, 1:100), a lissamine-rhodamine–conjugated goat anti-mouse IgG (Dianova, Hamburg, Germany; 715-085-151, 1:400), and an FITC-conjugated sheep anti-mouse Ig (Amersham; N1031, 1:50) were used. The following drugs were used: nocodazol (Sigma, St. Louis, MO; M-1404; final concentration, 20 μM) and latrunculin B (Calbiochem, La Jolla, CA; 428020-Q; final concentration, 12.6 μM). The cloning of the human Staufen-GFP (S65T mutation) construct was described by Wickham *et al.* (1999).

Hippocampal Cell Culture and Transient Transfection Protocol

Primary hippocampal neurons derived from rat embryos were cultured following the protocol of Goslin and Banker (1997) and de Hoop *et al.* (1998). Adult primary hippocampal neurons (stage 5) were transfected using a modified Ca^{2+}-phosphate precipitation protocol (Haubensack *et al.*, 1998). In brief, neurons grown on glass coverslips were transferred into 2 ml of conditioned culture medium in a 3.5 cm culture dish. The Ca^{2+}-phosphate precipitate was prepared by dropwise adding 60 μl of 2× BBS (280 mM NaCl, 1.5 mM Na_2HPO_4, 50 mM *N,N*-bis[2-hydroxyethyl]-2-aminoethanesulfonic acid, pH 7.1) to 3.5 μg of plasmid cDNA (1 μg/μl stock in 10 mM Tris-HCl, pH 8.5) dissolved in 60 μl of 250 mM $CaCl_2$ and incubated for 90 s at room temperature. The precipitate was added to the neurons, and the cells were incubated for 2 h at 2.5% CO_2 and 37°C. Neurons were washed twice with HEPES-buffered saline, returned to the original medium, and incubated overnight at 5% CO_2 and 36.5°C before fixation or performing subsequent experiments. To not saturate the cell with overexpressed or aggregated hStau-GFP, we chose a short time of expression (16–20 h). This allowed the detection of individual particles in dendrites and their subsequent intracellular transport.

SYTO14 labeling of cells was essentially performed as described (Knowles *et al.*, 1996; Kiebler *et al.*, 1999) with the following modification. In brief, cells were incubated in SYTO14-containing (1 μM) conditioned N2 medium for 15 min at 37°C and 5% CO_2. Neurons were briefly rinsed twice with N2 medium and then fixed.

Immunocytochemistry of neurons was performed as described by Kiebler *et al.* (1999). For microtubule staining, neurons were extracted before fixation using 0.1% saponin in microtubule-stabilizing buffer (2 mM $MgCl_2$, 10 mM EGTA, 60 mM 1,4-piperazinediethanesulfonic acid, pH 7.05) for 15 s and shortly rinsed in microtubule-stabilizing buffer.

Blotting

Stau-GFP transfected neurons as well as control neurons were incubated in conditioned medium containing 2 mm sodium butyrate. After 17 h, cells were lysed in 0.1% SDS and methanol-chloroform extracted (Kiebler *et al.*, 1999). Lysates of three neuron-containing dishes (3.5 cm) were pooled, run on a 10% minigel (Bio-Rad, Hercules, CA), and blotted onto nitrocellulose. Nonspecific binding sites were blocked by incubation for 2 h in blocking buffer (5% low-fat milk powder in PBS), and then filters were incubated for 2 h in blocking buffer and anti-GFP antiserum D2 (Wacker *et al.*, 1997). Intermediate wash steps were carried out with 0.2% Tween 20 in PBS. Detection of bound antibodies was performed with HRP-coupled donkey anti-rabbit secondary antibodies (Amersham) for 30 min in blocking buffer followed by ECL detection (Amersham).

Microscopy

Time-lapse video microscopy of living transiently transfected neurons grown on glass coverslips was performed using a metal slide. For recording at physiological temperature, the objective was heated at 36°C by an objective heating ring (Bioptechs, Butler, PA) (Bradke and Dotti, 1998). The following setup was used: a Zeiss (Thornwoodd, NY) Axiovert 135 inverted microscope with a 63× Plan apochromat objective and a 100-W HBO mercury arc bulb (Osram, Berlin, Germany), a shutter driver (Uniblitz D122; Vincent Associates, Rochester, NY), standard FITC and rhodamine filters, and a Cohu (San Diego, CA) charge-coupled device (CCD) camera controlled by a CCD camera control (C2400; Hamamatsu, Hamamatsu City, Japan). Images were taken either every 8 or 10 s using the Scion 1.58 software package (National Institutes of Health). Fluorescent microscopy was performed with a Zeiss Axioskop using a 63× objective, standard FITC and rhodamine filters, a 100-W HBO mercury arc lamp, and a Cohu CCD camera controlled by the NIH Image 1.59 software package.

For the Staufen-GFP and SYTO14 colocalization experiment (see Figure 3) the following filter sets were used: 1) enhanced GFP (EGFP) filter (excitation spectra, 470 ± 15 nm; emission spectra, 510 ± 10 nm); and 2) SYTO14 filter (excitation spectra, 546 ± 6 nm; emission spectra, 585 ± 20 nm). Although SYTO14 bound to RNA has its absorbance maximum at 521 nm and the emission maximum at 547 nm, we found a residual SYTO14 signal in the EGFP filter. For

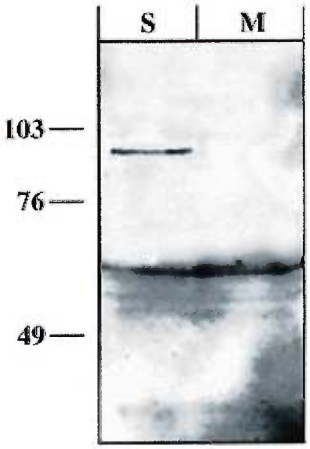

Figure 1. Transiently transfected hippocampal neurons express the full-length human Staufen-GFP fusion protein. Western blots of extracts from either transiently transfected (S) or mock-treated (M) rat hippocampal neurons were probed with a polyclonal GFP antibody. The antibody detects a 92-kDa band in the transfected but not in the untransfected neurons; this represents the expected size for the hStau-GFP fusion protein (65 + 27 kDa). Additionally, the antibody detects a 61-kDa band in all neuronal extracts, most likely representing an unspecific cross-reaction. The sizes of the molecular mass markers are indicated on the left in kilodaltons.

that reason, we devised a new method to separate both signals from each other. An image was taken with the SYTO14 filter that detected SYTO14 but not Staufen-GFP, and then this signal was depleted by photobleaching, another image was taken, demonstrating that there was no signal left, and finally a third picture was taken with the EGFP filter that now exclusively represented the Staufen-GFP signal. The first and the third pictures were compared in NIH Image, and individual Staufen-GFP–positive granules were scored for the presence of RNA. In total, 579 granules from 29 cells were examined: of these, 380 were found to contain RNA representing 65.6% of all particles. A representative picture of one of these cells is shown in Figure 3.

Image Analysis and Quantitation

Untransfected cells did not show detectable autofluorescence under identical illumination conditions (our unpublished observations). For quantitatation, transiently transfected cells were randomly chosen by green fluorescence and examined by phase contrast for health, and a fluorescent image was taken and evaluated. To calculate the velocity of individual granules, the distance traveled was measured between two adjacent video frames with the NIH Image 1.59 software package and divided by the time. To quantitate the maximal velocity, 18 different particles from 10 independent transfections were tracked; from these 42 different velocities were measured. The average speed was calculated from videos in which particles were moving at least during three or more consecutive frames (average number of frames, 7.9). In total, 14 different particles were tracked and analyzed.

To quantitate the effect of nocodazole on the localization of fluorescent granules, hStau-GFP–expressing neurons were grouped into two different categories (see Figure 7A): 1) neurons with the typical granular expression pattern of hStau-GFP ("localized"), as shown in Figure

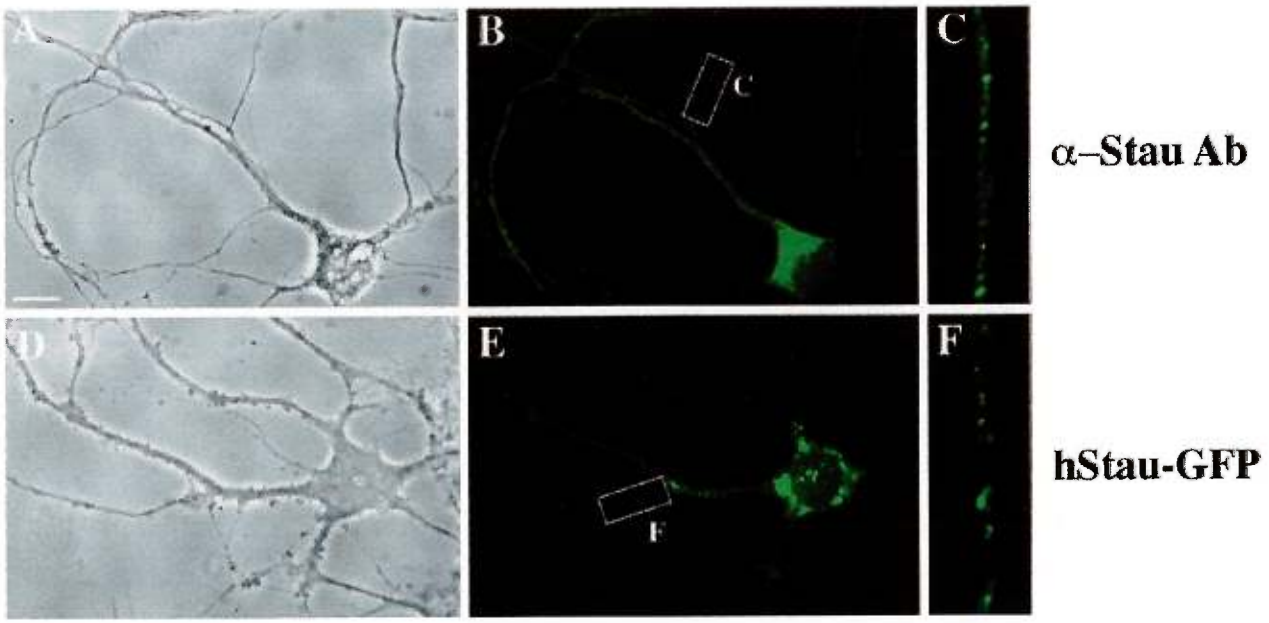

Figure 2. Expressed human Staufen-GFP and endogenous rat Staufen protein show a comparable punctate, dendritic expression pattern in hippocampal neurons. Adult rat hippocampal neurons were either fixed and labeled with anti-hStau antibodies (A–C) or transiently transfected with hStau-GFP and fixed, and green fluorescence was recorded (D–F). (A–C) Phase-contrast and hStau immunofluorescence of a representative neuron. C is an enlarged section of the white box in B. (D–F) Phase-contrast and hStau-GFP fluorescence of a representative neuron. F is an enlarged section of the white box in E. The small precipitate seen in D is due to CaP_i transfection. Note that two different types of fluorescent granules were routinely observed (E): large granules around the nuclear membrane and smaller granules in the periphery of the neurons. Bar, 10 μm.

2; and 2) neurons with an aberrant expression pattern with no apparent granules ("mislocalized"). In 42 control cells, only 7 cells (17%) showed a cytosolic expression pattern versus 26 of 58 nocodazole-treated cells (45%). This represents a 168% increase of transfected cells with mislocalized hStau-GFP. To analyze the effect of nocodazole on the transport of hStau-GFP–labeled granules, neurons with localized hStau-GFP were examined for the presence of granules in distal (>12 μm apart from the cell body) dendrites (see Figure 7B). Twenty-nine of the 32 mock-treated cells with localized expression had three or more hStau-GFP granules in distal parts of the dendrites versus 5 of 32 nocodazole-treated cells.

RESULTS AND DISCUSSION

Hippocampal neurons have been previously shown to be an appropriate model system to study the trafficking of heterologously expressed proteins (De Strooper *et al.*, 1995; Simons *et al.*, 1996; Haubensack *et al.*, 1998). Hence we used this cell system to analyze the trafficking of Staufen by transiently transfecting adult neurons with a plasmid coding for a fusion protein of human Staufen and GFP (hStau-GFP) (Wickham *et al.*, 1999). Our goal was twofold: first, to determine whether hStau-GFP is indeed incorporated into large RNA-containing granules as does the endogenous rat Staufen (rStau) (Kiebler *et al.*, 1999), and second, to study assembly of these particles and their subsequent dendritic transport in adult living hippocampal neurons.

Transfected Staufen-GFP is Present in Large RNA-containing Granules

We first tested whether hStau-GFP is expressed as a full-length fusion protein in rat hippocampal neurons. Therefore, we transiently transfected rat hippocampal neurons with hStau-GFP and performed Western blotting on extracts both from transfected and untreated neurons. As shown in Figure 1, we found that a specific 92-kDa band is detected with a GFP antibody, demonstrating that neurons exclusively express the correct fusion protein consisting of hStau (65 kDa) and GFP (27 kDa) and that there is no proteolytic cleavage.

We then analyzed the pattern of expression and localization of expressed fluorescent hStau-GFP (Figure 2, D–F) and compared that with the endogenous rStau, as visualized by immunofluorescence with an anti-hStau antibody (Figure 2, A–C). Sixteen to 20 h after transfection, hStau-GFP started to appear in small and large granules in the cell body and dendrites of these neurons (Figure 2, D–F). In contrast, cells transfected with GFP alone show an evenly distributed fluorescence throughout the whole cell. The observed hStau-GFP granules (Figure 2, D–F) were of the same size and showed the same cellular distribution as their endogenous rStau counterparts (Figure 2, A–C). However, it must be noted that the expression of hStau-GFP yielded fewer granules in dendrites (Figure 2F) compared with the endogenous Staufen (Figure 2C) and a reduced cytosolic background. There are several explanations for that phenomenon. First, we only allowed a moderate expression rate after transfection to not saturate the cell (see MATERIALS AND METHODS). Second, we only overexpressed Staufen and not any RNA; there is also increasing experimental evidence in other cells that Stau-containing granules can only move if newly synthesized mRNA is provided by the cells. In hippocampal neurons, we observed two different types of Staufen granules: 1) larger granules restricted to the cell body and 2) smaller granules in the periphery of the cell body and in dendrites (see Figures 2E and 6B).

To test whether those hStau-GFP granules indeed contain RNA, we transiently transfected rat hippocampal neurons with hStau-GFP and subsequently labeled RNA using the RNA-specific dye SYTO14 (Knowles *et al.*, 1996; Kiebler *et al.*, 1999). Based on corresponding pairs of fluorescent images, we exam-

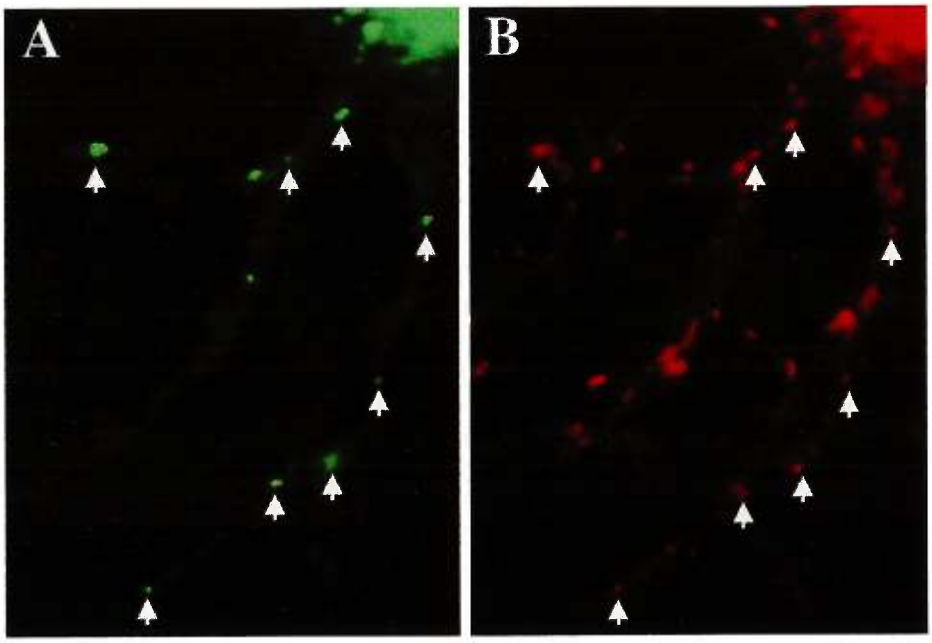

Figure 3. Human Staufen-GFP positive granules colocalize with RNA in transiently transfected rat hippocampal neurons. RNA was visualized using SYTO14 (Knowles *et al.*, 1996; Kiebler *et al.*, 1999), and the degree of colocalization with hStau-GFP was revealed by fluorescent microscopy (see MATERIALS AND METHODS). Individual green fluorescent hStau-GFP granules (A) were analyzed for the presence of RNA detected by SYTO14 labeling of the same cell (B). Arrowheads indicate hStau-GFP granules containing RNA. Overall, 65.6% of analyzed hStau-GFP granules were RNA positive. The additional SYTO14 labeling in B might reflect both RNA-positive granules containing endogenous Staufen as well as mitochondria (Knowles *et al.*, 1996).

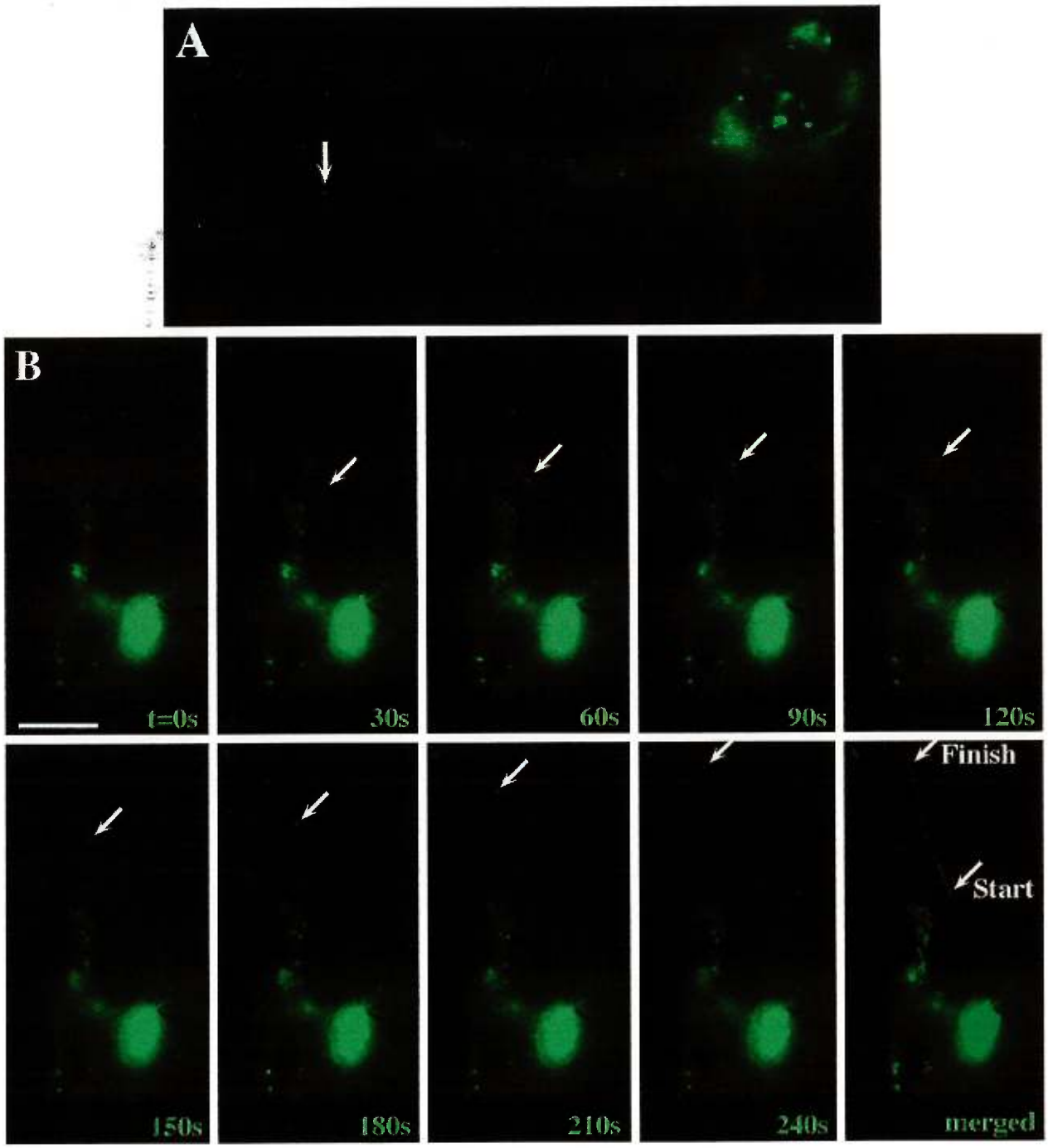

Figure 4. Individual hStau-GFP particles are transported into dendrites of living hippocampal neurons. Hippocampal neurons on glass coverslips were transfected with hStau-GFP as described in Figure 2, and individual motilities of green fluorescent granules were observed by time-lapse video microscopy. (A) Corresponding figure to Video 1; (B) corresponding figure to Video 2. In both videos as well as in B, moving particles are labeled by an arrow and were followed during its anterograde transport into the dendrite. The individual video frames were more highly integrated compared with Fig. 2 to detect individual granules in processes. Elapsed time is indicated in seconds in the lower right of each video frame in B. The last panel in B shows a merged picture of all frames depicting both the Brownian movement of most particles as well as the discontinuous, directed motility of the chosen granule. Bar, 10 μm.

ined whether individual hStau-GFP granules colocalize with ribonucleoprotein particles. Figure 3 shows a representative example of a hippocampal neuron in which the majority of hStau-GFP granules clearly contain RNA. In total, we analyzed 579 hStau-GFP granules from 29 different cells and found that 65.6% of these granules were also SYTO14 positive. Interestingly, larger granules found in the cell body were often SYTO14 negative, whereas the majority of the smaller granules in the periphery of the cell body and in dendrites were SYTO14 positive (Figure 3). Additionally, some of the observed SYTO14-negative hStau-GFP granules might represent recycling granules migrating in the retrograde direction toward the cell body (see below). Finally, taken into account that an immunolabeling of GFP-labeled secretory granules in neuroendocrine cells yielded a 75% colocalization of all green fluorescent structures (Kaether *et al.*, 1997), the calculated value (65.6%) of colocalization comes close to the expected theoretical upper limit of this quantitation method. In conclusion, these results demonstrate that hStau-GFP, like the endogenous Staufen, is dendritically targeted in RNA-containing granules.

Time-Lapse Fluorescent Microscopy Visualizes the Saltatory, Bidirectional Movement of hStau-GFP Granules into Dendrites of Living Neurons

We next sought to perform time-lapse video microscopy to follow the intracellular movement of these fluorescent granules in neurons. For this reason, transiently transfected adult hippocampal neurons were transferred to a video chamber, and the movement of individual green fluorescent granules was recorded using a heated objective (Figure 4). Figure 4A is the corresponding figure to Video 1; Figure 4B is the corresponding figure to Video 2; moving particles are labeled by an arrow (online versions of both figures in QuickTime format are available at www.molbiolcell.org). In contrast to previous experiments shown in Figure 2, individual video frames were more highly integrated to detect the smaller granules in processes.

As shown in Figure 4 and the two videos, we frequently observed one or more fluorescent granules moving from the cell body into distal dendrites (anterograde transport). However, retrograde transport was also frequently observed in adult neurons (Video 2). The anterograde transport of these particles into the distal part of the dendrite was then followed. Interestingly, almost all particles in motion were moving in a saltatory and not a linear, uninterrupted manner. In most cases, particles were moving for some 30–60 s and then suddenly stopped and remain stationary for some time. These pauses can be of significant durance until these particles continue their movement. In general, three different types of movements occurred: 1) particles in a stationary phase or showing Brownian movement, 2) particles moving in one direction only, and 3) particles moving bidirectionally.

During video microscopy, we observed two types of granules in living neurons: larger granules around the nuclear membrane, which seemed to be stationary, and smaller granules moving toward the periphery of the neurons. The large granules could correspond to newly synthesized hStau-GFP protein, which still has not bound to their cognate mRNA. This is further supported by the finding that those larger granules were often SYTO14-negative (Figure 3). In this scenario, one would then hypothesize that upon contact with newly synthesized mRNA, transport-competent granules form and begin to move toward the periphery, as seen in the videos representing active transport units. Indeed, we observed in some cases smaller granules attached to larger particles, which might be in the process of pinching off (Köhrmann and Kiebler, unpublished observation). Taken together, the videos and Figure 4B faithfully represent Staufen dynamics. The fact that only a small percentage of granules actually move in a neuron has also been found in SYTO14-labeled cortical neurons (Knowles and Kosik, 1997).

Measurement of the Velocity and Average Speed of Staufen-GFP Granules in Living Neurons

We then went on to characterize the observed transport of granules by determining the velocities and average speed of individual particles. We therefore analyzed 18 different particles to calculate their velocities and measured 42 distances that the particles traveled between two adjacent frames. Figure 5 shows a Gaussian distribution of the measured velocities arranged in increasing intervals.

We next determined the average speed as described in MATERIALS AND METHODS and calculated a value of 6.4 ± 3.2 (SEM) μm/min by analyzing 14 different hStau-GFP granules moving over an extended distance in adult hippocampal neurons. Videos 1 (Figure 4A) and 2 (Figure 4B) show two exceptional examples of such a movement. In Video 1 (Figure 4A), the particle observed travels 27.3 μm during the recorded 2.13 min, resulting in an average speed of 12.8 μm/min; in Video 2 (Figure 4B), the observed particle travels 22.5 μm during 4 min, which results in an average speed of 5.6 μm/min. The observed overall average speed of

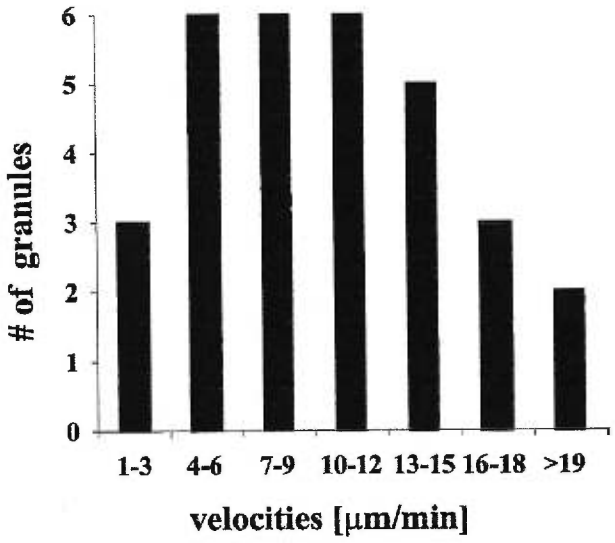

Figure 5. Gaussian distribution of measured velocities of individual hStau-GFP particles. Cells were transiently transfected, and fluorescence recording was performed as described in Figure 4. The velocities of moving hStau-GFP particles were calculated from the distance traveled between two adjacent video frames. Forty-two velocities from 18 particles were analyzed by time-lapse video microscopy, the resulting velocities arranged in increasing intervals and plotted. The mean velocity was 11.5 μm/min.

6.4 μm/min is more than one magnitude slower than vesicular, fast axonal transport (up to 278 μm/min) (Brady *et al.*, 1982) or vesicular, dendritic transport (120 μm/min) (Kaether and Dotti, unpublished results).

The measured speed, however, is in very good agreement with studies on RNA transport performed on oligodendrocytes, rat brain sections, and sympathetic and cortical neurons (Ainger *et al.*, 1993; Knowles *et al.*, 1996; Muslimov *et al.*, 1997; Wallace *et al.*, 1998). In oligodendrocytes, microinjected myelin-basic protein mRNA moved with a transport rate of ~6–12 μm/min (Ainger *et al.*, 1993). Wallace *et al.* (1998) studied the transport of the Arc/arg3.1 mRNA to dendrites by in situ hybridization and determined a transport rate of 5.0 μm/min. Muslimov *et al.* (1997) microinjected BC1, a small noncoding RNA transcript, into sympathetic neurons and found a delivery rate of 4.0 μm/min. Finally, Knowles *et al.* (1996) labeled RNA-containing granules in young cortical neurons with SYTO14 and measured an average rate of 6.0 μm/min. In conclusion, these transport rates strongly argue that the RNA-binding protein Staufen is the first known protein in neurons being recruited to discrete RNA-containing particles, which are then transported with the same kinetics than described for granular RNA transport.

Recruitment of hStau-GFP into Granules and Their Subsequent Transport into Dendrites Are Microtubule Dependent in Living Neurons

We next sought to examine whether these granules move along microtubules into dendrites of hippocampal neurons. To study the effect of microtubule depolymerization on the localization and transport of hStau-GFP, we transiently transfected adult hippocampal neurons and incubated the neurons in the presence or absence of nocodazole. Green fluorescence analysis showed that microtubule depolymerization resulted in a significant change in the overall expression pattern of hStau-GFP in all cells observed (Figure 6). In control neurons, only 17% of the cells had an evenly distributed, "nonlocalized" expression of hStau-GFP, whereas all other cells showed the granular expression pattern as described in Figure 2. In nocodazole-treated cells, however, 45% of all transfected cells had a nonclustered, evenly dis-

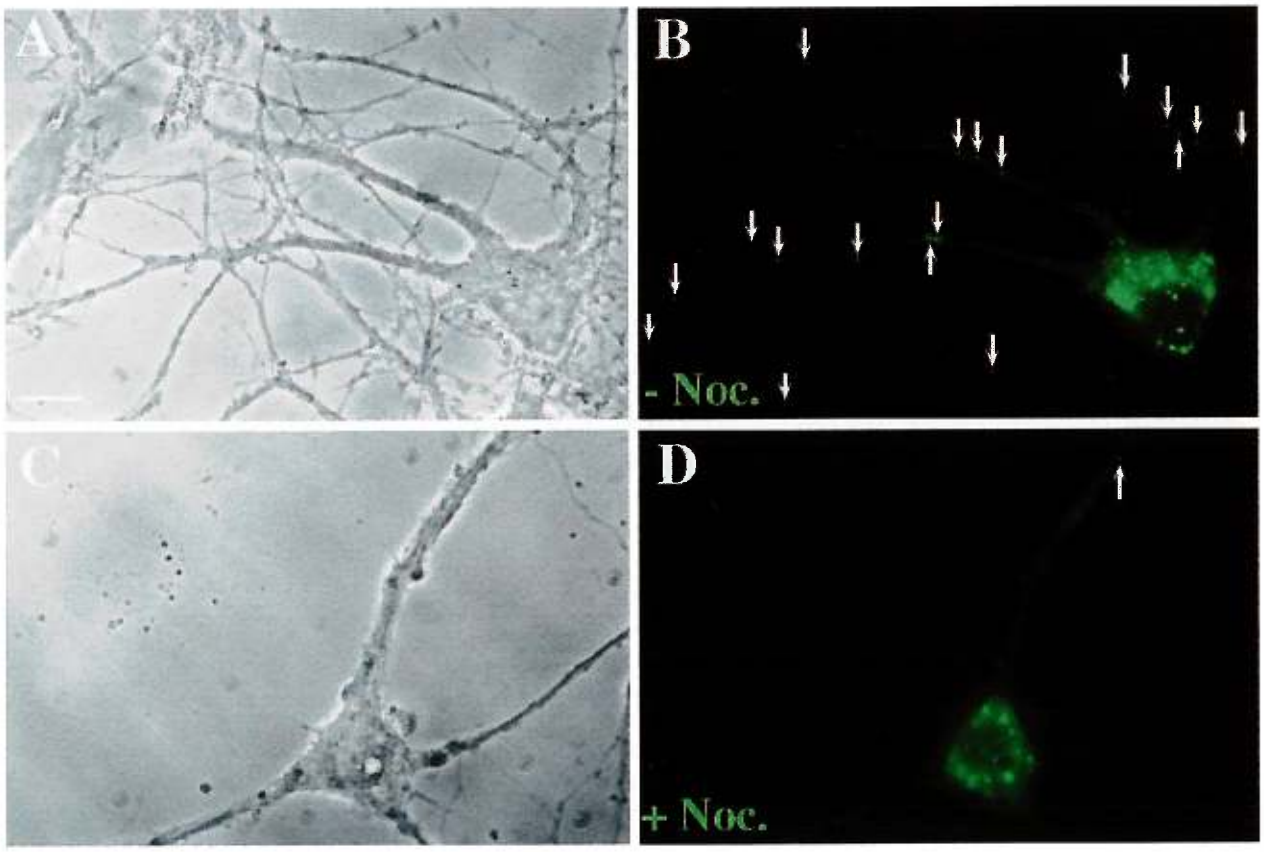

Figure 6. Nocodazole treatment of hippocampal neurons results in a diminished number of Stau-GFP particles in distal dendrites. Hippocampal neurons were transiently transfected as described in Figure 2 and the following day were treated with nocodazole (20 μM) for 3.5 h or mock treated. Cells were fixed, and fluorescence was recorded. (A and B) A representative cell is shown containing 19 Stau-GFP granules (arrows) in distal dendrites (>12 μm apart from the cell body). (C and D) A typical nocodazole-treated cell with a granular expression pattern is shown containing one granule (arrow) in distal dendrites. Bar, 10 μm.

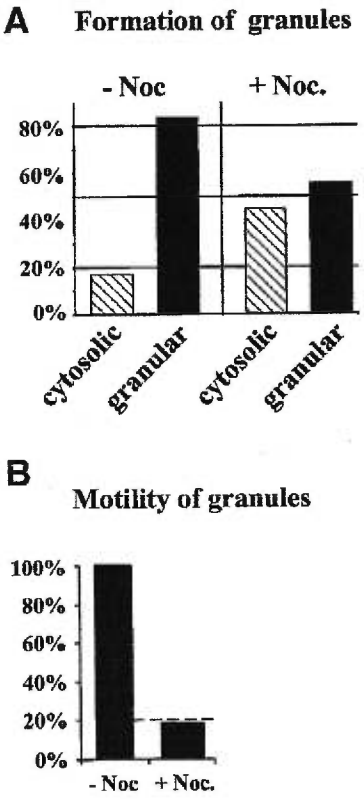

Figure 7. The transport of hStau-GFP particles into distal dendrites is microtubule dependent. Transfected neurons were treated as described in Figure 6. Pictures of 42 mock-treated and 58 nocodazole-treated cells were taken and analyzed for granular (localized) versus cytosolic (mislocalized) fluorescence (A) and subsequently for localization of hStau-GFP granules in distal (>12 μm apart from the cell body) dendrites (B).

tributed pattern with no apparent granules both in the cell body and in dendrites. This represents a 168% increase of cells with the described aberrant expression pattern of mislocalized hStau-GFP (Figure 7A). This finding clearly indicates that the recruitment and formation of hStau-GFP into granules requires an intact cytoskeleton.

We next analyzed the effect of nocodazole on the transport of hStau-GFP particles into the distal part of dendrites. For this we focused our attention on those cells that had a granular expression pattern (Figures 6 and 7B). Whereas 83% of the control cells (29 of 35) with a granular expression pattern had more than two granules in distal parts of the dendrites, only 16% (5 of 32) of the nocodazole-treated cells showed the same phenotype. When normalized, this reflects an 81% suppression of the number of neurons with fluorescent, dendritically transported hStau-GFP granules (Figure 7B). To study the role of the actin on hStau-GFP expression pattern, we used latrunculin B (Spector *et al.*, 1989), a G-actin–sequestering drug. Latrunculin B had no effect on both the localization and transport of hStau-GFP granules.

A similar microtubule dependence for mRNA transport has been observed in *Drosophila* embryos (Ferrandon *et al.*, 1994) and cortical neurons (Knowles *et al.*, 1996). In the embryo, the microtubule-depolymerizing drug colcemid but not the actin-depolymerizing drug cytochalasin B prevented both the formation of Staufen-bcd-3′-UTR particles after injection of bcd-3′-UTR mRNA into embryos as well as their subsequent movement. Ferrandon *et al.* (1994) introduced a model in which the binding of Staufen to its target RNA induces a conformational change in the Staufen protein. In our opinion it is conceivable that this would allow the Staufen-RNA complex to assemble either directly or indirectly to microtubules thereby leading to the assembly of the granules at the site of transport. In mammalian neurons this is further corroborated by the fact that human Staufen contains a (low-affinity) tubulin binding domain (Wickham *et al.*, 1999) allowing the Staufen–RNA complex to bind to the cytoskeleton directly. In cortical neurons, colchicine, another microtubule-depolymerizing drug, but not cytochalasin D prevented the transport of RNA-labeled granules into neurites of 4-d-old neurons. Taken together, we show for the first time that hStau-GFP is recruited to RNA-containing granules in adult hippocampal neurons. The existence of fluorescent granules now enabled us to examine their motility in living neurons. Video microscopy revealed that this transport occurs in a saltatory manner with many particles remaining in a stationary phase during recording and allowed us to calculate an average speed of 6.4 μm/min. Finally, we demonstrate that both the assembly and the dendritic transport of these granules require intact microtubules.

Perspectives

The RNA-binding protein Staufen is the first known protein being recruited to discrete particles, which then move into dendrites. Their visualization in living neurons (see attached videos) therefore faithfully represents for the first time the dynamics of this process. Interestingly, both the velocity and the microtubule dependence correlate well with studies in other organisms, suggesting a strong conservation of the mRNA transport mechanism through phylogeny. Moreover, the assay presented here will allow to experimentally address a central hypothesis in neurobiology: is dendritic mRNA transport (and subsequent local translation) to the synapse involved in forming synaptic memories? Finally, the biochemical isolation of these particles will lead to the identification of both transported mRNAs as well as other components of this transport machinery.

ACKNOWLEDGMENTS

This paper is dedicated to Walter Neupert at the occasion of his 60th birthday. Special thanks to Lola Ledesma, Bianca Hellias, Eugenia Piddini, Francesca Ruberti, Barbara Grunewald, Jürgen Löschinger, R. Carazo Salas, P. Fortes, H. McBride, P. Scheiffele, and F. Bonhoeffer for discussions and/or critically reading the manuscript. M.A.K. was supported by research fellowships from Deutsche Forschungsgemeinschaft and Human Frontier Science Program; C.K. was supported by a fellowship from the Fritz-Thyssen-Stiftung; C.G.D. was supported by Sonderforschungsbereich grant SFB 317; and L.D.G. was supported by a Natural Sciences and Engineering Research Council of Canada grant.

REFERENCES

Ainger, K., Avossa, D., Morgan, F., Hill, S.J., Barry, C., Barbarese, E., and Carson, J.H. (1993). Transport and localization of exogenous my-

elin basic protein mRNA microinjected into oligodendrocytes. J. Cell Biol. *123*, 431–441.

Bassell, G., Zhang, H., Byrd, A.L., Femino, A.M., Singer, R.H., Taneja, K.L., Lifshitz, L.M., Herman, I.M., and Kosik, K.S. (1998). Sorting of β-actin mRNA and protein to neurites and growth cones in culture. J. Neurosci. *18*, 251–265.

Bertrand, E., Chartrand, P., Schaefer, M., Shenoy, S.M., Singer, R.H., and Long, R.M. (1998). Localization of ASH1 mRNA particles in living yeast. Mol. Cell *2*, 437–445.

Bradke, F., and Dotti, C.G. (1998). Videomicroscopy of living microinjected hippocampal neurons in culture. In: Microinjection and Transgenesis: Strategies and Protocols, ed A. Cid-Arregui and A. Garcia-Carrancá, Heidelberg: Springer-Verlag, 81–94.

Bradke, F., and Dotti, C.G. (1999). The role of local actin instability in axon formation. Science *283*, 1931–1934.

Brady, S.T., Lasek, R.J., and Allen, R.D. (1982). Fast axonal transport in extruded cytoplasm from squid giant axon. Science *218*, 1129–1131.

Carson, J.H., Kwon, S., and Barbarese, E. (1998). RNA trafficking in myelinating cells. Curr. Opin. Neurobiol. *8*, 607–612.

Carson, J.H., Worboys, K., Ainger, K., and Barbarese, E. (1997). Translocation of myelin basic protein mRNA in oligodendrocytes requires microtubules and kinesin. Cell. Motil. Cytoskeleton *38*, 318–328.

de Hoop, M.J., Meyn, L., and Dotti, C.G. (1998). Culturing hippocampal neurons and astrocytes from fetal rodent brain. In: Cell Biology: A Laboratory Handbook, 2nd ed., ed. J.E. Celis, 2nd ed., San Diego: Academic Press, 154–163.

De Strooper, B., Simons, M., Multhaup, G., Van Leuven, F., Beyreuther, K., and Dotti, C.G. (1995). Production of intracellular amyloid-containing fragments in hippocampal neurons expressing human amyloid precursor protein and protection against amyloidogenesis by subtle amino acid substitutions in the rhodent sequence. EMBO J. *14*, 4932–4938.

Deshler, J.O., Highett, M.I., Abramson, T., and Schnapp, B.J. (1998). A highly conserved RNA-binding protein for cytoplasmic mRNA localization in vertebrates. Curr. Biol. *8*, 489–496.

Deshler, J.O., Highett, M.I., and Schnapp, B.J. (1997). Localization of *Xenopus* Vg1 mRNA by VERA protein and the endoplasmic reticulum. Science *276*, 1128–1131.

Driever, W., and Nüsslein-Volhard, C. (1988). The *bicoid* protein determines position in the *Drosophila* embryo in a concentration-dependent manner. Cell *54*, 95–104.

Ephrussi, A., Dickinson, L.K., and Lehmann, R. (1991). Oskar organizes the germ plasm and directs localization of the posterior determinant nanos. Cell *66*, 37–50.

Ferrandon, D., Elphick, L., Nüsslein-Volhard, C., and St. Johnston, D. (1994). Staufen protein associates with the 3-UTR of bicoid mRNA to form particles that move in a microtubule-dependent manner. Cell *79*, 1221–1231.

Goslin, K., and Banker, G. (1997). Rat hippocampal neurons in low-density culture. In: Culturing Nerve Cells, ed. G. Banker and K. Goslin, Cambridge, MA: MIT Press, 251–281.

Haubensack, W., Narz, F., Heumann, R., and Leßmann, V. (1998). BDNF-GFP containing secretory granules are localized in the vicinity of synaptic junctions of cultured cortical neurons. J. Cell Sci. *111*, 1483–1493.

Hazelrigg, T. (1998). The destinies and destinations of RNAs (meeting review). Cell *95*, 451–460.

Hoek, K., Kidd, G.J., Carson, J.H., and Smith, R. (1998). hnRNP A2 selectively binds the cytoplasmic transport sequence of myelin basic protein mRNA. Biochemistry *37*, 7021–7029.

Holmes, E., Hermanson, G., Cole, R., and de Vellis, J. (1988). Developmental expression of glial-specific mRNAs in primary cultures of rat brain visualized by in situ hybridization. J. Neurosci. *19*, 389–396.

Kaether, C., Salm, T., Glombik, M., Almers, W., and Gerdes, H.-H. (1997). Targeting of GFP to neuroendocrine secretory granules: a new tool for real time studies of regulated protein secretion. Eur. J. Cell Biol. *74*, 133–142.

Kiebler, M., Hemraj, I., Verkade, P., Köhrmann, M., Fortes, P., Marión, R.M., Ortín, J., and Dotti, C.G. (1999). The mammalian Staufen protein localizes to the somatodendritic domain of cultured hippocampal neurons: implications for its involvement in mRNA transport. J. Neurosci. *19*, 288–297.

Knowles, R.B., and Kosik, K.S. (1997). Neurotrophin-3 signals redistribute RNA in neurons. Proc. Natl. Acad. Sci. USA *94*, 14804–14808.

Knowles, R.B., Sabry, J.H., Martone, M.E., Deerinck, T.J., Ellisman, M.H., Bassell, G.J., and Kosik, K.S. (1996). Translocation of RNA granules in living neurons. J. Neurosci. *16*, 7812–7820.

Kuhl, D., and Skehel, P. (1998). Dendritic localization of mRNAs. Curr. Opin. Neurobiol. *8*, 600–606.

Marión, R.M., Fortes, P., Beloso, A., Dotti, C.G., and Ortín, J. (1999). A human sequence homologue of staufen is an RNA-binding protein that is associated with polysomes and localizes to the rough ER. Mol. Cell. Biol. *19*, 2212–2219.

Mayford, M., Baranes, D., Podsypanina, K., and Kandel, E.R. (1996). The 3'-untranslated region of CaMKII alpha is a *cis*-acting signal for the localization and translation of mRNA in dendrites. Proc. Natl. Acad. Sci. USA *93*, 13250–13255.

Muslimov, I.A., Santi, E., Homel, P., Perini, S., Higgins, D., and Tiedge, H. (1997). RNA transport in dendrites: a *cis*-acting targeting element is contained within neuronal BC1 RNA. J. Neurosci. *17*, 4722–4733.

Ross, A.F., Oleynikov, Y., Kislauskis, E.H., Taneja, K.L., and Singer, R.H. (1997). Characterization of a β-actin mRNA zipcode-binding protein. Mol. Cell. Biol. *17*, 2158–2165.

Simons, M., De Strooper, B., Multhaup, G., Tienari, P.J., Dotti, C.G., and Beyreuther, K. (1996). Amyloidogenic processing of the human amyloid precursor protein in primary cultures of rat hippocampal neurons. J. Neurosci. *16*, 899–908.

Spector, I., Shochet, N.R., Blasberger, D., and Kashman, Y. (1989). Latrunculins—novel marine macrolides that disrupt microfilament organization and affect cell growth: I. comparison with cytochalasin D. Cell Motil. Cytoskeleton *13*, 127–144.

St. Johnston, D. (1995). The intracellular localization of mRNAs. Cell *81*, 161–170.

St. Johnston, D., Beuchle, D., and Nuesslein-Volhard, C. (1991). staufen, a gene required to localize maternal RNAs in the *Drosophila* egg. Cell *66*, 51–63.

Tiedge H, Bloom FE, Richter D. (1999). RNA, whither goest thou? Science *283*, 186–187.

Wacker, I., Kaether, C., Krömer, A., Migala, A., Almers, W., and Gerdes, H.-H. (1997). Microtubule-dependent transport of secretory vesicles visualized in real time with a GFP-tagged secretory protein. J. Cell Sci. *110*, 1453–1463.

Wallace, C.S., Lyford, G.L., Worley, P.F., and Steward, O. (1998). Differential intracellular sorting of immediate early gene mRNAs depends on signals in the mRNA sequence. J. Neurosci. *18*, 26–35.

Wang, S., and Hazelrigg, T. (1994). Implications for bcd mRNA localization from spatial distribution of exu protein in *Drosophila* oogenesis. Nature *369*, 400–403.

Wickham, L., Duchaîne, T., Luo, M., Nabi, I.R., and DesGroseillers, L. (1999). Mammalian Staufen is a double-stranded RNA- and tubulin-binding protein which localizes to the rough ER. Mol. Cell. Biol. *19*, 2220–2230.

Wilhelm, J.E., and Vale, R.D. (1993). RNA on the move: the mRNA localization pathway. J. Cell Biol. *123*, 269–274.

VI- Discussion

The studies presented in this thesis describe the molecular characterization and functional investigation of the mammalian orthologues of *Drosophila* Staufen (dStau), the first known double-stranded RNA-binding protein that participates in intracellular RNA localization and local translation. Most of the work is shown in 4 manuscripts that have been included in the thesis. These studies have revealed that mammalian Staufen is an evolutionary conserved protein which has four distinct biochemical properties: binding to double-stranded RNA, binding to microtubules, association with the RER, co-fractionation with ribosomes. By a series of molecular mapping techniques, we further determined that each of these biochemical properties has its own molecular determinant. These results suggest that mammalian Stau may serve as a molecular bridge between the RER, ribosomes, and microtubules. Finally, by collaboration with two other groups, we have addressed the putative role of hStau in RNA transport in two different expression systems.

VI.1 Characterization of human and mouse *stau* genes and their genetic organization

VI.1.1 Mammalian stau genes may be derived from a common origin

Staufen is a protein with multiple dsRNA-binding domains that was first characterized in *Drosophila melanogaster*. It is essential for the asymmetric localization of *oskar*, *bicoid* and *prospero* mRNAs during oogenesis, early embryogenesis and neurogenesis, respectively. Our work in the study of human and mouse *Stau* genomic

organization reveals that mammalian *stau* genes may be derived from a common genetic origin (Brizard et al., 2000, Article 1). First, both human and mouse *stau* transcripts have conserved transcription initiation sites at the same position when mapped by 5'RACE. Second, the overall organization of the human and mouse *stau* genes is quite similar, especially the positions of the exon/intron junctions which are perfectly conserved in both species although three additional exons have been found in the human gene that are subject to differential splicing and generate four different transcripts. Even an alternative choice between two splicing acceptor sites, which caused an insertion of 18 nucleotides in exon E5, is conserved in both human and mouse. The alternative splicing of exon E5 may represent a conserved mechanism to regulate Staufen function in mammalian cells since the resulting insertion of 6 amino acids in dsRBD3 generates a protein with impaired RNA-binding activity and modulates the RNA content in Staufen-containing ribonucleoprotein complexes (Duchaîne et al., 2000).

VI.1.2 Staufen encodes a conserved RNA-binding protein across species

Staufen homologues of *Drosophila melanoganster* have been reported in two other insect species, *Drosophila virilis* (DvStau) and *Musca domestica* (MdStau), which diverged from *Drosophila melanogaster* over 60 and 100 million years ago, respectively (Micklem et al., 2000). The characterization of Staufen homologues from different mammalian species including human (hStau), mouse (mStau) and rat (rStau) (Kiebler et al., 1999; Marion et al., 1999; Wickham et al., 1999, Article 2) provides strong evidence that Staufen may be functionally conserved in these species. Mammalian Stau contains 4 dsRNA-binding domains which correspond to dsRBD2 to dsRBD5 of *Drosophila* Stau

(dStau), these corresponding domains share higher sequence similarity and identity compared to the dsRBDs of other dsRBD-containing proteins, suggesting that our cloned human and mouse proteins are real orthologues of dStau. In addition, the *Caenorhabditis elegans* genome also contains an uncharacterized open reading frame that shows similarity to human and mouse Staufen dsRBDs, suggesting that a functional homologue of Staufen is also present in worms (Wickham et al., 1999, Article 2). These findings, together with the conseved genomic organization of human and mouse *stau* genes, suggest that Staufen is an evolutionary conserved protein across species.

Drosophila Staufen contains three functional dsRNA-binding domains including dsRBD1, 3 and 4, although their binding capacity is different and dsRBD3 remains the strongest one. dsRBD2 of dStau contains a proline-rich insertion in the domain, and this insertion is important for dStau-mediated RNA transport (Micklem et al., 2000). Interestingly, this insertion is also conserved across other species suggesting that this split domain may play a conserved function across species although it could not bind any dsRNA *in vitro*.

Micklem et al (2000) have shown that the dsRBDs are the only conserved regions of dStau required for *oskar* mRNA localization since a transgene in which the large non-conserved N-terminal region was deleted can completely rescue the posterior localization and anchoring of *osk* mRNA in *dStau*-null background. Moreover, when the dsRBD-containing regions of dStau are replaced with the corresponding regions from *M. domestica* ($Stau^{DmMD}$), the transgene still rescues all the phenotypes of a *Stau*-null mutation. Thus, the functional domains of Stau have been conserved during evolution.

Interestingly, mammalian Stau has evolved a new domain that resembles the microtubule-binding domain of MAP1B. This domain binds microtubules *in vitro* (Wickham et al., 1998, Article 2). We recently demonstrated that hStau mediates RNA transport in neurons in a microtubule-dependent way (Köhrmann et al., 1999, Article 4). Immuno-electromicroscopy of rat hippocampal neurons has also shown that Stau is present in the vicinity of microtubules in dendrites (Kiebler et al., 1999). In COS cells, we only observed partial colocalization of hStau with the microtubules. This is not surprising since the small size of COS cells may not allow us to observe a strong colocalization. It has been reported that some RNA-binding protein such as β-actin mRNA zipcode binding protein mediates β-actin mRNA localization along the microfilaments in fibroblast cells (Ross et al., 1997) and along the microtubules in neurons (Bassell et al., 1998). Therefore it is possible that Staufen may mediate RNA transport along different cytoskeletal components in different cells. It will be interesting to determine whether mammalian Stau is directly associated with microtubules in neurons and if the putative TBD plays a role in this association.

VI.1.3 The dsRBDs of Stau have evolved independently

The sequence homology among Stau homologues in different species only exists in the corresponding functional domains. A ClustalW analysis of dsRBDs from many proteins reveals that a given Stau domain is most similar to the equivalent one in each of the other Stau homologues (see Fig.1). This suggests that evolution is not acting simply to maintain similarity to a dsRBD consensus sequence, but rather that each domain has

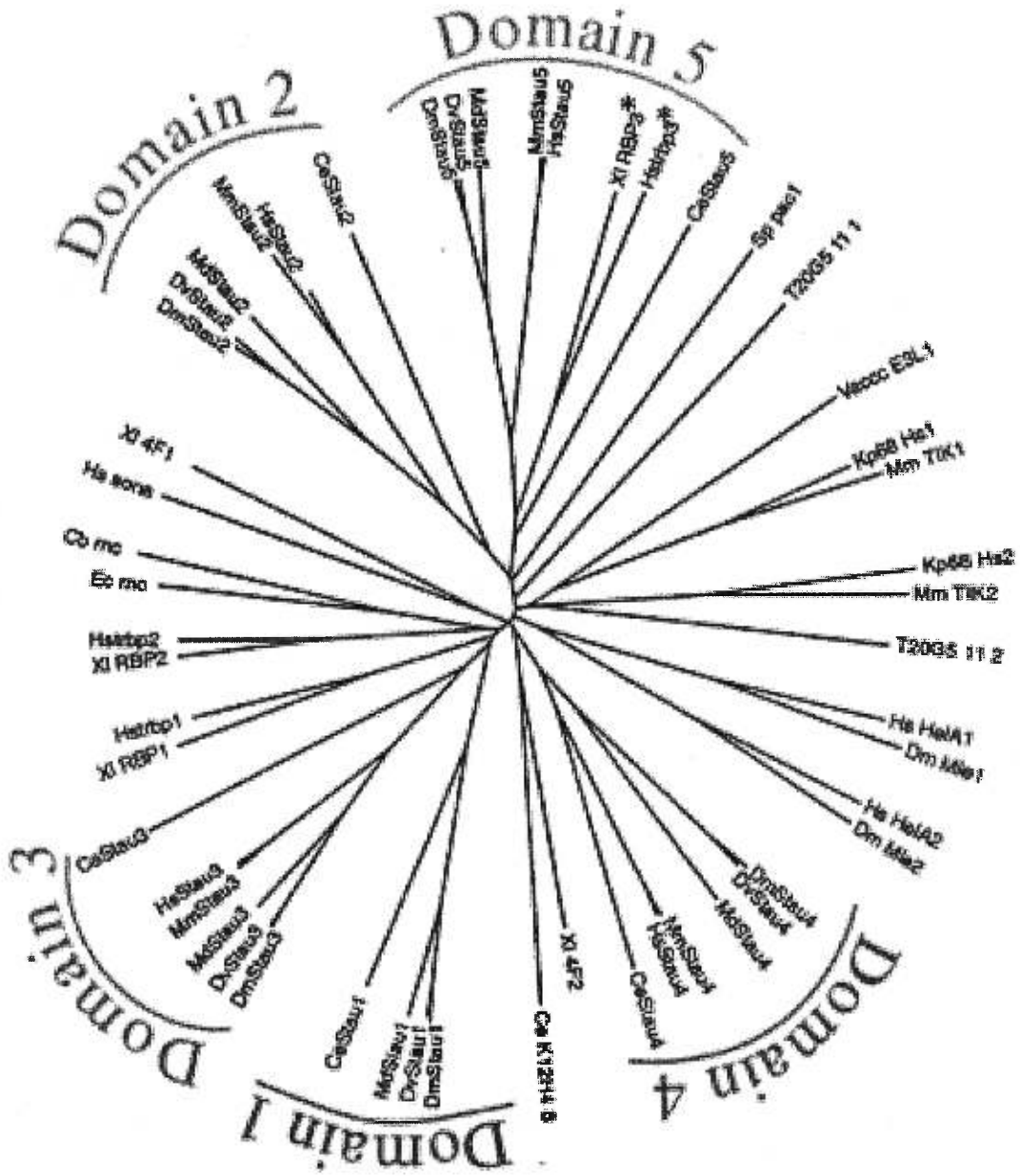

Fig. 1. An unrooted tree derived from a ClustalW alignment of dsRBDs from different proteins. Corresponding domains in the different Staufen homologues are more similar to each other than they are to any other dsRBDs, with exception of CeStau dsRBD5, which is approximately similar to the other Stau dsRBDs and to the third dsRBD of human TAR RNA-binding protein (HsTRBP) and *Xenopus* Xlrbpa (marked as asterisks). Adapted from Micklem et al., 2000.

unique feature that has been conserved during evolution therefore, each dsRBD of Stau may be evolved independently and may have distinct functions (Micklem et al, 2000).

Our mapping results of human and mouse genomic organization are consistent with the notion that each dsRBD of Staufen may have originated from a different ancestral gene or evolved independently. Comparison of the genomic organization of two other members of the dsRBD family of proteins, the human adenosine deaminase (*DRADA*, Wang et al., 1995) and the human interferon-inducible dsRNA-dependent protein kinase (*PKR*, Kuhen et al., 1996), with that of human and mouse *stau* genes further supports this notion (Brizard et al., 2000, Article 1). In the case of *DRADA* and *PKR* genes, introns divide each of their corresponding dsRBDs into NH_2 and COOH regions of identical size. However, the *stau* genes share different splicing patterns for each of their dsRBDs. Two full-sized domains, dsRBD3 and dsRBD4 contain one intron in each of the domains, but the position of the exon-intron junction is different. dsRBD2, the so-called split domain, in human and mouse Staufen, contains inserts of different sizes which share conserved sequences. Interestingly, each conserved region is flanked by introns. Finally, dsRBD5 contains two exon-intron junctions and is divided into three units, the well-conserved C-terminal consensus sequence being spliced. The distinct splicing pattern for each of the dsRBDs of mammalian Staufen suggests that these dsRBDs may have evolved from distinct origins and may have different functions.

VI.1.4 Mammalian stau may be a housekeeping gene

Our work in the identification of the 5' flanking region of mStau suggests that Stau may be driven by a housekeeping gene promoter (Brizard et al., 2000, Article 1).

This region has many features which are characteristic of promoters of housekeeping genes, for example, the absence of canonical TATA and CAAT boxes, the extremely G+C rich region (74%), the high frequency of potential methylation sites (CpG pairs) and multiple Sp1-binding consensus sites. The presence of such a promoter for the mouse *stau* gene is consistent with the broad expression of *stau* mRNA in different tissues and cell lines. Recently, a 2.5-kb mouse Staufen genomic DNA fragment covering the 5' flanking regions was further cloned upstream of the mStau cDNA in a mammalian expression vector which is devoid of a promoter. This fragment was able to drive the expression of Staufen protein in transiently transfected COS7 cells (Duchaîne T, personal communication), confirming that the G+C-rich region may represent a true promoter. Further work will be needed to map the exact region of the mouse Staufen promoter.

VI.2 Characterization of hStau protein isoforms

VI.2.1 The presence of multiple Stau isoforms

Our Western blotting experiments have shown that hStau contains at least two major protein isoforms which are ubiquitously expressed in almost every tested tissue and cell line. One isoform is approximately 63 kDa, and the other is approximately 55 kDa (Wickham et al., 1999, Article 2). These two major isoforms are also ubiquitously expressed in mouse and rat tissues and cell lines. In some experiments, doublets or triplets of approximately 55 kDa are also visible, suggesting that this isoform may have differential translation initiation sites. In addition, we have also observed a short protein

of around 30 kDa in most of the tested tissues and cell lines. Currently, we do not know if this short protein comes from proteolytic degradation during the experimental procedure or from alternative translation initiation from an internal AUG site. Since the 30-kDa band is constitutively expressed in every tested tissue and cell line, the latter case is most probably true. Indeed, an in-frame ATG which harbours a Kozak consensus sequence is present in the middle of dsRBD4, and translation initiation from this ATG is predicted to produce a 30-kDa protein. Therefore, the observed 30-kDa protein in Western blotting may correspond to this predicted 30-kDa protein. This small protein contains only the microtubule-binding domain and the last half-consensus dsRNA-binding domain, its function in vivo remains to be elucidated and it may serve as a negative regulating protein which can block Staufen-mediated RNA transport along the microtubules.

Interestingly, using cell fractionation analysis, we have found that these different Staufen isoforms have distinct subcellular distributions. Stau^{63} is mainly present in the rough endoplasmic reticulum (RER), Stau^{55} is predominantly associated with ribosomes (for details, see article 3), and the 30-kDa protein appears to be present in the cytosolic fractions that cofractionate with soluble proteins (our unpublished data). After isolating the nucleus and cytoplasm, we also found that Stau^{55} mainly co-fractionates with cytoplasmic fractions (our unpublished results), which is consistent with results obtained using immunofluorescence (Wickham et al., 1999, Article 2). Surprisingly, Stau^{63} is found to mainly cofractionate with the nucleus (our unpublished results), indicating this isoform is more nuclear and may shuttle between the nucleus and cytoplasm. However, once in the cytoplasm, Stau^{63} is mainly associated with the rough endoplasmic reticulum

(Article 3). The distinct localization of Staufen isoforms suggests that they may play different roles in mammalian cells.

VI.2.2 A differential splicing event generates two different proteins

Interestingly, an alternative splicing event generates 4 Staufen transcripts in human that are termed T1 to T4 (Wickham et al., 1999, Article 2). These four transcripts are outlined in Fig. 2. To directly confirm the presence of this differential splicing event and to test the abundance of each individual transcript, we have designed and completed an RT-PCR and hybridization analysis (the results are shown in Fig.1 of the Appendix). This experiment demonstrated that the four different transcripts of human Staufen are expressed in every tested human tissue and HeLa cells and transcript T2, which has a 75-bp insert compared to the shortest transcript T1, is the most abundant one *in vivo*.

We have demonstrated that the differential splicing event in humans generates two proteins. The cloned T1, T2 and T4 transcripts are capable of producing a protein approximately 55 kDa that comigrates with the endogenous short isoform, and the T3 transcript generates a protein of around 63 kDa which comigrates with the longer endogenous isoform (Wickham et al., 1999, Article 2). The cloned 55 and 63 kDa proteins are almost identical, except that the 63 kDa protein has an extension of 81 amino acids at the N-terminal extremity (Wickham et al., 1999, Article 2). Of the four *hStau* transcripts, T2, T3 and T4 harbour in-frame stop codons before their respectively translation initiation sites, however, transcript T1 is still open (see Fig. 2). It is possible

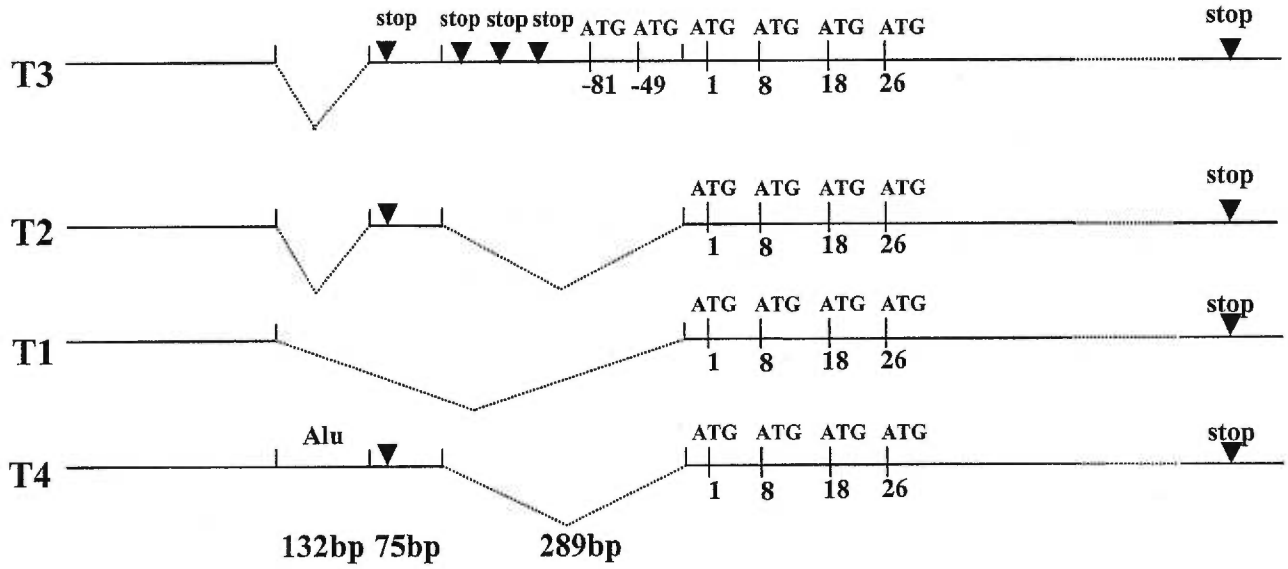

Fig. 2 Schematic representation of four alternatively spliced hStau transcripts

that some extra nucleotides which harbor another translation initiation site may be missing in the most 5' end of the transcript T1, and this transcript may encode the Stau[63] isoform that is widely expressed in different mammalian species.

In Western blotting assays, we consistently observed the presence of doublets around 55 kDa. One explanation is that the 55 kDa Staufen isoform may have alternative translation initiation sites. From the corresponding cDNA sequence, a single ATG codon at position –81 is expected to initiate the translation of the 63 kDa protein. However, four in-frame ATGs are clustered at the putative translation initiation site of the 55 kDa protein (see Fig. 2 in the discussion). In order to identify the translation initiation sites for each of the cloned 55 and 63 kDa proteins, we made a series of deletion mutants from each of the cloned cDNAs and expressed the resulting proteins in mammalian cells (the results are shown in Fig. 2 of the Appendix). These experiments have revealed that the second and the fourth ATG in the 4 ATG cluster of hStau cDNA are used to initiate the translation of the 55 kDa protein doublets. Interestingly, three in-frame ATGs are also present in the 5' end of mouse *Stau* cDNA coding for the 55 kDa protein, which correspond to the second to fourth ATG in the human transcript. Deletion analysis has shown that the first and third ATG of the mouse transcript, which correspond to the second and the fourth ATG of the human transcript, are also the real translation initiation sites (our unpublished results), demonstrating that the 55-kDa protein from human and mouse has conserved translation start sites.

VI.2.3 The possibility for an uncloned Stau isoform

In humans, we have shown that differentially spliced transcripts code for two proteins of 55 and 63 kDa. These two proteins comigrate with the two endogeneous isoforms when transiently expressed in HEK or HeLa cells (Wickham et al., 1999, Article 2), suggesting that both hStau isoforms are cloned. By confocal microscopy, both the cloned 55 and 63 kDa protein have the same RER localization pattern (Wickham et al., 1999, Article 2). By Western blotting, the two endogenous isoforms of 55 and 63 kDa Stau were also detected in mouse and rat tissues as well as cell lines (our unpublished results, Kiebler et al., 1999). However, screening of cDNA libraries, RT-PCR experiments and analysis of clones isolated from a mouse genomic library all failed to identify splicing events that would explain the presence of a long isoform as observed in humans (Brizard et al., 2000, Article 1). These results suggest that an additional ubiquitously-expressed 63 kDa isoform remains to be cloned in mammals while the 63 kDa protein expressed from the alternatively spliced human transcript T3 (Wickham et al., 1999, Article 2) may be barely expressed endogenously and distinct from the common 63 kDa protein. For clarity, we named the cloned human specific 63 kDa protein as hStau^{63h}.

When analyzed by sucrose gradient cell fractionation, we found that endogenous Stau^{55} and Stau^{63} are differentially associated with the ribosomes and the RER, respectively. Therefore, the two isoforms may be associated with different complexes *in vivo*. Further analysis of the overexpressed hStau^{55}-HA$_3$ and hStau^{63h}-HA$_3$ showed that both proteins are associated with ribosomes similar to the pattern of endogenous hStau^{55} in sucrose gradient. These results confirm that hStau^{63h} is not the common 63 kDa protein which is ubiquitously expressed in mammals and is associated with the RER. Therefore,

an additional Staufen isoform around 63 kDa is expressed from the *Stau* gene. Since the reading frames in the 5'UTR of the human and mouse cDNAs are open and in frame with the sequence of hStau^{55} (in human, transcript T1 is open), it is likely that Stau^{63} is translated from this sequence. The first ATG initiation codon remains to be identified due to the presence of a very rich GC region upstream from the 5'end of the longest cDNA (Brizard et al., 2000, Article 1). This isoform would also differ from the other isoforms by an insertion at its N-terminal extremity that is different from that of hStau^{63h}.

VI.3 Molecular determinants of hStau RER and ribosome association

VI.3.1 Staufen RER- and ribosome-binding determinants

Our results demonstrate that multiple domains are required for Staufen RER/ribosome association *in vivo*. dsRBD4 alone is sufficient for RER association although the other two N-terminal domains dsRBD2 and dsRBD3 are also required for full RER association implicating a structural/functional cooperation between dsRBD2, 3 and 4 for this function. Indeed, deletion of each RBD from both sides of the N-terminal region covering dsRBD2/3/4 strongly impaired RER association, confirming the notion that a structural/functional cooperation among the first three RBDs is important for Stau-RER association (our unpublished results). In contrast, TBD alone is not sufficient to promote detectable association with ribosomes or the RER. However, it is crucial for hStau^{55} ribosome association since the deletion of TBD from hStau^{55} shifts the distribution of the protein from ribosomes to the RER. Conversely, when the TBD is fused to the RER-associated dsRBD2/3/4, the resulting protein is relocalized to the ribosomes. Thus, TBD is a critical domain for hStau^{55} ribosome association. These

results also indicated that hStau^{55} contains a cryptic RER association domain (dsRBD2/3/4) in the presence of TBD. Therefore, hStau^{55} can associate not only with ribosomes but also with the RER through its overlapping determinants. Interestingly, our fine mapping reveals that a minimal region covering RBD4/TBD is able to confer basal ribosome association, suggesting that the presence of RER-associated RBD4 is important for TBD-mediated ribosome association. This hypothesis is further supported by the fact that the full-length Stau^{55} and Stau$^{55}\Delta5$, which contain the full-length RER-association-domain dsRBD2/3/4 and TBD, have stronger ribosome association than dsRBD4/TBD. Therefore, the determinants for RER and ribosome association are overlapped and the N-terminal RER association may be important for TBD-mediated ribosome association. Alternatively, the role of the N-terminal dsRBDs may be to stabilize the tertiary structure of TBD, allowing its stable association with ribosomes independent of RER association.

The RER association through dsRBD2/3/4 may be mediated by a complex mechanism. The isolated dsRBD4 itself has independent RER-binding activity. Together with dsRBD2 and 3, which have no independent RER binding activity separately, dsRBD4 can confer strong RER association. We propose that dsRBD4 constitutes a core RER-binding domain that directly interacts with RER components through protein-protein interactions, and that other domains facilitate this interaction. Protein-protein interactions mediated by dsRBDs have been reported for *Drosophila* Staufen and other members of the dsRNA-binding protein family (Schmedt et al., 1995; Cosentino et al., 1995; Li et al., 1997; Schuld et al., 1998). Besides protein-protein interaction, dsRBD3 RNA-binding activity plays additional roles for RER binding, since the F135A mutation in dsRBD3 (which destroys the RNA-binding activity of hStau) of the N-terminal

dsRBD2/3/4-HA releases a part of the RER-associated protein to the upper fractions that contain soluble proteins (our unpublished data). The same mutation in dsRBD4 has no effect on Staufen localization, confirming that the dsRBD4/RER interaction is not due to an RNA-protein interaction. Similar to RER association, Staufen association with ribosomes per se is not mainly due to its RNA-binding capacity since the basal ribosome association mediated through dsRBD4/TBD is totally independent of Staufen RNA-binding activity (see Article 3). Therefore, the molecular mechanism involving Staufen ribosome association is different from that involving other members of the dsRNA-binding protein family such as PKR, since association of PKR with ribosomes requires RNA-binding activity of its dsRBDs (Zhu et al., 1997). It is likely that the RNA-binding activity of dsRBD3 indirectly increases the stability of the Stau/ribosome complex and that RNA-binding may help to create a complete ribonucleoprotein complex that facilitates Stau-ribosome interactions. Alternatively, binding RNA may induce a structural change in RBD4/TBD that allows its stable binding to ribosomes.

VI.3.2 Distinct mechanisms may direct the differential localization of Stau isoforms

Both hStau^{55} and hStau^{63h} (and most probably the common Stau^{63} isoform) contain identical motifs: four dsRBDs and one TBD. dsRBD4, an independent RER-binding domain, in cooperation with dsRBD2 and dsRBD3, constitutes a full RER association domain. TBD, which is located next to dsRBD4 in Staufen protein, is crucial for ribosome association. Based on these lines of evidence, a picture of the Stau localization mechanism is emerging. With the cooperation of dsRBD2 and 3, dsRBD4 may first bind to its RER partner and dock Staufen to the RER. This Stau/RER

association will bring the neighbouring TBD in close proximity to the RER located ribosomes, and subsequently triggers TBD-mediated ribosome association. Binding to ribosomes may then induce a structural shift that causes the dissociation of hStau^{55}-containing complexes from the RER. dsRBD4, which is involved in both RER and ribosome association, may be the molecular switch for this transition. hStau^{55}/ribosome complexes may then be associated with the cytoskeleton and be resistant to Triton X-100 extraction (see Fig. 3 for the model of Staufen-mediated RER and ribosome association). The presence of ribosomes and of the translation machinery on the cytoskeleton is well documented (Pachter, 1992).

The model in Fig. 3 would explain the ribosome association of hStau^{55} and hStau^{63h}. Under this model, there is a transition between RER-docked and ribosome-associated Staufen protein. It is thus plausible that two peaks of Staufen protein may be present in the sucrose gradient. Indeed, we do find a major ribosome peak and a minor RER peak of endogenous hStau^{55} and overexpressed hStau^{55} and hStau^{63h} in our sucrose gradient assays. Moreover, when overexpressed, the ratio of RER-associated hStau^{55} is increased. This could be expected when a transition from RER to ribosome is saturated due to abnormal expression of the protein. Therefore, it seems that hStau^{55} (and probably the hStau^{63h}) has the potential to be present in both the RER and ribosomes. These different populations of protein may have different functions.

Given the fact that different Stau isoforms are differentially associated with the RER and ribosomes and the crucial role of TBD for ribosome association, it is possible that modulation of the TBD may be a mechanism underlying the differential RER or ribosome association of Staufen isoforms. To confirm this model it will be extremely

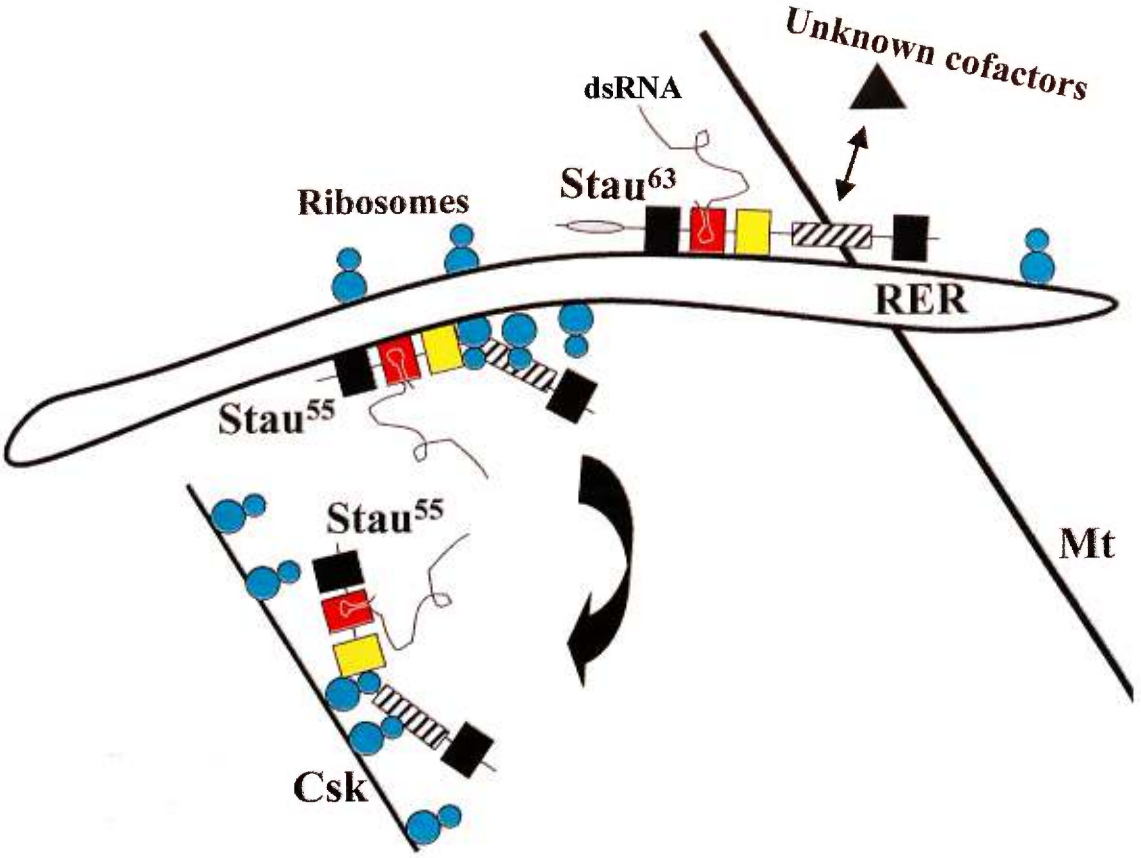

Fig. 3 A model for the differential association of two Stau isoforms with the RER and ribosomes. Stau^{55} first binds certain protein components on the RER using its N-terminal RER association determinant (dsRBD2/3/4). This RER association will bring the neighbouring TBD, a potential ribosome binding domain, in close proximity to the RER located ribosomes, and trigger TBD-mediated ribosome association. Ribosome association may induce a structural shift that causes the dissociation of Stau^{55}-containing complexes from the RER. Stau^{55}/ribosome complexes may then be associated with the cytoskeleton and be resistant to Triton treatment. For Stau^{63}, which is associated with the RER, its potential ribosome binding domain,TBD, may be masked by certain unknown cofactors. Thus, the protein is constitutively associated with the RER via the N-terminal RER-binding determinant. The red and yellow boxes represent the major and minor dsRNA-binding domain, respectively. The black boxes represent the half-consensus dsRNA-binding domains which have no dsRNA-binding capacity. The hatched box represent the tubulin-binding domain,TBD. Mt: microtubules, Csk: cytoskeleton.

important to clone the RER associated 63 kDa protein, and to identify the potential RER determinant. We expect that an extra domain at the N-terminal extremity and/or other unknown cofactors may mask the TBD to achieve its RER distribution (see Fig.3). Alternatively, the TBD may be deleted by an alternative splicing event so that the resultant protein contains only the RER association domain. However, this scenario does not seem likely since preliminary results using RT-PCR are not able to detect the alternative splicing events that remove the TBD from Staufen (Duchaîne et al., personal communication).

VI.3.3 Staufen as a molecular bridge between the RER, ribosome and microtubules

Our results demonstrated the ribosome-associated Stau[55] contains both RER- and ribosome-association determinants, and has the potential to be associated with not only ribosomes but also the RER. Thus, Stau[55] may act as a molecular link between the RER and ribosomes. Staufen is a protein presumably involved in RNA transport and localization. Its properties to bind both RER and ribosomes produce profound functional implications. On one hand, linking Stau to the RER may facilitate Stau-involved RNA transport since the ER has been implicated in RNA transport (Deshler et al., 1997). Alternatively, directly linking Stau to the RER may also help to bring Stau bound mRNA to the site of translation in the RER. On the other hand, a direct link between Stau and ribosomes will facilitate the translation activation of its transported mRNA, once localized. Indeed, previous results revealed that the transfected hStau[55] mostly colocalized with RER markers by immunofluorescence (Wickham et al., 1999, Article 2) but cofractionated with ribosomes on sucrose gradient (Marión et al., 1999). It is

possible that this 55 kDa isoform binds both targets at the same time via its two different determinants. At least for the 55 kDa isoform, both the RER and ribosome determinants are present in the protein and are necessary for its proper subcellular localization and function. This isoform may acts as a molecular link between the RER and ribosome.

The tubulin-binding domain of mammalian Staufen has been shown to bind tubulin *in vitro* (Wickham et al., 1999, Article 2). Thus, this domain seems to play multiple roles. In COS7 cells, we have no strong evidence for hStau/microtubule colocalization, but the small size of the cell may not allow the observation of the transport of a small population of Staufen-containing particles along the microtubules. However, in hippocampal neurons, Stau was found to be associated with both the RER and microtubules (Kiebler et al., 1999). In expression studies of hStau tagged with the green flurorescent protein (hStau-GFP), hStau was found to form RNA-containing granules that migrate to the distal dendrites bidirectionally, and these movements are sensitive to drugs that disrupt microtubules (Köhrmann et al., 1999, Article 4). Altogether, these results suggest that hStau also bridges the RER and the microtubules, at least in some subcellular compartments. A dynamic translocation of hStau-containing complexes between ribosomes, RER and microtubules may be important for the role of hStau in RNA transport and possibly in translation regulation.

VI.4 Differential localization of Stau isoforms in cytoplasm and nucleus

By immunofluorescence, both the cloned Stau^{55} and Stau^{63h} are mainly cytoplasmic, although a very small population of the transfected cells have nuclear or nucleolar localization. Interestingly, some of the mutants can be found in the nucleus or the nucleolus. For example, the N-terminal mutant RBD3/4-GFP is present in both cytoplasm and nucleus. While in the nucleus, it is exclusively found in the nucleolus of the transfected cells (see Fig.5 in the Appendix). This mutant contains a putative bipartite nuclear localization signal (KK-X_{10}-KPRIK). The nucleolar signal is Triton-resistant and specific. Localization to the nucleolus requires the RNA-binding activity of the protein since point mutation in RBD3 which breaks the RNA-binding activity of hStau abolishes its presence into the nucleolus (Fig.5 in the Appendix and our unpublished results). This also demonstrates that its presence in the nucleus is not simply due to passive diffusion through the nuclear pores. The C-terminal mutant (RBD4/TBD/5-HA) is randomly distributed throughout the cell including the nucleus. However, when fused to the bacterial gene *LacZ* which codes a 90 kDa protein β-galactosidase, RBD4/TBD/5-LacZ is exclusively expressed in the cytoplasm, indicating that RBD4/TBD/5 is not a nuclear protein (our unpublished results). Therefore, the nucleus/nucleolar localization signal most probably exists in the RBD3 and the spacer region between RBD3 and RBD4, and the putative bipartite nuclear localization signal is located in the spacer region. In order to assess the relevance of the putative bipartite localization signal, we isolated the signal and fused it to GFP. The fusion protein is predominantly nuclear (Luo and DesGroseillers, unpublished). Therefore, the putative bipartite nuclear localization signal is probably functional. These results suggest that Staufen may transit through the nucleus and/or the nucleolus before localizing or anchoring in the cytoplasm.

The RNA-binding dependent nucleolar localization of the N-terminal mutant (RBD3/4-GFP) suggests that Staufen may bind to ribosomal RNAs, since the nucleolus is the site of ribosomal RNA synthesis and assembly. Staufen is also found in the cytoplasm in association with ribosomes (Article 3, and Marion et al., 1999). Therefore, Staufen may enter the nucleus to form immature RNP complexes along with ribosome RNAs and/or other cofactors, and later exit the nucleus to localize in the cytoplasm. These cofactors may include some polymerase III transcripts such as BC200, a subset of specific RNAs, and hnRNPs, which have all been observed in the nucleolus and are known to be involved in RNA transport and localization.

VI.5 The putative roles of different Staufen isoforms

The differential association of Stau^{55} and Stau^{63} with the ribosomes and the RER implies that these two isoforms play different roles in the cell. We expected that the different Stau isoform-containing complexes will play distinct roles in mRNA transport and/or translation, as previously demonstrated for *Drosophila* hnRNP1 Squid (Norvell et al., 1999). Based on its cofractionation with the ribosomes, it is likely that Stau^{55} (and possibly hStau^{63h}) may be involved in translation regulation. Genetic studies involving *oskar* mRNA and Staufen in *Drosophila* (Kim-Ha et al., 1995) have suggested that Staufen activates *oskar* mRNA translation since homozygous *stau* mutants failed to express an *oskar* transgene even if the bruno-mediated translational repression is missing. It will be interesting to determine whether dsRBD5 functionally cooperates with the

identified ribosome association domain (TBD) to regulate translation since *Drosophila* dsRBD5 was shown to be involved in the derepression of *oskar* mRNA translation once localized (Micklen et al., 2000). In contrast, the 63 kDa isoform may be more directly involved in mRNA transport and localization via its association with the RER. A link between ER and RNA transport has been described in other species (Deshler et al., 1997, Wilsch-Bräuninger et al., 1997). It has been proposed that both the *trans*-acting factors and their cognate mRNAs may associate with the ER and that vesiculated ER may be involved in RNA transport (Kiebler and DesGroseillers, 2000). In dendrites of rat neurons in culture, endogenous Staufen was found in proximity to microtubules and ER, suggesting that ER may be important for RNA transport (Kiebler et al., 1999). Similarly, we showed that the RER-associated RBD2/3/4-HA mutant is sufficient to mediate HIV-1 RNA selection and encapsidation (Mouland et al., 2000). It is thus possible that the N-terminal half of Staufen which has full dsRNA-binding capacity links the RNAs to the RER and mediates RNA transport. A point mutation (F135A) in dsRBD3 of hStau^{55} or a differential splicing event that endogenously inserts 6 amino acids within dsRBD3 (Duchaîne et al., 2000) both impaired Staufen RNA-binding activity. Interestingly, the mutant proteins form large granules that are still colocalized with the RER marker. Thus, disruption of Staufen RNA-binding activity could impede the movement the Staufen contained ribosome complexes in the RER, or in some putative subdomains of the RER, which accumulates as large RER-associated granules in the cytoplasm (see Fig. 3 in the Appendix for the double labelling of hStau/3*-HA_3 and calnexin). We propose that the RNA-binding activity of Staufen may be somehow related to ribosome/RER dynamics in the cytoplasm. Therefore, disruption of Staufen RNA-binding activity may affect

Staufen-mediated RNA transport. In *Drosophila*, the RNA-binding activity of dsRBD3 has been shown to be essential for *bicoid* and *oskar* mRNA localization (Ramos et al., 2000).

VI.6 Staufen as a conserved component linked to the RNA transport machinery

VI.6.1 The hypothesis of a conserved RNA transport machinery

Asymmetrically localized mRNAs and/or local protein synthesis have been demonstrated in a growing number of organisms. They possess diverse physiological roles such as axis formation during oogenesis (St Johnston, 1995; Mowry and Cote, 1999), differential cell determination (Li *et al.*, 1997; Broadus *et al.*, 1998; Long *et al.*, 1997), cell polarity and motility (Kislauskis *et al.*, 1997), and synaptic plasticity (Martin *et al.*, 1997; Kang and Schuman, 1996; Kiebler and DesGroseillers, 2000). Studies over the past decade have revealed that the process of intracellular RNA localization is complex and occurs through multiple successive steps, which require the recognition of overlapping *cis*-acting sequences by a series of *trans*-acting RNA-binding proteins (St Johnston, 1995). This complex process shares several conserved features in different organisms and cell types. One of the conserved features is the presence of the *cis*-acting RNA targeting signal(s), which is usually located in the 3'-untranslated region of the localized transcripts. Deletion of this signal usually abolishes the localization of the transcript. Another most common feature is the formation of large ribonucleoprotein complexes as the RNA transport substrates, which are made of one or more RNA-binding proteins or cofactors as well as their cognate RNAs. The third common feature comes

from the dependence of an intact cytoskeleton network (either microtubules or microfilaments) as the RNA-transport scaffold and anchoring matrix. Finally, for the entire localization process the translation of the localized RNAs appears to be tightly regulated. Specific signals have been characterized in several localized mRNAs that are important for their repression during the transport, and their derepression once they reach their final destinations in the cell. These common features suggest that conserved RNA localization machinery may exist to govern this complex process.

VI.6.2 hStau as a component of the RNA transport unit in neurons

In *Drosophila,* genetic studies have shown that the activity of the *staufen* gene product is required for the proper localization of two maternal mRNAs, *bicoid and oskar,* to the anterior and posterior ends of the oocyte, respectively, and for *prospero* mRNA to one of the two daughter cells, the GMC, during the asymmetric divisions of the embryonic neuroblasts. Thus, Staufen is involved in RNA localization in both germline and somatic cells. So far, it remains to be one of the best-characterized *trans*-acting RNA-binding proteins that are involved in intracellular mRNA localization.

The molecular characterization of the mammalian homologue of the *Drosophila* Staufen has potentially revealed a common component of the mRNA localization machinery in mammalian cells, particularly in neurons, to that of mRNA trafficking in insect oocytes and neuroblasts. Mammalian Staufen contains four copies of the dsRBD consensus motif which correspond to the dsRBD2 to dsRBD5 of *Drosophila* Staufen, despite that fact that the first dsRBD of dStau is not present in mammalian Staufen. Analysis of the mammalian Staufen dsRBDs indicates that these regions are functional

homologues. Similar to its *Drosophila* counterpart, mammalian Stau was shown to bind dsRNA without sequence specificity *in vitro*, and this RNA-binding activity is mainly attributed to its dsRBD3, which is also the major RNA-binding domain in *Drosophila* Stau. Mammalian Staufen contains a putative microtubule-associated protein (MAP1B)-binding domain that is lacking in the *Drosophila* protein. Our study shows that this domain is a multiple functional domain since it is also important for ribosome association (Article 3). In fibroblasts, mammalian Staufen is associated with polysomes and the RER (Marion et al., 1999; Wickham et al., 1999), whereas in neurons, it is mainly associated with both the RER and microtubules (Kiebler et al., 1999). The biochemical features of mammalian Staufen indicate that it is good candidate for RNA transport and local translation in mammals.

In developing hippocampal neurons, Staufen was found to expressed in all neurites of young neurons. However, in mature neurons, Staufen is expressed only in the somatodendritic domain (the cell body and dendrites) and is present in large RNA-containing particles in dendrites as determined from its colocalization with SYTO14-postive granules (Kiebler et al., 1999). These granules had been previously suggested to represent ribonucleoprotein particles containing poly(A)$^+$ RNA, translational factors such as the elongation factor 1α, and even ribosomal subunits (Knowles et al., 1996). The evidence that Staufen is expressed in neurons and colocalizes with mRNA granules provides a potential mechanism for transport of mRNAs to the dendrites. Since the transport of certain mRNAs from the soma to distal dendrites provides a means to establish local translation at the synapses, Staufen may be a protein component of the

machinery that is involved in the formation of synaptic plasticity and even synaptic memory in mammalian nervous systems.

In order to gain more direct insight into the role of Staufen in RNA transport, we expressed a reporter consisting of hStau tagged with GFP in living hippocampal neurons. The dynamics of the hStau-GFP fusion protein was visualized in real time by time-lapse fluorescence microscopy (Köhrmann et al., 1999, Article 4). The distribution of hStau-GFP was compared with that of SYTO14-labelled RNPs in living neurons. Staufen was found to accumulate in large and small granules in the soma and dendrites. In dendrites, the Stau-GFP granules move in a saltatory fashion from the cell body into the distal dendrites and vice versa. This movement is very similar to that seen in labeled RNPs and the average speed of the particles (6.4 μm/min) is in good agreement with previous measurements (4-6 μm/min) of RNA transport in various systems (Knowles et al., 1996; Muslimov et al., 1998; Wallace et al., 1998). Interestingly, as in the transport of RNPs, Staufen-GFP recruitment and translocation are dependent on the presence of intact microtubules; treatment with nocodazole leads to an increase in cytosolic Staufen and a decrease in the percentage of Staufen granules.

Based on these observations, mammalian Staufen appears to be a component of RNA transport units in neurons. In the developing neuron, Staufen might be responsible for the formation of large RNPs that transport specific mRNAs along microtubules to the elaborating dendrite. This mRNA transport might contribute to dendrite morphogenesis by providing mRNAs for local protein synthesis. In the fully differentiated neurons, Staufen would continue to function in transporting specific mRNAs to the synapse to produce synaptic microenvironments through local protein synthesis. Recently, a

neuronal specific homologue of Staufen (Stau2) has been found in our laboratory, the characterization of this neuronal homologue will boost further research toward a molecular understanding of how mRNA transport is achieved in the nervous system.

VI.6.3 hStau is implicated in retrovirus genomic RNA encapsidation

The involvement of hStau in the replication of human immunodeficiency virus type 1 (HIV-1) was also explored by our collaboration with Dr. Andrew Mouland in the laboratory of Dr. Cohen , University of Montreal (see Mouland et al., 2000, not included in this thesis). hStau was found to be selectively incorporated in HIV-1 and other retrovirus particles. Using a series of hStau expressers and suppressors, we demonstrated that hStau incorporation in HIV-1 is dependent on an intact functional dsRNA-binding domain and quantitatively correlates with the level of encapsidated HIV-1 genomic RNA.

Our study of hStau incorporation in HIV-1 and several other retroviruses likely reflects an important biological function for this host cell dsRNA-binding protein in HIV-1 replication. Based on several lines of evidence, hStau is selectively, but not passively incorporated into HIV-1 particles due to its dsRNA-binding activity. First, PKR and TRBP, two host cellular proteins that possess similar dsRNA-binding motifs and have similar subcellular distributions, are not detectable in HIV-1 preparations. Second, both TRBP and hStau bind to HIV-1 genomic RNA. However, only hStau is incorporated in the HIV-1 virions, suggesting that HIV-1 RNA binding does not necessarily lead to incorporation. Several other host cell RNA-binding proteins such as hnRNP A1 (Black et al., 1996), CRM1 (Bogerd et al., 1998), and poly(A)-binding protein (Afonina et al., 1997) are also capable of binding HIV-1 RNA, but there is no evidence that these host

RNA-binding proteins are incorporated in the virions, supporting the notion that HIV-1 RNA binding is not necessary for viral incorporation of the protein. However, since hStau is not incorporated in the empty Gag VLPs (with no genomic RNA) and virion-incorporated levels of hStau correlate with the genomic RNA content of the virus particle, it appears that hStau HIV-1 incorporation depends on the interaction of hStau with the viral RNAs. Indeed, molecular mapping of hStau viral incorporation determinants and point mutation analysis confirmed that hStau RNA-binding activity is important for its HIV-1 virion incorporation. hStau is found to associate with HIV-1 RNA in both cytosolic and purified viral lysates. Thus, it appears to be involved in pre- and post-assembly of HIV-1 genomic RNA.

Although the full picture of hStau's function in HIV-1 genomic RNA encapsidation is still missing, we demonstrate that hStau overexpression can enhance several-fold the abundance of genomic HIV-1 RNA in virions. Conversely, after treatment with hStau antisense constructs, hStau viral incorporation was able to be downregulated by 40 to 50% (Mouland and Cohen, unpublished). In both of these conditions, the infectivity of the resulting viruses is impaired, suggesting that an appropriate amount of incorporated hStau is required to generate infectious viral particles. Further work is needed to address how different levels of hStau incorporation affect the viral infectivity, and to elucidate hStau's mechanism of action in HIV-1 replication.

In summary, hStau is associated with both cell and virus-associated HIV-1 RNA and is selectively incorporated in HIV-1 virions in an RNA-binding dependent way. Together with the possible role of hStau in RNA transport in hippocampal neurons, this

finding raises the intriguing possibility that hStau is also involved in the transport of HIV-1 genomic RNA during the retroviral replication cycles.

General conclusions

General conclusions

Article 1

1. **Two mammalian *Staufen* genes, *hStau* and *mStau*, share conserved transcriptional initiation sites.**

2. **The *mStau* gene contains a 5'-flanking region resembling a typical housekeeping gene promoter, suggesting that mammalian *Stau* may be a housekeeping gene.**

3. **The *hStau* and *mStau* genes are fragmented into 15 and 12 exons, distributed over at least 65 and 17 kb of genomic DNA, respectively.**

4. **The human and mouse *stau* genes share very conserved exon/intron genomic organization, suggesting that these two genes are derived from a common ancestor.**

Article 2

1. **hStau and mStau proteins share high sequence identity to *Drosophila* Staufen in the corresponding dsRNA-binding domains.**

2. **In humans, four transcripts arise by differential splicing and code for two proteins with different N-terminal extremities.**

3. **In vitro, hStau and mStau bind dsRNA via each of the two full-length dsRNA-binding domains and bind to tubulin via a region similar to the**

microtubule-binding domain of MAP-1B, suggesting that Stau cross-links cytoskeletal and RNA components.

4. **hStau is associated with the detergent-insoluble fraction in vivo, and colocalizes with the RER marker, implicating it in the transport of RNA to the site of translation.**

Article 3

1. **Two endogenous Stau isoforms Stau^{63} and Stau^{55}, are differentially associated with the RER and ribosomes, suggesting that they are incorporated into different complexes in vivo.**

2. **The cloned human 63-kDa protein, which is specifically expressed in humans, is associated with ribosomes similar to Stau^{55} suggesting that a new uncharacterized 63 kDa protein is expressed in vivo and associated with the RER.**

3. **Two overlapping regions dsRBD2/3/4 and dsRBD4/TBD/5, are differentially associated with the RER and ribosomes respectively, and both regions are necessary for hStau^{55} ribosome association.**

4. **dsRBD4 and TBD together constitute a basal ribosome association domain, this ribosome association is independent of Staufen RNA-binding activity.**

5. **dsRBD4 alone is sufficient for RER association and it cooperates with dsRBD2 and 3 to promote full RER association.**

6. **TBD is crucial for hStau^{55} ribosome association since its deletion from hStau^{55} relocates the protein from ribosomes to the RER.**

7. **Taken together, our results suggest that dsRBD4/TBD-mediated ribosome association may depend on prior or simultaneously RER binding, and show that hStau^{55} may be a bridging molecule between the RER and ribosomes via its overlapping determinants.**

Article 4

1. **The hStau-GFP fusion protein is capable of forming RNA-containing granules when transiently expressed in living hippocampal neurons.**

2. **hStau-GFP granules migrate into the distal dendrites of living hippocampal neurons in a bidirectional and microtubule-dependent manner.**

3. **The average speed of hStau-GFP particles was measured to be 6.4 μm/min with a maximum velocity of 24.3 μm/min. This velocity is in good agreement with that observed for typical RNA transport in neurons and oligodendrocytes.**

4. **Mammalian Stau may serve as a component of the ribonucleoprotein complexes involving RNA transport in neurons.**

Perspectives

Perspectives

Localization of mRNAs in the cytoplasm is now considered to be an essential step in the regulation of gene expression and an efficient way to unevenly distribute proteins in polarized cells. The work presented in this thesis contributes to our understanding of Staufen's role(s) in mammals and of mRNA transport mechanisms. Future work is needed to address the following issues:

1. **Molecular cloning of the RER associated 63-kDa Staufen isoform and identification of its RER association determinant;**
2. **Identification of the protein partners that interact with the RER association domain dsRBD4 and the ribosome association determinant dsRBD4-TBD;**
3. **Evaluating the potential role of ribosome-associated Stau^{55} in translation regulation;**
4. **Identification of the molecular determinants that are involved in Stau granule formation and movement in neurons and the domain responsible for the microtubule dependence;**
5. **Finally, the identification of endogenous RNA(s) and protein(s) that are bound to Staufen and transported in the cells will be very important to further evaluate the precise role(s) of mammalian Staufen.**

Reference bibliography

1. Afonina E, Neumann M, Pavlakis GN. (1997). Preferential binding of poly(A)-binding protein 1 to an inhibitory RNA element in the human immunodeficiency virus type 1 gag mRNA. *J. Biol. Chem.* 272: 2307-2311.

2. Ainger K, Avossa D, Morgan F, Hill SJ, Barry C, Barbarese E, Carson JH. (1993). Transport and localization of exogenous myelin basic protein mRNA microinjected into oligodendrocytes. *J Cell Biol* 123:431-441

3. Ainger K, Avossa D, Dinana AS, Barry C, Barbarese E, Carson JH. (1997). Transport and localization elements in myelin basic protein mRNA. *J. Cell Biol.* 138:1077-1087.

4. Ait-Ahmed O, Thomas-Cavallin M, Rosset R. (1987). Isolation and characterization of a region of the Drosophila genome which contains a cluster of differentially expressed maternal genes (yema gene region). *Dev Biol.* 122(1):153-62.

5. Alberts B, Bray B, Lewis J, Raff M, Roberts K, Watson JD. (1994a). Intracellular compartments and protein sorting. *In* " Molecular Biology of the cell," Chap. 12, pp. 551-598. Garland, New York.

6. Alberts B, Bray B, Lewis J, Raff M, Roberts K, Watson JD. (1994b). Vesicular traffic in the secretory and endocytic pathways. *In* " Molecular Biology of the cell," Chap. 13, pp. 599-651. Garland, New York.

7. Baker NE. (1988). Embryonic and imaginal requirements for wingless, a segment-polarity gene in Drosophila. *Dev Biol.* 125(1):96-108.

8. Banerjee U, Renfranz PJ, Pollock JA, Benzer S. (1987). Molecular characterization and expression of sevenless, a gene involved in neuronal pattern formation in the Drosophila eye. *Cell* 49(2):281-91.

9. Barbarese E, Koppel DE, Deutscher MP, Smith CL, Ainger K, Morgan F, Carson JH. (1995). Protein translation components are colocalized in granules in oligodendrocytes. *J. Cell Sci.* 108: 2781-2790.

10. Bashirullah A, Cooperstock RL, Lipshitz HD. (1998). RNA localization in development. *Annu. Rev. Biochem.* 67:335-394.

11. Bassell GJ, Oleynikov Y., Singer RH. (1999). The travels of mRNAs through all cells large and small. *FASEB J.* 13: 447-454.

12. Bassell GJ, Singer RH. (1997). mRNA and cytoskeletal filaments. *Curr. Opin. Cell Biol.* 9:109-115.

13. Bassell GJ, Zhang H, Byrd AL, Femino AM, Singer RH, Taneja KL, Lifshitz LM, Herman IM, and Kosik KS. (1998). Sorting of β-actin mRNA and protein to neurites and growth cones in culture. *J. Neurosci.* 18, 251-265.

14. Beach DL, Salmon ED, Bloom K. (1999). Localization and anchoring of mRNA in budding yeast. *Curr Biol* 9: 569-578.

15. Berleth T, Burri M, Thoma G, Bopp D, Richstein S, Frigerio G, Noll M, Nusslein-Volhard C. (1988). The role of localization of bicoid RNA in organizing the anterior pattern of the Drosophila embryo. *EMBO J.* 7:1749-1756.

16. Bertrand E, Chartrand P, Schaefer M, Shenoy SM, Singer RH, Long RM. (1998). Localization of ASH1 mRNA particles in living yeast. *Mol. Cell* 2: 437-445.

17. Bevilacqua PC, George CX, Samuel CE, Cech TR. (1998). Binding of the protein kinase PKR to RNAs with secondary structure defects: role of tandem A-G mismatch and noncontiguous helices. *Biochemistry*, **37**, 6303-6316.

18. Black AC, Luo J, Chun S, Bakker A, Fraser JK, Rosenblatt JD. (1996). Specific binding of polypyrimidine tract binding protein and hnRNP A1 to HIV-1 CRS elements. *Virus Genes* 12: 275-285.

19. Blichenberg A, Schwanke B, Rehbein M, Garner CC, Richter D, Kindler S. (1999). Identification of a *cis*-Acting Dendritic Targeting Element in MAP2 mRNAs. *J. Neurosci.* 19: 8818-8829.

20. Bilger A, Fox CA, Wahle E, Wickens M. (1994). Nuclear polyadenylation factors recognize cytoplasmic polyadenylation elements. *Genes Dev* 8:1106-1116.

21. Bobola N, Jansen RP, Shin TH, Nasmyth K. (1996). Asymmetric accumulation of Ash1p in postanaphase nuclei depends on a myosin and restricts yeast mating-type switching to mother cells. *Cell* 84:699-709.

22. Bogerd HP, Echarri A, Ross TM, Cullen BR. (1998) Inhibition of human immunodeficiency virus Rev and human T-cell leukemia virus Rex function, but not Mason-Pfizer monkey virus constitutive transport element activity, by a mutant human nucleoporin targeted to Crm1. *J. Virol.* 72:8627-8635.

23. Bouget FY, Gerttula S, Shaw SL, Quatrano RS. (1996) Localization of actin mRNA during the establishment of cell polarity and early cell divisions in fucus embryos. *Plant cell* 8: 189-201.

24. Bouvet P, Omilli F, Arlot-Bonnemains Y, Legagneux V, Roghi C. (1994). The deadenylation conferred by the 3' untranslated region of a developmentally controlled mRNA in *Xenopus* embryos is switched to polyadenylation by deletion of short sequence element. *Mol. Cell Biol.* 14: 1893-1900.

25. Breitwieser W, Markussen FH, Horstmann H, Ephrussi A (1996) Oskar protein interaction with Vasa represents an essential step in polar granule assembly. *Genes Dev* 10:2179-2188.

26. Brizard F, Luo M, DesGroseillers L. (2000). Genomic organization of the human and mouse *staufen* genes. *DNA & Cell Biol. 19*, 331-339.

27. Broadus J, Doe CQ. (1997). Extrinsic cues, intrinsic cues and microfilaments regulate asymmetric localization in Drosophila neuroblasts. *Curr. Biol.* 7: 827-835.

28. Broadus J, Fuerstenberg S, Doe CQ. (1998). Staufen-dependent localization of prospero mRNA contributes to neuroblast daughter-cell fate. *Nature* 391: 792–795.

29. Brosius J, Tiedge H. (1995). Neural BC1 RNA: dendritic localization and transport. In Localized RNAs. H.D. Lipshitz, editor. R.G. Landes, Austin, TX. 289-300.

30. Burgin KE, Washam MN, Rickling S, Westgate SA, Mobley WC, Kelly PT (1990). In situ hybridization histochemistry of Ca^{++} /calmodulin-dependent protein kinase in developing rat brain. *J Neurosci.* 10: 1788-1798.

31. Burz DS, Rivera-Pomar R, Jäckle H, Hanes SD. (1998). Cooperative DNA-binding by Bicoid provides a mechanism for threshold-dependent gene activation in the *Drosophila* embryo. *EMBO J* 17(20): 5998-6009.

32. Bycroft M, Grünert S, Murzin AG, Proctor M, St Johnston D. (1995). NMR solution structure of a dsRNA binding domain from Drosophila Staufen protein reveals homology to the N terminal domain of ribosomal protein S5. *EMBO J.* 14: 3563-3571.

33. Carson JH, Worboys K, Ainger K, Barbarese E. (1997). Translocation of myelin basic protein mRNA in oligodendrocytes requires microtubules and kinesin. *Cell. Motil. Cytoskeleton* 38, 318-328.

34. Carson JH, Kwon S, Barbarese E. (1998). RNA trafficking in myelinating cells. *Curr. Opin. Neurobiol.* 8, 607-612.

35. Chartrand P, Meng XH, Singer RH, Long RM. (1999). Structural elements required for localization of *ASH1* mRNA and a GFP reporter particle in vivo. *Curr Biol* 9: 333-336.

36. Cheng H, Bjerknes M. (1989). Asymmetric distribution of actin mRNA and cytoskeletal pattern generation in polarized epithelial cells. *J Mol Biol.* 210(3):541-9.

37. Cheung HK, Serano TL, Cohen RS. (1992). Evidence for a highly selective RNA transport system and its role in establishing the dorsoventral axis of the *Drosophila* egg. *Development* 114(3):653-61.

38. Clark I, Giniger E, Ruohola-Baker H, Jan LY, Jan YN. (1994). Transient posterior localization of a kinesin fusion protein reflects anteroposterior polarity of the Drosophila oocyte. *Curr. Biol.* 4: 289-300.

39. Comery TA, Harris JB, Willems PJ, Oostra BA, Irwin SA, Weiler IJ, Greenough WT. (1997). Abnormal dendritic spines in fragile X knockout mice: maturation and pruning deficits. *Proc Natl Acad Sci USA* 94: 5401–5404.

40. Cosentino GP, Venkatesan S, Serluca FC, Green S, Mathews MB, Sonenberg N. (1995). Double-stranded-RNA-dependent protein kinase and TAR RNA-binding protein form homo- and heterodimers *in vivo*. *Proc. Natl. Acad. Sci. USA.* 92: 9445-9449.

41. Cote CA, Gautreau D, Denegre JM, Kress TL, Terry NA, Mowry KL. (1999). A *Xenopus* protein related to hnRNP I has a role in cytoplasmic RNA localization. *Mol. Cell.* 4:431-437.

42. Curtis D, Lehmann R, Zamore PD. (1995). Translational regulation in development. *Cell.* 81: 171-178.

43. Dahanukar A., Wharton R. P.(1996). The Nanos gradient in *Drosophila* embryos is generated by translational regulation. *Genes Dev* 10:2610-2620.

44. Davis I, Ish-Horowicz D. (1991). Apical localization of pair-rule transcripts requires 3' sequences and limits protein diffusion in the *Drosophila* blastoderm embryo. *Cell* 67(5):927-40.

45. Deshler JO, Highett MI, Schnapp BJ. (1997). Localization of Xenopus Vg1 mRNA by VERA protein and the endoplasmic reticulum. *Science* 276, 1128-1131.

46. Deshler JO, Highett MI, Abramson T, Schnapp BJ. (1998). A highly conserved RNA-binding protein for cytoplasmic mRNA localization in vertebrates. *Curr. Biol.* 8, 489-496.

47. Ding D, Lipshitz HD.(1993). A molecular screen for polar-localised maternal RNAs in the early embryo of *Drosophila. Zygote.* 1(3):257-71.

48. Ding D, Parkhurst SM, Halsell SR, Lipshitz HD. (1993). Dynamic Hsp83 RNA localization during Drosophila oogenesis and embryogenesis. *Mol Cell Biol.* 13(6):3773-81.

49. Ding D, Parkhurst SM, Lipshitz HD. (1993). Different genetic requirements for anterior RNA localization revealed by the distribution of Adducin-like transcripts during Drosophila oogenesis. *Proc Natl Acad Sci USA.* 90(6):2512-6.

50. Doe CQ, Chu-LaGraff Q, Wright DM, Scott MP. (1991). The prospero gene specifies cell fates in the *Drosophila* central nervous system. *Cell* 65: 451-465.

51. Dreyfuss G, Matunis MJ, Pinol-Roma S, Burd CG. (1993). hnRNP proteins and the biogenesis of mRNA. *Annu. Rev. Biochem.* 62: 289-321.

52. Driever W, Nüsslein-Volhard, C. (1988). The bicoid protein determines position in the Drosophila embryo in a concentration-dependent manner. *Cell* 54, 95-104.

53. Driever W, Nüsslein-Volhard C. (1989a) The bicoid protein is a postive regulator of hunchback transcription in the early *Drosophila* embryo. *Nature* 337: 138-143.

54. Driever W, Nüsslein-Volhard C. (1989b) Determination of spatial domains of zygotic gene expression in the *Drosophila* embryo by the affinity of binding sites for the bicoid morphogen. *Nature* 340: 363-367.

55. Dubnau J, Struhl G. (1996) RNA recognition and translational regulation by a homeodomain protein. *Nature* 379:694-699.

56. Duchaîne T, Wang H-J, Luo M, Steinberg SV, Nabi IR, DesGroseillers L. (2000). A novel murine Staufen isoform modulates the RNA content of the Staufen complexes. *Mol. Cell. Biol. 20*, 5592-5601.

57. Dugich-Djordjevic MM, Tocco G, Willoughby DA, Najm I, Pasinetti G, Thompson RF, Baudry M, Lapchak PA, Hefti F. (1992) BDNF mRNA expression in the developing rat brain following Kainic acid-induced seizure activity. *Neuron* 8:1127-1138.

58. Edgar BA, Odell GM, Schubiger G. (1987). Cytoarchitecture and the patterning of fushi tarazu expression in the Drosophila blastoderm. *Genes Dev.* 1(10):1226-37

59. Elinson RP, King ML, Forristall C. (1993). Isolated vegetal cortex from Xenopus oocytes selectively retains localized mRNAs. *Dev Biol.* 160(2):554-62.

60. Elisha Z, Havin L, Ringel I, Yisraeli JK. (1995). Vg1 RNA binding protein mediates the association of Vg1 RNA with microtubules in Xenopus oocytes. *EMBO J.* 14: 5109-5114.

61. Ephrussi A, Dickinson LK, Lehmann R. (1991). Oskar organizes the germ plasm and directs localization of the posterior determinant nanos. *Cell* 66, 37-50.

62. Ephrussi AL, Lehmann R. (1992). Induction of germ cell formation by oskar. *Nature* 358: 387-392.

63. Erdelyi M, Michon AM, Guichet A, Glotzer JB, Ephrussi A. (1995). Requirement for Drosophila cytoplasmic tropomyosin in oskar mRNA localization. *Nature* 377: 524-527.

64. Ferrandon D, Elphick L, Nusslein-Volhard C, St Johnston D. (1994). Staufen protein associates with the 3' UTR of bicoid mRNA to form particles that move in a microtubule-dependent manner. *Cell* 79: 1221–1232.

65. Ferrandon D, Koch I, Westhof E, Nusslein-Volhard C. (1997). RNA-RNA interaction is required for the formation of specific bicoid mRNA 3'UTR-staufen ribonucleoprotein particles. *EMBO J.* 16: 1751-1758.

66. Fox C, Sheets M, Wickens M. (1989). Poly(A) addition during maturation of the frog oocytes: distinct nuclear and cytoplasmic activities and regulation by the sequence UUUUUAU. *Genes Dev* 3:2152-2162.

67. Frigerio G, Burri M, Bopp D, Baumgartner S, Noll M. (1986). Structure of the segmentation gene *paired* and the Drosophila PRD gene set as part of gene network. *Cell* 47: 735-746.

68. Frise E, Knoblich JA, Younger-Shepherd S, Jan LY, Jan YN. (1996). The *Drosophila* Numb protein inhibits signaling of the Notch receptor during cell-cell interaction in sensory organ lineage. *Proc. Natl. Acad. Sci. USA* 93:11925-32.

69. Furuichi T, Simon-Chazottes D, Fujino I, Yamads N, Hasegawa M, Miyawaki A, Yoshikawa S, Guénet JL, Mikoshiba K. (1993). Widespread expression of inositol 1,45-trisphosphate receptor type 1 gene (Insp 3r 1) in the mouse central nervous system. *Receptors Channels* 1:11-24.

70. Gao FB. (1998). Messenger RNAs in dendrites: localization, stability, and implications for neuronal function. *Bioessays* 20: 70–78.

71. Garner CC, Tucker RP, Matus A. (1988). Selective localization of messenger RNA for cytoskeletal protein MAP2 in dendrites. *Nature* 336: 674-677.

72. Gautreau D, Cote CA, and Mowry KL. (1997). Two copies of a subelement from the Vg1 RNA localization sequence are sufficient to direct vegetal localization in Xenopus oocytes. *Development* 124: 5013-5020.

73. Gavis ER, Curtis D, Lehmann R. (1996). Identification of *cis*-acting sequences that control *nanos* RNA localization. *Dev. Biol.* 176:36-50.

74. Gavis ER, Lunsford L, Bergsten SE, Lehmann R. (1996). A conserved 90 nucleotide element mediates translational repression of *nanos* RNA. *Development* 122:2791-2800.

75. Gavis ER, and Lehmann R. (1992). Localization of nanos RNA controls embryonic polarity. *Cell* 71: 301-313.

76. Gavis ER, and Lehmann R. (1994). Translational regulation of nanos by RNA localization. *Nature* 369: 315-318.

77. Gergen JP, Butler BA.(1988). Isolation of the Drosophila segmentation gene runt and analysis of its expression during embryogenesis. *Genes Dev.* 2(9):1179-93.

78. Golumbeski GS, Bardsley A, Tax F, Boswell RE. (1991). tudor, a posterior-group gene of *Drosophila* melanogaster, encodes a novel protein and an mRNA localized during mid-oogenesis. *Genes Dev.* 5(11):2060-70.

79. Gonzalez I, Buonomo SBC, Nasmyth K, von Ahsen U. (1999) *ASH1* mRNA localization in yeast involves multiple secondary structural elements and Ash1 protein translation. *Curr Biol* 9:337-340.

80. González-Reyes A, Elliott H, St. Johnston D. (1995). Polarization of both major body axes in *Drosophila* by gurken-torpedo signalling. *Nature* (London) 375:654-658.

81. Gunkel N, Yano T, Markussen FH, Olsen LC, Ephrussi A. (1998). Localization-dependent translation requires a functional interaction between the 5' and 3' ends of oskar mRNA. *Genes Dev.* 12:1652-1664.

82. Guo M, Jan LY, Jan YN. (1996). Control of daughter cell fates during asymmetric division: interaction of Numb and Notch. *Neuron* 17:27-41.

83. Guzowski JF, Lyford GL, Stevenson GD, Houston FP, McGaugh JL, Worley PF, Barnes CA. (2000). Inhibition of Activity-Dependent Arc Protein Expression in the Rat Hippocampus Impairs the Maintenance of Long-Term Potentiation and the Consolidation of Long-Term Memory. *J. Neurosci.* 20: 3993-4001.

84. Hake LE, Richter JD. (1994). CPEB is a specificity factor that mediates cytoplasmic polyadenylation during *Xenopus* oocyte maturation. *Cell* 79: 617-628.

85. Han JR, Yiu GK, Hecht NB. (1995). Testis/Brain RNA-binding protein attaches translationally repressed and transported mRNAs to microtubules. *Proc. Natl. Acad. Sci. USA*. 92:9550-9554.

86. Hannan AJ, Schevzov G, Gunning P, Jeffrey PL, Weinberger RP.(1995). Intracellular localization of tropomyosin mRNA and protein is associated with development of neuronal polarity. *Mol Cell Neurosci.* 6(5):397-412.

87. Havin L, Git A, Elisha Z, Oberman F, Yaniv K, Schwartz SP, Standart N, and Yisraeli JK. (1998). RNA-binding protein conserved in both microtubule- and microfilament-based RNA localization. *Genes Dev.* 12:1593-1598.

88. Hazelrigg T. (1998). The destinies and destinations of RNAs (meeting review). *Cell* 95: 451-460.

89. Hendry SHC, Kennedy MB. (1986). Immunoreactivity for a calmodulin-dependent protein kinase is selectively increased in macaque striate cortex after monocular deprivation. *Proc Natl Acad Sci USA* 83:1536-1540.

90. Hill MA, Gunning P. (1993). β and γ actin mRNAs are differentially located within myoblasts. *J Cell Biol* 122:825-832.

91. Hinkley CS, Martin JF, Leibham D, Perry M. (1992). Sequential expression of multiple POU proteins during amphibian early development. *Mol Cell Biol.* 12(2):638-49.

92. Hirata J, Nakagoshi H, Nabeshima Y, and Matsuzaki F. (1995). Asymmetric segregation of the homeodomain protein Prospero during *Drosophila* development. *Nature* 377: 627-630.

93. Hoek K, Kidd GJ, Carson JH, Smith R. (1998). hnRNP A2 selectively binds the cytoplasmic transport sequence of myelin basic protein mRNA. *Biochemistry* 37, 7021-7029.

94. Houston DW, Zhang J, Maines JZ, Wasserman SA, King ML. (1998). A *Xenopus* DAZ-like gene encodes an RNA component of germ plasm and is a functional homologue of Drosophila *boule. Development* 125:171-180.

95. Hudson C, Woodland HR. (1998). Xpat, a gene expressed specifically in germ plasm and primordial germ cells of Xenopus laevis. *Mech Dev* 73:159-168.

96. Hudson JW, Alarcon VB, Elinson RP. (1996). Identification of new localized RNAs in the Xenopus oocyte by differential display PCR. *Dev Genet* 19:190-198.

97. Hyatt BA, Yost J. (1998). The left-right coordinator: the role of *Vg1* in organizing left-right axis formation. *Cell* 93:37-46.

98. Ikeshima-Kataoka H, Skeath JB, Nabeshima Y, Doe CQ, Matsuzaki F. (1997). Miranda directs Prospero to a daughter cell during Drosophila asymmetric divisions. *Nature* 390: 625-629.

99. Irish V, Lehmann R, Akam M. (1989) The *Drosophila* posterior group gene *nanos* functions by repressing *hunchback* activity. Nature 338:646-648.

100. Jacobs C, Shapiro L. (1998). Microbial asymmetric cell division: localization of cell fate determinants. *Curr. Opin. Genet. Dev.* 8:386-391.

101. Jackson RJ. (1993). Cytoplasmic regulation of mRNA function: The importance of the 3' untranslated region. *Cell* 74:9-14.

102. Jan Y-N, Jan LY. (2000). Polarity in cell division: what frames thy fearful asymmetry? *Cell* 100: 599-602.

103. Jansen RP. (1999). RNA-cytoskeletal associations. *FASEB J.* 13: 455-466.

104. Jansen RP, Dowzer C, Michaelis C, Galova M, Nasmyth K. (1996). Mother cell-specific *HO* expression in budding yeast depends on the unconventional myosin Myo4p and other cytoplasmic proteins. *Cell* 84: 687-697.

105. Jeffery WB, Tomlinson CR, Brodeur RD. (1983). Localization of actin messenger RNA during early ascidian development. *Dev. Biol.* 99: 408-417.

106. Jirikowski GF, Sanna PP, Bloom FE. (1990). mRNA coding for oxytocin is present in axons of the hypothalamo-neurohypophysial tract. *Proc Natl Acad Sci U S A.* 87(19):7400-4.

107. Jongens TA, Ackerman LD, Swedlow JR, Jan LY, Jan YN. (1994). Germ cell-less encodes a cell type-specific nuclear pore-associated protein and functions early in the germ-cell specification pathway of *Drosophila*. *Genes Dev.* 8(18):2123-36.

108. Jongens TA, Hay B, Jan LY, Jan YN. (1992). The germ cell-less gene product: a posteriorly localized component necessary for germ cell development in Drosophila. *Cell* 70(4):569-84.

109. Joseph E, Melton D. (1998) Mutant *Vg1* ligands disrupt endoderm and mesoderm formation in *Xenopus* embryos. *Development* 125:2677-2685.

110. Kang H, Schuman EM. (1996). A requirement for local protein synthesis in neurotrophin-induced hippocampal synaptic plasticity. *Science* 273: 1402–1406.

111. Kelley RL. (1993). Initial organization of the *Drosophila* dorsoventral axis depends on an RNA-binding protein encoded by the squid gene. *Genes Dev.* 7:948-960.

112. Kessler DS, Melton DA. (1995). Induction of dorsal mesoderm by soluble, mature Vg1 protein. *Development* 121:2155-2164.

113. Kharrat A, Macias MJ, Gibson TJ, Nilges M, Pastore A. (1995). Structure of the dsRNA binding domain of *E.coli* RNase III. *EMBO J.* 14: 3572-3584.

114. Kiebler MA, Hemraj I, Verkade P, Kohrmann M, Fortes P, Marion RM, Ortin J, Dotti CG. (1999). The mammalian staufen protein localizes to the somatodendritic

domain of cultured hippocampal neurons: implications for its involvement in mRNA transport. *J Neurosci* 19: 288–297

115. Kiebler MA, DesGroseillers L. (2000). Molecular insights into mRNA transport and local translation in the mammalian nervous system. *Neuron 25*, 19-28.

116. Kim-Ha J, Smith JL, Macdonald PM. (1991). *oskar* mRNA is localized to the posterior pole of the *Drosophila* oocyte. *Cell* 66: 23-25.

117. Kim-Ha J, Webster PJ, Smith JL, Macdonald PM. (1993). Multiple RNA regulatory elements mediate distinct steps in localization of oskar mRNA. *Development* 119: 169-178.

118. Kim-Ha J, Kerr K, Macdonald PM. (1995). Translational regulation of oskar mRNA by bruno, an ovarian RNA-binding protein, is essential. *Cell.* 81: 403-412.

119. King ML. (1995). mRNA localization during frog oogenesis. In: Lipshitz HD, editor. Localized RNAs. Austin, Texas:R.G. Landes company; pp 137-148.

120. King ML, Zhou Y, Bubunenko M. (1999). Polarizing genetic information in the egg: RNA localization in the frog oocyte. *BioEssays* 21:546-557.

121. Kislauskis EH, Li Z, Taneja KL, Singer RH. (1993). Isoform-specific 3-untranslated sequences sort α-cardiac and β-cytoplasmic actin messenger RNAs to different cytoplasmic compartments. *J Cell Biol* 123:165-172.

122. Kislauskis EH, Singer RH. (1992). Determinants of mRNA localization. *Curr. Opin. Cell Biol.* 4:975-978.

123. Kislauskis EH, Zhu X, Singer RH. (1994). Sequences responsible for intracellular localization of β-actin messenger RNA also affect cell phenotype. *J Cell Biol* 127:441-451.

124. Kislauskis EH, Zhu X, Singer RH. (1997). β-actin messenger RNA localization and protein synthesis augment cell motility. *J Cell Biol.* 136: 1263-1270.

125. Kleiman R, Banker G, Steward O. (1993). Inhibition of protein synthesis alters the subcellular distribution of mRNA in neurons but does not prevent dendritic transport of RNA. *Proc Natl Acad Sci USA* 90:11192-11196.

126. Kleiman R, Banker G, Steward O. (1993). Subcellular distribution of rRNA and poly (A) RNA in hippocampal neurons in culture. *Mol Brain Res* 20:305-312.

127. Kleiman R, Banker G, Steward O. (1994). Development of subcellular mRNA compartmentation in hippocampal neurons in culture. *J Neurosci* 14:1130-1140.

128. Kloc M, and Etkin LD. (1995). Two distinct pathways for the localization of RNAs at the vegetal cortex in Xenopus oocytes. *Development* 121: 287-297.

129. Kloc M, Etkin LD. (1994). Delocalization of *Vg1* mRNA from the vegetal cortex in *Xenopus* oocytes after destruction of *Xlsirt* RNA. Science 265:1101-1103.

130. Kloc M, Larabell C, Etkin LD. (1996). Elaboration of the messenger transport organizer pathway for localization of RNA to the vegetal cortex of *Xenopus* oocytes. *Dev. Biol* 180:119-130.

131. Kloc M, Larabell C, Etkin LD. (1998). Contribution of METRO pathway localized moleculars to the organization of the germ cell lineage. *Mech Dev* 75:81-93.

132. Kloc M, Miller M, Carrasco AE, Eastman E, Etkin L. (1989). The maternal store of the xlgv7 mRNA in full-grown oocytes is not required for normal development in Xenopus. *Development* 107(4):899-907.

133. Kloc M, Reddy BA, Miller M, Eastman E, Etkin LD. (1991). x121: a localized maternal transcript in Xenopus laevis. *Mol Reprod Dev.* 28(4):341-5.

134. Kloc M, Spohr G, Etkin LD.(1993). Translocation of repetitive RNA sequences with the germ plasm in Xenopus oocytes. *Science* 262:1712-4.

135. Knoblich JA, Jan LY, Jan YN. (1995). Asymmetric segregation of Numb and Prospero during cell division. *Nature* 377: 624-630.

136. Knowles RB, Sabry JH, Martone ME, Deerinck DJ, Ellisman MH, Bassell GJ, Kosik KS. (1996). Translocation of RNA granules in living neurons. *J Neurosci* 16:7812-7820.

137. Knowles RB, Kosik KS. (1997). Neurotrophin-3 signals redistribute RNA in neurons. *Proc. Natl. Acad. Sci. USA* 94:14804-14808.

138. Kobayashi S, Amikura R, Okada M. (1993). Presence of mitochondrial large ribosomal RNA outside mitochondria in germ plasm of Drosophila melanogaster. *Science* 260:1521-4.

139. Köhrmann M, Luo M, Kaether C, DesGroseillers L, Dotti CG, Kiebler MA. (1999). Microtubule-dependent Recruitment of Staufen-Green Fluorescent Protein into Large RNA-containing Granules and Subsequent Dendritic Transport in Living Hippocampal Neurons. *Mol. Biol. Cell* 10: 2945-2953.

140. Kraut R, Campos-Ortega JA. (1996). inscuteable, a neural precursor gene of *Drosophila*, encodes a candidate for a cytoskeletal adapter protein. *Dev. Biol.* 174: 65-81.

141. Kraut R, Chia W, Jan LY, Jan YN, Knoblich JA. (1996). Role of inscuteable in orienting asymmetric cell divisions in *Drosophila*. *Nature* 383: 50-55.

142. Ku M, Melton DA. (1993). *Xwnt-11*: A maternally expressed wnt gene. *Development* 119:1161-1173.

143. Kuchinke U, Grawe F, Knust E. (1998). Control of spindle orientation in Drosophila by the Par-3-related PDZ-domain protein Bazooka. *Curr. Biol.* 8:1357-1365.

144. Kuhen KL, Shen X, Carlisle ER, Richardson AL, Weier HUG, Tanaka H, Samuel CE. (1996). Structural organization of the human gene (PKR) encoding an interferon-inducible RNA-dependent protein kinase (PKR) and differences from its mouse homology. *Genomics* 36: 197-201.

145. Kuhl D, Skehel P. (1998). Dendritic localization of mRNAs. *Curr. Opin. Neurobiol.* 8, 600-606.

146. Kwon S, Barbarese E, Carson JH. (1999). The *cis*-acting RNA trafficking signal from myelin basic protein mRNA and its cognate trans-acting ligand hnRNP A2 enhance cap-dependent translation. *J Cell Biol.* 147(2): 247-256.

147. Kwon YK, Hecht NB. (1991). Cytoplasmic protein binding to highly conserved sequences in the 3' untranslated region of mouse protamine 2 mRNA, a translationally regulated transcripts of male germ cells. *Proc. Natl Acad Sci USA.* 88:3584-3588.

148. Kwon YK, Hecht NB. (1993). Binding of a phosphoprotein to the 3'untranslated region of the mouse protamine 2 mRNA temporally represses its translation. *Mol Cell Biol.* 13:6547-6557.

149. Laitala-Leinonen T, Howell ML, Dean GE, Vaananen HK. (1996). Resorption-cycle-dependent polarization of mRNAs for different subunits of V-ATPase in bone-resorbing osteoclasts. *Mol Biol Cell.* 7(1):129-42.

150. Lall S, Francis-Lang H, Flament A, Norvell A, Schupbach T, Ish-Horowicz D. (1999). Squid hnRNP protein promotes apical cytoplasmic transport and localization of *Drosophila* pair-rule transcripts. *Cell* 98: 171-180.

151. Lane M., Kalderon D. (1994). RNA localization along the anteroposterior axis of the *Drosophila* oocyte requires PKA-mediated signal transduction to direct normal microtubule organization. *Genes Dev* 8:2986-2995.

152. Lantz V, Ambrosio L, Schedl P. (1994) The *Drosophila orb* RNA-binding protein is required for the formation of egg chamber and establisment of polarity. *Genes Dev.* 8: 598-613.

153. Lantz V, Ambrosio L, Schedl P. (1992). The *Drosophila orb* gene is predicted to encode sex-specific germline RNA-binding proteins and has localized transcripts in ovaries and early embryos. *Development* 115:75-88.

154. Lasko P. (1999). RNA sorting in *Drosophila* oocytes and embryos. *FASEB J.* 13:421-433.

155. Latham V, Kislauskis E, Singer R, Ross A. (1994). β-actin mRNA localization is regulated by signal transduction mechanisms. *J Cell Biol* 126: 1211-1219.

156. Lawrence JB, Singer RH (1986) Intracellular localization of messenger RNAs for cytoskeletal proteins. *Cell* 45: 407-415.

157. Lehmann AK, Bass BL. (1999). The importance of internal loop within RNA substrates of ADAR1. *J. Mol. Biol.* 291: 1-13.

158. Li M-G, McGrail M, Serr M, Hays TS. (1994). *Drosophila* cytoplasmic dynein, a microtubule motor that is asymmetrically localized in the oocyte. *J. Cell. Biol.* 126:1475-1494.

159. Li P, Yang X, Wasser M, Cai Y, Chia W. (1997). Inscuteable and staufen mediate asymmetric localization and segregation of prospero RNA during Drosophila neuroblast cell division. *Cell* 90:437-447.

160. Liang L, Diehl-Jones W, Lasko PF. (1994). Localization of vasa protein to the *Drosophila* pole plasm is independent of its RNA-binding and helicase activities. *Development* 120:1201-1211.

161. Lieberfarb ME, Chu T, Wreden C, Theurkauf W, Gergen JP, Strickland S. (1996). Mutations that perturb poly(A)-dependent maternal mRNA activation block the initiation of development. *Development* 122:579-588.

162. Link W, Konietzko U, Kauselmann G, Krug M, Schwanke B, Freu U, Kuhl D (1995) Somatodendritic expression of an immediate early gene is regulated by synaptic activity. *Proc Natl Acad Sci USA* 92:5734-5738.

163. Linnen JM, Bailey CP, Weeks DL.(1993). Two related localized mRNAs from Xenopus laevis encode ubiquitin-like fusion proteins. *Gene* 128(2):181-8.

164. Litman P, Behar L, Elisha Z, Yisraeli JK, Ginzburg I. (1996). Exogenous Tau RNA is localized in oocytes: possible evidence for evolutionary conservation of localization mechanisms. *Dev. Biol.* 176:86-94.

165. Litman P, Barg J, Rindzoonski L, Ginzburg I. (1993). Subcellular localization of tau mRNA in differentiating neuronal cell culture: implications for neuronal polarity. *Neuron* 10(4):627-38.

166. Long RM, Singer RH, Meng X, Gonzalez I, Nasmyth K, Jansen RP. (1997). Mating type switching in yeast controlled by asymmetric localization of ASH1 mRNA. *Science* 277: 383-387.

167. Lu B, Jan L, Jan Y-N. (2000). Control of cell divisions in the nervous systems: symmetry and asymmetry. *Annu. Rev. Neurosci.* 23: 531-556.

168. Lu B, Rothenberg M, Jan LY, Jan YN. (1998). Partner of Numb colocalizes with Numb during mitosis and directs Numb asymmetric localization in Drosophila neural and muscle progenitors. *Cell* 95: 225-35.

169. Lyford G, Yamagata K, Kaufmann W, Barnes C, Sanders L, Copeland N, Gilbert D, Jenkins N, Lanahan A, Worley P. (1995). Arc, a growth factor and activity-regulated gene, encodes a novel cytoskeleton-associated protein that is enriched in neuronal dendrites. *Neuron* 14:433-445.

170. Ma X, Yuan D, Diepold K, Scarborough T, Ma J. (1996). The Drosophila morphogenetic protein Bicoid binds DNA cooperatively. *Development* 122: 1195-1206.

171. Macdonald PM. (1990). bicoid mRNA localization signal: Phylogenetic conservation of function and RNA secondary structure *Development* 110:161-171.

172. Macdonald PM. (1992). The Drosophila pumilio gene: an unusually long transcription unit and an unusual protein. *Development* 114(1):221-32.

173. Macdonald PM, Ingham P, Struhl G. (1986). Isolation, structure, and expression of even-skipped: a second pair-rule gene of Drosophila containing a homeo box. *Cell* 47(5):721-34.

174. Macdonald PM, Leask A, Kerr K. (1995). exl protein specifically binds BLE1, a bicoid mRNA localization element, and is required for one phase of its activity. *Proc. Natl. Acad. Sci. USA.* 92:10787-10791.

175. Macdonald PM, Kerr K. (1997). Redundant RNA recognition events in bicoid mRNA localization. *RNA.* 3:1413-1420.

176. Macdonald PM, Kerr K. (1998). Mutational analysis of an RNA recognition element that mediates localization of *bicoid* mRNA. *Mol. Cell. Biol.* 18:3788-3795.

177. Macdonald PM, Kerr K, Smith L, Leask A. (1993). RNA regulatory element BLE1 directs the early steps of bicoid mRNA localization. *Development* 118: 1233-1243.

178. Macdonald PM, Smibert CA. (1996). Translational regulation of maternal mRNAs. *Curr. Opin. Genet. Dev.* 6:403-407.

179. Macdonald PM, Struhl G. (1988). *Cis*-acting sequences responsible for anterior localization of *bicoid* mRNA in *Drosophila* embryos. *Nature* 336:595-598.

180. Mach JM, Lehmann R. (1997). An Egalitarian-BicaudalD complex is essential for oocyte specification and axis determination in *Drosophila*. *Genes Dev* 11:423-435.

181. Mahone M, Saffman EE, Lasko PF. (1995). Localized Bicaudal-C RNA encodes a protein containing a KH domain, the RNA binding motif of FMR1. *EMBO J.* 14(9):2043-55.

182. Marión RM, Fortes P, Beloso A, Dotti CG, Ortín J. (1999). A human sequence homologue of staufen is an RNA-binding protein that is associated with polysomes and localizes to the rough ER. Mol. Cell. Biol. 19, 2212-2219.

183. Markussen FH, Michon AM, Breitwieser W, Ephrussi A. (1995). Translational control of *oskar* generates short Osk, the isoform that induces pole plasm assembly. *Development*, **121**, 3723-3732.

184. Marsden K, Doll T, Ferralli J, Botteri F, Matus A. (1996). Transgenic expression of embryonic MAP2 in adult mouse brain: implications for neuronal polarization. *J Neurosci* 16:3265-3273.

185. Martin KC, Casadio A, Zhu HEY, Rose JC, Chen M, Bailey CH, Kandel ER. (1997). Synapse-specific, long-term facilitation of Aplysia sensory to motor synapses: a function for local protein synthesis in memory storage. *Cell* 91: 927–938.

186. Martone ME, Pollock JA, Jones YZ, Ellisman MH. (1996). Ultrastructural localization of dendritic messenger RNA in adult rat hippocampus. *J Neurosci* 16:7437-7446.

187. Matsuzaki F, Koisumi K, Hama C, Yoshioka T, Nabeshima T. (1992). Cloning of the Drosophila prospero gene and its expression in ganglion mother cells. *Biochem. Biophys. Res. Comm.* 182: 1326-1332.

188. Matsuzaki F, Ohshiro T, Ikeshima-Kataoka H, Izumi H. (1998) *miranda* localizes *staufen* and *prospero* asymmetrically in mitotic neuroblasts and epithelial cells in early *Drosophila* embryogenesis. *Development*, 125, 4089-4098.

189. Mayford M, Baranes D, Podsypanina K, Kandel E. (1996). The 3-untranslated region of CaMKII is a cis-acting signal for the localization and translation of mRNA in dendrites. *Proc Natl Acad Sci USA* 93:13250-13255.

190. McGrew LL, Dworkin-Rastl E, Dworkin MB, Richter JD. (1989). Poly(A) elongation during *Xenopus* oocyte maturation is required for translational recruitment and is mediated by a short sequence element. *Genes Dev* 3:803-815.

191. Melton DA. (1987). Translocation of a localized maternal mRNA to the vegetal pole of Xenopus oocytes. *Nature* 328:80-82.

192. Micklem DR. (1995). mRNA localization during development. *Dev. Biol.* 172:377-395.

193. Micklem DR, Adams J, Grünert S, St Johnston D. (2000). Distinct roles of two conserved Staufen domains in *oskar* mRNA localization and translation. *EMBO J.* 19:1366-1377.

194. Miyashiro K, Dichter M, Everwine J. (1994) on the nature and differential distributin of mRNA in hippocampal neurites: implications for neuronal funcioning. *Proc Natl Acad Sci USA* 91:10800-10804.

195. Mlodzik M, Gehring WJ. (1985) Expression of the *caudal* gene in the germ line of *Drosophila*: formation of an RNA and protein gradient during early embryogenesis. *Cell* 48:465-478.

196. Mohr E, Fehr S, Richter D. (1991). Axonal transport of neuropeptide encoding mRNAs within the hypothalamo-hypophyseal tract of rats. *EMBO J.* 10(9):2419-24.

197. Mohr E, Morris JF, Richter D. (1995). Differential subcellular mRNA targeting: deletion of a single nucleotide prevents the transport to axons but not to dendrites of rat hypothalamic magnocellular neurons. *Proc Natl Acad Sci USA* 92:4377-4381.

198. Morales CR, Wu XQ, Hecht NB. (1998). The DNA/RNA-binding protein, TB-RBP, moves from the nucleus to the cytoplasm and through intercellular bridges in male germ cells. *Dev. Biol* 201:113-123.

199. Morris EJ, Fulton AB. (1994). Rearrangement of mRNA for costamere proteins during costamere development in cultured skeletal muscle from chicken. *J cell Sci* 107: 377-386.

200. Mosquera L, Forristall C, Zhou Y, King ML. (1993). A mRNA localized to the vegetal cortex of Xenopus oocytes encodes a protein with nanos-like zinc finger domain. *Development* 117: 377-386.

201. Mouland AJ, Mercier J, Luo M, Bernier L, DesGroseillers L, Cohen EA. (2000). Staufen is incorporated in Human Immunodeficiency Virus 1 (HIV-1) and enhances genomic RNA encapsidation. *Journal of Virology 74*: 5441-5451.

202. Mowry KL, Melton DA. (1992). Vegetal messenger RNA localization directed by a 340-nt RNA sequence element in Xenopus oocytes. *Science* 255:991-994.

203. Mowry KL. (1996). Complex formation between stage-specific oocyte factors and a Xenopus mRNA localization element. *Proc. Natl. Acad. Sci. USA* 93: 14608-14613.

204. Mowry KL, Cote CA. (1999). RNA sorting in *Xenopus* oocytes and embryos. *FASEB J.* 13: 435-445.

205. Mueller-Pillasch F, Lacher U, Wallrapp C, Micha A, Zimmerhackl F, Hameister H, Varga G, Friess H, Buchler M, Beger HG, Vila MR, Adler G, and Gress TM. (1997). Cloning of a gene highly overexpressed in cancer coding for a novel KH-domain containing protein. *Oncogene* 14: 2729-2733.

206. Muller H-AJ, Wieschaus E. (1996). *Armadillo*, *bazooka* and *stardust* are critical for early stages in formation of the polarized blastoderm epithelium in *Drosophila*. *J. Cell Biol.* 134:149-63.

207. Münchow S, Sauter C, Jansen RP. (1999). Association of the class V myosin Myo4p with a localized messenger RNA in budding yeast depends on She proteins. *J Cell Sci* 112: 1511-1518.

208. Muramatsu T, Ohmae A, and Anzai K. (1998). BC1 RNA protein particles in mouse brain contain two y-, h-element-binding proteins, translin and a 37 kDa protein. *Biochem. Biophys. Res. Commun.* 247:7-11.

209. Murata Y, Wharton RP. (1995). Binding of pumilio to maternal *hunchback* mRNA is required for posterior patterning in *Drosophila* embryos. *Cell* 80:747-756.

210. Muslimov IA, Santi E, Homel P, Perini S, Higgins D, Tiedge H (1997). RNA transport in dendrites: a cis-acting targeting element is contained within neuronal BC1 RNA. *J Neurosci* 17:4722-4733.

211. Muslimov IA, Banker G, Brosius J, Tiedge H. (1998). Activity-dependent Regulation of Dendritic BC1 RNA in Hippocampal Neurons in Culture. *J. Cell Biol.* 141: 1601-1611.

212. Nakamura A, Amikura R, Mukai M, Kobayashi S, Lasko PF. (1996). Requirement for a noncoding RNA in *Drosophila* polar granules for germ cell establishment. *Science* 274:2075-9.

213. Nanduri S, Carpick BW, Yang Y, Williams BRG, Qin J. (1998). Structure of the double stranded RNA-binding domain of the protein kinase PKR reveals the molecular basis of its dsRNA-mediated activation. *EMBO J.* 17: 5458-5465.

214. Neuman-Silberberg FS, Schüpbach T. (1993). The *Drosophila* dorsoventral patterning gene *gurken* produces a dorsally localized RNA and encodes a TGF-alpha-like protein. *Cell* 75:165-174.

215. Neuman-Silberberg FS, Schüpbach T. (1994). Dorsoventral axis formation in Drosophila depends on the correct dosage of the gene *gurken*. *Development* 120: 2457-2463.

216. Newmark PA, Boswell RE. (1994). The *mago nashi* locus encodes an essential product required for germ plasm assembly in *Drosophila*. *Development* 120: 1303-1313.

217. Nicholson AW. (1996). Structure, reactivity and biology of double-stranded RNA. *Prog. Nucleic Acids Res. Mol. Biol.* 52: 1-65.

218. Norvell A, Kelley RL, Wehr K, Schüpbach T. (1999). Specific isoforms of Squid, a *Drosophila* hnRNP, perform distinct roles in Gurken localization during oogenesis. *Genes & Dev.* 13: 864-876.

219. Oleynikov Y, Singer RH. (1998). RNA localization: different zipcodes, same postman? *Trends Cell Biol.* 8:381-383.

220. Ostarreck-Lederer A, Ostareck DH, Standart N, Thiele BJ. (1994) Translation of 15-lipoxygenase messenger RNA is inhibited by a protein that binds to a repeated sequence in the 3' untranslated region. *EMBO J* 13: 1476-1481.

221. Otte AP, McGrew LL, Olate J, Nathanson NM, Moon RT.(1992). Expression and potential functions of G-protein alpha subunits in embryos of Xenopus laevis. *Development* 116(1):141-6.

222. Otte AP, Moon RT.(1992). Protein kinase C isozymes have distinct roles in neural induction and competence in Xenopus. *Cell* 68(6):1021-9.

223. Ouyang Y, Kantor D, Harris KM, Schuman EM, Kennedy MB. (1997) Visualization of the distribution of autophosphorylated calcium/calmodulin-dependent protein kinase II after tetanic stimulation in the CA1 area of the hippocampus. *J Neurosci* 17: 5416–5427.

224. Ouyang Y, Rosenstein A, Kreiman G, Schuman EM, Kennedy MB. (1999). Tetanic stimulation leads to increased accumulation of Ca(2+)/calmodulin-dependent protein kinase II via dendritic protein synthesis in hippocampal neurons. *J Neurosci* 19: 7823–7833.

225. Pachter JS. (1992). Association of mRNA with the cytoskeletal framework: its role in the regulation of gene expression. *Crit. Rev. Euk. Gene Exp. 2*: 1-18.

226. Perry BA, Capco DG. (1988). Spatial reorganization of actin, tubulin and histone mRNAs during meiotic maturation and fertilization in Xenopus oocytes. *Cell Differ Dev.* 25(2):99-108.

227. Pokrywka NJ, Stephenson EC. (1991). Microtubules mediate the localization of bicoid RNA during *Drosophila* oogenesis. *Development* 113: 55-66.

228. Pokrywka NJ, Stephenson EC. (1995). Microtubules are a general component of mRNA localization systems in *Drosophila* oocytes. *Dev. Biol.* 167:363-370.

229. Pollard VW, Michael WM, Nakielny S, Siomi MC, Wang F, Dreyfuss G. (1996). A novel receptor-mediated nuclear import pathway. *Cell* 86: 985-994.

230. Pomeroy ME, Lawrence JB, Singer RH, Billings-Gagliardi S. (1991). Distribution of myosin heavy chain mRNA in embryonic muscle tissue visualized by ultrastructural in situ hybridization. *Dev Biol.* 143(1):58-67.

231. Prakash N, Fehr S, Mohr E, Richter D (1997) Dendritic localization of rat vasopressin mRNA ultrastructural analysis and mapping of targeting elements. *Eur J Neurosci* 9:523-532.

232. Racca C, Gardiol A, Triller A. (1997). Dendritic and postsynaptic localizations of glycine receptor subunit mRNAs. *J Neurosci* 17:1691-1700.

233. Raff JW, Whitfield WG, Glover DM. (1990). Two distinct mechanisms localise cyclin B transcripts in syncytial Drosophila embryos. *Development* 110(4):1249-61.

234. Ramos A, Grünert S, Adams J, Micklem DR, Proctor MR, Freund S, Bycroft M, St Johnston D, Varani G. (2000) RNA recognition by a Staufen double-stranded RNA binding domain. *EMBO J.*, 19: 997-1009.

235. Ran B, Bopp R, Suter B. (1994). Null alleles reveal novel requirements of *Bic-D* during *Drosophila* oogenesis and Zygotic development. *Development* 120: 1233-42.

236. Rebagliati MR, Weeks DL, Harvey RP, Melton DA. (1985). Identification and cloning of localized maternal RNAs from Xenopus eggs. *Cell* 42: 769-777.

237. Reddy BA, Kloc M, Etkin LD. (1992). The cloning and characterization of a localized maternal transcript in Xenopus laevis whose zygotic counterpart is detected in the CNS. *Mech Dev.* 39(3):143-50.

238. Ressler KJ, Sullivan SL, Buck LB. (1994). Information coding in the olfactory system: evidence for a stereotyped and highly organized epitope map in the olfactory bulb. *Cell* 79(7):1245-55.

239. Richter J. (1996). Dynamics of poly(A) addition and removal during development. In *Translational Control.* Cold Spring Harbor, New York: Cold Spring Harbor Laboratory Press, 411-450.

240. Rivera-Pomar R, Niessing D, Schmidt-Ott U, Gehring W J, Jäckle H. (1996). RNA binding and translational suppression by bicoid. *Nature* 379:746-749.

241. Rhyu MS, Jan LY, Jan YN. (1994). Asymmetric distribution of Numb protein during division of the sensory organ precursor cell confers distinct fates to daughter cells. *Cell* 76: 477-491.

242. Rongo C, Gavis ER, Lehmann R. (1995). Localizationof *oskar* RNA regulates *oskar* translation and requires Oskar protein. *Development* 121:2737-2746.

243. Rosenthal ET, Tansey TR, Ruderman JV. (1983). Sequence-specific adenylations and deadenylation accompany changes in the translation of maternal messenger RNA after fertilization of Spisula oocytes. *J. Mol. Biol.* 166: 309-327.

244. Ross AF, Oleynikov Y, Kislauskis EH, Taneja KL, Singer RH. (1997). Characterization of a β-actin mRNA zipcode-binding protein. *Mol. Cell. Biol.* 17:2158-2165.

245. Roth S, Neuman-Silberberg FS, Barcelo G, Schüpbach T. (1995) *cornichon* and the EGF receptor signaling process are necessary for both anterior-posterior and dorsal-ventral pattern formation in *Drosophila. Cell* 81: 967-978.

246. Ruohola H, Bremer K, Baker D, Swedlow J, Jan L, and Jan Y. (1991). Role of neurogenic genes in establishmemt of follicle cell fate and oocyte polarity during oogenesis in Drosophila. *Cell* 66: 433-449.

247. Ryter JM, Schultz SC. (1998). Molecular basis of double-stranded RNA-protein interactions: structure of a dsRNA-binding domain complexed with dsRNA. *EMBO J.*, 17, 7505-7513.

248. Salles FM, Lieberfarb C, Wreden J, Gergen JP, Strickland S. (1994). Coordinate initiation of *Drosophila* development by regulated polyadenylation of maternal messenger RNAs. *Science* 266: 1996-1999.

249. Schaefer M, Shevchenko A, Shevchenko A, Knoblich J. (2000). A protein complex containing Inscuteable and the Galpha-binding protein Pins orients asymmetric cell divisions in *Drosophila. Curr Biol.* 10(7): 353-62.

250. Schnorrer F, Bohmann K, Nusslein-Volhard C. (2000). The molecular motor dynein is involved in targeting swallow and *bicoid* RNA to the anterior of *Drosophila* oocytes. *Nat Cell Biol.* 2(4): 185-90.

251. Schober M, Schaefer M, Knoblich J. (1999). Bazooka recruits Inscuteable to orient asymmetric cell divisions in *Drosophila* neuroblasts. *Nature* 402: 548-551.

252. Schuldt A, Adams JHJ, Davidson CM, Micklem DR, Haseloff J, St Johnson D, Brand AH. (1998). Miranda mediates asymmetric protein and RNA localization in the developing nervous system. *Genes Dev* 12: 1847–1857.

253. Schumacher JM, Artzt K, Braun RE. (1998). Spermatid perinuclear ribonucleic acid-binding protein binds microtubules in vitro and associates with abnormal manchettes in vitro in mice. *Biol. Reprod.* 59:69-76.

254. Schumacher JM, Lee K, Edelhoff S, Braun RE. (1995). Spnr, a murine RNA-binding protein that is localized to the cytoplasmic microtubules. *J. Cell Biol.* 129:1023-1032.

255. Schwartz SP, Aisenthal L, Elisha Z, Oberman F, Yisraeli JK. (1992). A 69 kDa RNA binding protein from *Xenopus* oocytes recognizes a common motif in two vegetally localized maternal mRNAs. *Proc. Natl. Acad. Sci.* 89:11895-11899.

256. Seeger MA, Kaufman TC. (1990). Molecular analysis of the bicoid gene from Drosophila pseudoobscura: Identification of conserved domains within coding and noncoding regions of the *bicoid* mRNA. *EMBO J* 9:2977-2987.

257. Severt WL, Biber TU, Wu X, Hecht NB, DeLorenzo RJ, Jakoi ER. (1999). The suppression of testis-brain RNA binding protein and kinesin heavy chain disrupts mRNA sorting in dendrites. *J. Cell Sci.* 112:3691-3702.

258. Seydoux G. (1996). Mechanisms of translational control in early development. *Curr. Opin. Genet. Dev.* 6: 555-561

259. Shen CP, Jan LY, Jan YN. (1997). Miranda is required for the asymmetric localization of Prospero during mitosis in Drosophila. *Cell* 90: 449-458.

260. Sil A, Herskowitz I. (1996). Identification of an asymmetrically localized determinant, Ash1p, required for lineage-specific transcription of the yeast HO gene. *Cell* 84: 711-722.

261. Siomi H, Dreyfuss G. (1995). A nuclear localization domain in the hnRNP A1 protein. *J Cell Biol.* 129: 551-560.

262. Siomi MC, Eder PS, Kataoka N, Wan L, Liu Q, Dreyfuss G. (1997). Transportin-mediated nuclear import of heterogeneous nuclear RNP proteins. *J Cell Biol.* 138: 1181-1192.

263. Smibert CA, Wilson JE, Kerr K, Macdonald PM. (1996). Smaug protein represses translation of unlocalized *nanos* mRNA in the *Drosophila* embryo. *Genes Dev* 10:2600-2609.

264. Smith JL, Wilson JE, Macdonald PM. (1992). Overexpression of oskar directs ectopic activation of nanos and presumptive pole cell formation in *Drosophila* embryos. *Cell.* 70:849-859.

265. Spana EP, Doe CQ. (1995). The Prospero transcription factor is asymmetrically localized to the cell cortex during neuroblast mitosis in Drosophila. *Development* 121: 3187-3195.

266. Spana E, Kopczynski C, Goodman CS, Doe CQ. (1995). Asymmetric localization of numb autonomously determines sibling neuron identity in the Drosophila CNS. *Development* 121: 3489-3494.

267. Spradling AC. (1993). Developmental genetics of oogenesis. The Development of *Drosophila melanogaster*. Vol. 1. Cold Spring Harbor Laboratory Press, Plainview, N.Y. 1–70.

268. Stebbins-Boaz B, Richter JD. (1994). Multiple sequence elements and a maternal mRNA product control cdk2 RNA polyadenylation and translation during early Xenopus development. *Mol. Cell Biol.* 14:5870-5880.

269. Stebbins-Boaz B, Hake LE, Richter JD. (1996). CPEB controls the cytoplasmic polyadenylation of cyclin, Cdk2 and c-mos mRNAs and is necessary for oocyte maturation in *Xenopus*. *EMBO J* 15: 2582-2592.

270. Stennard F, Carnac G, Gurdon JB. (1996). The Xenopus T-box gene, Antipodean, encodes a vegetally localised maternal mRNA and can trigger mesoderm formation. *Development* 122(12):4179-88.

271. Stephenson EC, Chao YC, Fackenthal JD. (1988). Molecular analysis of the swallow gene of *Drosophila melanogaster*. *Genes Dev.* 2:1655-1665.

272. Steward O. (1983). Polyribosomes at the base of dendritic spines of CNS neurons: their possible role in synapse construction and modification. *Cold Spring Harb Symp Quant Biol* 48: 745-759.

273. Steward O, Fass B. (1983). Polyribosomes associated with dendritic spines in the denervated dentate gyrus: Evidence for local regulation of protein synthesis during reinnervation. *Prog Brain Res* 58: 131-136.

274. Steward O, Halpain S. (1999). Lamina-Specific Synaptic Activation Causes Domain-Specific Alterations in Dendritic Immunostaining for MAP2 and CAM Kinase II. *J. Neurosci.* 19: 7834-7845

275. Steward O, Kleiman R, Banker G. (1995). Subcellular localization of mRNA in neurons. In: *Localized RNAs*. Pp.235-255. Ed. H. D. Lipshitz. Springer-Verlag, Heidelberg.

276. Steward O, Lewy WB. (1982). Preferential localization of polyribosomes under the base of dendritic spines in granule cells of the dentate gyrus. *J.Neurosci* 2:284-291.

277. Steward O, Wallace CS, Lyford GL, Worley PF. (1998). Synaptic activation causes the mRNA for the IEG Arc to localize selectively near activated postsynaptic sites on dendrites. *Neuron* 21: 741–751.

278. St Johnston D. (1995). The intracellular localization of messenger RNAs. *Cell* 81:161-170.

279. St. Johnston D, Beuchle D, Nuesslein-Volhard C. (1991). staufen, a gene required to localize maternal RNAs in the *Drosophila* egg. *Cell* 66, 51-63.

280. St Johnston D, Brown NH, Gall JG, Jantsch M. (1992). A conserved double-stranded RNA-binding domain. *Proc. Natl. Acad. Sci. USA* 89: 10979-10983.

281. St Johnston D, Driever W, Berleth T, Richstein S, Nusslein-Volhard C. (1989). Multiple steps in the localization of *bicoid* RNA to the anterior pole of the *Drosophila* oocyte. *Development.* 107:13-19.

282. St Johnston, D, Nüsslein-Volhard, C. (1992). The origin of pattern and polarity in the *Drosophila* embryo. *Cell*. 68:201-219.

283. Struhl G., Johnston P., Lawrence P. A. (1992). Control of *Drosophila* body pattern by the hunchback morphogen gradient. *Cell* 69:237-249.

284. Struhl G, Struhl K, Macdonald PM. (1989). The gradient morphogen bicoid is concentration-dependent transcriptional activator. *Cell* 57: 1259-1273.

285. Sundell CL, Singer RH. (1990). Actin mRNA localizes in the absence of protein synthesis. *J. Cell Biol.*111: 2397-2403.

286. Sundell CL, Singer RH. (1991). Requirement of microfilaments in sorting of actin messenger RNA. *Science* 253:1275-1277.

287. Suter B, Romberg LM, Steward R. (1989). Bicaudal-D, a *Drosophila* gene involved in developmental asymmetry localized transcript accumulation in ovaries and sequence similarity to myosin heavy chain tail domains. *Genes Dev* 3:1957-1968.

288. Suter B, Steward R. (1991), Requirement for phosphorylation and localization of the Bicaudal-D protein in Drosophila oocyte differentiation. *Cell* 67:917-26.

289. Swalla BJ, Jeffery WR. (1995). A maternal RNA localized in the yellow crescent is segregated to the larval muscle cells during ascidian development. *Dev Biol.* 170(2):353-64.

290. Swalla BJ, Jeffery WR. (1996). Localization of ribosomal protein L5 mRNA in myoplasm during ascidian development. *Dev Genet.* 19(3):258-67.

291. Swalla BJ, Jeffery WR. (1996). PCNA mRNA has a 3'UTR antisense to yellow crescent RNA and is localized in ascidian eggs and embryos. *Dev Biol.* 178(1):23-34.

292. Swan A, Suter B. (1996). Role of *Bicaudal-D* in patterning the *Drosophila* egg chamber in mid-oogenesis. *Development* 122:3577-3586.

293. Takizawa PA, Sil A, Swedlow JR, Herskowitz I, Vale RD. (1997). Actin-dependent localization of an RNA encoding a cell-fate determinant in yeast. *Nature* 389: 90-93.

294. Tautz D. (1988). Regulation of the *Drosophila* segmentation gene *hunchback* by two maternal morphogenetic centres. *Nature* 332: 281-284.

295. Tepass U, Theres C, Knust E. (1990). crumbs encodes an EGF-like protein expressed on apical membranes of Drosophila epithelial cells and required for organization of epithelia. *Cell* 61(5):787-99.

296. Tetzlaff MT, Jackle H, Pankratz MJ. (1996). Lack of *Drosophila* cytoskeletal tropomyosin affects head morphogenesis and the accumulation of oskar mRNA required for germ cell formation. *EMBO (Eur. Mol. Biol. Organ.) J.* 15:1247-1254.

297. Theurkauf W. (1994). Premature microtubule-dependent cytoplasmic streaming in *cappuccino* and *spire* mutant oocytes. *Science.* 265:2093-2095.

298. Theurkauf WE, Alberts BM, Jan YN, Jongens TA. (1993). A central role for microtubules in the differentiation of *Drosophila* oocytes. *Development* 118:1169-1180.

299. Thomsen GH, Melton DA. (1993). Processed *Vg1* protein is an axial mesoderm inducer in *Xenopus*. *Cell* 74:433-441.

300. Tian B, White RJ, Xia T, Welle S, Turner DH, Mathews MB, Thornton CA. (2000). Expand CUG repeats RNAs form hairpins that activate the double-stranded-RNA-dependent protein kinase PKR. *RNA* 6: 79-87.

301. Tiedge H, Bloom FE, Richter D. (1999). RNA, whither goest thou? *Science* 283: 186–187.

302. Tiedge H, Brosius J. (1996). Translational machinery in dendrites of hippocampal neurons in culture. *J. Neurosci.* 15:7171-7181.

303. Tiedge H, Chen W, Brosius J. (1993). Primary structure, neural-specific expression, and dendritic location of human BC200 RNA. *J Neurosci.* 13(6):2382-90.

304. Tiedge H, Fremeau RT Jr, Weinstock PH, Arancio O, Brosius J. (1991). Dendritic locaion of neural BC1 RNA. *Proc Natl Acad Sci USA* 88:2093-2097.

305. Tiedge H, Zhou A, Thorn NA, Brosius J. (1993). Transport of BC1 RNA in hypothalamo-neurohypophyseal axons. *J Neurosci.* 13(10):4214-9.

306. Torre ER, Steward O. (1996). Glycosylation of newly synthesized proteins in dendrites of hippocampal neurons in culture. *J neurosci* 16: 5967-5978.

307. Trapp BD, Moench T, Pully M, Barbosa E, Tennekoon G, Griffin J. (1987) Spacial segregation of mRNA encoding myelin-specific proteins. *Proc. Natl. Acad. Sci. USA* 84: 7773-7777.

308. Trembleau A, Calas A, Fevre-Montange M. (1990). Ultrastructural localization of oxytocin mRNA in the rat hypothalamus by in situ hybridization using a synthetic oligonucleotide. *Mol Brain Res.* 8(1):37-45.

309. Uemura T, Shepherd S, Ackerman L, Jan LY, Jan YN. (1989). numb, a gene required in determination of cell fate during sensory organ formation in *Drosophila* embryos. *Cell* 58: 349-360.

310. Vaessin H, Grell E, Wolff E, Bier E, Jan LY, Jan YN. (1991). prospero is expressed in neuronal precursors and encodes a nuclear protein that is involved in the control of axonal outgrowth in *Drosophila*. *Cell* 67:941-953.

311. Van Eeden F, St Johnston D. (1999). The polarisation of the anterior-posterior and dorsal-ventral axes during *Drosophila* oogenesis. *Curr. Opin. Genet. Dev.* 9: 396-404.

312. Vassar R, Chao SK, Sitcheran R, Nunez JM, Vosshall LB, Axel R. (1994). Topographic organization of sensory projections to the olfactory bulb. *Cell* 79(6):981-91.

313. Vlahou A, Gonzalez-Rimbau M, Flytzanis CN. (1996). Maternal mRNA encoding the orphan steroid receptor SpCOUP-TF is localized in sea urchin eggs. *Development* 122(2):521-6.

314. Wallace CS, Lyford GL, Worley PF, Steward O. (1998). Differential intracellular sorting of immediate early gene mRNAs depends on signals in the mRNA sequence. *J Neurosci*, 18: 26–35.

315. Wang C, Lehmann R. (1991) *Nanos* is the localized posterior determinant in Drosophila. *Cell* 66:637-647.

316. Wang C, Dickinson LK, Lehmann R. (1994). Genetics of nanos localization in Drosophila. *Dev. Dynam.* 199:103-115.

317. Wang Y., Zeng Y, Murry JM, Nishikura K. (1995). Genomic organization and chromosomal location of the human dsRNA adenosine deaminase gene: The enzyme for glutamate-activated ion channel RNA editing. *J. Mol. Biol.* 254: 184-195.

318. Wanner I, Baader SL, Brich M, Oberdick J, Schilling K. (1997). Subcellular localization of specific RNAs and their protein products in Purkinje cells by combined fluorescence in situ hybridization and immunocytochemistry. *Histochem Cell Biol.* 108:345-357.

319. Watson JB, Suteliffe JG, Fischer RS. (1992). Localization of the protein kinase C phosphorylation calmodulin-binding substrate RC3 in dendritic spines of neostriatal neurons. *Proc. Natl. Acad. Sci. USA* 89:8581-8585.

320. Webster PJ, Liang L, Berg CA, Lasko P, Macdonald PM. (1997). Translational repressor bruno plays multiple roles in development and is widely conserved. *Genes & Dev.* 11: 2510-2521.

321. Weeks DL, Melton DA. (1987). A maternal mRNA localized to the vegetal hemisphere in Xenopus eggs codes for a growth factor related to TGF-β. *Cell.* 51: 861-867.

322. Weiler IJ, Irwin SA, Klintsova AY, Spencer CM, Brazelton AD, Miyashiro K, Comery TA, Patel B, Eberwine J, Greenough WT (1997). Fragile X mental retardation protein is translated near synapses in response to neurotransmitter activation. *Proc Natl Acad Sci USA* 94: 5395–5400.

323. Wickham L, Duchaine T, Luo M, Nabi IR, DesGroseillers L. (1999). Mammalian staufen is a double-stranded RNA and tubulin binding protein which localizes to the rough endoplasmic reticulum. *Mol Cell Biol* 19: 2220–2230.

324. Wilhelm JE, Vale RD. (1993). RNA on the move: the mRNA localization pathway. *J Cell Biol* 123:269-274.

325. Wilsch-Brauninger M, Schwarz H, Nusslein-Volhard C. (1997). A sponge-like structure involved in the association and transport of maternal products during *Drosophila* oogenesis. *J. Cell Biol.* 139:817-829.

326. Wilson JE, Connell JE, Macdonald PM. (1996). *aubergine* enhances *oskar* translation in the *Drosophila* ovary. *Development* 122:1631-1639.

327. Wharton RP, Sonoda J, Lee T, Patterson M, Murata Y. (1998). The Pumilio RNA-binding domain is also a translational regulator. *Mol. Cell* 1:863-872.

328. Wharton RP, Struhl G. (1991). RNA regulatory elements mediate control of *Drosophila* body pattern by the posterior morphogen nanos. *Cell*, **67**, 955-967.

329. Whitfield WG, Gonzalez C, Sanchez-Herrero E, Glover DM. (1989). Transcripts of one of two *Drosophila* cyclin genes become localized in pole cells during embryogenesis. *Nature.* 338:337-40.

330. Wodarz A, Ramrath A, Kuchinke U, Knust E. (1999). Bazooka provides an apical cue for Inscuteable localization in *Drosophila* neuroblasts. *Nature* 402:544-547.

331. Worffe AP, Meric F. (1996). Coupling transcription to translation: a novel site for the regulation of gene expression. *Int J. Biochem. Cell Biol.* 28: 247-257.

332. Wu S, Kumar K, Kaufman RJ. (1998). Identification and requirements of three ribosome binding domains in dsRNA-dependent protein kinase (PKR). *Biochem.* 37, 13816-13826.

333. Yeh B, Svoboda KKH. (1994). Intracellular distribution of β-actin mRNA is polarized in embryonic corneal epithelia. *J cell Sci* 107: 105-115.

334. Yisraeli JK, Sokol S, Melton DA. (1990). A two step model for the localization of maternal mRNA in Xenopus oocytes: involvement of microtubules and microfilaments in the translocation and anchoring of Vg1 mRNA. *Development* 108: 289-298.

335. Yoon C, Kawakami K, Hopkins N. (1997). Zebrafish vasa homologue RNA is localized to the cleavage planes of 2- and 4-cell-stage embryos and is expressed in the primordial germ cells. *Development* 124(16):3157-65.

336. Yu F, Morin X, Cai Y, Yang X, Chia W. (2000). Analysis of *partner of inscuteable*, a novel player of *Drosophila* asymmetric divisions, reveals two distinct steps in Inscuteable apical localization. *Cell* 100: 399-409.

337. Yue L, Spradling AC. (1992). hu-li tai shao, a gene required for ring canal formation during Drosophila oogenesis, encodes a homolog of adducin. *Genes Dev.* 6(12B):2443-54.

338. Zamore PD, Williamson JR, Lehmann R. (1997). The Pumilio protein binds RNA through a conserved domain that defines a new class of RNA-binding proteins. *RNA* 3:1421-1433.

339. Zhang J, Houston DW, King ML, Payne C, Wylie C, Heasman J. (1998). The role of maternal VegT in establishing the primary germ layers in *Xenopus* embryos. *Cell* 94:515-524.

340. Zhang J, King ML. (1996). Xenopus VegT RNA is localized to the vegetal cortex during oogenesis and encodes a novel T-box transcription factor involved in mesodermal patterning. *Development* 122: 4119-4129.

341. Zhou Y, King ML. (1996). Localization of Xcat-2 RNA, a putative germ plasm component, to the mitochondrial cloud in Xenopus stage I oocytes. *Development* 122: 2947-2953.

342. Zhu S, Romano PR, Wek RC. (1997). Ribosome targeting of PKR is mediated by two double-stranded RNA-binding domains and facilitates in vivo phosphorylation of eukaryotic initiation factor-2. *J. Biol. Chem.* 272: 14434-14441.

Appendix

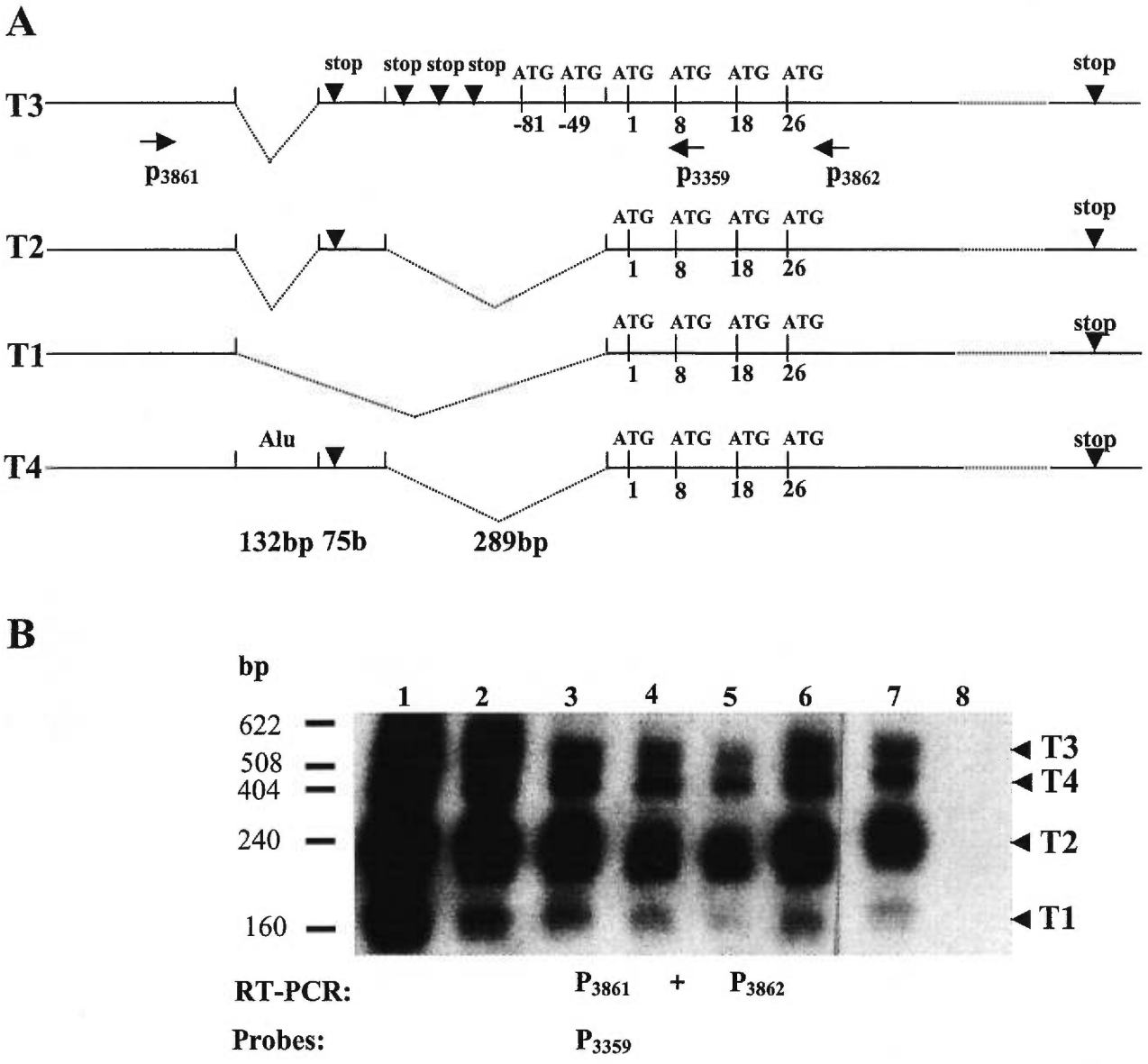

Fig. 1. The expression pattern of 4 alternative splicing transcripts of hStau in different human tissues and HeLa cells. A. The schematic representation of 4 hStau transcripts. **B.** RT-PCR and hybridization to examine the expression of the 4 transcripts in different human tissues and cell line. Lane 1: HeLa cells, Lane 2: CNS, Lane 3: Spleen, Lane 4: Calveria, Lane 5: Thymus, Lane 6: Pancreas, Lane 7: Kidney, Lane 8: Negative control.

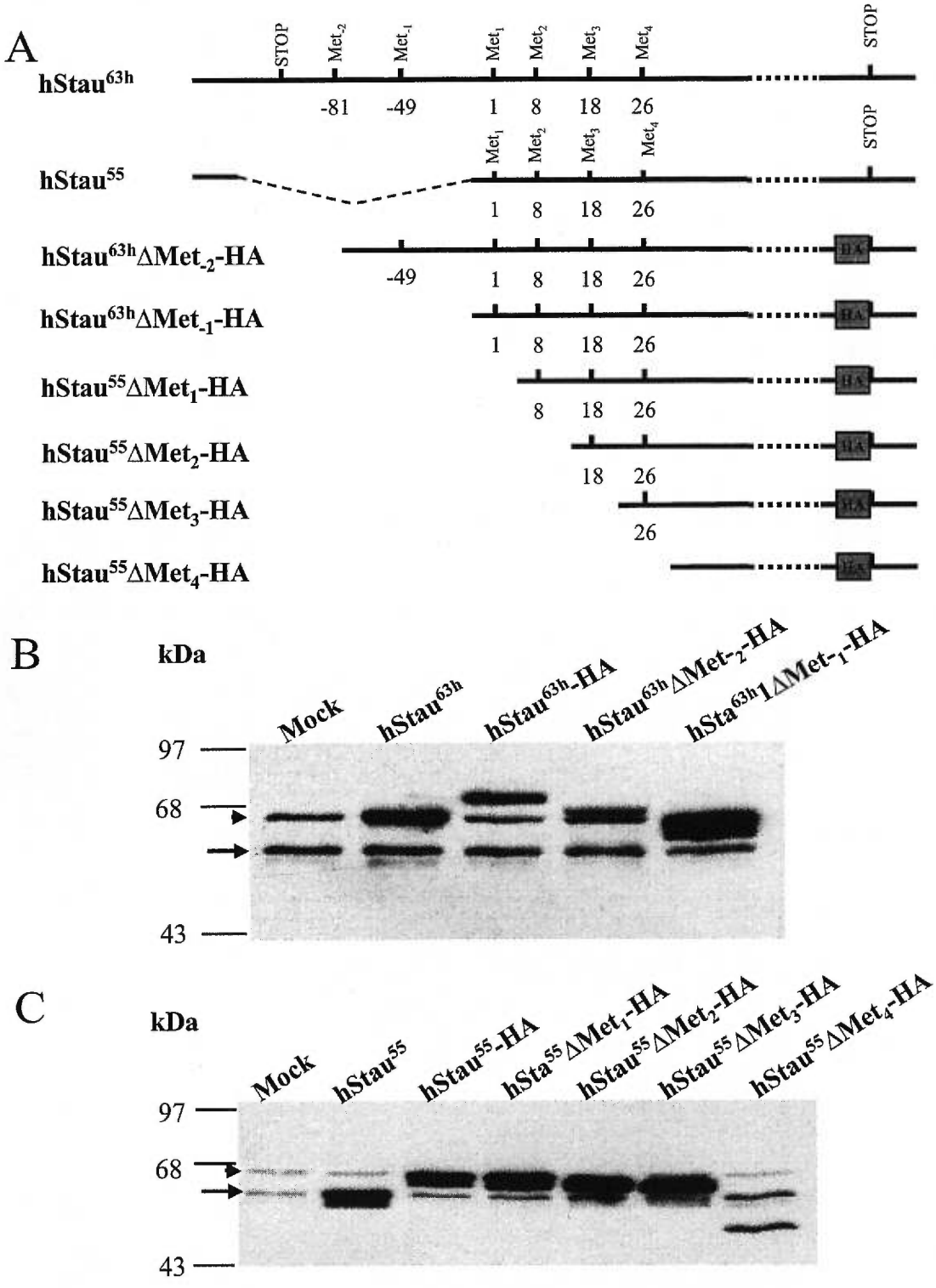

Fig. 2. Molecular mapping of the translation initiation sites of hStau^{63h} and hStau^{55}
A. Schematic representation of a series of deletion mutants from hStau^{63h} and hStau^{55}. **B.** The translation initiation site of hStau^{63h} maps to ATG$_{-81}$. **C.** The translation initiation site of hStau^{55} maps to ATG$_{8}$. Arrow head: Stau^{63}, Arrow: Stau^{55}.

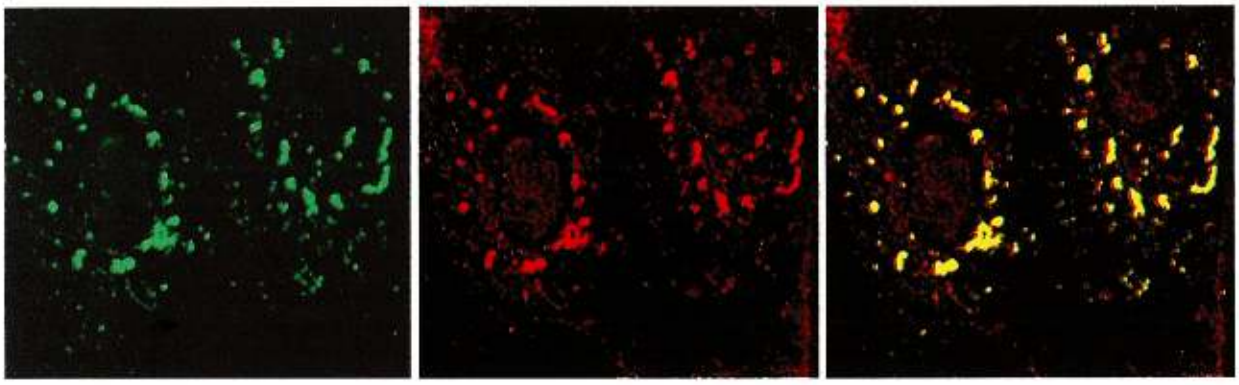

hStau^{55}/3*/4*-HA$_3$ **Calnexin** **Merged image**

Fig. 3. hStau^{55}/3*/4*-HA$_3$ forms clusters that colocalize with the RER marker in mammalian cells.

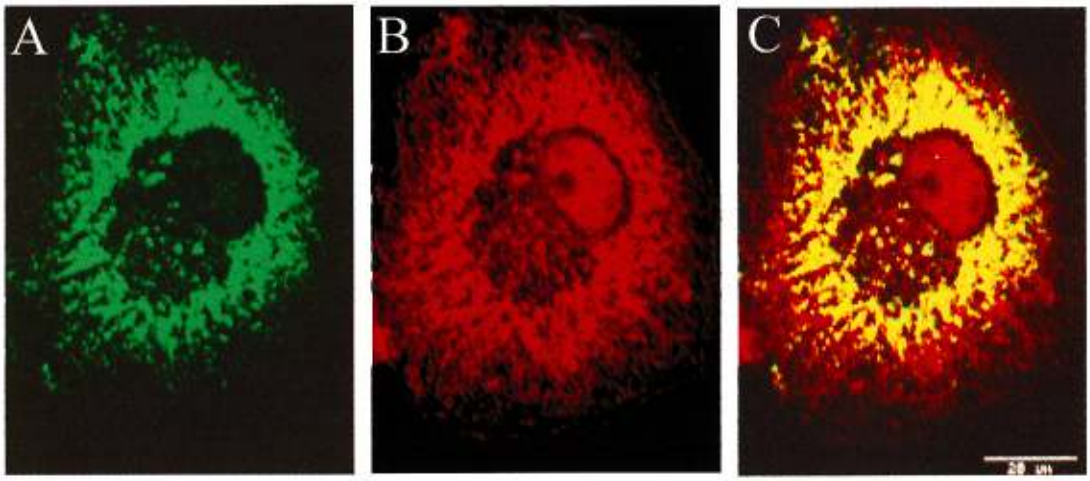

Fig. 4. The N-terminal mutant RBD2/3/4-HA_3 localizes to the rough endoplasmic reticulum.

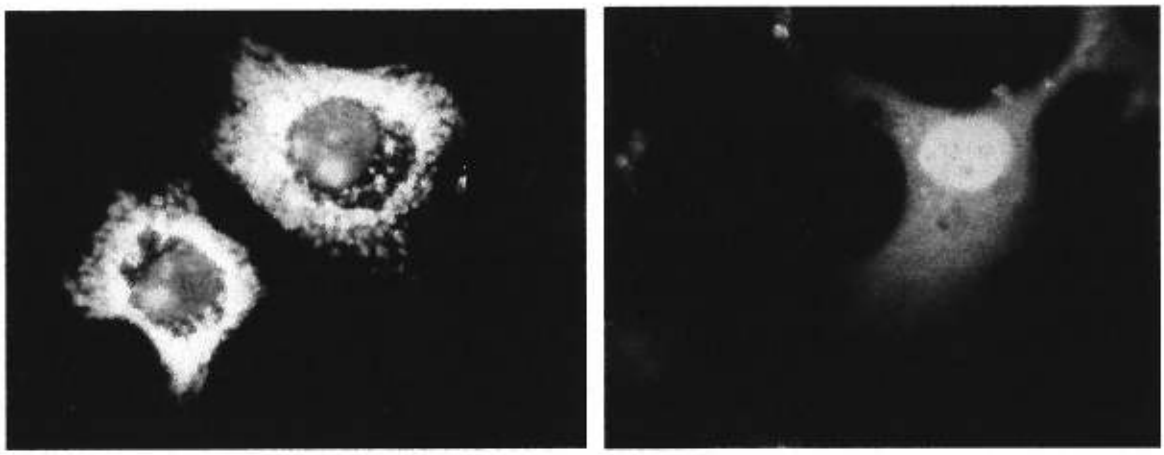

RBD3/4-GFP **RBD3*/4*-GFP**

Fig. 5. hStau mutant RBD3/4-GFP is localized to the nucleolus and cytoplasm, the nucleolus localization is dependent of hStau RNA-binding activity.

Publication List

Publications:

1. Wickham L, Duchaîne T, Luo M, Nabi IR, DesGroseillers L. Mammalian Staufen is a double-stranded-RNA- and tubulin-binding protein which localizes to the rough endoplasmic reticulum. *Mol Cell Biol* 1999, 19: 2220-30.

2. Köhrmann M, Luo M, Kaether C, DesGroseillers L, Dotti CG, Kiebler MA. Microtubule-dependent recruitment of Staufen-green fluorescent protein into large RNA-containing granules and subsequent dendritic transport in living hippocampal neurons. *Mol Biol Cell* 1999, 10(9): 2945-53.

3. DesGroseillers L, Duchaîne T, Luo M. Transport et localisation d'ARN messagers chez les mammifères: rôle de la protéine staufen. *Médecine/sciences* 1999, 15: 1164-1167.

4. Mouland AJ, Mercier J, Luo M, Bernier L, DesGroseillers L, Cohen EA. The Double-Stranded RNA-Binding Protein Staufen Is Incorporated in Human Immunodeficiency Virus Type 1: Evidence for a Role in Genomic RNA Encapsidation. *J Virology* 2000, 74(12): 5441-5451.

5. Brizard F, Luo M, DesGroseillers L. Genomic organization of the human and mouse *stau* genes. *DNA and Cell Biol* 2000, 19:331-339.

6. Duchaîne T, Wang HJ, Luo M, Steinberg SV, Nabi IR, DesGroseillers L. A novel murine Staufen isoform modulates the RNA content of Staufen ribonucleoprotein complexes. *Mol Cell Biol* 2000, 20:5592-5601.

7. Luo M, DesGroseillers L. Multiple Determinants in Human RNA-Binding Protein Staufen Are Involved in Ribosome and Rough Endoplasmic Reticulum Association. *J Biol Chem*, submitted.